CHAPTER 1

INTRODUCTION

1.1 <u>Foundations: Their Importance and Purpose</u>

All engineered construction resting on the earth must be carried by some kind of interfacing element called *a foundation.* The foundation is the part of an engineered system that transmits to, and into, the underlying soil or rock the loads supported by the foundation and its self-weight.

The term *superstructure* is commonly used to describe the engineered part of the system bringing load to the foundation, or *substructure*. The term *superstructure* has particular significance for buildings and bridges; however, foundations also may carry only machinery, support industrial equipment (pipes, towers, tanks), act as sign bases, and the like. For these reasons it is better to describe a foundation as that part of the engineered system that interfaces the load-carrying components to the ground.

Foundation engineering can be defined as the science and art of applying the principles of soil and structural mechanics together with engineering judgment to solve the interfacing problem. The foundation engineer is concerned directly with the structural members which affect the transfer of the load from the superstructure to the soil such that the resulting soil stability and estimated deformations are tolerable.

1.2 <u>Foundation Classification</u>

Foundations may be classified based on where the load carried by the ground, producing:

1. Shallow foundations: Spreading loads laterally with $D \leq B$ (where D is the depth of footing and B is the width of footing). These include pad or isolated footing, strip (or wall) footing, continuous footing, combined footing (rectangular, trapezoid and strap), and mat (or raft) foundation.
2. Deep foundations: Distribute the load vertically with $D > (4\text{-}5)\,B$. These include piles, drilled piers and drilled caissons.
3. Retaining Structures.

   Such as retaining walls, sheet pile walls and walls for excavations.

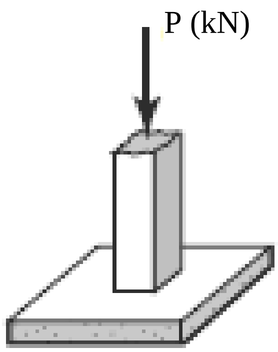

Pad

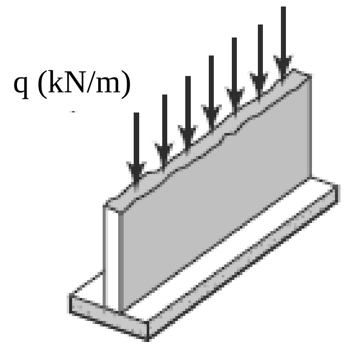

Wall

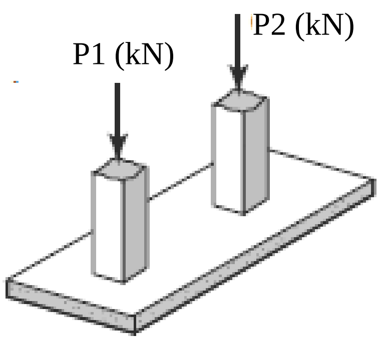

Rectangular

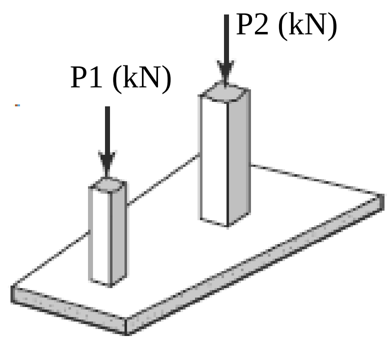

Trapezoidal

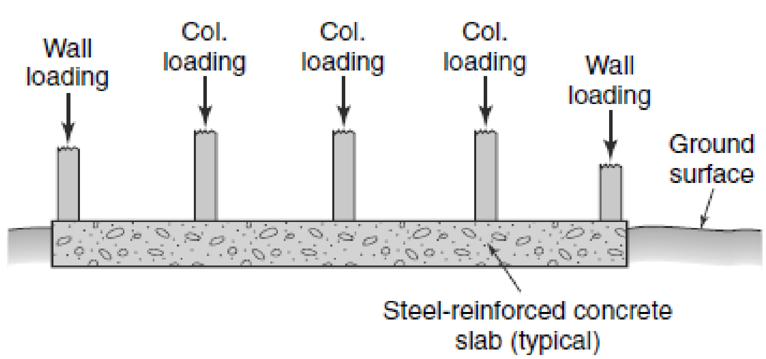

Mat

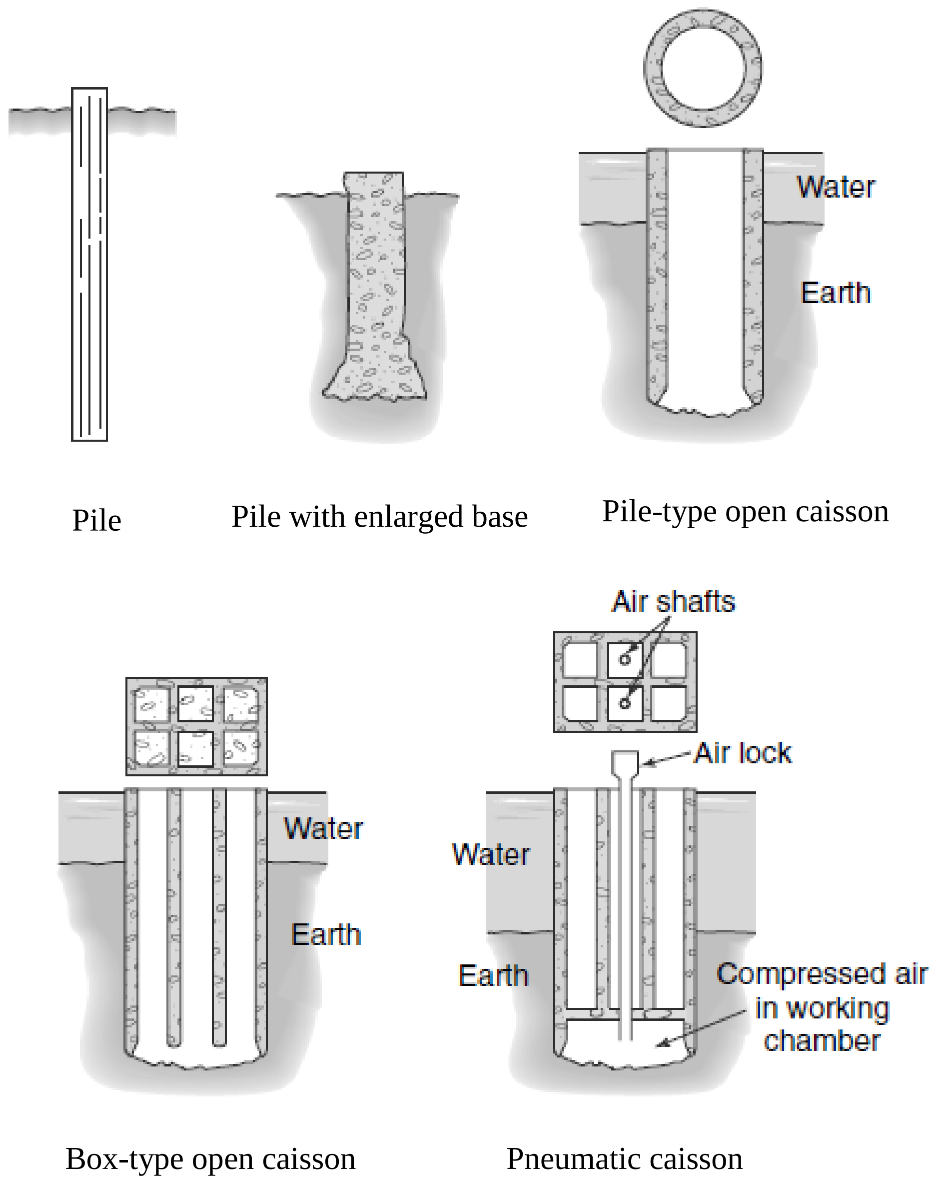

Fig. 1.1 General types of foundations

1.3 <u>General Requirements of Foundations</u>

A foundation must be capable of satisfying several stability and deformation requirements such as:

1. Depth must be adequate to avoid lateral expulsion of material from beneath the foundation.
2. Depth must be below the zone of seasonal volume changes caused by freezing, thawing and plant growth.

3. System must be safe against overturning, rotation, sliding, or soil rupture (shear failure).
4. System must be safe against corrosion or deterioration due to harmful materials present in the soil.
5. System should be adequate to sustain some changes in later site or construction geometry, and be easily modified should later changes be major in scope.
6. The foundation should be economical in terms of the method of installation.
7. Total and differential earth movements (settlements) should be tolerable for both the foundation and superstructure elements.
8. The foundation and its construction, must meet environmental protection standards.

1.4 Foundation Selection

See Fig. (1.2).

Soil conditions	Appropriate foundation type and location	Design comments
(1) 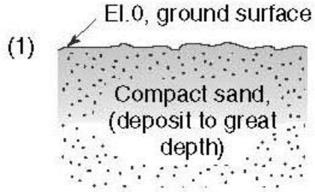	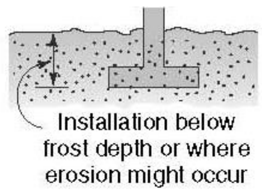	*Spread footings* most appropriate for conventional foundation needs. A deep foundation such as *piles* could be required if uplift or other unusual forces (e.g., seismic, effect of flood) could act.
(2) 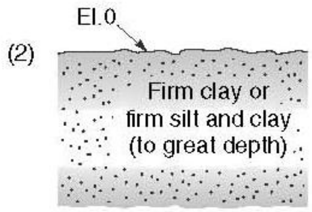	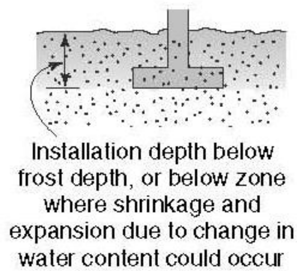	*Spread footings* most appropriate for conventional foundation needs. Also see comment for (1) above.
(3) 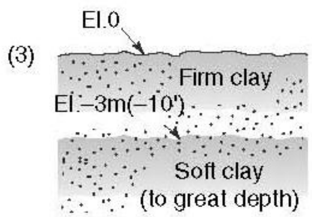	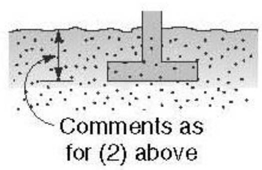	*Spread footing* would be appropriate for low to medium range of loads, if not installed too close to soft clay layer. If heavy loads are to be carried, *deep foundations* might be required.
(4) 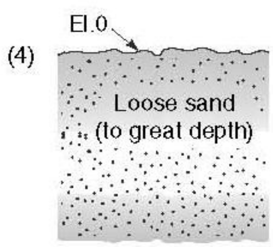	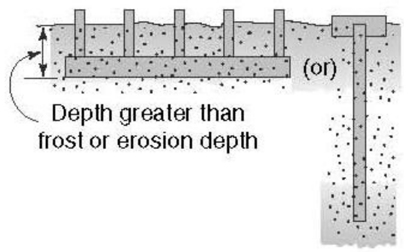	Spread footing may settle excessively or require use of very low bearing pressures. Consider *mat foundation*, or consider compacting sand by vibroflotation or other method, *then* use *spread footings*. Driven *piles* could be used and would densify the sand. Also consider *augered cast-in-place piles*.
(5) 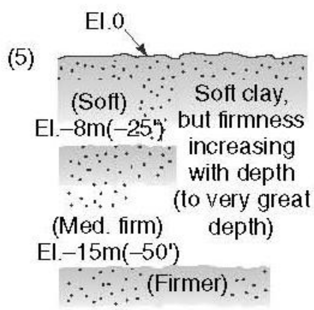	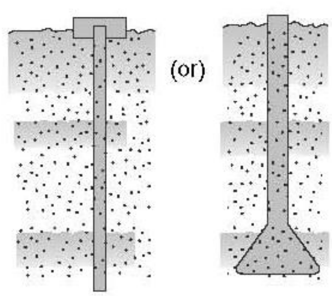	Spread footings probably not appropriate. *Friction piles* or *piers* would be satisfactory if some settlement could be tolerated. *Long piles* would reduce settlement problems. Should also consider *mat* foundation or *floating foundation*.

Soil conditions	Appropriate foundation type and location	Design comments

(6)

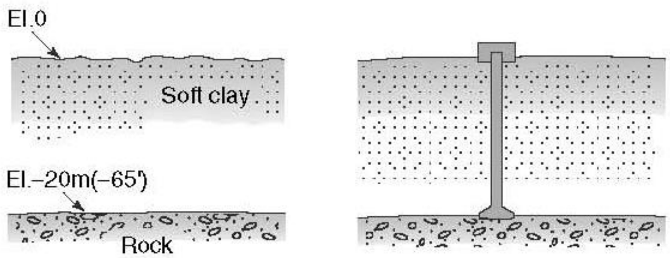

Deep foundation—*piles, piers, caissons*—bearing directly on/in the rock.

(7)

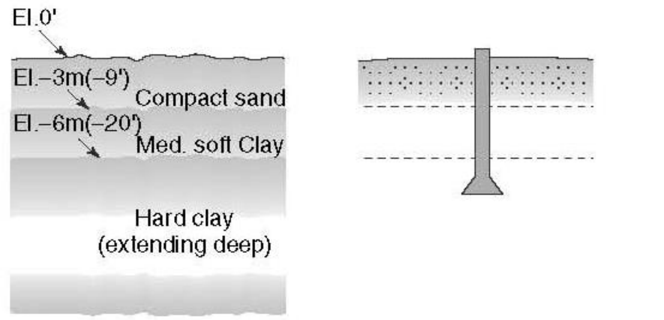

Spread footings in upper sand layer would probably experience large settlement because of underlying soft clay layer. Consider *drilled piers* with a bell formed in hard clay layer, or other *pile foundation* into hard clay layer.

(8)

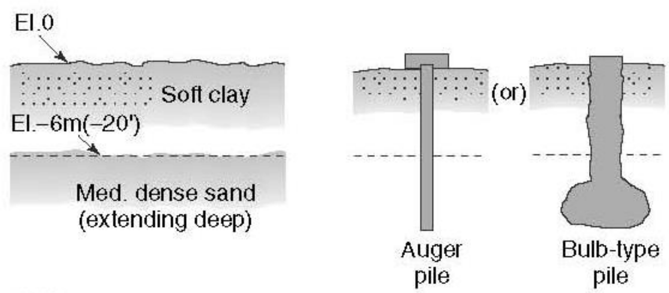

Deep foundation best—*cast-in-place* piles such as *auger piles* or *bulb piles* into sand layer appear most appropriate.

(9)

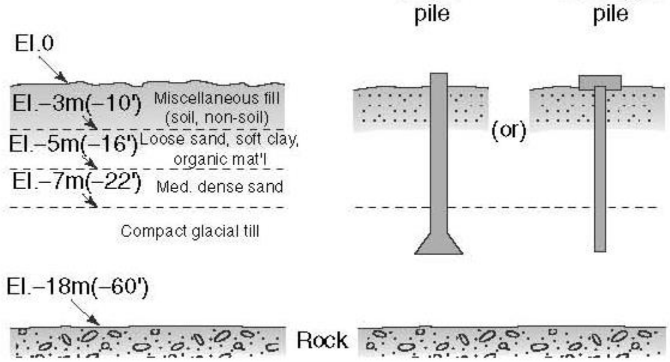

Deep foundation types extending into medium dense sand, or more preferably, into compact glacial till. *Strong* possibility for *drilled pier* with *bell* constructed in till. Also consider *cast-in-place* and *driven concrete pile, wood pile, pipe pile*.

(10)

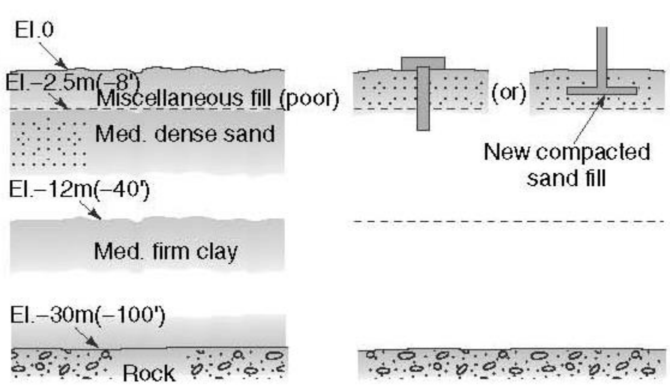

Deep foundations penetrating through fill are appropriate. With *piles* or *piers*, consider stopping in upper zone of sand layer so as to limit compression of clay layer. Also consider replacing poor fill with a *compacted fill* and then using *spread footings* in the new fill.

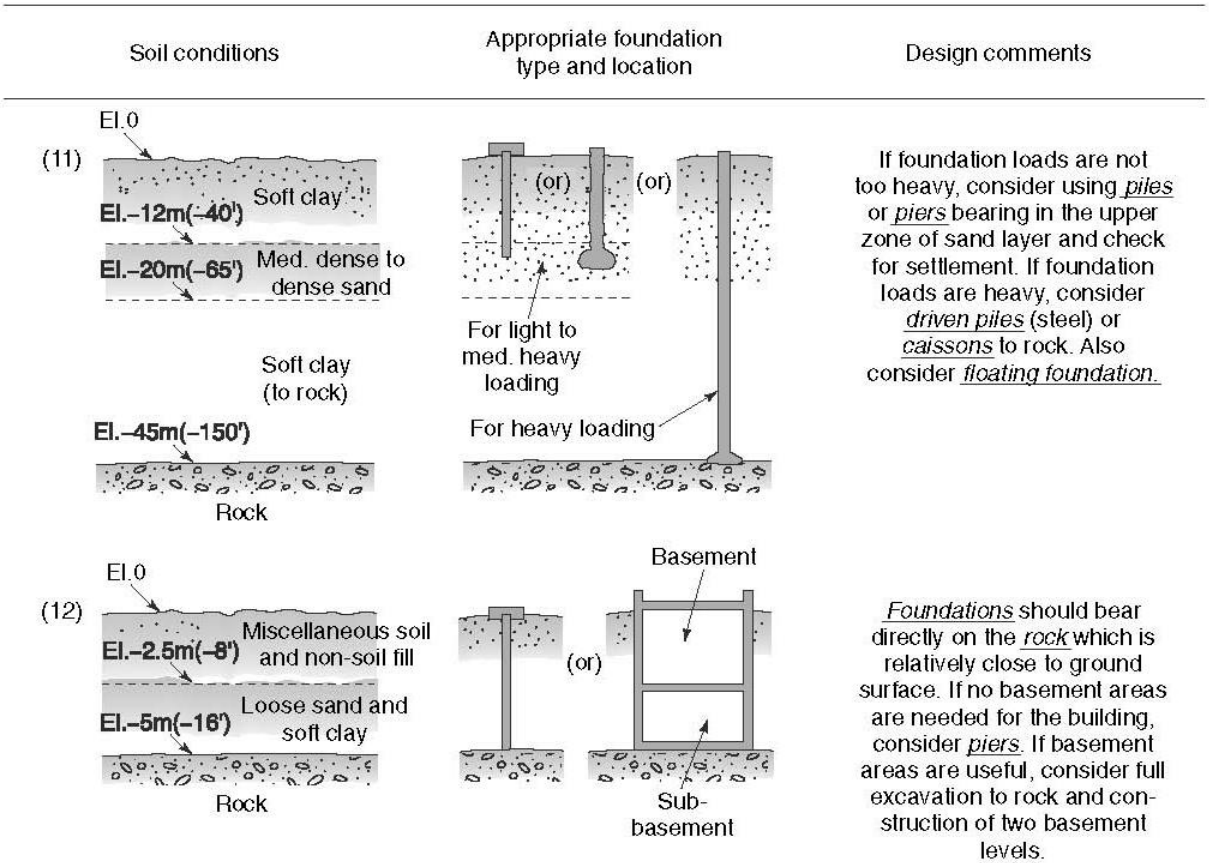

Fig. 1.2 Illustrations relating soil conditions and appropriate foundation types

CHAPTER 2

SOIL EXPLORATION

Soil exploration refers to the procedure of determining surface and sub-surface conditions in an area of proposed construction.

2.1 <u>Purpose of Subsurface Exploration</u>

The purpose of the exploration program is to determine the stratification and engineering properties of the soils underlying the site. The principal properties of interest will be the strength, deformation, and hydraulic characteristics. The elements of site investigation depend heavily on the project but generally should include the following:

1. Determining the nature of soil at the site and its stratification.
2. Obtaining disturbed and undisturbed soil samples for visual identification and appropriate laboratory tests.
3. Determining the depth and nature of bedrock, if and when encountered.
4. Performing some in-situ field tests.
5. Observing drainage conditions from and into the site.
6. Assessing any special construction problems with respect to the existing structure(s) nearby.

2.2 <u>Planning for Subsurface Exploration</u>

The actual planning of a subsurface exploration program includes some or all of the following steps:

1. Assembly of all available information on dimensions, anticipated loads, type and use of the structure, and the requirements of local building codes.
2. Reconnaissance of the area: This may be in the form of;
   A. A Field trip; accessibility of the site, nature of drainage conditions, open cuts, cracks in nearby structures.
   B. Useful information gathered from; geological survey maps, aerial photographs, existing soil exploration reports, published soil manuals, agronomy maps.
3. A preliminary site investigation. Few borings are made or a test pit is opened to establish

in a general manner the stratification, types of soil to be expected and possibly the location of the ground water table.

4. A detailed site investigation. Additional borings are made, laboratory tests to have design information and finally the report is prepared.

There are two complementary stages:

5. Verification (during construction); compare the actual soil conditions with soil report information.
6. Observation (after construction); compare the actual foundation behavior with the expected one.

2.3 <u>Methods of Soil Exploration</u>

A soil exploration program usually involves test (or trial) pits, soil borings (boreholes) and/or geophysical methods.

1. Trial pits: excavations into the earth that permit visual inspection of the conditions exposed in the wall of the pit. Samples can be taken. Limited for shallow depths (3 to 4m), see Fig. (2.1).
2. Soil Borings (Boreholes): Boreholes are conducted using one of the following methods:
   A. Auger (hand and mechanical); see Fig. (2.2).
   B. Percussion drilling; see Fig. (2.3).
   C. Wash boring; see Fig. (2.4).
   D. Rotary drilling; see Fig. (2.5).
3. Geophysical explorations:
   A. Seismic; refraction and reflection.
   B. Electrical resistivity.

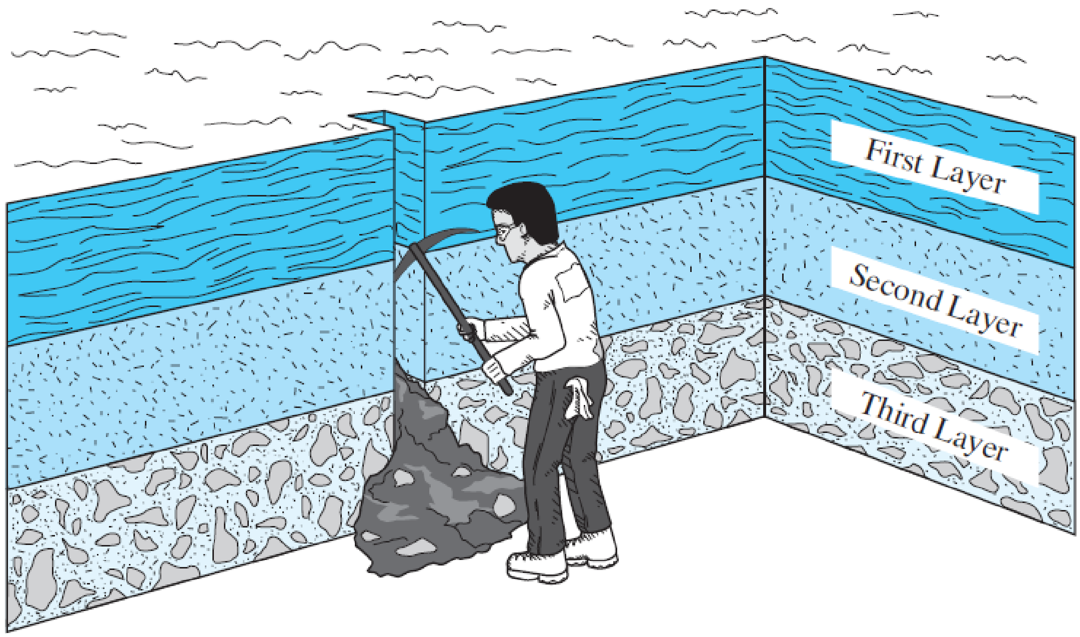

Fig. 2.1 Trial Pit

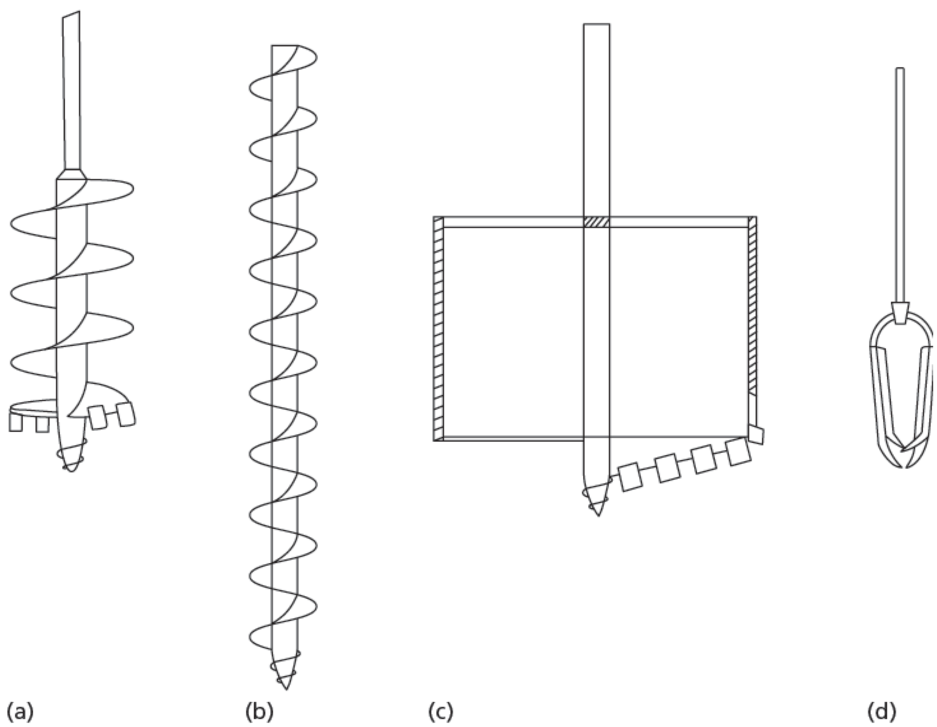

Fig. 2.2 (a) Short-flight auger, (b) continuous-flight auger, (c) bucket auger, and (d) Iwan (hand) auger.

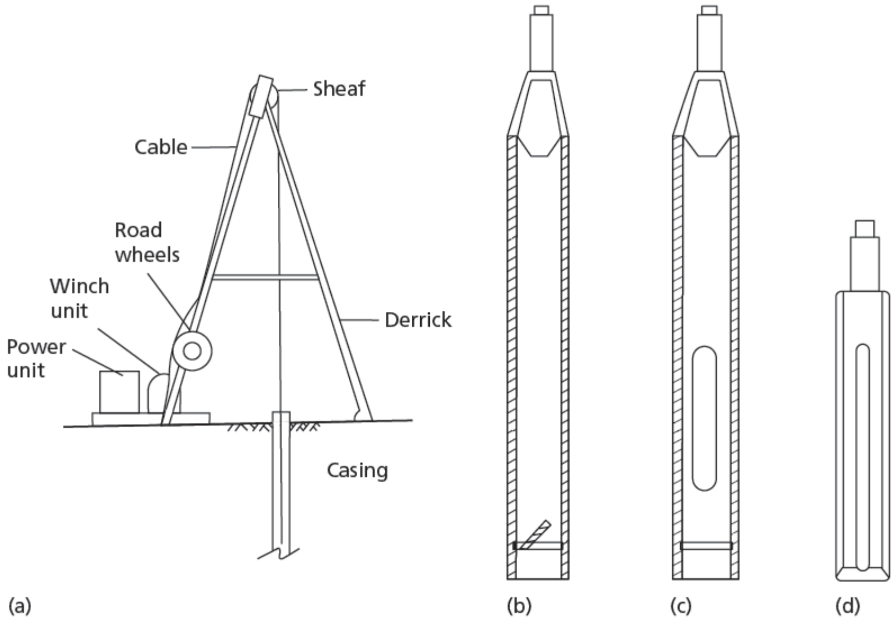

Fig. 2.3 (a) Percussion boring rig, (b) shell, (c) clay cutter, and (d) chisel.

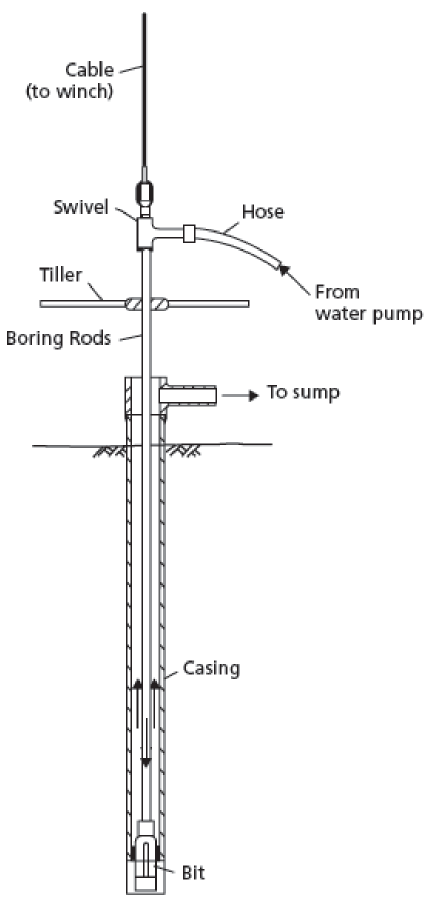

Fig. 2.4 Wash boring.

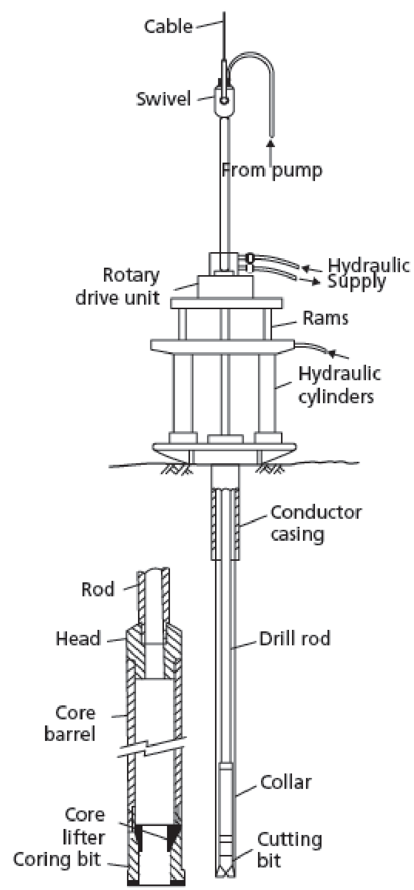

Fig. 2.5 Rotary drilling.

2.4 Soil Samples

There are two types of samples:

1. Disturbed samples; in which the in-situ properties of soil do not retain during the collection process. Such samples are usually used for identification, chemical and classification tests.
2. Undisturbed samples; in which the structural integrity of the soil is retained and has a high recovery ratio. Such samples are usually used to determine the mechanical properties of soil.

2.5 Causes of Disturbance

There are several factors that cause disturbance of soil samples:

1. Stress relief.
2. Volume displacement of the sampler [see Fig. (2.6a)].

$$area\ ratio = Ar = \frac{D_o^2 - D_i^2}{D_i^2} \times 100\%$$

For good samples; $Ar \leq 12$ % for 50 mm diameter samples

≤ 15 % for 75 mm diameter samples

≤ 20 % for 100 mm diameter samples

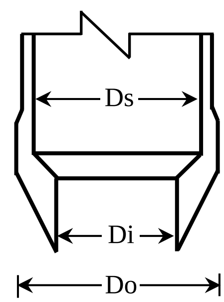

Fig. 2.6a

3. Friction (bearing capacity failure) [see Fig. (2.6b)].

$$inside\ clearence\ ratio = Cr = \frac{D_s - D_i}{D_i} \times 100\%$$

For good samples; $0.5 \leq Cr \leq 3$

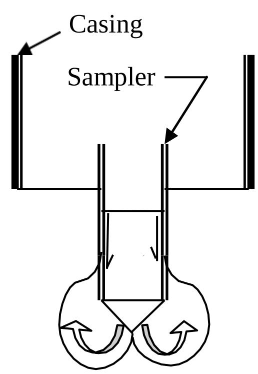

Fig. 2.6b

4. Soil shattering [see Fig. (2.6c)].
5. Water table.
6. Loss of hydrostatic pressure.
7. Environment.
8. Handling and transporting.

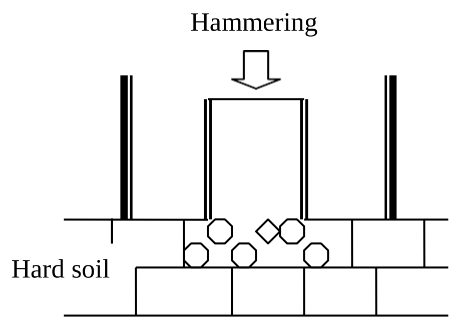

Fig. 2.6c

Another measure of disturbance is the recovery ratio;

$$Lr = \frac{actual\ length\ of\ recovered\ sample}{theoretical\ length\ of\ recovered\ sample}$$

For good samples; $Lr \approx 1$

2.6 <u>Soil Samplers</u>

The most common samplers used for in-situ testing and sampling are:

1. Split spoon sampler [Fig. (2.7a)]
2. Thin wall (Shelby) tube sampler [Fig. (2.7b)]
3. Stationary piston sampler [Fig. (2.8a)]
4. Swedish foil sampler [Fig. (2.8b)]
5. Osterberg piston sampler [Fig. (2.8c)]

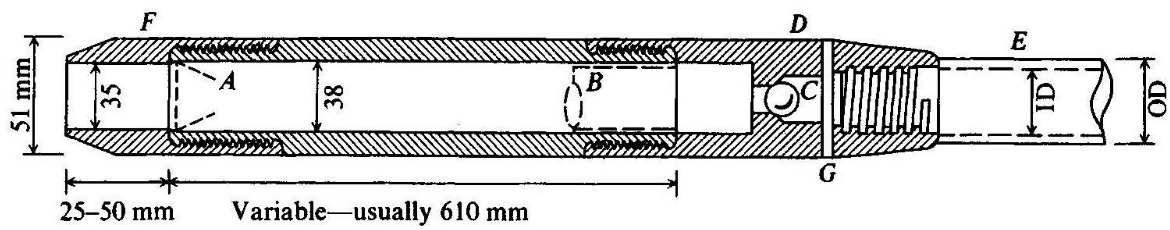

A—insert if used *B*—liner if used
C—ball check valve (provide suction on sample)
D—sampler-to-drill rod coupling
E—drill rod (A or AW)
F—drive shoe *G*—vent holes (used with *C*)

Drill rod sizes:
A: 41 OD × 29 ID mm 5.51 kg/m
AW: 44 OD × 32 ID mm 6.25 kg/m

(a) Standard split barrel sampler (also called a split spoon).
Specific sampler dimensions may vary by ± 0.1 to 1.0 mm.

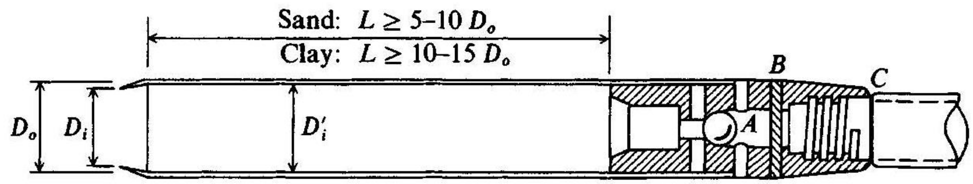

A—ball check valve to hold sample in tube on withdrawal
B—tube-to-drill rod coupling
C—drill rod

$$\text{Inside clearance ratio} = \frac{D_i' - D_i}{D_i}$$

Common D_o: 51, 64, 76, and 89 mm

(*b*) Thin wall tube sampler.

Fig. 2.7 Commonly used in situ testing and sample recovery equipment. For both split barrel and thin wall tube details, see (ASTM D 1586 and D 1587).

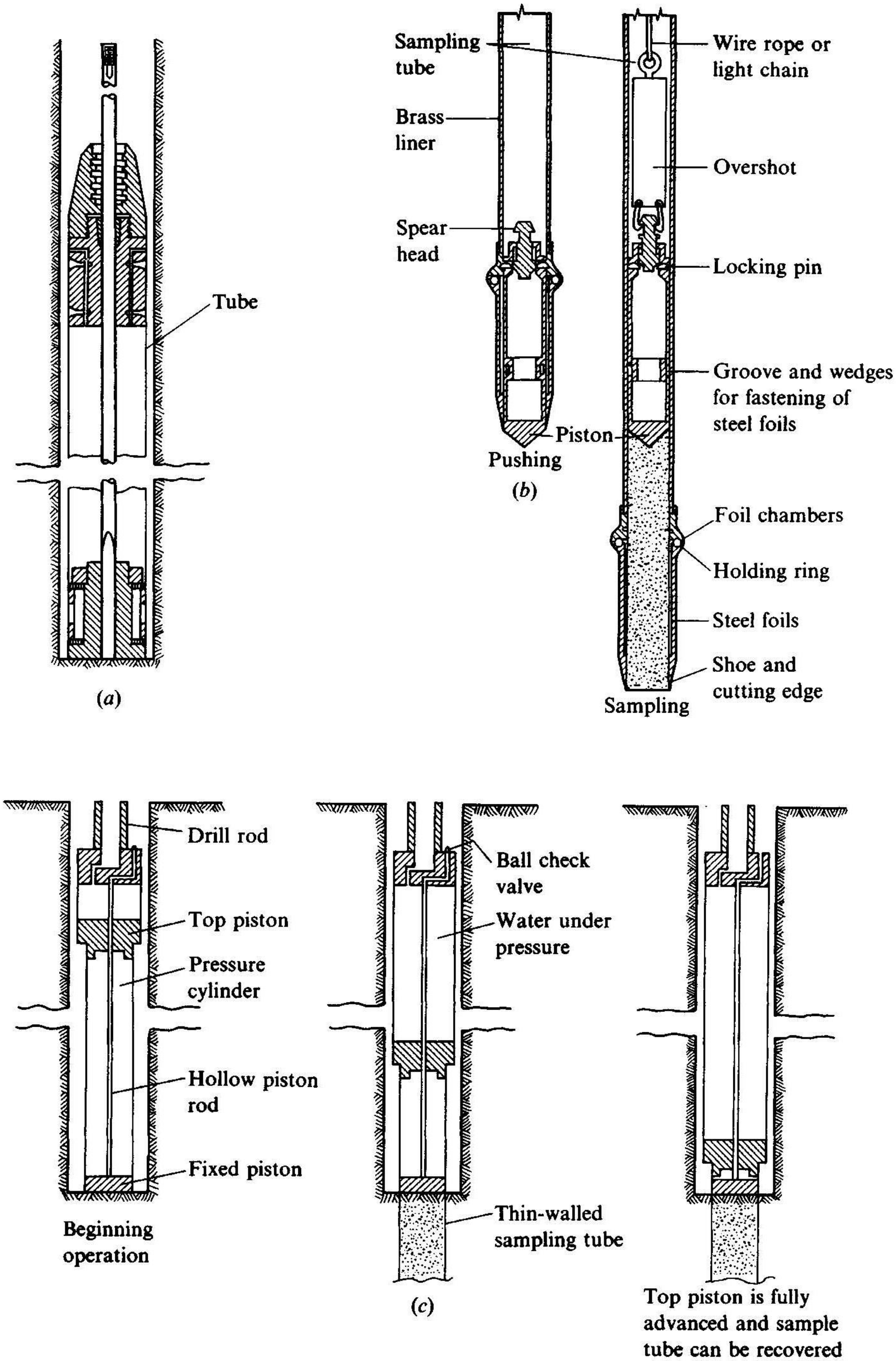

Fig. 2.8 Typical piston samplers, (*a*) Stationary piston sampler for recovery of "undisturbed" samples of cohesive soils. Piston remains stationary on soil and tube is pushed into the soil; piston is then clamped and sample is recovered; (*b*) Swedish foil sampler; (*c*) Osterberg piston sampler. [*Hvorslev* (1949)].

2.7 <u>Number of Borings</u>

The required number of boreholes which need to be sunk on any particular location is a difficult problem which is closely bound up with the relative costs of the investigation and the project for which it is undertaken. Obviously the more boreholes that are sunk the more is known of the soil conditions and greater economy can be achieved in foundation design, and the risks of meeting unforeseen and difficult soil conditions which would greatly increase the costs of the foundation work become progressively less. However, an economic limit is reached when the cost of borings outweighs any savings in foundation costs and merely adds to the overall cost of the project. Below are general guidelines on the number of borings versus type of project.

- For individual buildings of less than (300 m^2) plan area; (3) B.Hs. are the minimum [not to be on a straight line].
- For large sites or group of buildings; (5) B.Hs. are the minimum [(4) at corners and (1) at the middle].
- For large sites; probes are needed (penetration tests, geophysical investigations) to obtain information in areas between B.Hs. As a general rule the area enclosed among any (4) B.Hs. ≈ 10 % of the site area [Fig. (2.9)].

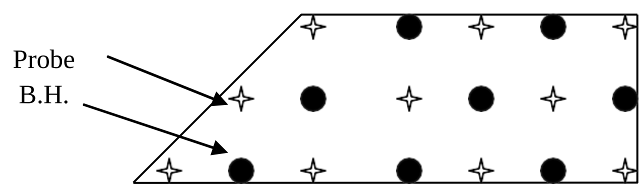

Fig. 2.9

- In case of limestone (from geological information), use a seismic method between B.Hs. to check any cavities.
- For some special structures;
  - A. Retaining walls; maximum spacing is (120 m) at centerline with some B.Hs. located on both sides of the centerline [Fig. (2.10a)].
  - B. Slope stability problems; (3-4) B.Hs. at critical zone and (1) B.H. outside this zone [Fig. (2.10b)].
  - C. Highways; (250-300) m spacing.
  - D. Earth dams; (25-50) m spacing.

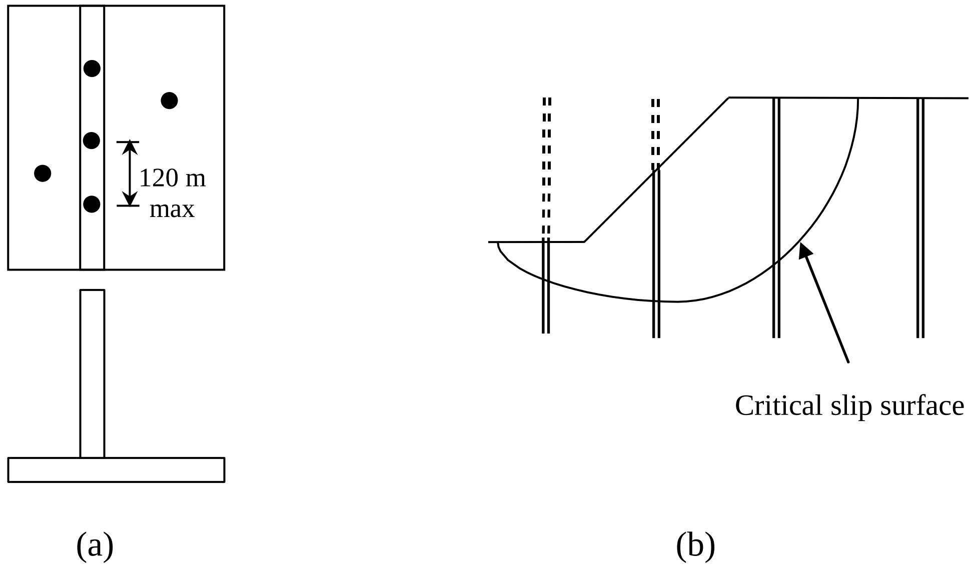

Fig. 2.10

Table (2.1) provides additional guidelines for the number of boreholes based on the phase of investigation.

Table 2.1

Phase of Investigations	**Geological Structure**	**Number and Spacing of Borings**	**Location of Borings in the Field**
Preliminary Investigation (to assess the suitability of the site)	Uniform	5-10 B.Hs. per km^2	Depending on topography of the site
	Irregular or Unknown	10-30 B.Hs. per km^2	
General Investigation (selection of areas of most favorable ground)	Uniform	300 m x 300 m	Regular square network of borings parallel to contour lines
	Irregular or Unknown	100 m x 100 m	
Detailed Investigation (for individual buildings where location has been fixed)	Uniform	At least 3 B.Hs. (30-50) m apart	As regular as possible network to suit individual buildings taking into consideration preliminary investigations
	Irregular or Unknown	3-5 B.Hs. for each building, (10-30) m apart	

2.8 Depth of Borings

Similar to the boring layout, the depth of subsurface exploration for a particular project must be based on judgment and experience. Borings should always be extended through unsuitable foundation bearing material, such as uncompacted fill, peat, soft clays and organic soil, and loose sands, and into dense soil or hard rock of adequate bearing capacity. In a general sense, the depth of subsurface exploration will depend on the size and loading of the proposed foundation, the sensitivity of the proposed structure to settlements, and the stiffness and coefficient of compressibility of the strata that will underlie the foundation. Below are some guidelines for different types of geotechnical and foundation projects.

- Highways and airfields; minimum depth is (3 m) but should extend below artificial fill or compressible layers.
- Retaining walls and slope stability problem:
  A. Below artificial fill or compressible layers.
  B. Deeper than possible surface of sliding.
  C. Deeper than wall base width.
  D. Equal to the width of bottom of cuts.
- Shallow foundations:

  Tomlinson (1986) suggested that for;
  A. Single narrow strip footings; depth ≈ (1 to 3) B > 6 m [Fig. (2.11a)].
  B. Group of overlapping stress zones footings or raft; depth ≈ 1.5 B [Figs. (2.11c and 2.11b)].

  The American Society of Civil Engineers, ASCE (1972) suggested that the minimum depth of boring is the smallest depth of the following (unless bedrock is encountered):
  A. The depth of B.Hs. should extend to the point where the net increase in stress due to the building load is less than (10 %) of the contact pressure [see Fig. (2.12)].
  B. The depth of B.Hs. should extend to the point at which the net increase in stress due to the building load is less than (5 %) of the effective overburden pressure [see Fig. (2.12)].

For hospitals and office buildings, Sowers and Sowers (1970) used the following rules:

A. For light steel or narrow concrete buildings; depth (m) = 3 $S^{0.7}$

B. For heavy steel or wide concrete buildings; depth (m) = 6 $S^{0.7}$; where S is the number of stories.

- If bedrock is countered, the minimum depth of core boring into the bedrock is about 3m.
- Deep Foundations: If piled foundation is expected, depth of boring should satisfy the following:

A. Depth of boring should extend to (3-5) times pile diameter (or width) or 3m into the bearing stratum.

B. Tomlinson suggested that the boring depth should extend below the pile-point of at least ($1.5\text{ B} - \frac{D}{3}$) as shown in Fig. (2.11 d).

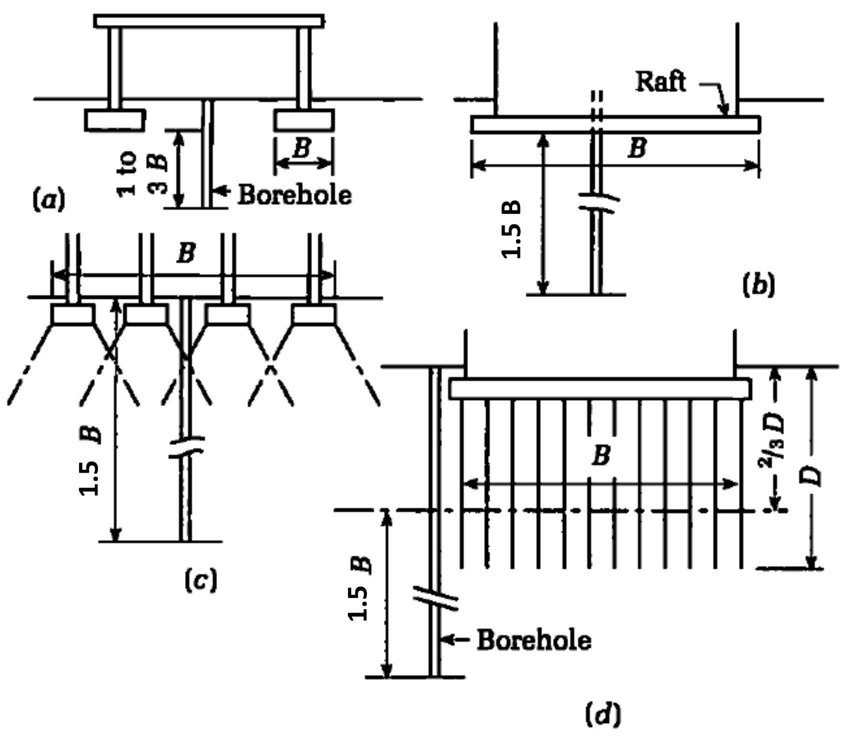

Fig. 2.11 Depths of boreholes for various foundation conditions

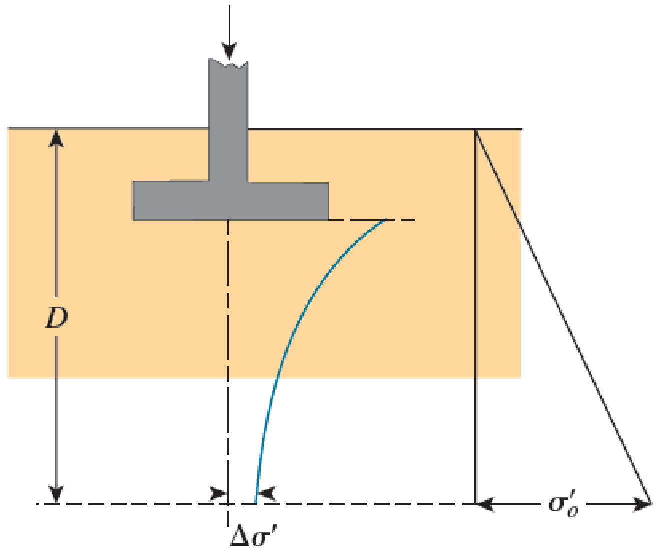

Fig. 2.12 Determination of the minimum depth of boring

2.9 In-Situ (Field) Tests

In-situ tests are used to identify soils at a site and to provide soil parameters for design. The results are available quickly, often during the tests or soon after, compared with laboratory tests. There are a variety of in-situ tests available. The most commonly used in-situ tests are:

- Standard penetration test (SPT)
- Cone penetration test (CPT)
- Vane shear test (VST)
- Plate load test (PLT)

2.9.1 Standard Penetration Test - ASTM-D1586

It is the most popular and economical method to obtain sub-surface information. The test consists of driving the standard split-barrel sampler [see Fig. (2.7a)] a distance of 460 mm (18″) into the soil at the bottom of the boring, using a 63.5 kg (140 lb) driving mass falling free from a height of 760 mm (30″), see Fig. (2.13). The number of blows required to drive the tube the last 305 mm (12″) should be counted to obtain the (*N*) value.

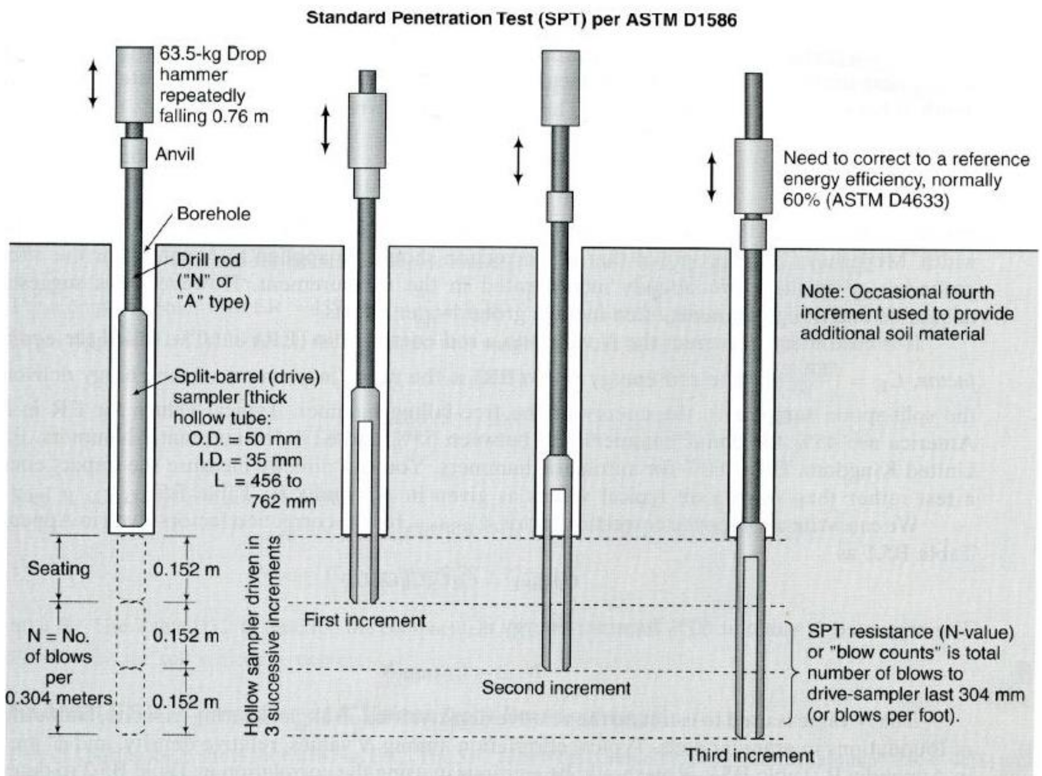

Fig. 2.13 Driving sequence in an SPT

Advantages of SPT

1. The test is too economical.
2. It produces a visual profile of a great percentage of boring depth.
3. The test results in recovery of samples.
4. Long service life of equipment in use.
5. The accumulation of a large SPT data-base which is continually expanding.

Corrections of *N*-values

Various corrections are applied to the *N*-values to account for hammer efficiency, borehole diameter, rod length, sampler type, overburden pressure and pore water pressure effect. Only two corrections for *N* values are considered in this class:

A. Fine saturated sands; in very fine, or silty saturated sand, Terzaghi and Peck recommended that (N) be corrected if (N > 15) as;

$$N' = 15 + \frac{1}{2}(N - 15)$$

where:

N = measured N-value

N' = corrected N-value

B. Overburden effect; Peck, Hanson and Thornburn (1974) proposed the following empirical correlation for converting the field standard penetration number to an effective overburden pressure of 95.76 kPa, see Fig. (2.14).

$$N' = C_N \cdot N = 0.77 \log \frac{2000}{\sigma'_o} N \qquad for\ \sigma'_o > 23.9\ kPa$$

where σ'_o is the effective overburden pressure.

Note: when the two corrections are justified, the pore water pressure correction must be done first.

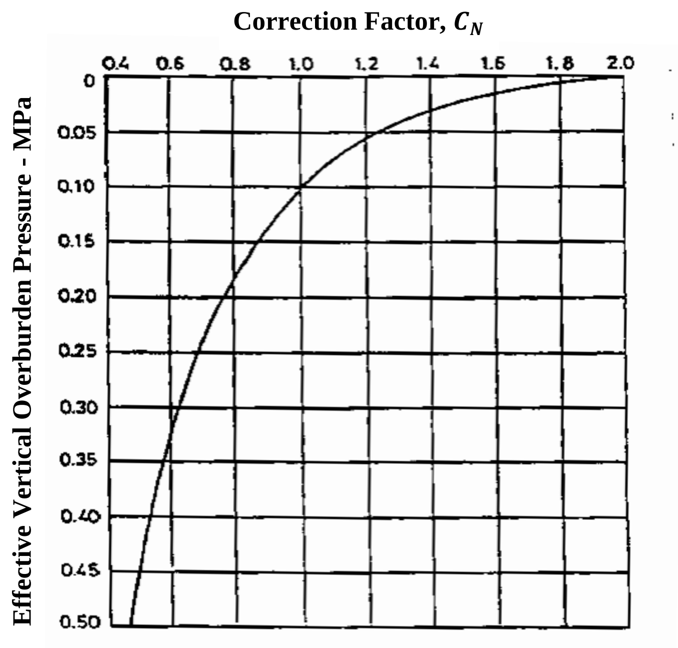

Fig. 2.14 Chart for correction of N-values for influence of overburden pressure (After Peck, Hanson and Thornburn, 1974)

<u>Correlation for SPT</u>

The standard penetration number is commonly used to correlate several parameters of soil. See tables (2.2 and 2.3) and Fig. (2.15).

Table 2.2 Empirical values for ϕ, D_r, and unit weight of granular soils based on the standard penetration number with corrections for depth and for fine saturated sands.

Description		Very loose		Loose		Medium		Dense		Very dense
Relative density D_r*	0		0.15		0.35		0.65		0.85	1.00
Standard penetration no. N			5–10		8–15		10–40		20–70	> 35
Approx. angle of internal friction ϕ°†	25–30°		27–32°		30–35°		35–40°		38–43°	
Approx. range of moist unit weight γ, pcf (kN/m³)		70–100‡ (11–16)		90–115 (14–18)		110–130 (17–20)		110–140 (17–22)		130–150 (20–23)

* Depends on p_o ranging from 70 to 500 kPa. Low value of N corresponds to lesser p_o.

† After Meyerhof (1956). $\phi = 25 + 25D_r$ with more than 5 percent fines and $\phi = 30 + 25D_r$ with less than 5 percent fines. Use larger values for granular material with 5 percent or less fine sand and silt. See also Eq. (4-10) for estimate of ϕ.

‡ It should be noted that excavated material or material dumped from a truck will weigh 70 to 90 pcf. Material must be quite dense and hard to weigh much over 130 pcf. Values of 105 to 115 pcf for nonsaturated soils are common.

Table 2.3 Empirical values for q_u* and consistency of cohesive soils based on the standard penetration number.

Consistency		Very soft		Soft		Medium		Stiff		Very stiff		Hard
q_u, ksf (kPa)	0		0.5 (25)		1.0 (50)		2.0 (100)		4.0 (200)		8.0 (400)	
N, standard penetration resistance	0		2		4		8		16		32	
γ_{sat}, pcf (kN/m³)		100–120 (16–19)				110–130 (17–20)				120–140 (19–22)		

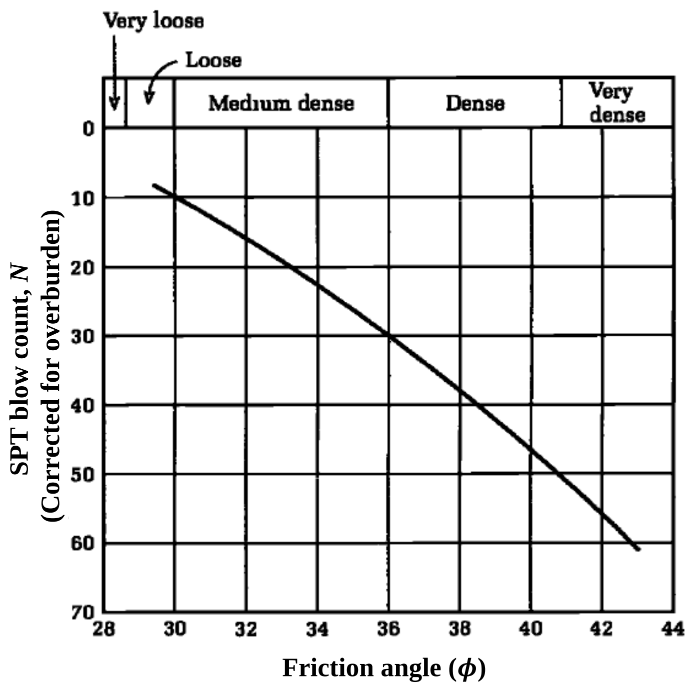

Fig. 2.15 SPT blow count (N) versus friction angle (ϕ)

2.9.2 Cone Penetration Test (CPT) - ASTM-D5778

The CPT is a simple test that is now widely used in lieu of the SPT particularly for fine sands, silty fine sands and clay deposits. In outline, the cone is pushed into the soil stratum of interest and the corresponding resistance is measured. The resistance may be of the cone alone, or a cone resistance and the side or skin resistance of a sleeve. The cone is forced into the ground at a rate varying from (10 to 20 mm/s). The cone resistance is related to the undrained shear strength, since the test is so rapid [see Fig. (2.16)]. The data obtained are used to estimate bearing capacity and settlement for footings or static pile capacity.

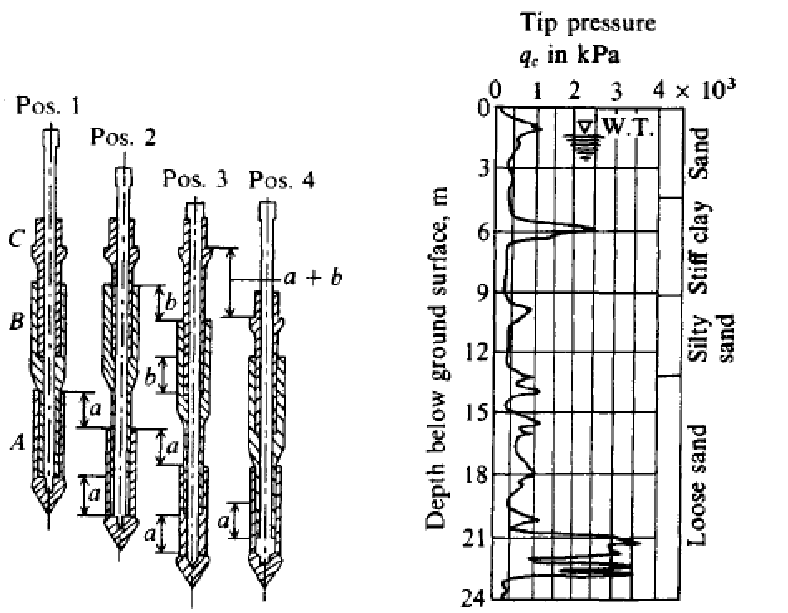

(a) Positions of the Dutch cone during a pressure record.

(b) Typical output (usually electronically made).

Fig. 2.16 Mechanical (or Dutch) cone, operations sequence, and tip resistance data

Advantages of CPT

1. Quick and economical.
2. Gives a continuous resistance of strata.
3. Gives skin friction of soil.
4. Reliable for sand below water table.
5. No boring is required.

Limitations of CPT

1. Not suitable for gravel deposits or stiff/hard cohesive deposits.
2. Does not reveal types of soils encountered.
3. No samples are taken.
4. Test depth (15-25) m.

Correlations for CPT: see Table (2.4).

Table 2.4 Approximate relationships between cone point resistance q_c (kPa) and SPT value of N and static stress-strain modulus E_s (kPa)

Soil type	q_c/N*	E_s, kPa
Silts, fine sands, slightly cohesive soils	150–300	$1.5–2q_c$
Fine to medium sands, slightly silty fine to medium sands	300–450	$2–4q_c$
Coarse sands	450–700	$1.5–3q_c$
Sandy gravel, gravelly sands	700–2000†	
Stiff clay, sandy clay		$5–7q_c$

* After Trofimenkov (1974) and others and usually converted by author to kPa from kg/cm^2 or other units. Values should be verified on a local basis rather than making arbitrary use of, say, the midvalue.

† May give much too large N in gravel; so 1500 to 2000 may be best estimate.

2.9.3 Vane Shear Test (VST) - ASTM D 2573M

The VST is substantially used method to estimate the in-situ undrained shear strength of very soft, sensitive, fine-grained soil deposits. It consists of inserting a four blades vane [Fig. (2.17)] into the soil at the required depth and measuring the required torque (T) for rotating the vane (i.e. shearing the soil), see Fig. (2.18). The measured torque is converted to undrained shear strength using;

$$s_u = \frac{2T}{\pi d^3 \left(\frac{h}{d} + \frac{1}{3}\right)}$$

where;

s_u: undrained shear strength

T : maximum torque

h : height of the vane

d : diameter of the vane

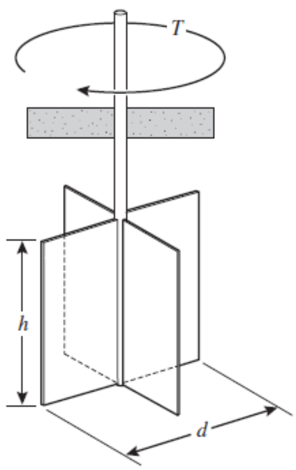

Fig. 2.17 Vane tester

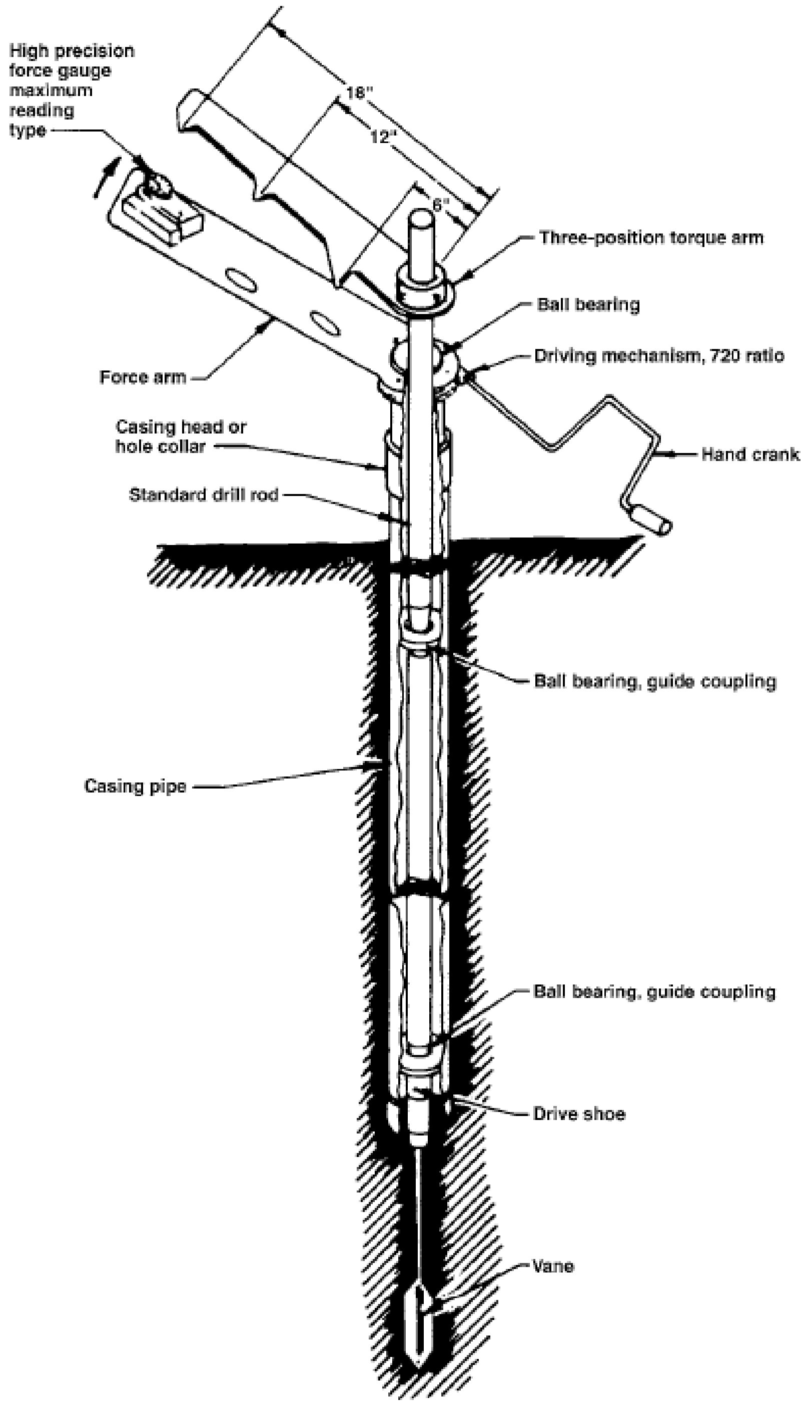

Fig. 2.18 Diagram illustrating the field vane test.
(*From NAVFAC DM-7.1, 1982*.)

2.9.4 Plate Loading Test (PLT) - ASTM-D1194

Plate load tests [Fig. (2.19)] are used to estimate bearing capacity and settlement of shallow footings. It involves loading a horizontal plate, while monitoring the settlement. The test is usually carried out, in a test pit, by applying a series of loads in increments of (1/5) the working load to be applied by the foundation, up to at least twice the working stress. The deformation is monitored under constant load until the settlement rate drops to less than (0.25 mm/hr). Plate load test is used in the following situations;

1. On soft jointed and fractured rocks.
2. On granular or cohesive soils containing boulders.
3. Where a structure is particularly sensitive to settlement.

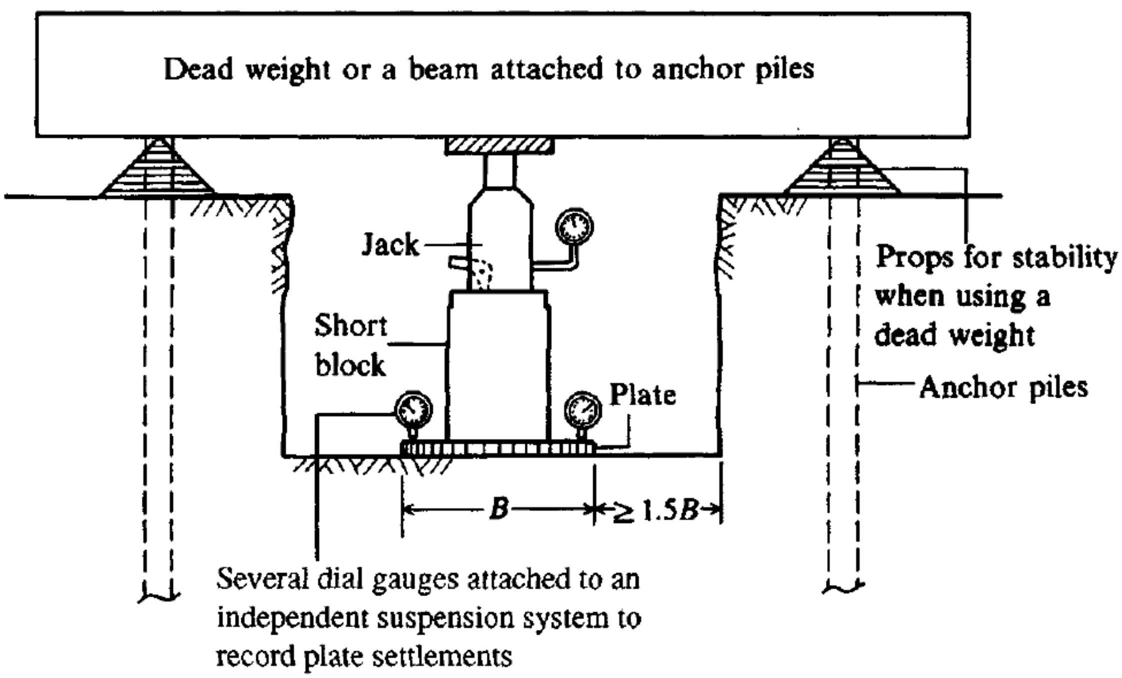

Fig. 2.19 Plate-load testing. The method of performing this test is outlined in some detail in ASTM D 1194.

In conducting the plate loading test, the following factors must be considered:

1. Size of plate; the diameter (or width) of the plate should be at least (6) times the size of the largest soil particle, or in rock should be more than (6) times the spacing between horizontal fractures. The minimum plate size is (300 mm). Also, the stress zone is influenced by the plate size [see Fig. (2.20)].

2. Number of tests; soils are highly variable. To obtain the variation of soil properties, series of tests should be carried out at different locations and depths.

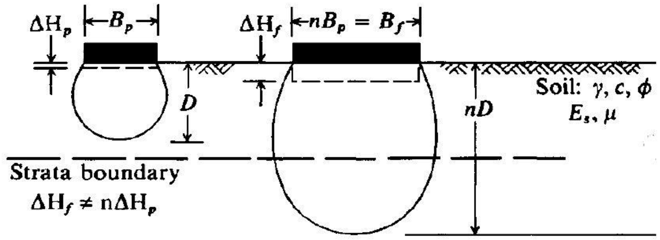

Fig. 2.20

2.10 Soil Exploration Report

At the end of the soil exploration program, a soil exploration report is prepared for the use of the planning and design office. Any soil exploration report should contain the following information:

1. Scope of investigation.
2. General description of the proposed structure for which the exploration has been conducted.
3. General description of the site.
4. Details of boring.
5. Description of sub-soil conditions as determined from the soil samples collected.
6. Ground water table as observed from the B.Hs.
7. Details of foundation recommendations and alternatives.
8. Any anticipated construction problems.
9. Limitations of the investigation.

The following graphic representations also need to be attached to the soil exploration report:

1. Site location map.
2. Location of borings with respect to the proposed structure.
3. Boring logs, [see Fig. (2.21)].
4. Laboratory test results.
5. Other special presentations.

Boring Log

Name of the Project: Two-story apartment building

Location: Johnson & Olive St. Date of Boring: March 2, 2015

Boring No.: 3 Type of Boring: Hollow-stem auger Ground Elevation: 60.8 m

Soil description	Depth (m)	Soil sample type and number	N_{60}	w_n (%)	Comments
Light brown clay (fill)					
Silty sand (SM)	1				
	2	SS-1	9	8.2	
°G.W.T. 3.5 m	3	SS-2	12	17.6	LL = 38 PI = 11
	4				
Light gray clayey silt (ML)	5	ST-1		20.4	LL = 36 q_u = 112 kN/m^2
	6	SS-3	11	20.6	
Sand with some gravel (SP)	7				
End of boring @ 8 m	8	SS-4	27	9	

N_{60} = standard penetration number
w_n = natural moisture content
LL = liquid limit; PI = plasticity index
q_u = unconfined compression strength
SS = split-spoon sample; ST = Shelby tube sample

°Groundwater table observed after one week of drilling

Fig. 2.21 A typical boring log

CHAPTER 3

BEARING CAPACITY OF SHALLOW FOUNDATIONS

3.1 Introduction

Foundations are structural members which are designed to transfer building loads safely to the underlying ground. They must satisfy the following two design criteria:

1. **Bearing capacity:** The foundation must be stable against shear failure of the supporting soil.
2. **Settlement:** The foundation must not settle beyond a tolerable limit to avoid damage to the structure.

3.2 Bearing Capacity

Bearing capacity refers to the ability of a soil to support or hold up a foundation and structure. The *ultimate bearing capacity* of a soil refers to the loading per unit area that will just cause shear failure in the soil. It is given the symbol q_{ult}. The *allowable bearing capacity* (symbol q_a) refers to the loading per unit area that the soil is able to support without unsafe movement. It is the "design" bearing capacity. The allowable load is equal to allowable bearing capacity multiplied by area of contact between foundation and soil. The allowable bearing capacity is equal to the ultimate bearing capacity divided by the factor of safety. A factor of safety of 2 to 3 is commonly applied to the value of q_{ult}.

3.3 Modes of Soil Failure

Three distinct modes of soil failure have been identified as shown in Fig. (3.1):

1. **General shear failure:**
   - Associated with dense soils of relatively low compressibility.
   - The slip surface is continuous from the edge of the footing to the soil surface.
   - Full shear resistance of the soil is developed along the failure surface.
   - Sudden and may be accompanied by tilting.
   - Bulging of the soil near the footing is usually apparent.

2. **Local shear failure:**
   - Associated with medium soils.
   - The failure surface extends from the edge of the footing to approximately the boundary of the Rankine passive zone.
   - The shear resistance is fully developed over only part of the failure surface.
   - There is a certain degree of bulging on the sides and considerable vertical compression under the footing. This is not usually apparent until significant vertical penetration occurs.

3. **Punching shear failure:**
   - A condition common for loose and very compressible soils.
   - The pattern is not easily detected.
   - Generally, some vertical shear deformation is visible around the periphery of the footing.
   - No apparent bulging of the soil around the footing.

General shear failure does not exist when the relative density for sandy soils (Dr < 30 %) and when the sensitivity for clayey soils (S_t > 10).

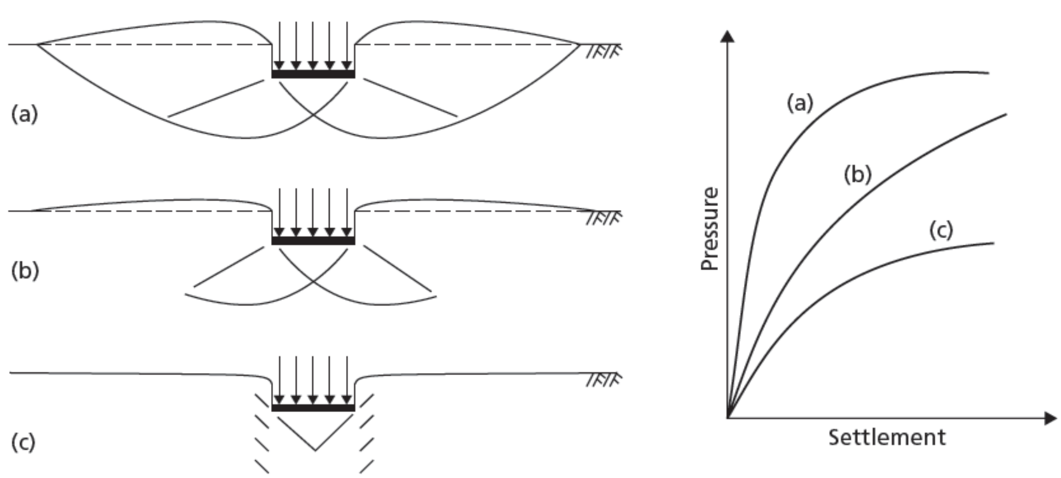

Fig. 3.1 Modes of failure: (a) general shear, (b) local shear, and (c) punching shear.

3.4 Terzaghi's Bearing Capacity Equation

Terzaghi (1943) was the first to present a comprehensive theory for the evaluation of the ultimate bearing capacity of rough shallow foundations. According to this theory, the following assumptions were adopted;

1. $D_f \leq B$
2. Soil is plastic.
3. Rough surface of footing.
4. Neglected shear resistance along cd [Fig. (3.2a)].
5. Replaced the soil above foundation level with surcharge ($\bar{q}$) placed at foundation level.
6. $\beta = \phi$
7. ad is log-spiral

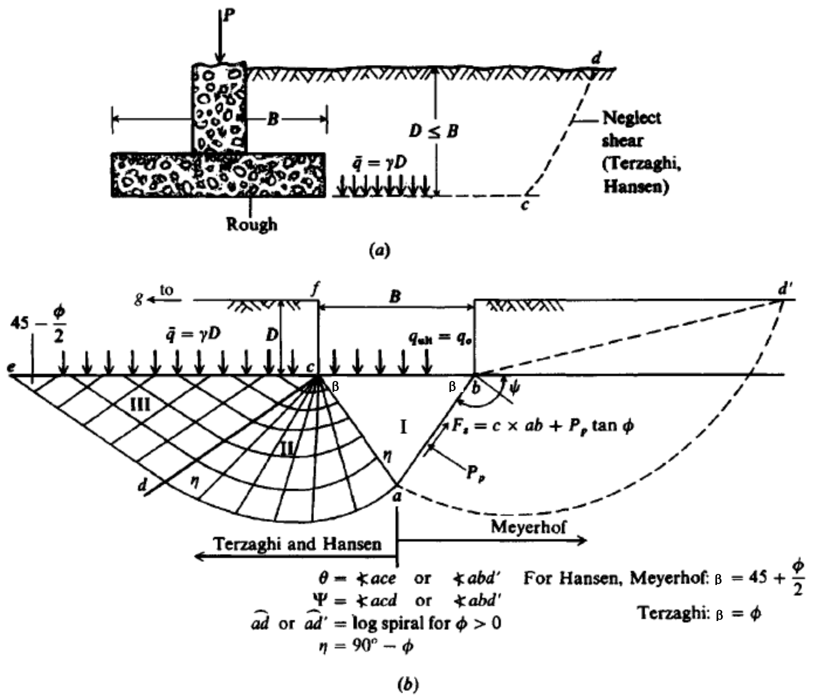

Fig. 3.2 (*a*) Shallow foundation with rough base defined. Terzaghi and Hansen equations of Table 4-1 neglect shear along *cd*; (*b*) general footing-soil interaction for bearing-capacity equations for strip footing—left side for Terzaghi (1943), Hansen (1970), and right side Meyerhof (1951).

By applying static equilibrium for the above mechanism, the following equations can be developed (Table 3.1):

For a continuous footing, $q_{ult} = c \cdot N_c + \bar{q} \cdot N_q + 0.5\gamma \cdot B \cdot N_\gamma$

For a square footing, $q_{ult} = 1.3\, c \cdot N_c + \bar{q} \cdot N_q + 0.4\, \gamma \cdot B \cdot N_\gamma$

For a circular footing, $q_{ult} = 1.3\, c \cdot N_c + \bar{q} \cdot N_q + 0.3\, \gamma \cdot B \cdot N_\gamma$

For a rectangular footing, $q_{ult} = \left(1 + 0.3\frac{B}{L}\right) c \cdot N_c + \bar{q} \cdot N_q + 0.5\left(1 - 0.2\frac{B}{L}\right) \gamma \cdot B \cdot N_\gamma$

where

q_{ult} : ultimate gross bearing capacity

c : soil cohesion below foundation level

ϕ : angle of internal friction below foundation level

$\bar{q}$: effective overburden pressure at foundation level

D_f : depth of footing below lowest adjacent soil surface

γ : unit weight of soil below foundation level

B : width or diameter of footing

L : length of footing

N_c, N_q, N_γ: bearing capacity factors = $f(\phi)$ [see Tables (3.1 and 3.2) and Figs. (3.3) and (3.4)]

In case of the local shear failure, use reduced shear strength parameters [i.e. (2/3)c and (2/3) tan ϕ] for Terzaghi's bearing capacity equation.

Table 3.1 **Bearing-capacity equations by the several authors indicated**

Terzaghi (1943). See Table 3.2 for typical values and for $K_{p\gamma}$ values.

$$q_{ult} = cN_c s_c + \bar{q}N_q + 0.5\gamma B N_\gamma s_\gamma \qquad N_q = \frac{a^2}{2\cos^2(45+\phi/2)}$$

$$a = e^{(0.75\pi - \phi/2)\tan\phi}$$

$$N_c = (N_q - 1)\cot\phi$$

$$N_\gamma = \frac{\tan\phi}{2}\left(\frac{K_{p\gamma}}{\cos^2\phi} - 1\right)$$

For:	strip	round	square	rectangule
s_c =	1.0	1.3	1.3	1+0.3B/L
s_γ =	1.0	0.6	0.8	1-0.2B/L

Meyerhof (1963).* See Table 3.3 for shape, depth, and inclination factors.

Vertical load: $q_{ult} = cN_c s_c d_c + \bar{q}N_q s_q d_q + 0.5\gamma B' N_\gamma s_\gamma d_\gamma$

Inclined load: $q_{ult} = cN_c d_c i_c + \bar{q}N_q d_q i_q + 0.5\gamma B' N_\gamma d_\gamma i_\gamma$

$$N_q = e^{\pi\tan\phi}\tan^2\left(45 + \frac{\phi}{2}\right)$$

$$N_c = (N_q - 1)\cot\phi$$

$$N_\gamma = (N_q - 1)\tan(1.4\phi)$$

Hansen (1970).* See Table 3.5 for shape, depth, and other factors.

General:† $q_{ult} = cN_c s_c d_c i_c g_c b_c + \bar{q}N_q s_q d_q i_q g_q b_q + 0.5\gamma B' N_\gamma s_\gamma d_\gamma i_\gamma g_\gamma b_\gamma$

when $\phi = 0$

use $q_{ult} = 5.14 s_u(1 + s'_c + d'_c - i'_c - b'_c - g'_c) + \bar{q}$

$$N_q = \text{same as Meyerhof above}$$

$$N_c = \text{same as Meyerhof above}$$

$$N_\gamma = 1.5(N_q - 1)\tan\phi$$

*These methods require a trial process to obtain design base dimensions since width B and length L are needed to compute shape, depth, and influence factors.

Table 3.2 Bearing-capacity factors for the Terzaghi equations

Values of N_γ for ϕ of 0, 34, and 48° are original Terzaghi values and used to back-compute $K_{p\gamma}$

ϕ, deg	N_c	N_q	N_γ	$K_{p\gamma}$
0	5.7*	1.0	0.0	10.8
5	7.3	1.6	0.5	12.2
10	9.6	2.7	1.2	14.7
15	12.9	4.4	2.5	18.6
20	17.7	7.4	5.0	25.0
25	25.1	12.7	9.7	35.0
30	37.2	22.5	19.7	52.0
34	52.6	36.5	36.0	
35	57.8	41.4	42.4	82.0
40	95.7	81.3	100.4	141.0
45	172.3	173.3	297.5	298.0
48	258.3	287.9	780.1	
50	347.5	415.1	1153.2	800.0

3.5 Factor of Safety

Referring to Fig. (3.5), let;

$(q_{ult})_{gross} = q_{ult} =$ The total intensity of pressure applied at the level of foundation base will cause failure of soil.

$$(q_{ult})_{net} = q_{ult} - \bar{q}$$

where; $\bar{q} = \gamma D_f$

γ is the effective unit weight of the soil above the footing base. Then we define:

$$(q_a)_{gross} = q_a = \frac{q_{ult}}{F}$$

$$(q_a)_{net} = \frac{(q_{ult})_{net}}{F} = \frac{q_{ult} - \bar{q}}{F}$$

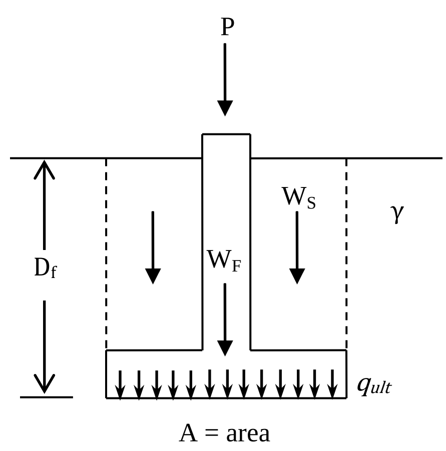

Fig. 3.5

where F is the factor of safety which is usually taken between 2 and 3.

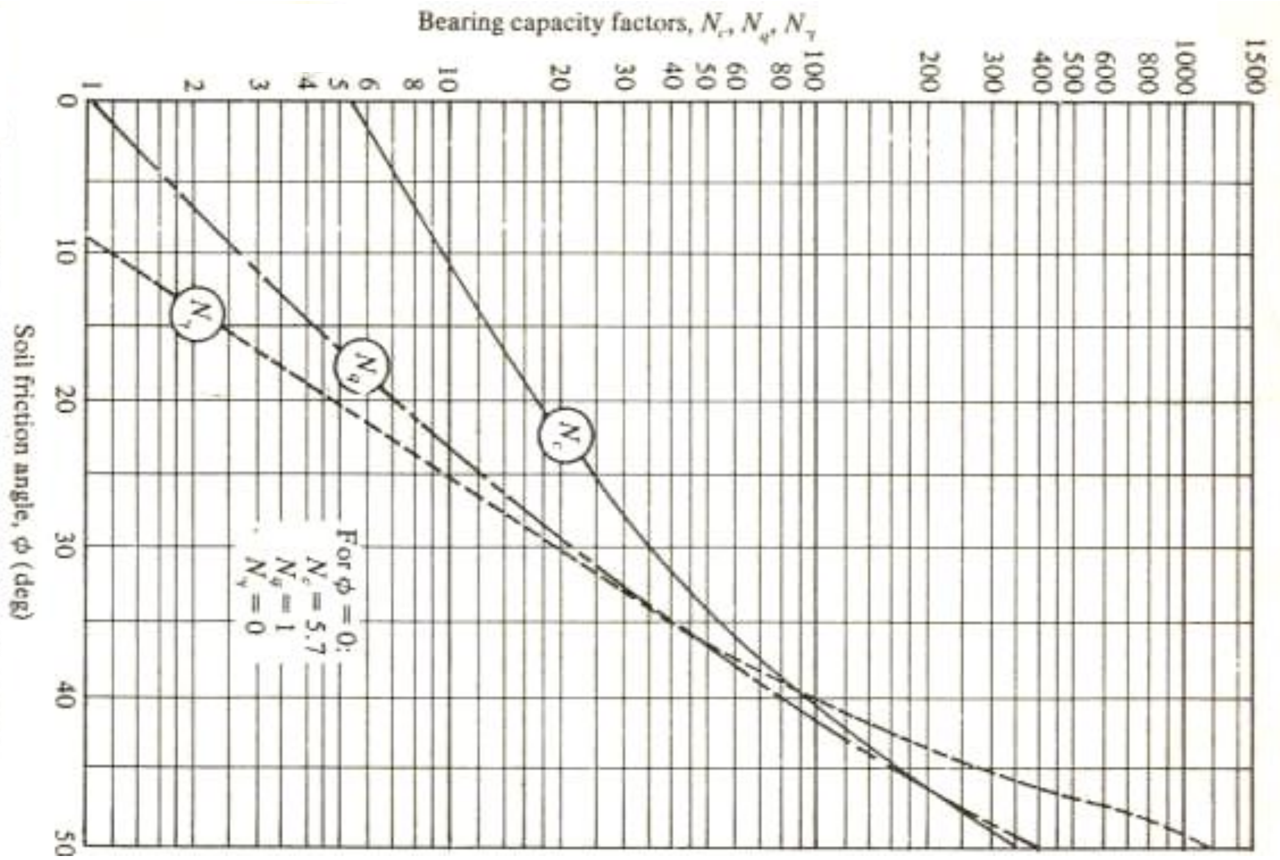

Fig. 3.3 Terzaghi's bearing capacity factors for general shear failure

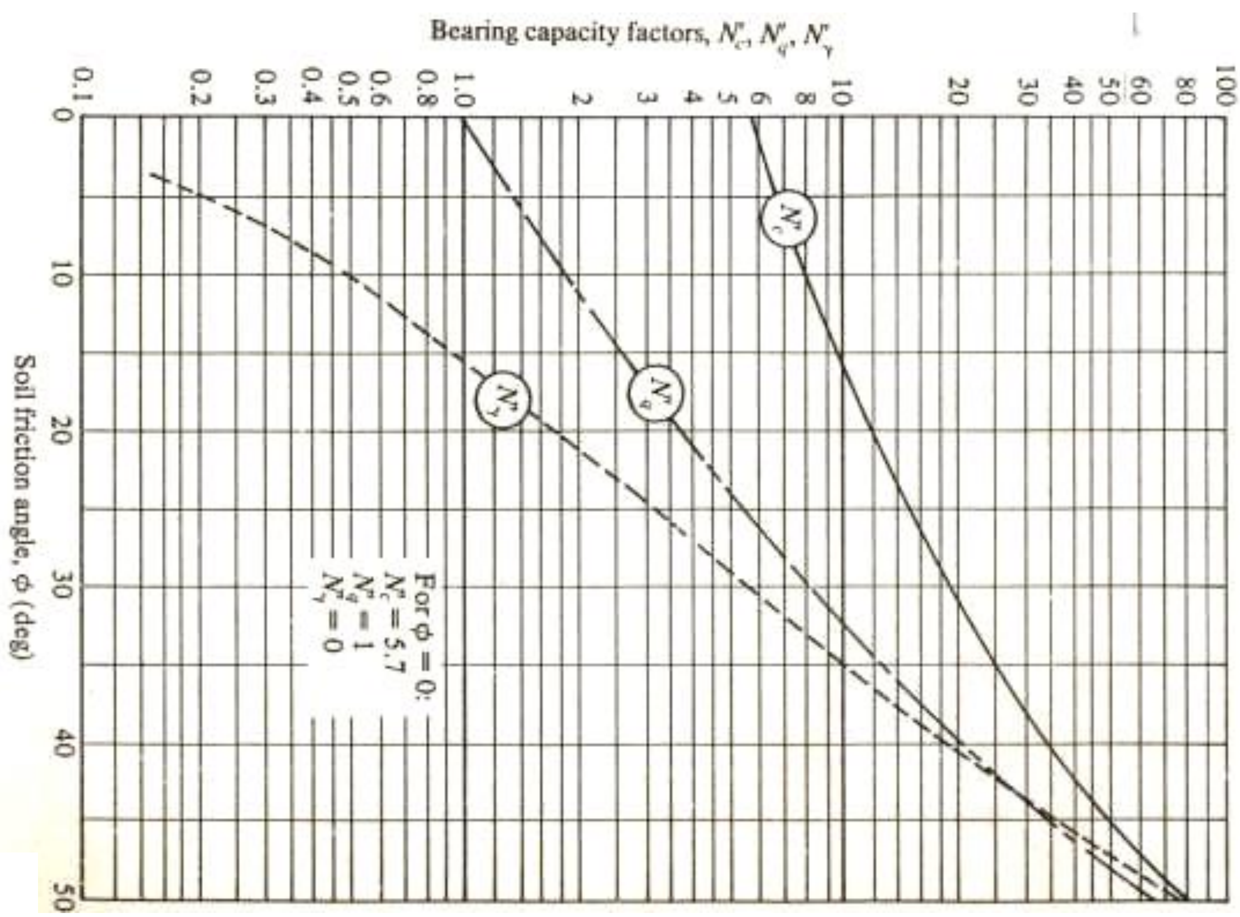

Fig. 3.4 Terzaghi's bearing capacity factors for local shear failure

3.6 Effect of Water Table on B.C.

The bearing capacity equation developed in section (3.4) based on the assumption that the water table is located well below the foundation (d_w > B). However, if the water table is close to the foundation, it reduces the unit weight of soil, so some modifications of the bearing capacity equations will be necessary. Referring to Fig. (3.6), let;

γ_t = wet (or total) unit weight (above W.T.)

γ_{sat} = saturated unit weight (below W.T.)

γ' = effective unit weight;

$\gamma' = \gamma_{sat} - \gamma_w$

$$q_{ult} = c \cdot N_c \,.\, s_c + \bar{q} \cdot N_q + 0.5\,.\gamma \cdot B \cdot N_\gamma . s_\gamma$$

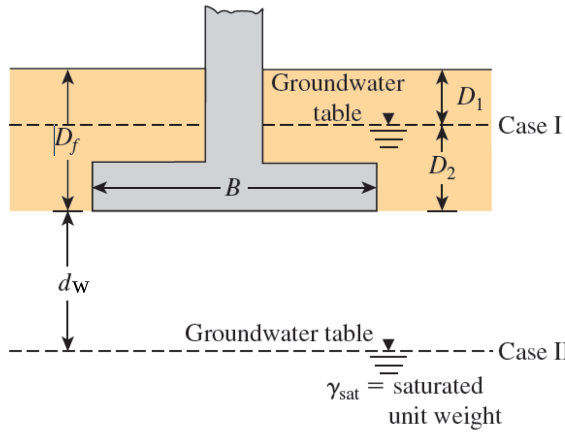

Fig. 3.6 Modification of bearing capacity equations for water table

The presence of W.T. close to the foundation will affect $\bar{q}$ (in the second term) and γ (in the third term). Three cases can be recognized:

Case	Depth of the W.T.	$\bar{q}$ in the second term	γ in the third term
I	$0 \le D_1 \le D_f$	$\bar{q} = D_1 \cdot \gamma_t + D_2 \cdot \gamma'$	$\gamma = \gamma'$
II	$0 \le d_w \le B$	$\bar{q} = D_f \cdot \gamma_t$	$\gamma = \bar{\gamma}$ $\bar{\gamma} = \gamma' + \frac{d_w}{B}(\gamma_t - \gamma')$
III	$d_w \ge B$	The W.T. has no effect on bearing capacity	

3.7 Meyerhof's Bearing Capacity Equation

1. Considered shear resistance along cd [Fig. (3.2a)].
2. $\beta = 45° + \frac{\phi}{2}$
3. Adjusted the angle of internal friction when (ϕ_{tr} > 34°) as follows:

   a. for $L/B \leq 2$, use $\phi_{ps} = \phi_{tri}$

   b. for $L/B > 2$, use $\phi_{ps} = 1.5\,\phi_{tri} - 17$

   where, ϕ_{ps} : plane strain value of ϕ and ϕ_{tri}: ϕ from triaxial test.
4. Used shape, depth and load inclination factors.

Basic equations:

For vertical load; $q_{ult} = c \cdot N_c \cdot s_c \cdot d_c + \bar{q} \cdot N_q \cdot s_q \cdot d_q + 0.5\gamma \cdot B \cdot N_\gamma \cdot s_\gamma \cdot d_\gamma$

For inclined load; $q_{ult} = c \cdot N_c \cdot i_c \cdot d_c + \bar{q} \cdot N_q \cdot i_q \cdot d_q + 0.5\gamma \cdot B \cdot N_\gamma \cdot i_\gamma \cdot d_\gamma$

where N_c, N_q, N_γ: Meyerhof's bearing capacity factors, [see tables (3.1 and 3.4)].

s_c , s_q , s_γ : shape factors
d_c , d_q , d_γ : depth factors
i_c , i_q , i_γ : load inclination factors

(see Table 3.3)

Table 3.3 Shape, depth, and inclination factors for the Meyerhof bearing-capacity equations of Table 3.1

Factors	Value	For
Shape:	$s_c = 1 + 0.2K_p\frac{B}{L}$	Any ϕ
	$s_q = s_\gamma = 1 + 0.1K_p\frac{B}{L}$	$\phi > 10°$
	$s_q = s_\gamma = 1$	$\phi = 0$
Depth:	$d_c = 1 + 0.2\sqrt{K_p}\frac{D}{B}$	Any ϕ
	$d_q = d_\gamma = 1 + 0.1\sqrt{K_p}\frac{D}{B}$	$\phi > 10$
	$d_q = d_\gamma = 1$	$\phi = 0$
Inclination:	$i_c = i_q = \left(1 - \frac{\theta°}{90°}\right)^2$	Any ϕ
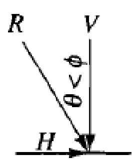	$i_\gamma = \left(1 - \frac{\theta°}{\phi°}\right)^2$	$\phi > 0$
	$i_\gamma = 0$ for $\theta > 0$	$\phi = 0$

where $K_p = \tan^2(45 + \phi/2)$
θ = angle of resultant R measured from vertical without a sign: if θ = 0, all i_i = 1.0.

Table 3.4 Bearing-capacity factors for the Meyerhof and Hansen bearing-capacity equations

ϕ	N_c	N_q	$N_{\gamma(H)}$	$N_{\gamma(M)}$	N_q/N_c	$2\tan\phi(1-\sin\phi)^2$
0	5.14*	1.0	0.0	0.0	0.195	0.000
5	6.49	1.6	0.1	0.1	0.242	0.146
10	8.34	2.5	0.4	0.4	0.296	0.241
15	10.97	3.9	1.2	1.1	0.359	0.294
20	14.83	6.4	2.9	2.9	0.431	0.315
25	20.71	10.7	6.8	6.8	0.514	0.311
26	22.25	11.8	7.9	8.0	0.533	0.308
28	25.79	14.7	10.9	11.2	0.570	0.299
30	30.13	18.4	15.1	15.7	0.610	0.289
32	35.47	23.2	20.8	22.0	0.653	0.276
34	42.14	29.4	28.7	31.1	0.698	0.262
36	50.55	37.7	40.0	44.4	0.746	0.247
38	61.31	48.9	56.1	64.0	0.797	0.231
40	75.25	64.1	79.4	93.6	0.852	0.214
45	133.73	134.7	200.5	262.3	1.007	0.172
50	266.50	318.5	567.4	871.7	1.195	0.131

Note that N_c and N_q are same for both methods.

3.8 <u>General (Hansen's) Bearing Capacity Equation</u>

$$q_{ult} = c \cdot N_c \cdot s_c \cdot d_c \cdot i_c \cdot g_c \cdot b_c + \bar{q} \cdot N_q \cdot s_q \cdot d_q \cdot i_q \cdot g_q \cdot b_q + 0.5\gamma \cdot B \cdot N_\gamma \cdot s_\gamma \cdot d_\gamma \cdot i_\gamma \cdot g_\gamma \cdot b_\gamma$$

For $\phi = 0$; $q_{ult} = 5.14 s_u (1 + s_c' + d_c' - i_c' - g_c' - b_c') + \bar{q}$

where N_c, N_q, N_γ: Hansen's bearing capacity factors, [see tables (3.1 and 3.4)].

$$\left.\begin{array}{l} s_c, s_q, s_\gamma : \text{shape factors} \\ d_c, d_q, d_\gamma : \text{depth factors} \\ i_c, i_q, i_\gamma : \text{load inclination factors} \\ g_c, g_q, g_\gamma : \text{ground inclination factors} \\ b_c, b_q, b_\gamma : \text{base inclination factors} \end{array}\right\} \text{(see Table 3.5)}$$

s_u : undrained shear strength

<u>Notes</u>:

- Do not use shape factors in combination with load inclination factors.
- The $B.N_\gamma$ term does not cause an increase in bearing capacity without bound. A suggested reduction factor is;

$$r_\gamma = 1 - 0.25 log\frac{B}{2} \qquad for\ B > 2m$$

This factor can be used with any bearing capacity equation by multiplying it by the third term.

3.9 Skempton's Method [$\phi = 0$]

$$q_{ult} = c \cdot N_c + \bar{q}$$

where N_c is obtained from Fig. (3.7).

For rectangular, N_c can be obtained using the following equation;

$$Nc_{,rec} = N_{c,sq} \cdot \left(0.84 + 0.16\frac{B}{L}\right)$$

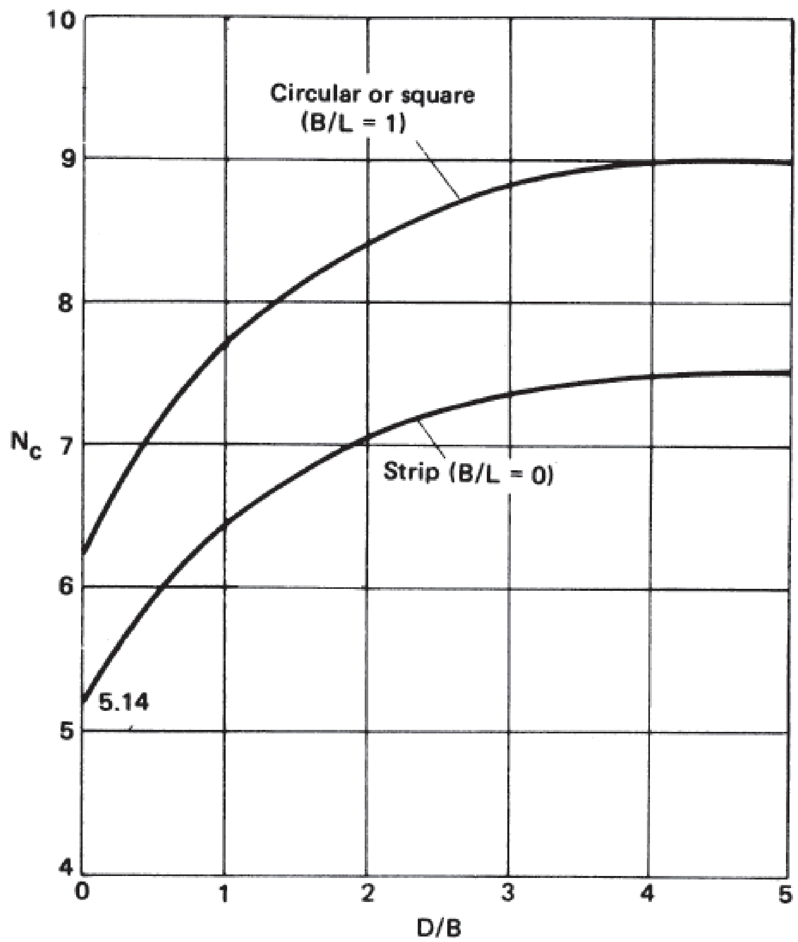

Fig. 3.7 Skempton's Values of N_c for $\phi_u = 0$

Table 3.5 **Shape, depth, inclination, and other factors for use in the Hansen bearing capacity equation in Table** 3.1

Table combined from Hansen (1970), De Beer (1970), and Vesic (1973). Primed factors for undrained (U) conditions and $\phi = 0$

Shape factors	Depth factors		Inclination factors	Ground factors (see figure)
$s'_c = 0.2B/L$	$d'_c = 0.4D/B$	$D \le B$	$i'_c = 0.5 - 0.5\sqrt{1 - H/A_f c_a}$	$g'_c = \psi°/147°$
$s_c = 1 + N_q B/N_c L$	$d'_c = 0.4 \tan^{-1} \dfrac{D}{B}$	$D > B$	$i_c = i_q - (1 - i_q)/(N_q - 1)$	for horizontal ground use $g'_c = 0.0$
	$d_c = 1 + 0.4 \dfrac{D}{B}$	$D \le B$		$g_c = 1 - \psi°/147°$ $g_q = g_\gamma = (1 - 0.5 \tan \psi°)^5$
	$d_c = 1 + 0.4 \tan^{-1} \dfrac{D}{B}$	$D > B$		Base factors (see figure)
$s_q = 1 + (B/L) \tan \phi$	$d_q = 1 + 2 \tan \phi (1 - \sin \phi)^2 \dfrac{D}{B}$	$D \le B$	$i_q = \left(1 - \dfrac{0.5H}{V + A_f c_a \cot \phi}\right)^5$	$b'_c = \eta°/147°$
	$d_q = 1 + 2 \tan \phi (1 - \sin \phi)^2 \tan^{-1} \dfrac{D}{B}$	$D > B$		for horizontal ground use $b'_c = 0.0$ $b_c = 1 - \eta°/147°$
$s_\gamma = 1 - 0.4B/L$	$d_\gamma = 1.00$ for all ϕ		Horizontal ground: $i_\gamma = \left(1 - \dfrac{0.7H}{V + A_f c_a \cot \phi}\right)^5$ Sloping ground: $i_\gamma = \left(1 - \dfrac{(0.7 - \eta°/450°)H}{V + A_f c_a \cot \phi}\right)^5$	$b_q = b_\gamma = \exp(-2\eta \tan \phi)$ η = radians for b_q

where A_f = effective footing contact area $B'L'$
L' = effective footing length = $L - 2e_L$
B' = effective footing width = $B - 2e_B$
D = depth of footing in ground
e_B, e_L = eccentricity of load with respect to center of footing area
c = cohesion of base soil
ϕ = angle of internal friction of soil
H, V = load components parallel and perpendicular to footing, respectively
$\tan \delta$ = coefficient of friction between footing and base soil {use $\delta = \phi$ for concrete poured on ground [Schultze and Horn (1967)]}
η, ψ = as shown in accompanying figure with positive directions shown

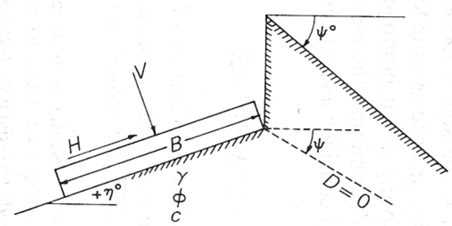

Notes: Do not use shape factors in combination with inclination factors. Use d_i and i_i only in combination or s_i with d_i, g_i and b_i. When triaxial ϕ is used for plane-strain conditions, one may adjust as follows:

for $L/B \le 2$, use ϕ_{tri}

$L/B > 2$, use $\phi_{ps} = 1.5\,\phi_{tri} - 17$

$\phi_{tr} \le 34°$, use $\phi_{tri} = \phi_{ps}$

Limitations: $H \leqq V \tan \delta + c_a A_f$

$i_q, i_\gamma > 0$

$\psi \leqq \phi$

$\eta + \psi \leqq 90°$

3.10 Footings with Eccentric Loadings

Meyerhof (1953) introduced the concept of effective area in which the non-uniform soil pressure is reduced to a uniform by considering a new footing area called the "effective area" instead of original dimensions of the footing [see Fig. (3.8)].

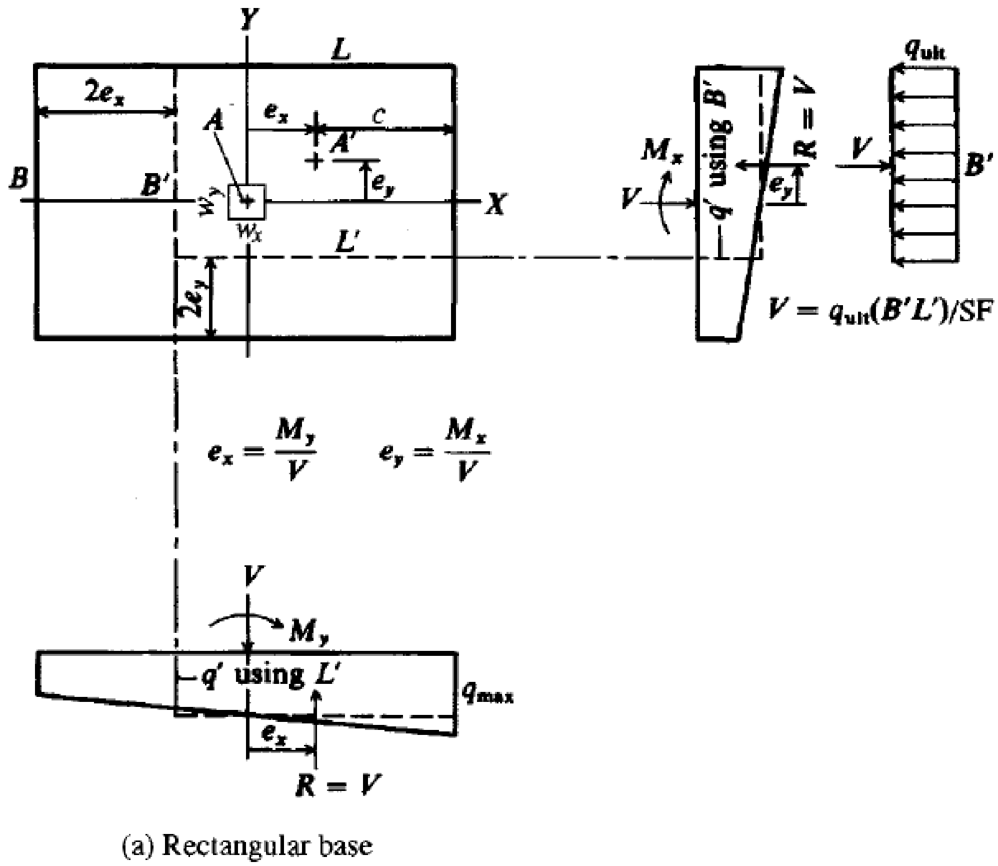

Fig. 3.8 Method of computing effective footing dimensions when footing is eccentrically loaded for rectangular footing

$$A' = B' \cdot L' \qquad \text{(effective area)}$$

$$B' = B - 2e_y \quad , \quad e_y = \frac{M_x}{V}$$

$$L' = L - 2e_x \quad , \quad e_x = \frac{M_y}{V}$$

Notes:

- (B) must be replaced by (B') in the third term of the bearing capacity equations.
- While computing the shape factors, (B') should be used for (B) and (L') for (L).

- If $(L - 2e_x) < (B - 2e_y)$ then $(L - 2e_x) \Rightarrow B'$ and $(B - 2e_y) \Rightarrow L'$
- Use the effective dimensions in calculating the allowable load:

$$P_a = q_a \cdot B' \cdot L'$$

For a circular footing [see Fig. (3.9)] of radius R, the effective area A′ = 2 × (area of circular segment ADC). Consider A′ to be a rectangle with $\frac{L'}{B'} = \frac{AC}{BD}$

$$e = \frac{\sum M}{\sum Q}$$

$$A' = 2S = B'L'$$

$$L' = \left(2S\sqrt{\frac{R+e}{R-e}}\right)^{1/2}$$

$$B' = L'\sqrt{\frac{R-e}{R+e}}$$

$$S = \frac{\pi R^2}{2} - \left[e\sqrt{R^2 - e^2} + R^2 \sin^{-1}\left(\frac{e}{R}\right)\right]$$

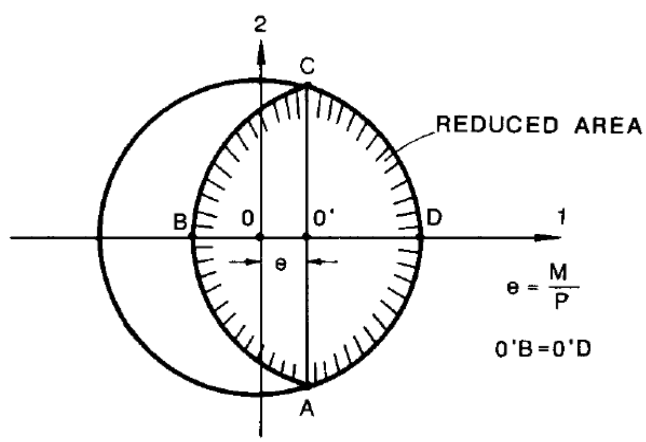

Fig. 3.9 Reduced (effective) area for circular footing

3.11 Footing on Layered Soils

When the thickness of the top stratum is less than the depth of rupture zone, some modifications are required in calculation of q_{ult}. Two cases will be considered:

Case 1: Footing on layered clays (ϕ = 0 condition).

The ultimate bearing capacity of a foundation can be given as (Reddy and Srinivasan, 1967);

$$q_{ult} = c_{u1} \cdot N_c(1 + s'_c + d'_c) + \bar{q}$$

where:

c_{u1}, c_{u2}: undrained shear strength of the upper and lower layers [Fig. (3.10)].

N_c : bearing capacity factor depending on c_{u2}/c_{u1} and d/b [Fig. (3.11)].

d: depth measured from the bottom of the foundation to the interface of the two clay layers [Fig. (3.10)].

s'_c, d'_c : shape and depth factors of general bearing capacity equation (Hansen).

Note:

The constant *b* in Fig. (3.11) is defined as:

b = B / 2 (B = width of footing)

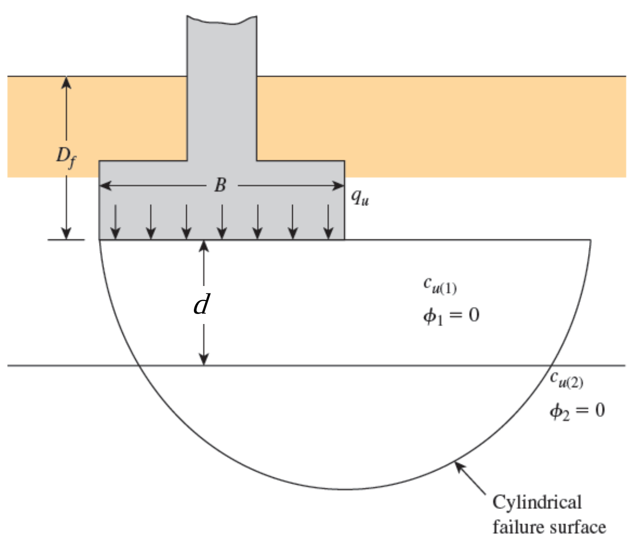

Fig. 3.10 Footing on layered clays

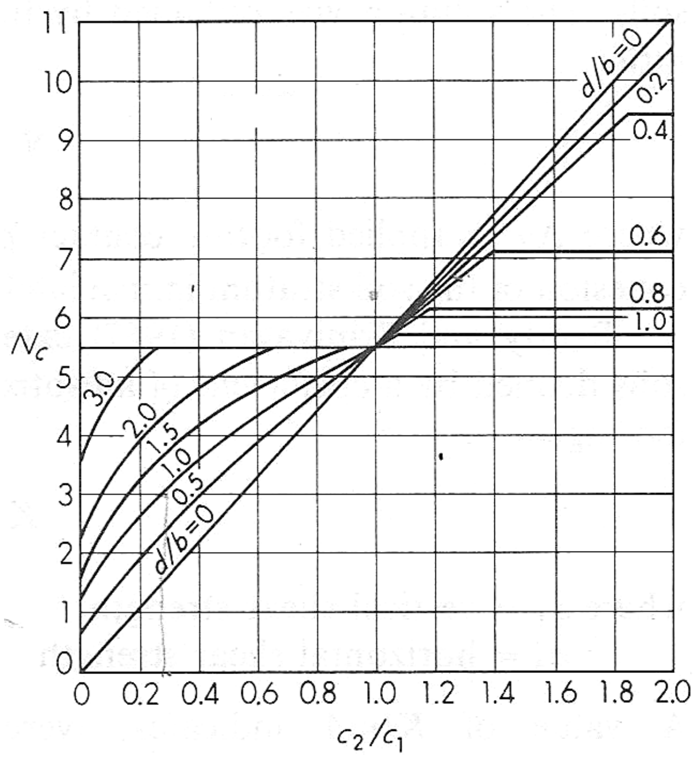

Fig. 3.11 Bearing capacity factor N_c for a footing on layered clays

<u>Case 2</u>: Footing on layered $c-\phi$ soil [Fig. (3.12)]

In this case, the weighted average values of c and ϕ are used in the bearing capacity equation.

$$c_{av} = \frac{\sum_{i=1}^{n} c_i \cdot H_i}{\sum_{i=1}^{n} H_i}$$

$$\phi_{av} = \tan^{-1}\left(\frac{\sum_{i=1}^{n} H_i \cdot \tan\phi_i}{\sum_{i=1}^{n} H_i}\right)$$

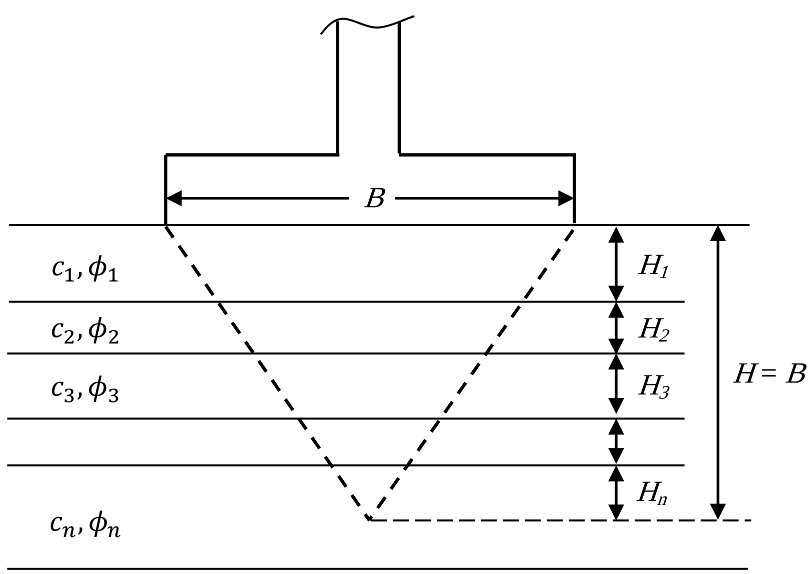

Fig. 3.12 Footing on layered $c-\phi$ soil where:

c_i= cohesion of stratum of thickness H_i; c may be zero.

ϕ_i = angle of internal friction in stratum of thickness H_i; ϕ may be zero.

$$\sum_{i=1}^{n} H_i = H \approx B$$

3.12 <u>Bearing Capacity of Footings Adjacent to a Slope</u>

The lack of soil on the slope side of the footing will tend to reduce the stability of the footing. Table (3.6) has been developed to provide the values of the modified factors (N_c' and N_q') for the slope effects.

$$q_{ult} = c \cdot N_c' \cdot s_c \cdot i_c + \bar{q} \cdot N_q' \cdot s_q \cdot i_q + 0.5\gamma \cdot B \cdot N_\gamma \cdot s_\gamma \cdot d_\gamma \cdot i_\gamma$$

Notes:

- N_γ is not corrected for slope effects.
- The effect of depth is included in both (N_c' and N_q') when ($\frac{D}{B} > 0$), so that (d_i) factors should not again be used.
- A (ϕ_{tri}) should not be adjusted to (ϕ_{ps}) since the slope edge distorts the failure patterns such that plane-strain conditions may not develop except for large ($\frac{b}{B}$) ratios.
- The overall slope stability should be checked for the effect of footing load.
- To simplify the calculations, linear interpolation will be used for intermediate values. The accurate method is to estimate (N_c' and N_q') by plotting.

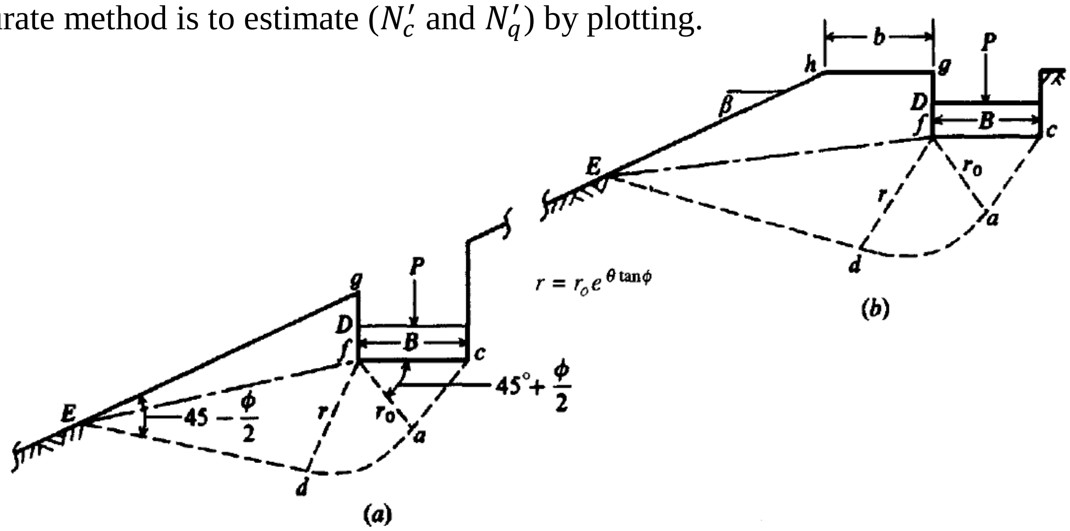

Fig. 3.13 Footings on or adjacent to a slope.

Table 3.6

Bearing capacity N'_c, N'_q for footings on or adjacent to a slope

Refer to Fig. 4-4 for variable identification. Base values ($\beta = 0$) may be used when length or area ratios > 1 or when $b/B > 1.5$ to 2.0 (approximate). Values given should cover usual range of footing locations and depths of embedment.

	$D/B = 0$ $b/B = 0$					**$D/B = 0.75$ $b/B = 0$**					**$D/B = 1.50$ $b/B = 0$**				
$\beta\downarrow$	**$\phi = 0$**	**10**	**20**	**30**	**40**	**0**	**10**	**20**	**30**	**40**	**0**	**10**	**20**	**30**	**40**
0° N'_c =	5.14	8.35	14.83	30.14	75.31	5.14	8.35	14.83	30.14	75.31	5.14	8.25	14.83	30.14	75.31
N'_q =	1.03	2.47	6.40	18.40	64.20	1.03	2.47	6.40	18.40	64.20	1.03	2.47	6.40	18.40	64.20
10°	4.89	7.80	13.37	26.80	64.42	5.14	8.35	14.83	30.14	75.31	5.14	8.35	14.83	30.14	75.31
	1.03	2.47	6.40	18.40	64.20	0.92	1.95	4.43	11.16	33.94	1.03	2.47	5.85	14.13	40.81
20°	4.63	7.28	12.39	23.78	55.01	5.14	8.35	14.83	30.14	66.81	5.14	8.35	14.83	30.14	75.31
	1.03	2.47	6.40	18.40	64.20	0.94	1.90	4.11	9.84	28.21	1.03	2.47	5.65	12.93	35.14
25°	4.51	7.02	11.82	22.38	50.80	5.14	8.35	14.83	28.76	62.18	5.14	8.35	14.83	30.14	73.57
	1.03	2.47	6.40	18.40	64.20	0.92	1.82	3.85	9.00	25.09	1.03	2.47	5.39	12.04	31.80
30°	4.38	6.77	11.28	21.05	46.88	5.14	8.35	14.83	27.14	57.76	5.14	8.35	14.83	30.14	68.64
	1.03	2.47	6.40	18.40	64.20	0.88	1.71	3.54	8.08	21.91	1.03	2.47	5.04	10.99	28.33
60°	3.62	5.33	8.33	14.34	28.56	4.70	6.83	10.55	17.85	34.84	5.14	8.34	12.76	21.37	41.12
	1.03	2.47	6.40	18.40	64.20	0.37	0.63	1.17	2.36	5.52	0.62	1.04	1.83	3.52	7.80
	$D/B = 0$ $b/B = 0.75$					**$D/B = 0.75$ $b/B = 0.75$**					**$D/B = 1.50$ $b/B = 0.75$**				
10°	5.14	8.33	14.34	28.02	66.60	5.14	8.35	14.83	30.14	75.31	5.14	8.35	14.83	30.14	75.31
	1.03	2.47	6.40	18.40	64.20	1.03	2.34	5.34	13.47	40.83	1.03	2.47	6.40	15.79	45.45
20°	5.14	8.31	13.90	26.19	59.31	5.14	8.35	14.83	30.14	71.11	5.14	8.35	14.83	30.14	75.31
	1.03	2.47	6.40	18.40	64.20	1.03	2.47	6.04	14.39	40.88	1.03	2.47	6.40	16.31	43.96
25°	5.14	8.29	13.69	25.36	56.11	5.14	8.35	14.83	30.14	67.49	5.14	8.35	14.83	30.14	75.31
	1.03	2.47	6.40	18.40	64.20	1.03	2.47	6.27	14.56	40.06	1.03	2.47	6.40	16.20	42.35
30°	5.14	8.27	13.49	24.57	53.16	5.14	8.35	14.83	30.14	64.04	5.14	8.35	14.83	30.14	74.92
	1.03	2.47	6.40	18.40	64.20	1.03	2.47	6.40	14.52	38.72	1.03	2.47	6.40	15.85	40.23
60°	5.14	7.94	12.17	20.43	39.44	5.14	8.35	14.38	23.94	45.72	5.14	8.35	14.83	27.46	52.00
	1.03	2.47	6.40	18.40	64.20	1.03	2.47	5.14	10.05	22.56	1.03	2.47	4.97	9.41	20.33
	$D/B = 0$ $b/B = 1.50$					**$D/B = 0.75$ $b/B = 1.50$**					**$D/B = 1.50$ $b/B = 1.50$**				
10°	5.14	8.35	14.83	29.24	68.78	5.14	8.35	14.83	30.14	75.31	5.14	8.35	14.83	30.14	75.31
	1.03	2.47	6.40	18.40	64.20	1.03	2.47	6.01	15.39	47.09	1.03	2.47	6.40	17.26	49.77
20°	5.14	8.35	14.83	28.59	63.60	5.14	8.35	14.83	30.14	75.31	5.14	8.35	14.83	30.14	75.31
	1.03	2.47	6.40	18.40	64.20	1.03	2.47	6.40	18.40	53.21	1.03	2.47	6.40	18.40	52.58
25°	5.14	8.35	14.83	28.33	61.41	5.14	8.35	14.83	30.14	72.80	5.14	8.35	14.83	30.14	75.31
	1.03	2.47	6.40	18.40	64.20	1.03	2.47	6.40	18.40	55.20	1.03	2.47	6.40	18.40	52.97
30°	5.14	8.35	14.83	28.09	59.44	5.14	8.35	14.83	30.14	70.32	5.14	8.35	14.83	30.14	75.31
	1.03	2.47	6.40	18.40	64.20	1.03	2.47	6.40	18.40	56.41	1.03	2.47	6.40	18.40	52.63
60°	5.14	8.35	14.83	26.52	50.32	5.14	8.35	14.83	30.03	56.60	5.14	8.35	14.83	30.14	62.88
	1.03	2.47	6.40	18.40	64.20	1.03	2.47	6.40	18.40	46.18	1.03	2.47	6.40	16.72	36.17

3.13 Bearing Capacity from Field Tests

It is difficult to obtain undisturbed samples of coarse-grained soils for testing in the laboratory. Consequently, the allowable bearing capacity and settlement of foundations on coarse-grained soils are often based on empirical methods using test data from in-situ tests. Various empirical equations have been proposed and only a few of these equations are presented here.

3.13.1 Bearing Capacity from SPT

A. Peck, Hanson and Thornburn (1974)

They presented empirical correlations [Fig. (3.15)] between standard penetration resistance, width of footing and the allowable bearing pressure limiting maximum settlement to 25 mm. The correlations are applicable to situations in which the W.T. is greater than B below the footing. A correction should be made if the W.T. is within a depth B below the foundation [see Fig. (3.14)]. Thus, the allowable bearing pressure obtained should be multiplied by a factor C_w, given by:

$$C_w = 0.5 + 0.5\frac{d_w}{B}$$

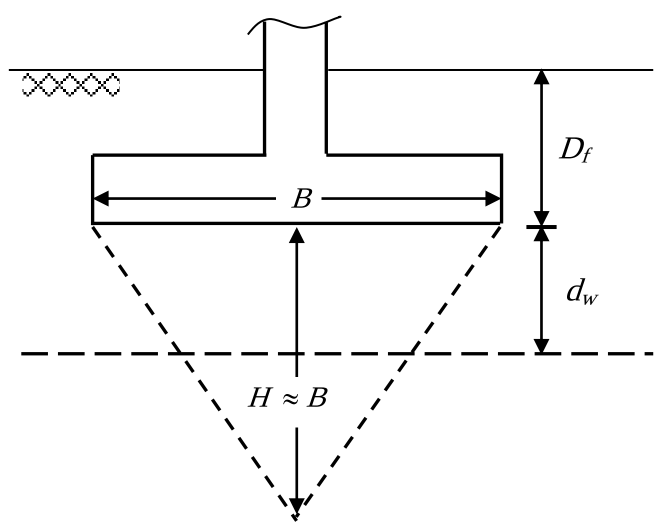

Fig. 3.14 Correction of $(q_a)_{net}$ for water table

In the case of rafts, the allowable bearing pressure should be doubled because a maximum settlement of 50 mm is considered acceptable.

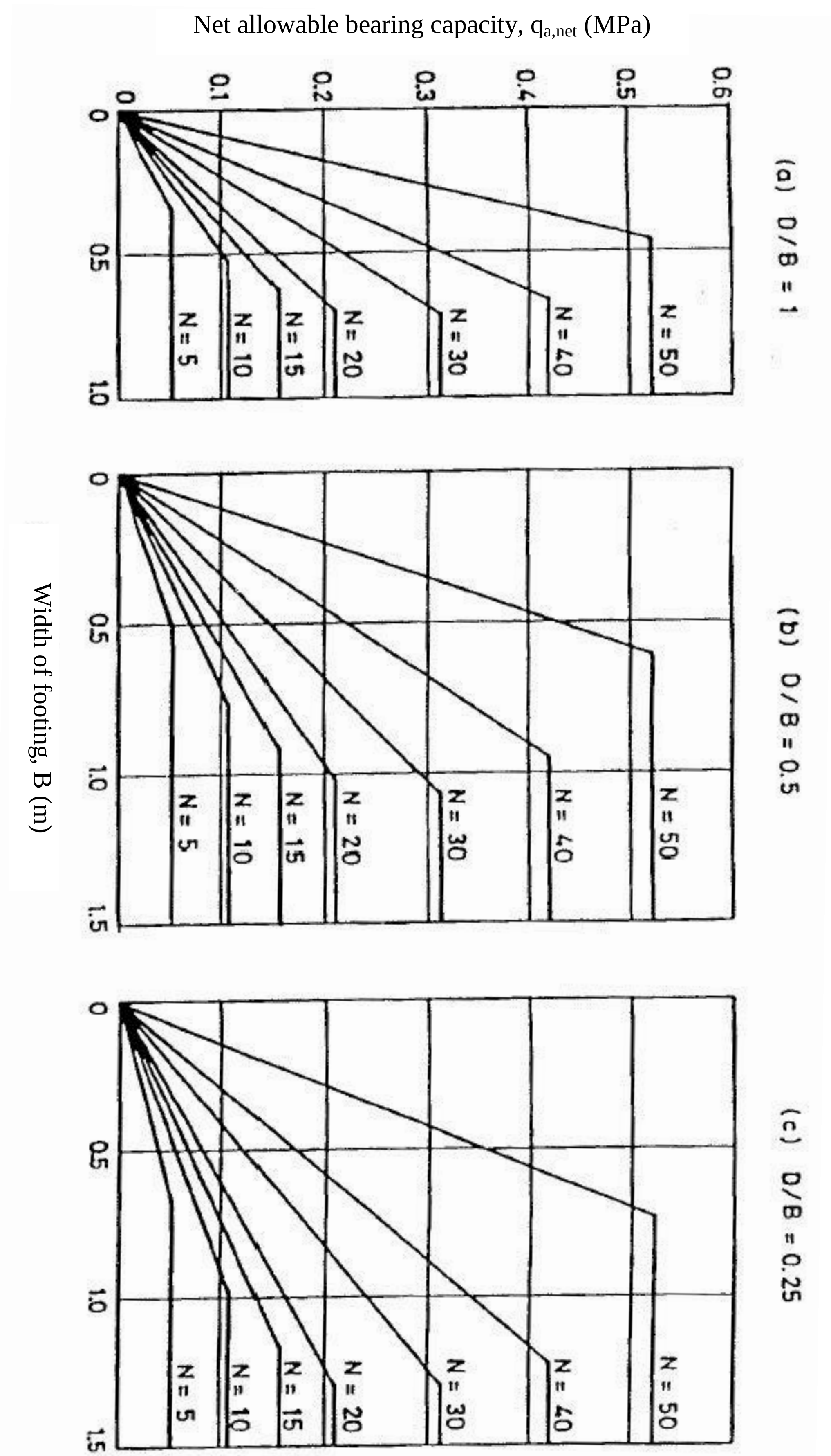

Fig. 3.15 Correlation of net allowable bearing capacity with standard penetration number for foundation settlements not exceeding 1 in (25.4 mm) (after Peck, Hanson, and Thornburn, 1974)

Note: The N-value is the average value within the footing influence zone (B below footing base) and should be corrected for the effect of overburden pressure.

B. Meyerhof (1974)

Meyerhof proposed an approach which is similar to the earliest published relationships obtained by Peck, Hanson and Thornburn. Bowles (1999) compared the two relations with the available field observations and concluded that the two relations are overly conservative. Consequently, he adjusted the Meyerhof equations for an approximate 50% increase in allowable bearing capacity to obtain the following:

For $B \leq 1.2\ m$ $\qquad q_a = \frac{N}{0.05} K_d$

For $B > 1.2\ m$ $\qquad q_a = \frac{N}{0.08} \left(\frac{B + 0.3}{B}\right)^2 K_d$

where $K_d = 1 + 0.33 \frac{D_f}{B} \leq 1.33$

q_a is in (kPa), [see Fig. (3.16)].

Notes

- The N-value is the average value of the corrected standard penetration number for the footing influence zone of about 0.5B above footing base to 2B below.
- In the above equations q_a is for an assumed 25.4 mm settlement. In general, q_a for any settlement is given by:

$$(q_a)_{any\ sett} = (q_a)_{25.4mm\ sett} \times \frac{Tolerable\ settlement}{25.4\ mm}$$

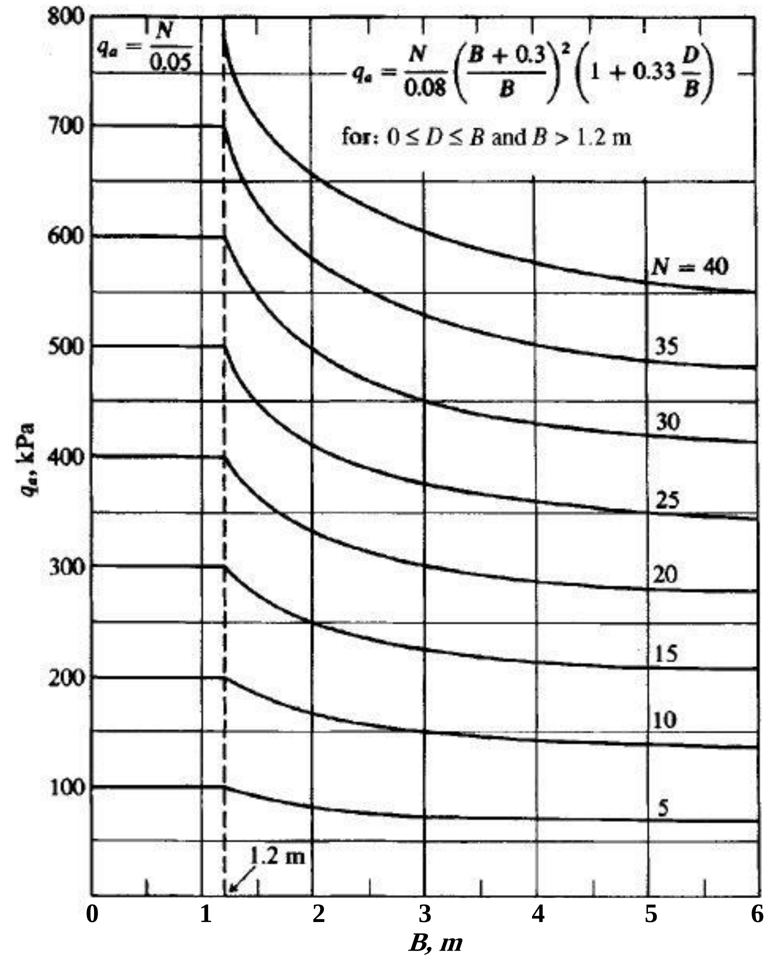

Fig. 3.16 Allowable bearing capacity for surface-loaded footings with settlement limited to approximately 25 mm. Equation used is shown on figure.

3.13.2 Bearing Capacity from CPT

Meyerhof (1965) suggested the bearing capacity for an estimated 25 mm settlement could be obtained directly as:

For $B \le 1.2\ m$ $$q_a = \frac{q_c}{30}$$

For $B > 1.2\ m$ $$q_a = \frac{q_c}{50}\left(\frac{B+0.3}{B}\right)^2$$

where q_c : cone-point resistance (kPa).

Values of q_a calculated from the above formulae should be halved if the sand within the stressed zone is submerged. Meyerhof suggests that the allowable bearing pressure should be doubled for raft foundation.

3.14 Foundations Subjected to Uplift or Tension Forces

The foundation behaves as shallow or deep according to its embedment ratio compared to the limiting one that obtained from Table (3.7).

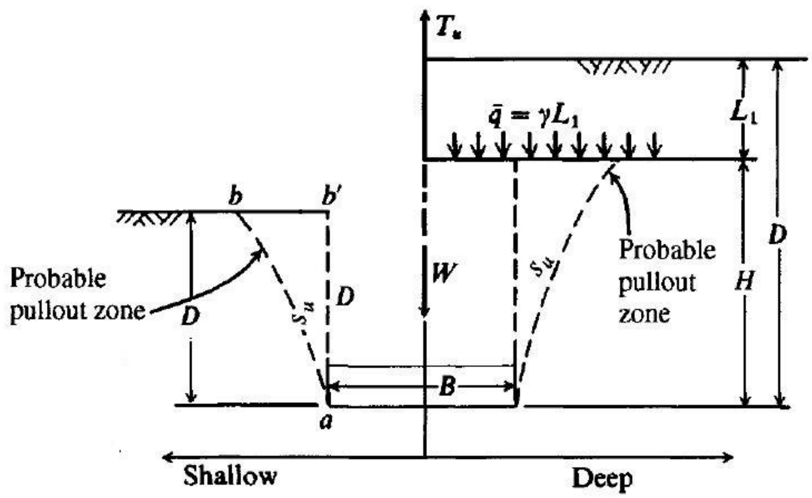

Fig. 3.17 Footings subjected to uplift or tension forces

For shallow circular footing:

$$T_u = \pi \cdot B \cdot c \cdot D + \frac{\pi}{2} \cdot s_f \cdot B \cdot \gamma \cdot D^2 \cdot K_u \cdot \tan\phi + W$$

For shallow rectangular footing:

$$T_u = 2c \cdot D \cdot (B + L) + \gamma \cdot D^2 \cdot (2s_f \cdot B + L - B) \cdot K_u \cdot \tan\phi + W$$

For deep circular footing:

$$T_u = \pi \cdot B \cdot c \cdot H + 1.57 \cdot s_f \cdot B \cdot \gamma \cdot (2D - H) \cdot H \cdot K_u \cdot \tan\phi + W$$

For deep rectangular footing:

$$T_u = 2c \cdot H \cdot (B + L) + \gamma \cdot (2D - H) \cdot (2s_f \cdot B + L - B) \cdot H \cdot K_u \cdot \tan\phi + W$$

where B = footing width (or diameter)

L = footing length

$W = W_f + W_s$ + any additional loads.

s_f = shape factor = $\left(1 + \frac{m.D}{B}\right) \leq \left(1 + \frac{m \cdot H}{B}\right)$

K_u = coefficient of earth pressure [K_o is one of the suggested values of it].

$K_o = (1 - \sin\phi)\sqrt{OCR}$

Table 3.7 Values of m, s_f, and H/B for various ϕ angles

ϕ	20°	25°	30°	35°	40°	45°	48°
Limiting H/B	2.5	3.0	4.0	5.0	7.0	9.0	11.0
m	0.05	0.10	0.15	0.25	0.35	0.50	0.60
Maximum s_f	1.12	1.30	1.60	2.25	3.45	5.50	7.60

CHAPTER 4
FOUNDATION SETTLEMENT

4.1 Introduction

In general, the settlement in soil due to loading consists of three parts:

1. **Immediate settlement** (S_i), which is due to the elastic deformation of dry soils and of moist and saturated soils without any change in the water content.
2. **Consolidation settlement** (S_c), which is the result of volume change in saturated fine-grained soils due to the expulsion of water occupying the void spaces.
3. **Secondary compression** (S_s), which is due to the plastic adjustment of soil fabrics. It is measured after complete dissipation of excess pore water pressure.

The total settlement (S_t) is the sum of the above three components:

$$S_t = S_i + S_c + S_s$$

4.2 Contact Pressure

It is the pressure transformed to the soil at foundation level. The actual contact pressure distributions are shown in figures (4.1, 4.2), [discuss]. In practice, it is generally assumed that the pressure distribution beneath the footing is uniform for concentric loading and linearly increasing for eccentric loading.

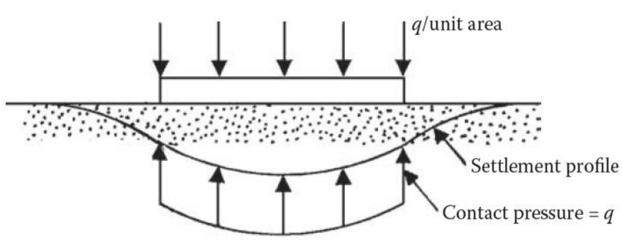

(a)

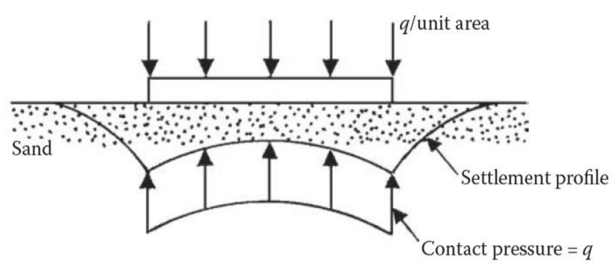

(a)

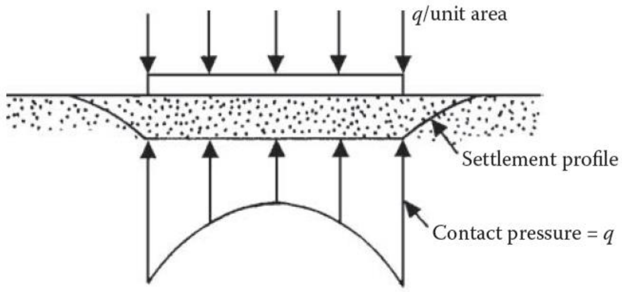

(b)

Fig. 4.1 Flexible (a) and rigid (b) foundations on clay

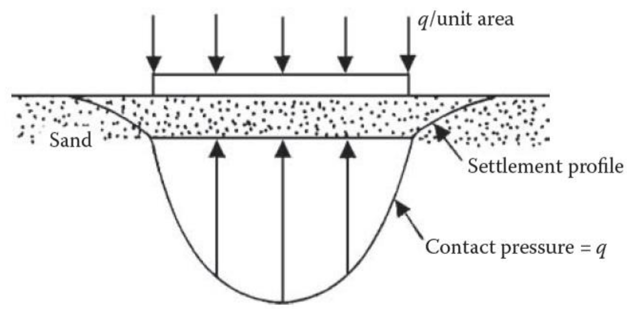

(b)

Fig. 4.2 Flexible (a) and rigid (b) foundations on sand

4.3 Stresses in a Soil Mass

The foundation settlement depends on the loading, size, and shape of the foundation, along with the properties of the underlying soil. Several methods can be used to estimate the increased pressure at some depth in the strata below the loaded area.

4.3.1 2:1 Slope Method

An early method (not much used at present) is to use 2:1 slope as shown in Fig. (4.3). This had a great advantage of simplicity. Others have proposed the slope angle anywhere from 30^o to 45^o. This (2:1 slope) method compares well with theoretical methods for a depth ranged between $z = B$ and $z = 4B$, but should not be used for $z < B$ (B = width of footing).

In this approach, the vertical pressure (σ_z) at a depth z beneath the loaded area due to load Q is:

$$\sigma_z = \frac{Q}{A_z}$$

where;

$A_z = (B + Z)(L + Z)$	Rectangular
$A_z = (B + Z)^2$	Square
$A_z = \frac{\pi}{4}(B + Z)^2$	Round
$A_z = (B + Z) \times 1$	Continuous

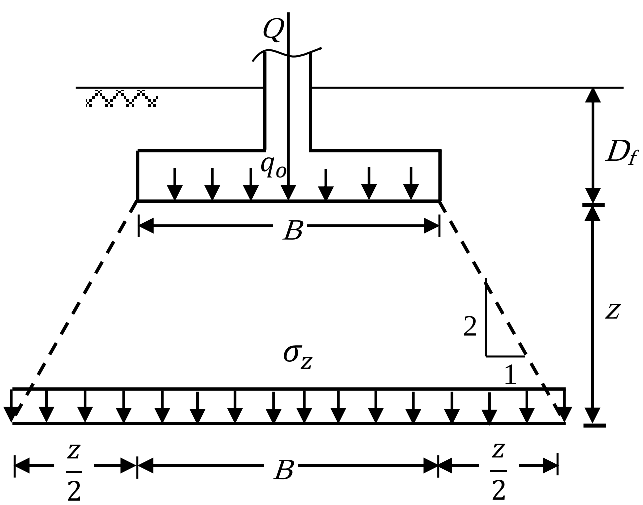

Fig. 4.3 Stress distribution according to 2:1 slope method

4.3.2 Boussinesq Method

Based on the theory of elasticity, Boussinesq developed a mathematical relationship for determining the normal stress at any point inside *homogeneous*, *elastic* and *isotropic* mediums due to a concentrated point load located at the surface, as shown in Fig. (4.4), to obtain:

$$\sigma_z = \frac{3Q}{2\pi z^2\left[1+\left(\frac{r}{z}\right)^2\right]^{5/2}}$$

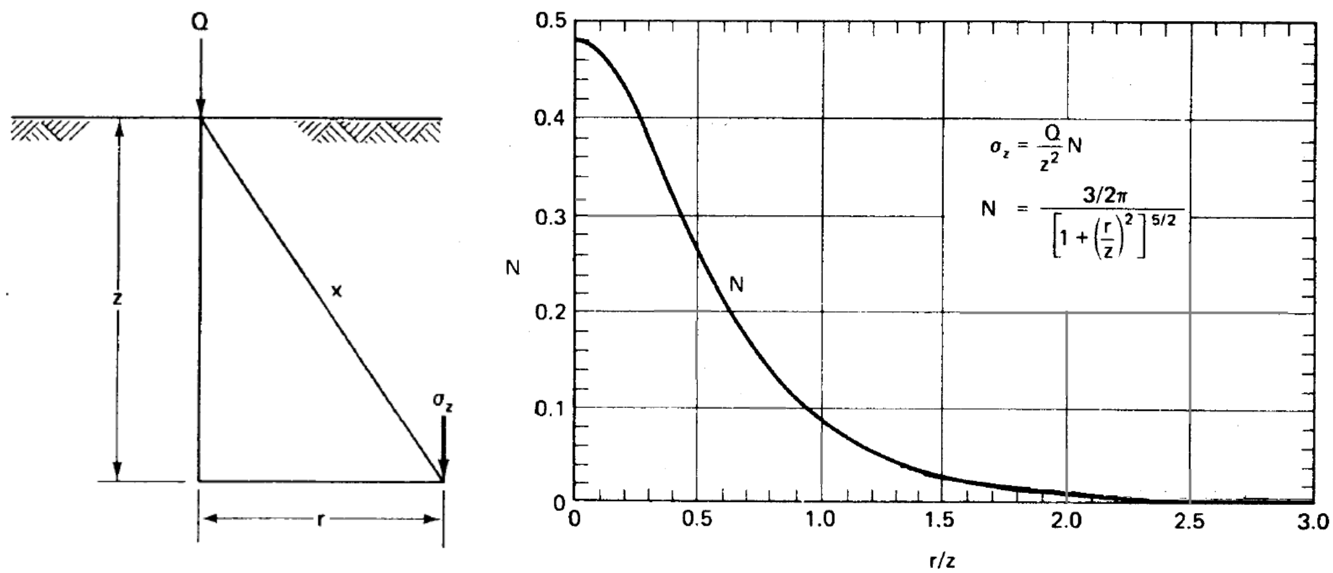

Fig. 4.4 Vertical stress under point load

The vertical stress at any point in a medium due to a distributed load on different shapes of footing can be found by integrating the above Boussinesq relation within the loaded area. This will result in the following charts:

- Circular loaded area [see Fig. (4.5)].
- Square loaded area [see Fig. (4.6)].
- Uniform strip load [see Fig. (4.7)].
- Rectangular loaded area [see Fig. (4.8)].
- Triangular strip load [see Fig. (4.9)].
- Embankment loading [see Fig. (4.10)].
- For any shape loaded area, use “Newmark influence chart” [see Fig. (4.11)].

Newmark's Influence Chart

Newmark constructed an influence chart, based on the Boussinesq solution, enabling the vertical stress to be determined at any point below an area of any shape carrying a uniform pressure q_o. The loaded area is drawn on tracing paper to a scale such that the length of the scale line on the chart [line $\overline{AB}$ in Fig. (4.11)] represents the depth z at which the vertical stress is required. The position of the loaded area on the chart is such that the point at which the vertical stress required is at the center of the chart. Referring to Fig. (4.11), the vertical stress is given by:

$$\sigma_v = I \cdot N \cdot q_o = 0.005\ N \cdot q_o$$

where;

σ_v: increase intensity of soil pressure

q_o: foundation contact pressure

I: influence factor of the chart ($I = \frac{1}{200} = 0.005$)

N: number of units counted (partial units are estimated)

Scale: $z = \overline{AB} = 35\ mm$

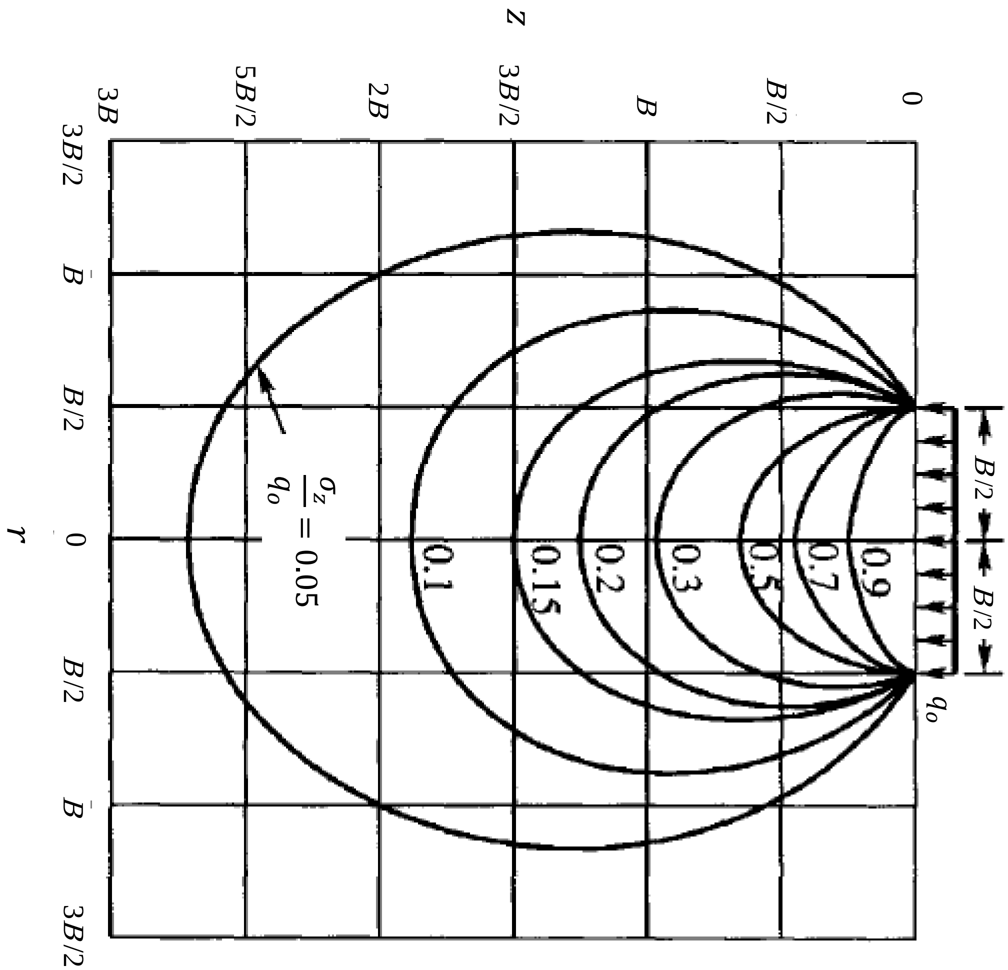

Fig. 4.5 Vertical stress under circular loaded area

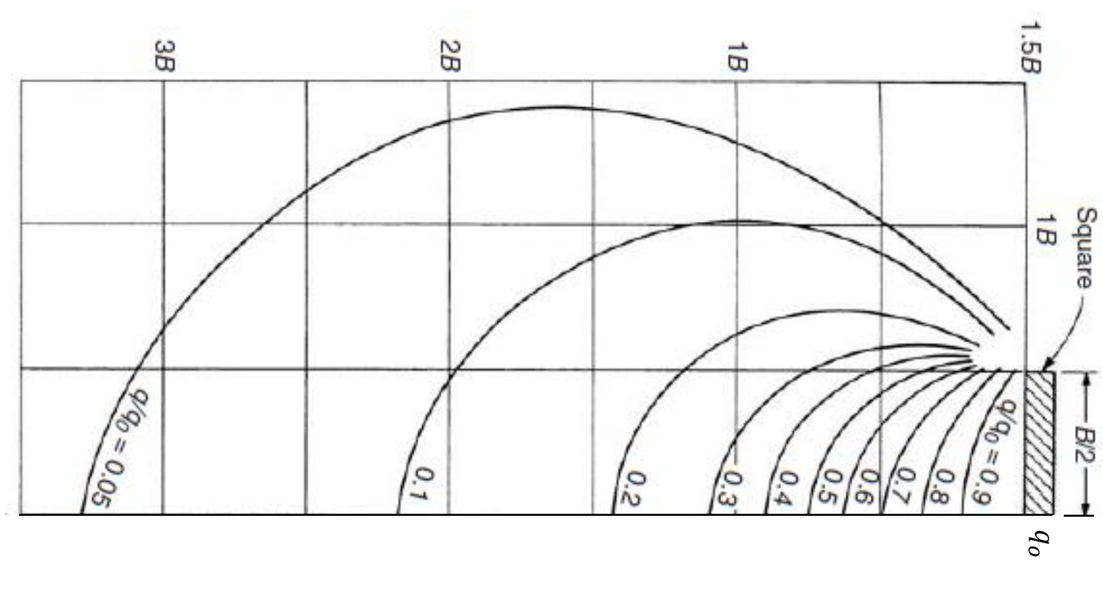

Fig. 4.6 Vertical stress under square loaded area

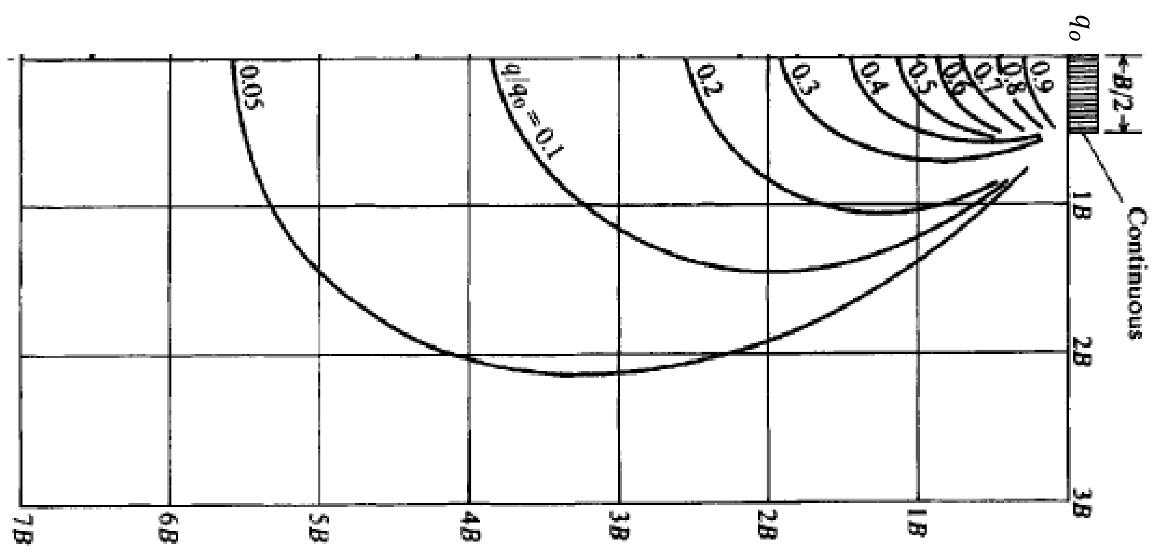

Fig. 4.7 Vertical stress under uniform strip load

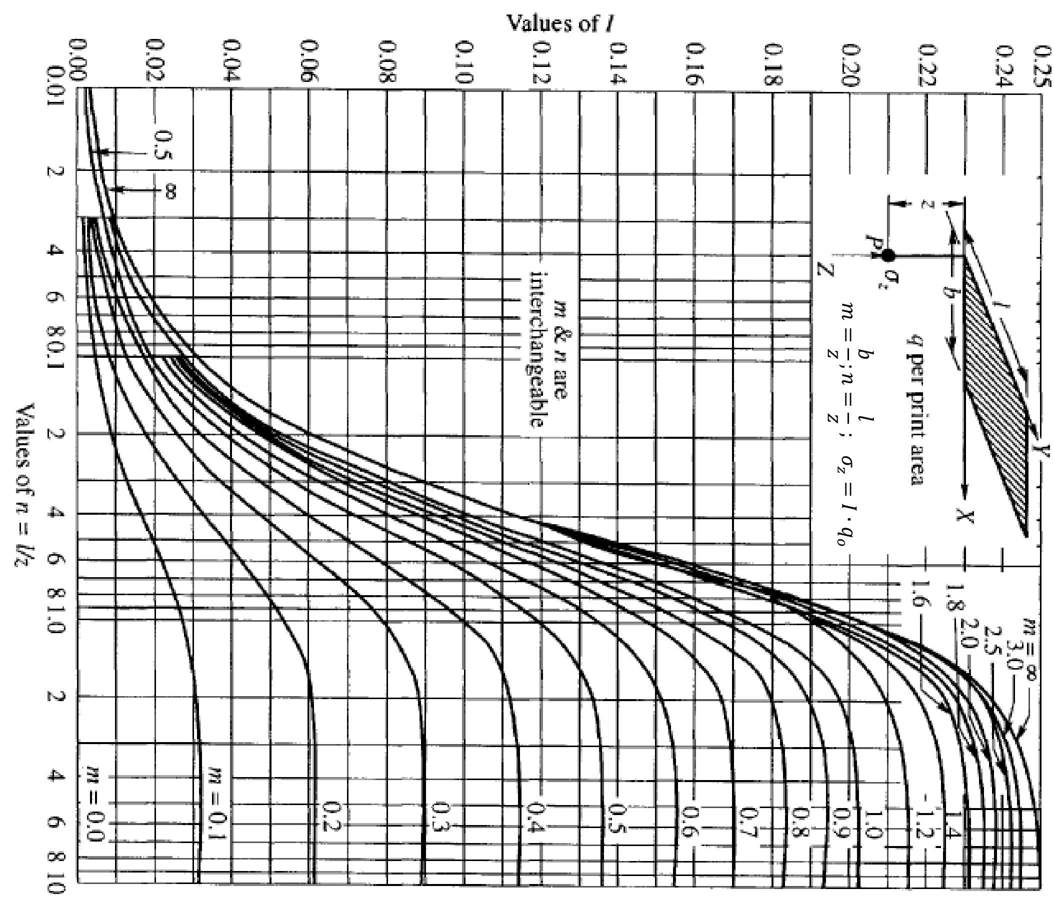

Fig. 4.8 Vertical stress under rectangular loaded area

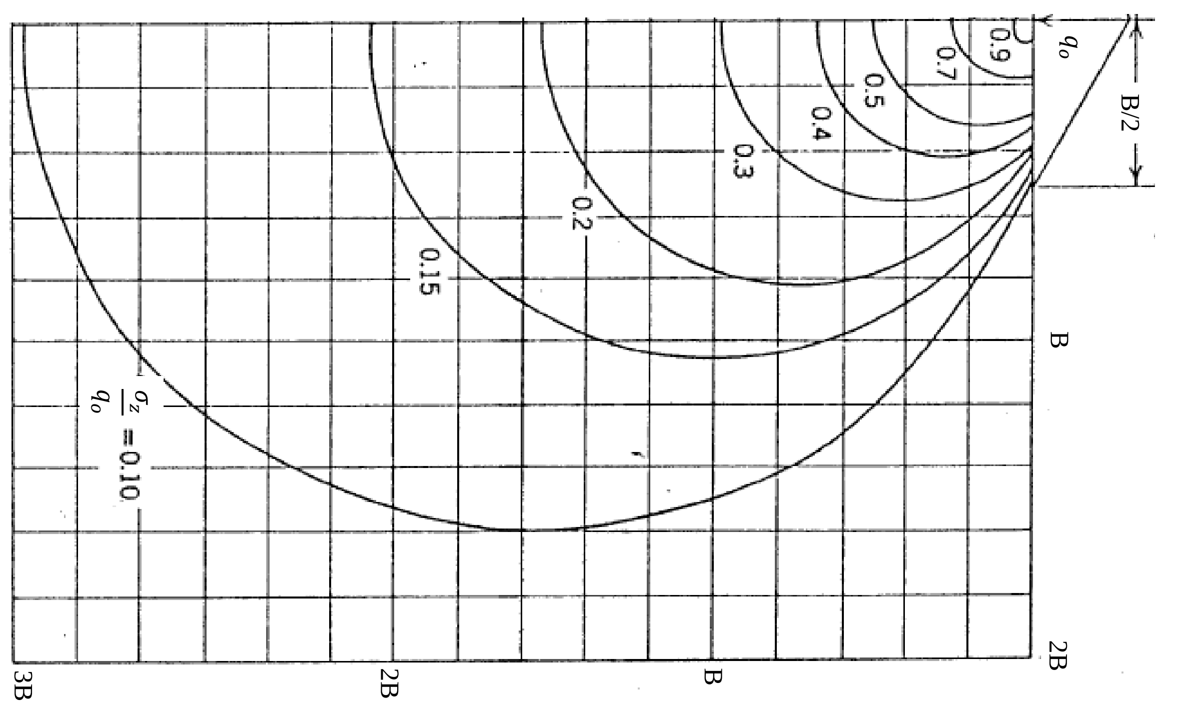

Fig. 4.9 Vertical stress under triangular strip load

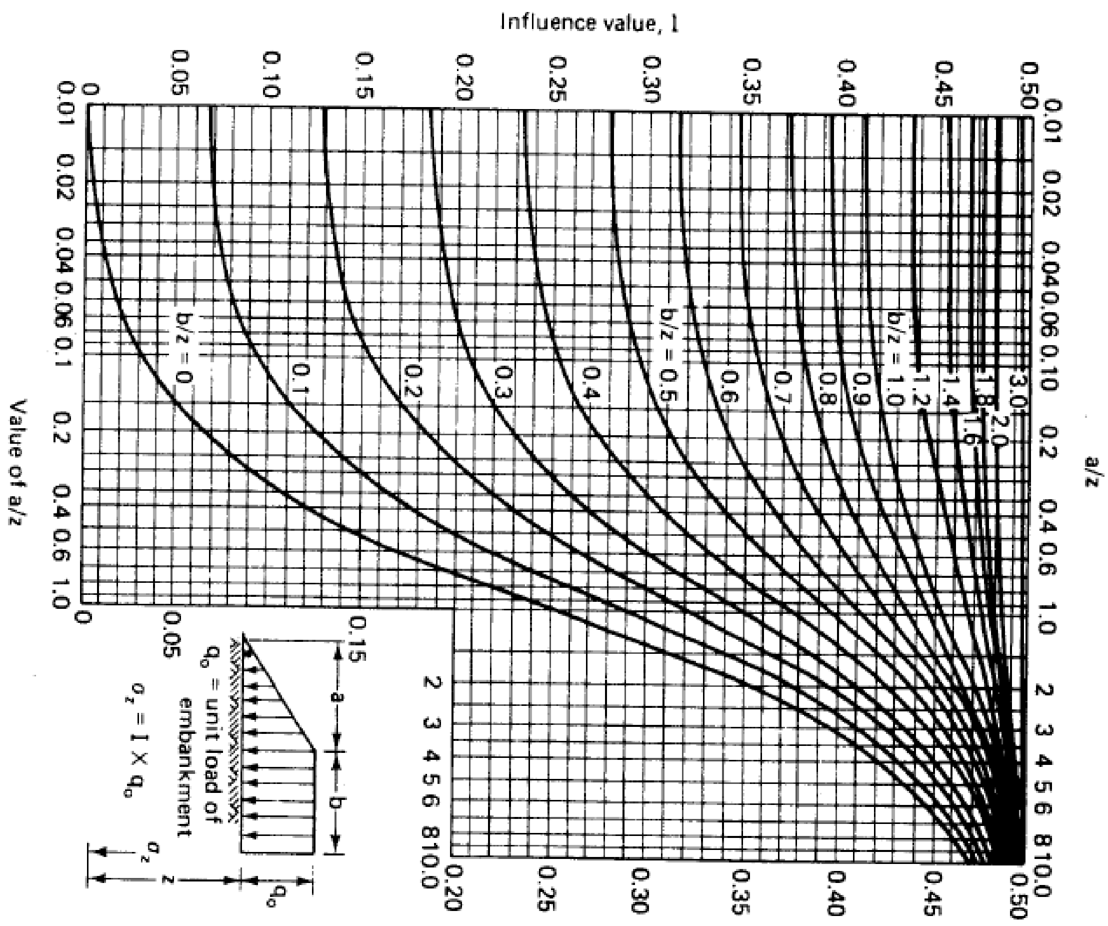

Fig. 4.10 Vertical stress under very long embankment

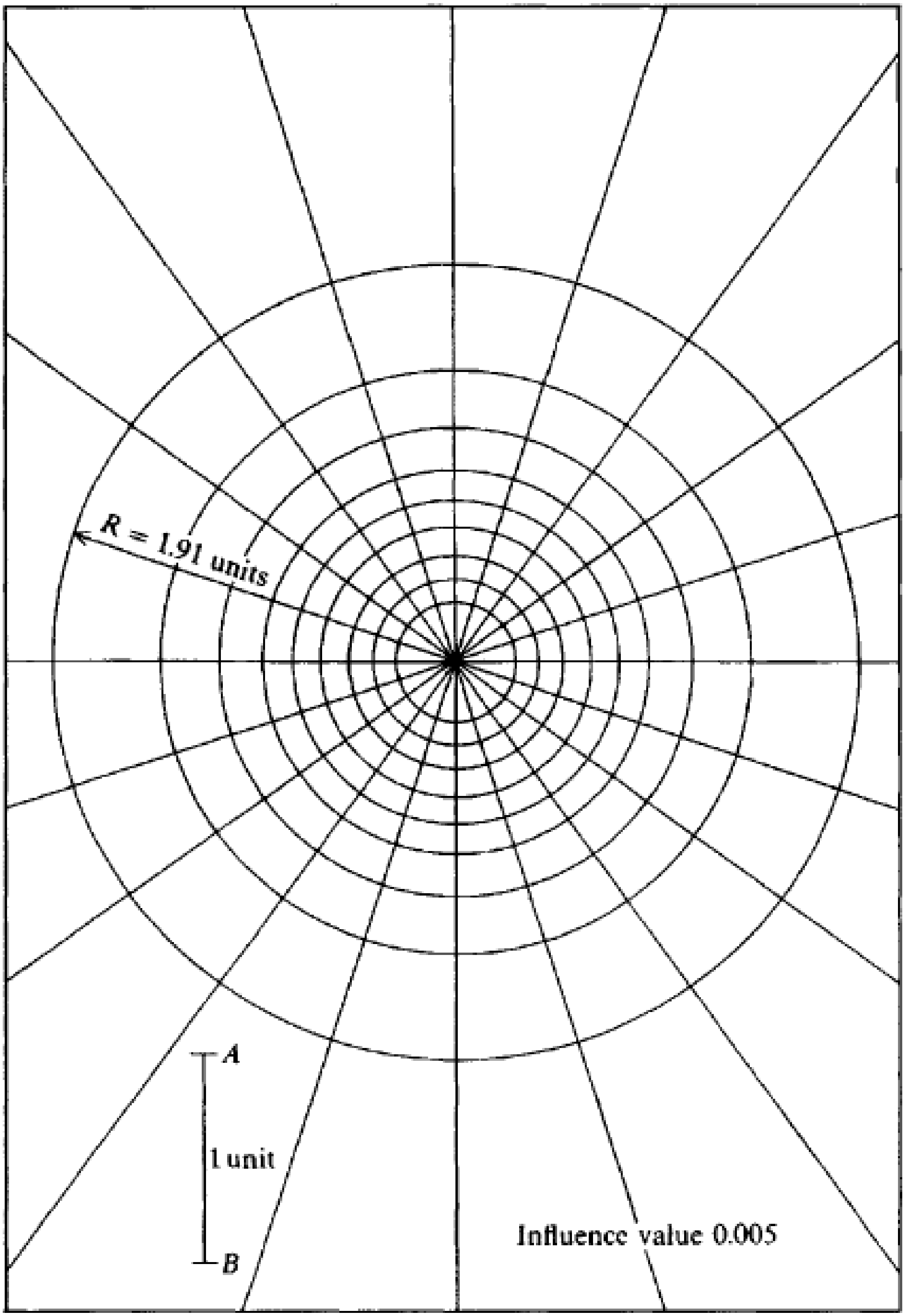

Fig. 4.11 Influence chart for vertical stress (Newmark chart)

4.4 Immediate (Elastic) Settlement

Immediate settlement takes place as soon as the load is applied. It occurs in partially saturated fine grained soils (silts and clays) and all cohesionless soils (sands and gravels) for any degree of saturation.

The immediate settlement can be computed using different approaches:

4.4.1 Elastic Settlement Based on the Theory of Elasticity

$$S_i = \frac{q \cdot B}{E_s}(1-\nu^2) \cdot I_w \cdot F_3$$

where

q : intensity of contact pressure.

B : lesser dimension of footing.

E_s : Young's modulus of soil, [see Table (4.1)].

ν : Poisson's ratio of soil, [see Table (4.2)].

I_w : influence factor, [see Table (4.3)].

F_3 : depth correction factor, [see Fig. (4.12)]

Note: For depth ratio D/B < 0.5, use depth factor, F3 = 1.0.

Table 4.1 Typical range of values for the static stress-strain modulus for selected soils

Soil	E_s, MPa
Clay	
Very soft	2–15
Soft	5–25
Medium	15–50
Hard	50–100
Sandy	25–250
Glacial till	
Loose	10–150
Dense	150–720
Very dense	500–1440
Loess	15–60
Sand	
Silty	5–20
Loose	10–25
Dense	50–81
Sand and gravel	
Loose	50–150
Dense	100–200
Shale	150–5000
Silt	2–20

*Value range is too large to use an "average" value for design.

Table 4.2 Typical range of values for Poisson's ratio

Type of soil	ν
Clay, saturated	0.4–0.5
Clay, unsaturated	0.1–0.3
Sandy clay	0.2–0.3
Silt	0.3–0.35
Sand, gravelly sand	−0.1–1.00
commonly used	0.3–0.4
Rock	0.1–0.4 (depends somewhat on type of rock)
Loess	0.1–0.3
Ice	0.36
Concrete	0.15
Steel	0.33

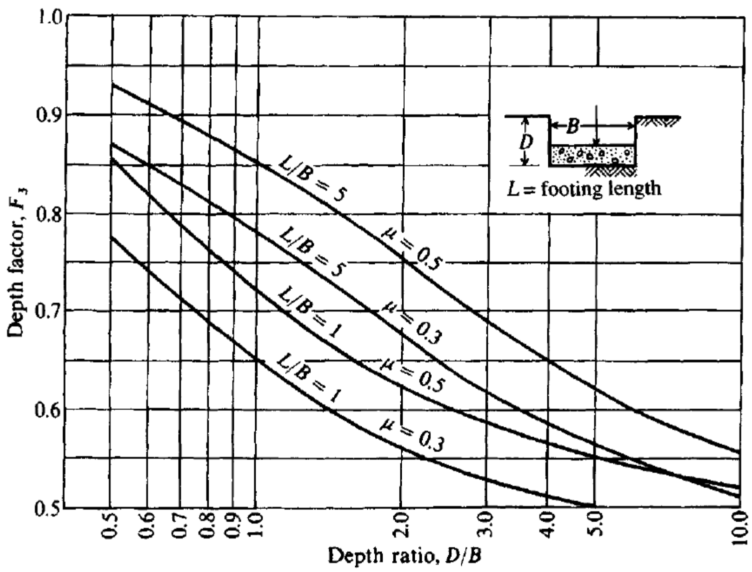

Fig. 4.12 Influence depth factor (F_3)

Table 4.3 Influence factor (I_w) for footings

	Flexible			Rigid
Shape	Center	Corner	Average	I_w
Circle	1.00	0.64 (edge)	0.85	0.88†
Square	1.12	0.56	0.95	0.82
Rectangle:				
$L/B = 0.2$				
0.5				
1.5	1.36	0.68	1.15	1.06
2	1.53	0.77	1.30	1.20
5	2.10	1.05	1.83	1.70
10	2.54	1.27	2.25	2.10
100	4.01	2.00	3.69	3.40

4.4.2 Elastic Settlement of Shallow Foundation on Saturated Clay (ν = 0.5)

For saturated clay layer underlain by a hard stratum, the average elastic settlement is given by:

$$S_i = \mu_1 \cdot \mu_o \cdot \frac{q \cdot B}{E_s}$$

where

μ_1 : correction factor for finite thickness of elastic soil layer, [see Fig. (4.13)].

μ_o : correction factor for depth of embedment of footing, [see Fig. (4.13)].

4.5 Consolidation Settlement

Consolidation is the gradual reduction in volume of a fully saturated soil of low permeability due to drainage of some of the pore water. The process continuing until the excess pore water pressure set up by an increase in total stress has completely dissipated.

The characteristics of a soil during consolidation or swelling can be determined by means of the oedometer test. The compressibility characteristics are represented by plots of void ratio (e) against effective stress (σ') [see Fig. (4.14)]. The shapes of the curves are related to the stress history of the clay. The $e - \log \sigma'$ relationship for a normally consolidated clay is linear and is called the virgin compression line. If the clay is overconsolidated, its state will be represented by a point on the expansion or recompression parts of the plot. The plots show that a clay in the overconsolidated state will be much less compressible than the same clay in a normally consolidated state.

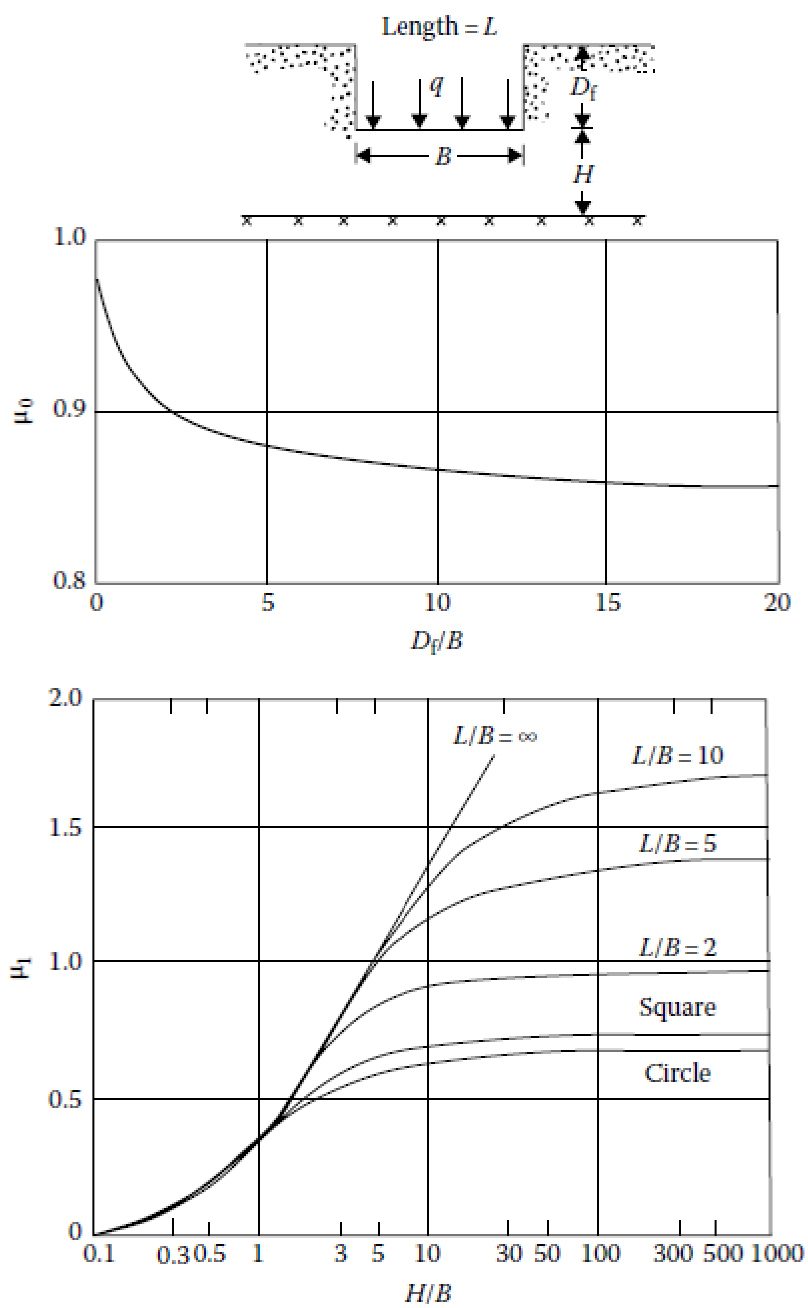

Fig. 4.13 Coefficients for vertical displacement of foundations on saturated clays

4.5.1 Compressibility Characteristics

The compressibility of the clay can be represented by [see Fig. (4.14)]:

1. *Compression index* (C_c), which represents the slope of the linear portion of the ($e - \log\sigma'$) plot and is dimensionless:

$$C_c = \frac{|\Delta e|}{\Delta(\log\sigma')} = \frac{e_o - e}{\log\dfrac{\sigma'}{\sigma'_o}}$$

where;

e_o : initial void ratio

σ'_o : initial effective overburden stress

For normally consolidated clay, it can be estimated using the following approximate formulae: C_c = 0.009(*L.L* - 10); where *L.L* = liquid limit.

The expansion portion of the ($e - \log\sigma'$) plot can be approximated to a straight line, the slope of which is referred to as the *expansion index* (C_e) or *swell index* or *recompression index* (C_r), [$C_r \approx$ (0.1-0.2) C_c].

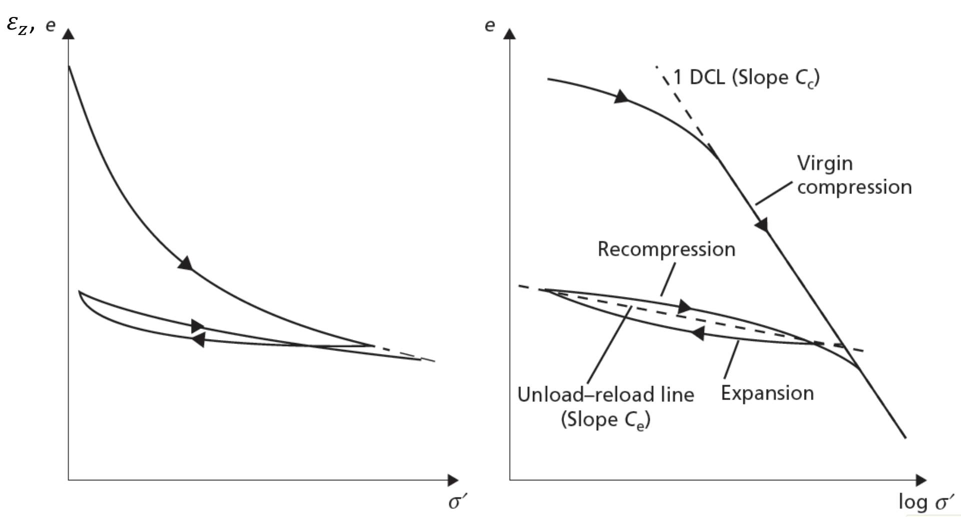

Fig. 4.14 Void ratio-effective stress relationship

2. The *coefficient of volume compressibility* (m_v): which represents the slope of $\varepsilon_z - \sigma'$ plot and has the units of the inverse of stress (L^2/F).

$$m_v = \frac{|\Delta\varepsilon_z|}{\Delta\sigma'} = \frac{1}{1+e_o}\cdot\frac{|\Delta e|}{\Delta\sigma'} = \frac{1}{H_o}\left(\frac{H_o - H}{\sigma' - \sigma'_o}\right)$$

where H_o is the initial thickness.

The slope of the expansion-recompression part of $\varepsilon_z - \sigma'$ plot is called the coefficient of volume recompressibility (m_{vr}) and is expressed as:

$$m_{vr} = \frac{|(\Delta\varepsilon_z)_r|}{\Delta\sigma'}$$

In calculating either m_v or m_{vr}, the vertical stress difference ($\Delta\sigma'$) should not exceed 100 kPa because of the nonlinearity of the $\varepsilon_z - \sigma'$ curve.

4.5.2 <u>Overconsolidation Ratio and Preconsolidation Pressure</u>

The degree of overconsolidation, called *overconsolidation ratio* (OCR), is defined as:

$$OCR = \frac{\sigma_c'}{\sigma_o'}$$

where;

σ_c' = the maximum effective vertical stress that has acted on the clay in the past which is called the *preconsolidation pressure* [see Fig. (4.15)].

σ_o' = present effective vertical stress.

Accordingly, we can define two types of clayey soils based on stress history:

1. Normally consolidated clay (O.C.R = 1), whose present effective overburden pressure is the maximum pressure that the soil has been subjected to.
2. Over consolidated clay (O.C.R > 1), whose present effective overburden pressure is less than that which the soil has experienced in the past.

Whenever possible, the pre-consolidation pressure for an over consolidated clay should not be exceeded in construction.

Casagrande (1936) suggested a simple graphic construction to determine the preconsolidation pressure (σ_c') from the laboratory $e - \log\sigma'$ plot. The procedure is as follows [see Fig. (4.15)]:

Step 1. By visual observation, establish point *a*, at which the $e - \log\sigma'$ plot has a minimum radius of curvature.

Step 2. Draw a horizontal line *ab*.

Step 3. Draw the line *ac* tangent at *a*.

Step 4. Draw the line *ad*, which is the bisector of the angle *bac*.

Step 5. Project the straight-line portion *gh* of the $e - \log \sigma'$ plot back to intersect line *ad* at *f*. The abscissa of point *f* is the preconsolidation pressure, σ_c'.

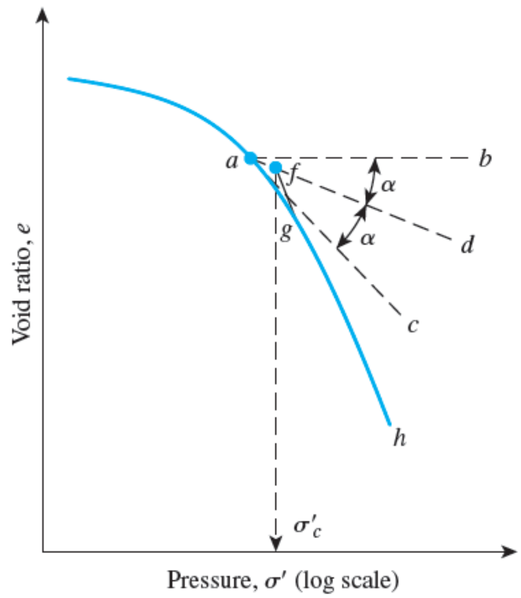

Fig. 4.15 Graphic procedure for determining preconsolidation pressure

4.5.3 Effect of Disturbance on $e - \log \sigma'$ Curve

A soil specimen will be remolded when it is subjected to some degree of disturbance. This remolding will result in some deviation of the $e - \log \sigma'$ plot as observed in the laboratory from the actual behavior in the field. The field $e - \log \sigma'$ plot can be reconstructed from the laboratory test results in the manner described in this section (Terzaghi and Peck, 1967).

Normally Consolidated Clay of Low to Medium Plasticity [Fig. (4.16)]

Step 1. In Fig. (4.16), curve 2 is the laboratory $e - \log \sigma'$ plot. From this plot, determine the preconsolidation pressure, $\sigma_c' = \sigma_o'$ (that is, the present effective overburden pressure). Knowing where $\sigma_c' = \sigma_o'$, draw vertical line *ab*.

Step 2. Calculate the void ratio in the field, e_o. Draw horizontal line *cd*.

Step 3. Calculate $0.4e_o$ and draw line *ef*. (*Note: f* is the point of intersection of the line with curve 2.)

Step 4. Join points *f* and *g*. Note that *g* is the point of intersection of lines *ab* and *cd*. This is the *virgin compression curve.*

It is important to point out that if a soil is remolded completely, the general position of the $e - \log \sigma'$ plot will be as represented by curve 3.

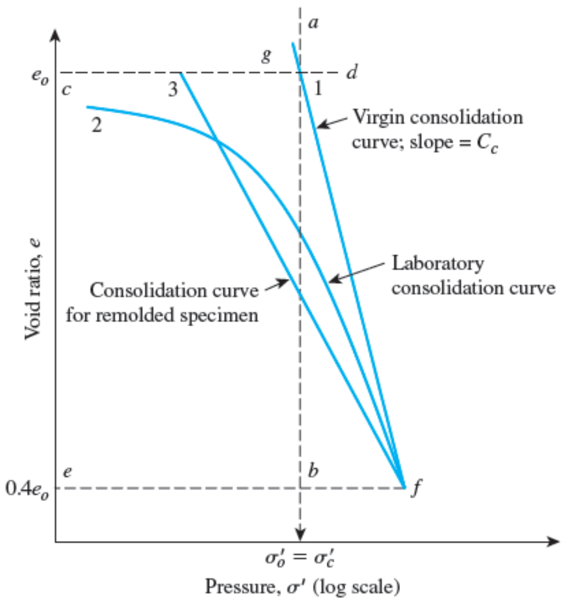

Fig. 4.16 Consolidation characteristics of normally consolidated clay of low to medium sensitivity

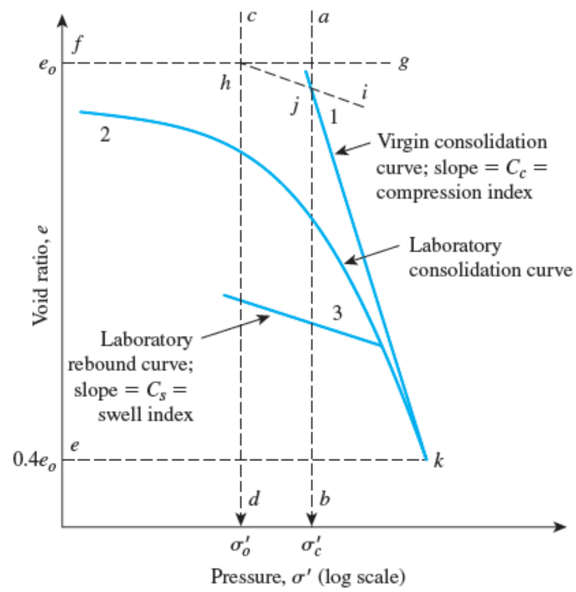

Fig. 4.17 Consolidation characteristics of overconsolidated consolidated clay of low to medium sensitivity

<u>Overconsolidated Clay of Low to Medium Plasticity [Fig. (4.17)]</u>

Step 1. In Fig. (4.17), curve 2 is the laboratory $e - \log \sigma'$ plot (loading), and curve 3 is the laboratory unloading, or rebound, curve. From curve 2, determine the preconsolidation pressure σ'_c. Draw the vertical line *ab.*

Step 2. Determine the field effective overburden pressure σ'_o. Draw vertical line *cd.*

Step 3. Determine the void ratio in the field, e_o. Draw the horizontal line *fg*. The point of intersection of lines *fg* and *cd* is *h.*

Step 4. Draw a line *hi*, which is parallel to curve 3 (which is practically a straight line). The point of intersection of lines *hi* and *ab* is *j.*

Step 5. Join points *j* and *k*. Point *k* is on curve 2, and its ordinate is $0.4e_o$.

The field consolidation plot will take a path *hjk*. The recompression path in the field is *hj* and is parallel to the laboratory rebound curve (Schmertmann, 1953).

4.5.4 <u>One-Dimensional Consolidation Settlement Calculations</u>

Referring to Fig. (4.18), the consolidation settlement can be estimated as follows:

A. For N.C. clay

$$S_c = \frac{C_c}{1+e_o} H_o \log \frac{\sigma_o' + \Delta\sigma}{\sigma_o'}$$

where;

S_c: final consolidation settlement ($t = \infty$)

C_c: compression index

H_o: thickness of clay layer

e_o: initial void ratio at mid of clay layer

σ_o': effective overburden pressure at the center of clay layer.

$\Delta\sigma$: increase in pressure induced at the center of clay layer.

B. For O.C. clay:

(i) if $\sigma_o' + \Delta\sigma \le \sigma_c'$

$$S_c = \frac{C_r}{1+e_o} H_o \log \frac{\sigma_o' + \Delta\sigma}{\sigma_o'}$$

(ii) if $\sigma_o' + \Delta\sigma > \sigma_c'$

$$S_c = \frac{C_r}{1+e_o} H_o \log \frac{\sigma_c'}{\sigma_o'} + \frac{C_c}{1+e_o} H_o \log \frac{\sigma_o' + \Delta\sigma}{\sigma_c'}$$

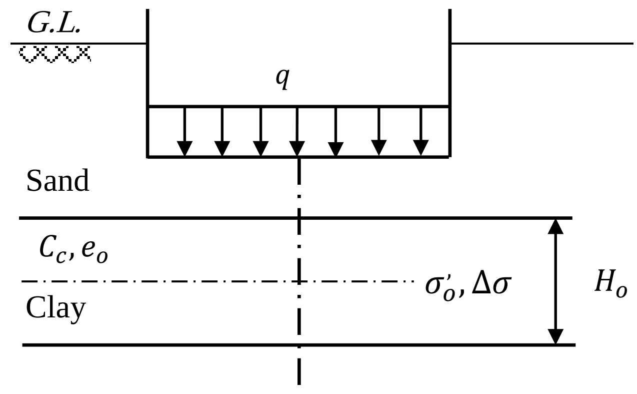

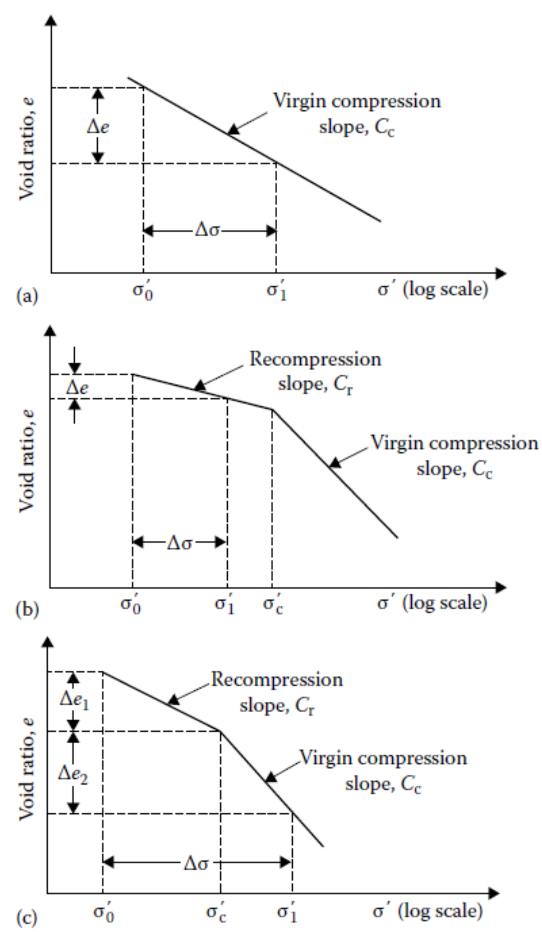

Fig. 4.18

4.5.5 Consolidation Settlement for Thick Layer

The average pressure increase can be obtained by simply averaging the top and bottom value for H_o up to about 1 m. For greater thickness (H_o > 1.5 – 2 m), the following methods may be adopted:

1. Dividing into thin layers [Fig. (4.19)]:

$$S_c = \sum_{i=1}^{n} (S_c)_i$$

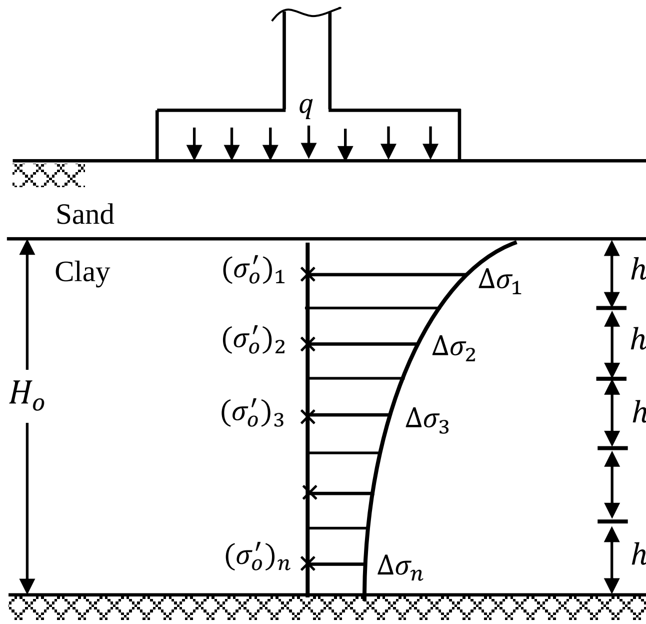

Fig. 4.19

2. Calculation of $\Delta\sigma$ using Trapezoidal Rule [Fig. (4.20)]:

$$\Delta\sigma \cdot H_o = \frac{h}{2}(\Delta\sigma_1 + \Delta\sigma_2) + \frac{h}{2} \cdot (\Delta\sigma_2 + \Delta\sigma_3) + \cdots + \frac{h}{2} \cdot (\Delta\sigma_{n-1} + \Delta\sigma_n) + \frac{h}{2} \cdot (\Delta\sigma_n + \Delta\sigma_{n+1})$$

$$\Delta\sigma = \frac{h}{H_o}\left(\frac{\Delta\sigma_1 + \Delta\sigma_{n+1}}{2} + \Delta\sigma_2 + \cdots + \Delta\sigma_n\right)$$

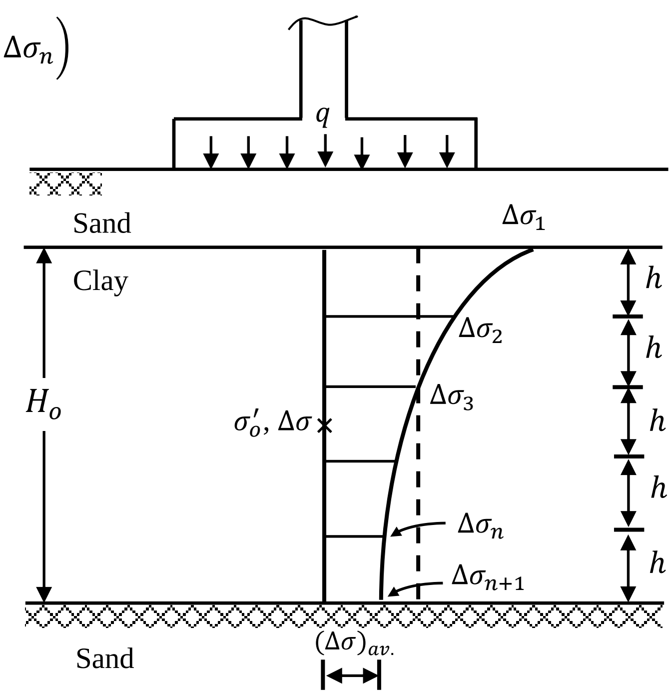

Fig. 4.20

4.5.6 Rate of Consolidation Settlement

Terzaghi's theory of one-dimensional consolidation settlement results in the following differential equation:

$$\frac{\partial u}{\partial t} = c_v \frac{\partial^2 u}{\partial z^2} \qquad (1)$$

where;

u = excess pore water pressure (p.w.p)

c_v = coefficient of consolidation = $\dfrac{k}{\gamma_w \cdot m_v}$ (dimensions: L^2/T)

k = coefficient of permeability

m_v = coefficient of volume compressibility

For a uniform initial excess p.w.p. and boundary conditions as shown in Fig. 4.21, the solution of the above D.E. (Eq. 1) yields:

$$u = \sum_{m=0}^{\infty} \left[\frac{2u_i}{M} \sin\left(\frac{M \cdot z}{d}\right)\right] e^{-M^2 \cdot T_v} \qquad (2)$$

where;

u = excess p.w.p. at time = t and depth = z.

m = an integer

$M = \dfrac{\pi}{2}(2m + 1)$

u_i = initial excess p.w.p.

d = the longest drainage path

= $H_o/2$ for two-way drainage

= H_o for one-way drainage

T_v = time factor = $\dfrac{c_v \cdot t}{d^2}$ (dimensionless)

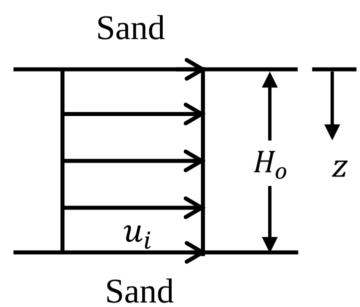

$z = 0 \quad , \quad u = 0$

$z = H_o \quad , \quad u = 0$

$t = 0 \quad , \quad u = u_i$

Fig. 4.21 Distribution of initial excess p.w.p.

The degree of consolidation at a distance z at any time t is:

$$U_z = \frac{\sigma' - \sigma'_o}{\Delta\sigma} = \frac{u_i - u}{u_i} = 1 - \frac{u}{u_i} \qquad (3)$$

Equations (2 and 3) can be combined to obtain the degree of consolidation at any depth z. This is shown in Fig. (4.22).

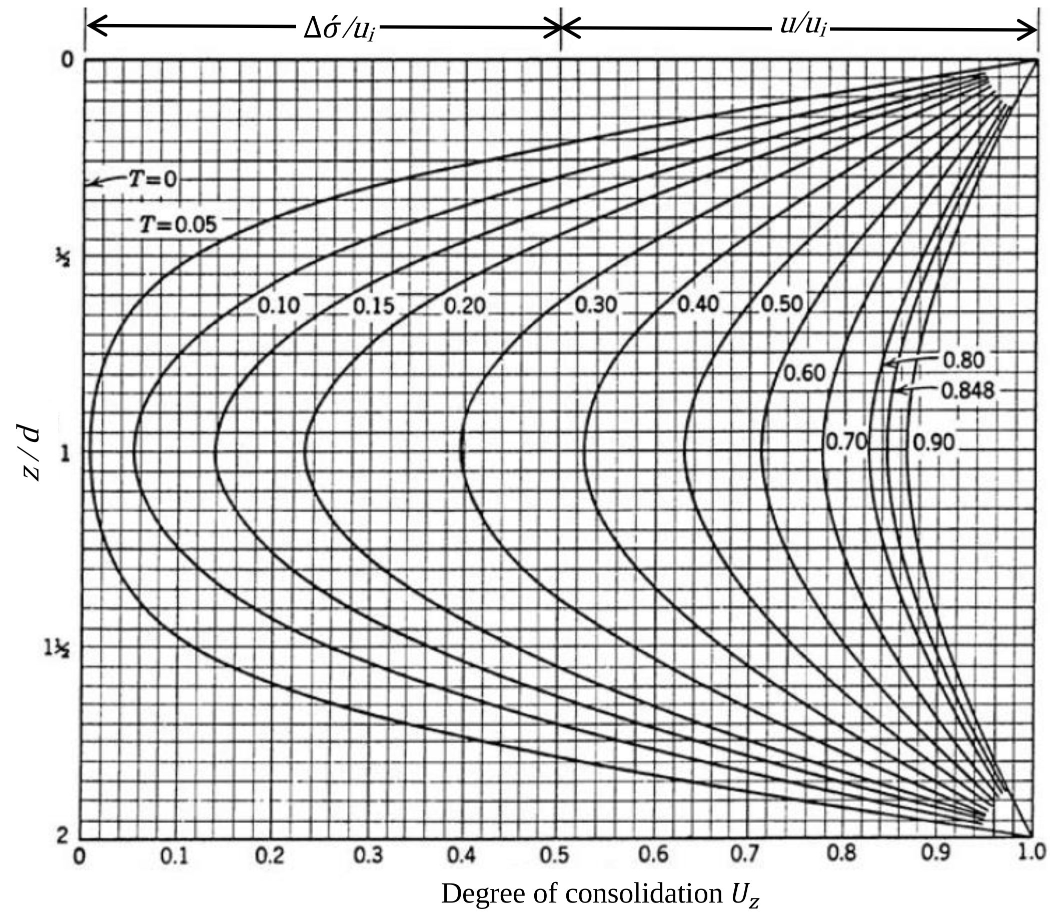

Fig. 4.22 Variation of U_z with T_v and z/d

The average degree of consolidation (U_{av} or U) and (T_v) relation for a uniform initial excess pore water pressure can be expressed using Fig. (4.23) or the following equations:

$$T_v = \frac{\pi}{4} U_{av}^2 \qquad for\ U_{av} < 0.6$$

$$T_v = -0.933 \log(1 - U_{av}) - 0.085 \qquad for\ U_{av} \geq 0.6$$

The consolidation settlement at any time can be calculated as:

$$S_{c\ at\ any\ time} = U_{av} \cdot S_c$$

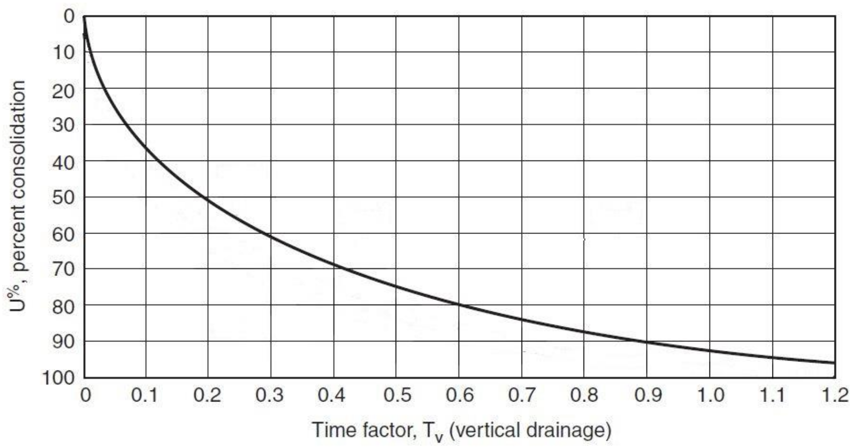

Fig. 4.23 Variation of time factor T_v with percentage of consolidation U.

Results of Terzaghi for a linear distribution of excess pore pressure

Average degree of consolidation U_{av} %	Time factor T_v
0	0
5	0.002
10	0.008
15	0.017
20	0.031
25	0.049
30	0.071
35	0.092
40	0.126
45	0.159
50	0.197
55	0.238
60	0.286
65	0.340
70	0.403
75	0.477
80	0.567
85	0.683
90	0.848
95	1.13
100	∞

Assumptions: Terzaghi theory of consolidation, linear initial excess pore water pressures, and instantaneous loading.

Note: The above values are based on the following approximate equations by Casagrande (unpublished notes) and Taylor (1984):

For $U_{avg} < 60\%$, the time factor $T = \frac{1}{4}\pi(U_{avg}/100)^2$

For $U_{avg} \geq 60\%$, the time factor $T = 1.781 - 0.933 \log(100 - U_{avg})$

4.5.7 Correction for Construction Period

In practice, structural loads are applied to the soil not instantaneously but over a period of time. Terzaghi proposed an empirical method of correcting the instantaneous time-settlement curve to allow for the construction period.

A. Analytically:

during construction period; $$[S_{c\ at\ t}]_{act} = [S_{c\ at\ \frac{t}{2}}]_{inst} \times \frac{P}{P'}$$

after construction period; $$[S_{c\ at\ t}]_{act} = [S_{c\ at\ (t-\frac{t_c}{2})}]_{inst}$$

where;

P = instantaneous load during construction period

P' = load at the end of construction period

B. Graphically [see Fig. (4.24)]:

- Project vertically from (t_c/2) on the instantaneous curve and then horizontally. The intersection with (t_c) locates point (B).
- For any time (t) less than (t_c), project from (t/2) vertically on the instantaneous curve and then horizontally to intersect (AB) at point (C). The intersection of (CO) and (t) locates another point on the corrected curve.
- For any time after (t_c), the horizontal distance between the two curves is (t_c/2).

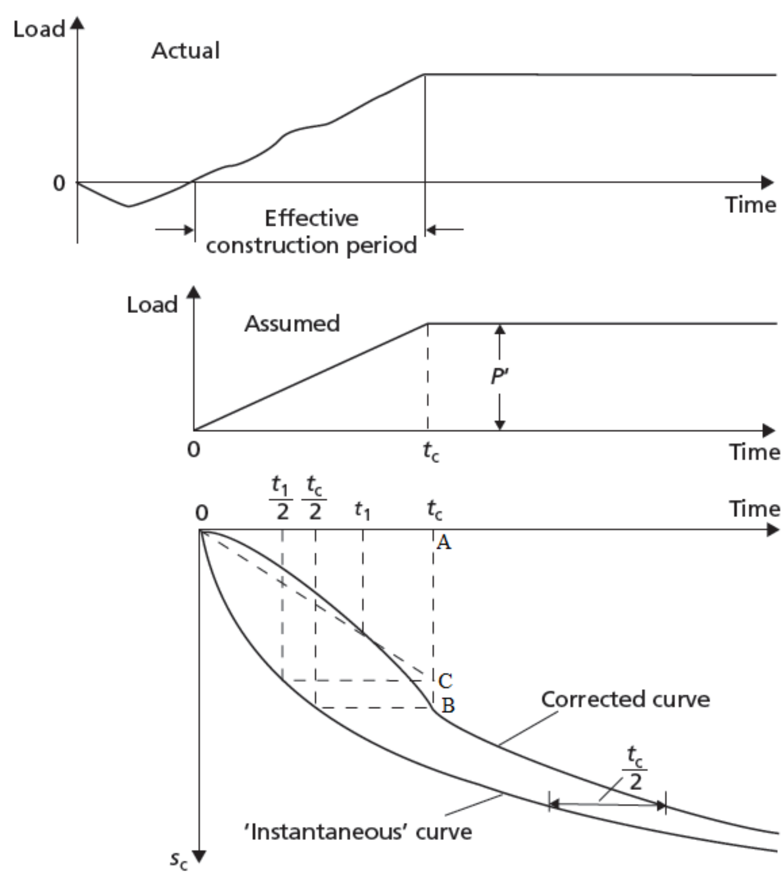

Fig. 4.24 Correction for construction period

4.6 <u>Secondary Settlement</u>

Experimental results show that compression does not cease when the excess p.w.p. has dissipated to zero but continues at a gradually decreasing rate under constant effective stress. Secondary compression is thought to be due to the gradual readjustment of the clay particles into a more stable configuration.

A plot of deformation against the logarithm of time during secondary consolidation is practically linear as shown in Fig. (4.25).

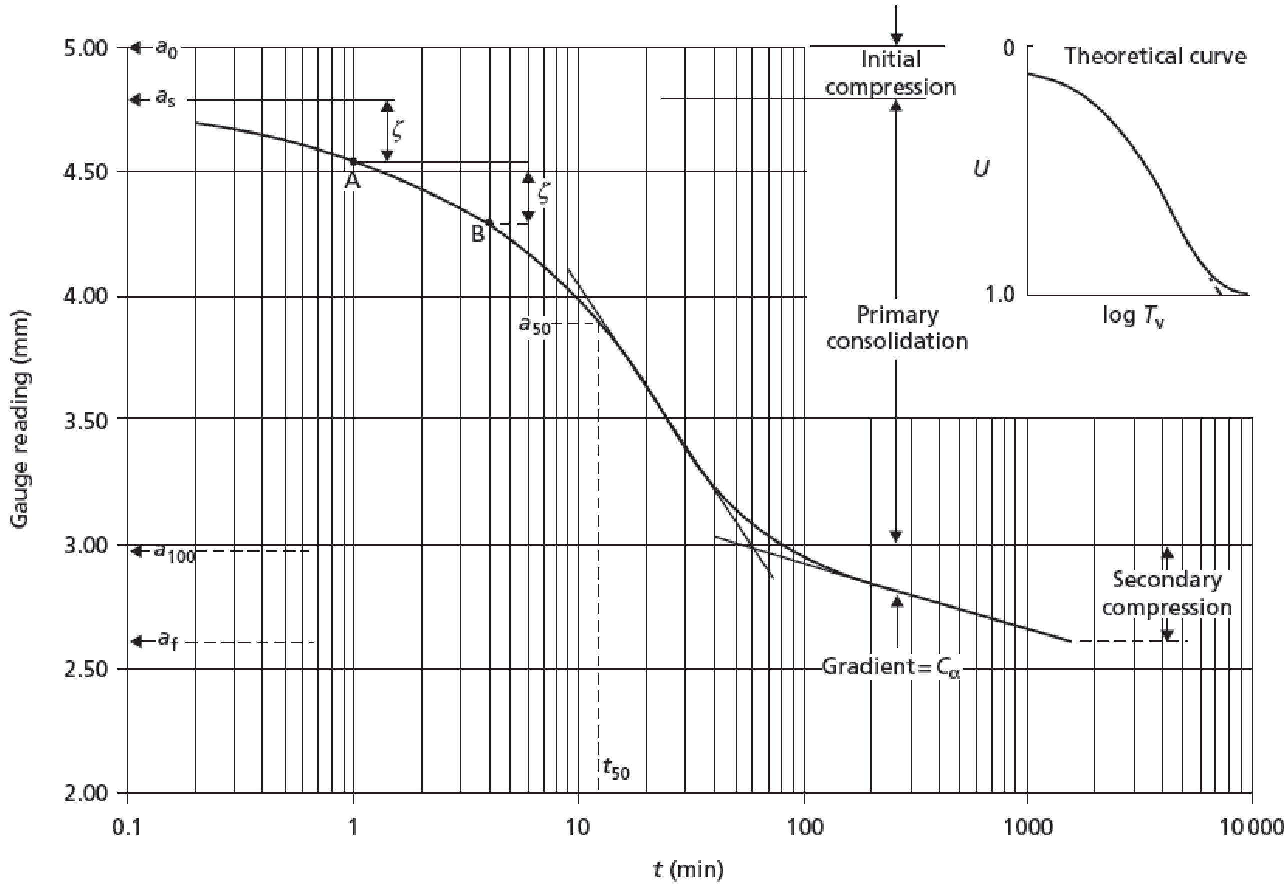

Fig. 4.25 The log time method

The magnitude of the secondary consolidation can be calculated as:

$$S_s = \frac{C_\alpha}{1 + e_p} H_p \log \frac{t}{t_p}$$

where;

C_α : coefficient of secondary compression.

t_p : time required for 100% primary consolidation. (T_v =1 → $t_p = d^2/C_v$)

e_p : void ratio at the end of primary consolidation.

H_p : thickness of layer at the end of primary consolidation.

For practical purposes: $C_\alpha / C_c \approx 0.05$

Note: e_o and H_o may be used for e_p and H_p, respectively, without much loss of accuracy.

4.7 Allowable Settlement

Settlement can be important, even though no rupture is imminent, for three reasons: appearance of the structure, utility of the structure, and damage to the structure.

Settlement can detract from the appearance of a building by causing cracks in exterior masonry walls and/or the interior plaster walls. It can also cause a structure to tilt enough to be detected by human eye.

Settlement can interface with the function of a structure in a number of ways, e.g. cranes and other such equipment may not operate correctly, pumps, compressors may get out of line, and tracking units such as radar become inaccurate.

Settlement can cause structure to fail structurally and collapse even though the F.S. against a shear failure is high.

The following measures of settlement should be considered:

1. Total settlement [(S_1 or S_2) in Fig. (4.26)]
2. Differential settlement [(S_1 - S_2) in Fig. (4.26)]
3. Angular Distortion [{(S_1 - S_2)/L} in Fig. (4.26)]

See Tables (4.4, 4.5, and 4.6) and Fig. (4.27).

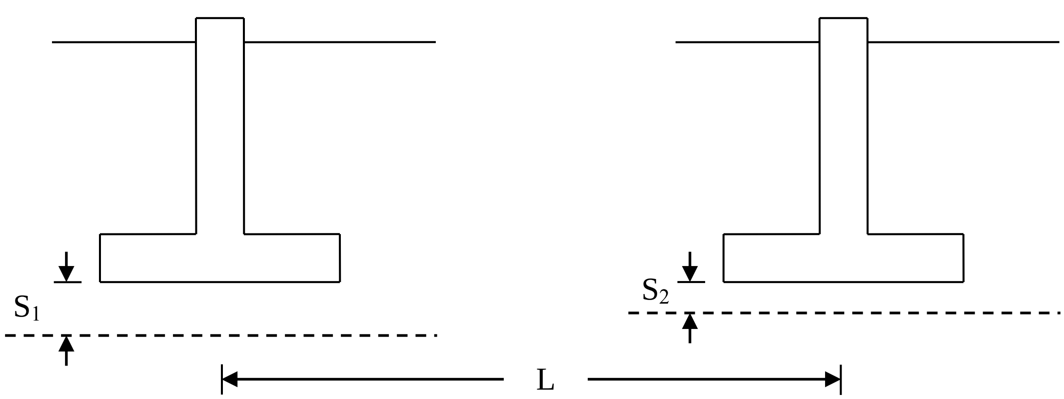

Fig. 4.26

Table 4.4 Allowable Settlement

Type of movement	Limiting factor	Maximum settlement
Total settlement	Drainage	15–30 cm (6–12 in.)
	Access	30–60 cm (12–24 in.)
	Probability of nonuniform settlement:	
	Masonry walled structure	2.5–5 cm (1–2 in.)
	Framed structures	5–10 cm (2–4 in.)
	Smokestacks, silos, mats	8–30 cm (3–12 in.)
Tilting	Stability against overturning	Depends on H and W
	Tilting of smokestacks, towers	$0.004L$
	Rolling of trucks, etc.	$0.01L$
	Stacking of goods	$0.01L$
	Machine operation—cotton loom	$0.003L$
	Machine operation—turbogenerator	$0.0002L$
	Crane rails	$0.003L$
	Drainage of floors	$0.01–0.02L$
Differential movement	High continuous brick walls	$0.0005-0.001L$
	One-story brick mill building, wall cracking	$0.001–0.002L$
	Plaster cracking (gypsum)	$0.001L$
	Reinforced-concrete-building frame	$0.0025–0.004L$
	Reinforced-concrete-building curtain walls	$0.003L$
	Steel frame, continuous	$0.002L$
	Simple steel frame	$0.005L$

Source: Sowers (1962).
Notes: L = distance between adjacent columns that settle different amounts, or between any two points that settle differently. Higher values are for regular settlements and more tolerant structures. Lower values are for irregular settlement and critical structures. H = height and W = width of structure.

Table 4.5 Tolerable differential settlements of buildings, in inches,* recommended maximum values in parentheses

Criterion	Isolated foundations	Rafts
Angular distortion (cracking)	1/300	
Greatest differential settlement:		
Clays	$1\frac{3}{4}(1\frac{1}{2})$	
Sands	$1\frac{1}{4}(1)$	
Maximum settlement:		
Clays	$3(2\frac{1}{2})$	$3–5(2\frac{1}{2}–4)$
Sands	$2(1\frac{1}{2})$	$2–3(1\frac{1}{2}–2\frac{1}{2})$

* MacDonald and Skempton (1955).

Table 4.6 Permissive differential building slopes by the U.S.S.R. code on both unfrozen and frozen ground

All values to be multiplied by L = length between two adjacent points under consideration. H = height of wall above foundation*

Structure	On sand or hard clay	On plastic clay	Average max. settlement, cm
Crane runway	0.003	0.003	
Steel and concrete frames	0.0010	0.0013	10
End rows of brick-clad frame	0.0007	0.001	15
Where strain does occur	0.005	0.005	
Multistory brick wall L/H to 3	0.003	0.004	8 $L/H \geq 2.5$ 10 $L/H \leq 1.5$
Multistory brick wall L/H over 5	0.005	0.007	
One-story mill buildings	0.001	0.001	
Smokestacks, water towers, Ring foundations	0.004	0.004	30
	Structures on permafrost		
Reinforced concrete	0.002–0.0015		15 at 4 cm/year†
Masonry, precast concrete	0.003–0.002		20 at 6 cm/year
Steel frames	0.004–0.0025		25 at 8 cm/year
Timber	0.007–0.005		40 at 12 cm/year

* From Mikhejev et al. (1961) and Polshin and Tokar (1957).
† not to exceed this rate per year.

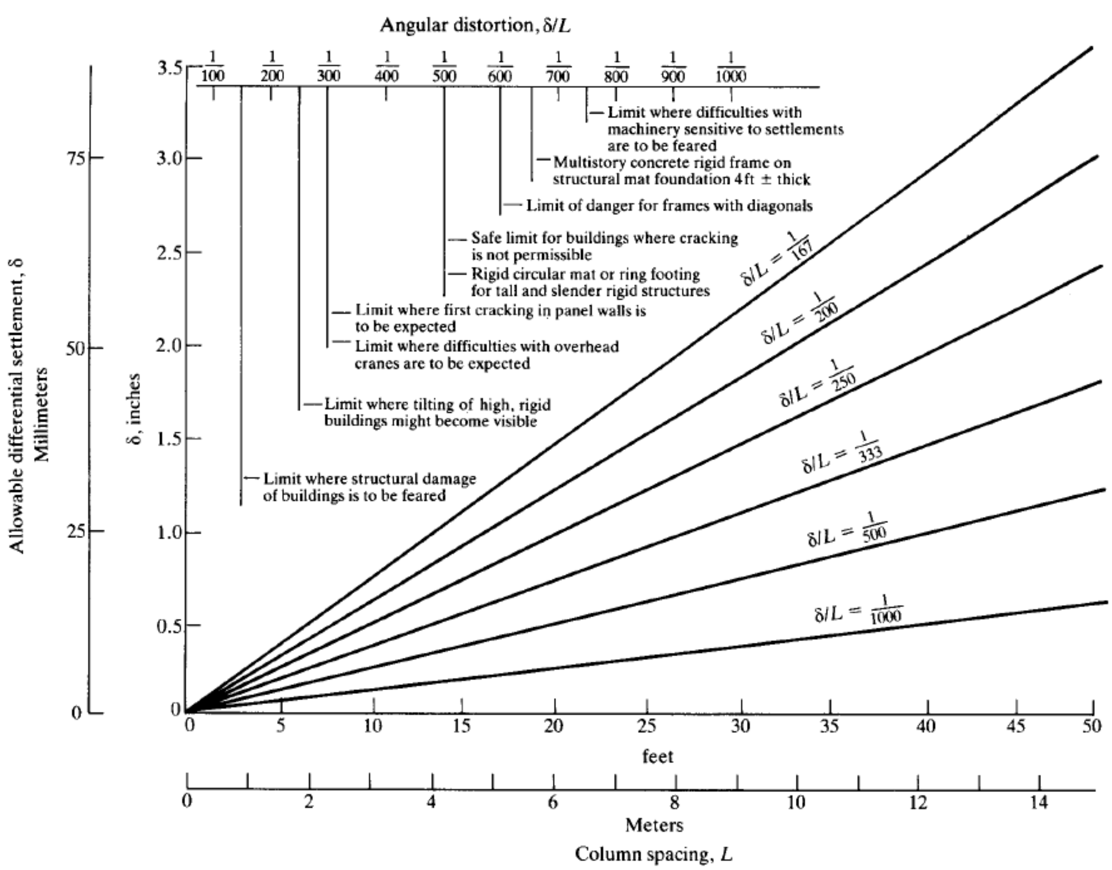

Fig. 4.27 Tolerable settlements for buildings. *(Bjerrum, 1963; Navy, 1982)*

CHAPTER 5
SPREAD FOOTING DESIGN

5.1 Ultimate Strength Design Method (USD) (ACI: 318 - 19)

The ultimate strength design will be used for the structural design of footings (spread, combined, and raft foundation). This method requires converting working design loads to ultimate loads through the use of load factors [ACI: 318-19; Table 5.3.1] as:

$$P_u = 1.2\ DL + 1.6\ LL$$

or $$P_u = 1.2\ DL + 1.0\ W + 1.0\ LL$$

or $$P_u = 0.9\ DL + 1.0\ W$$

For earthquake loading, substitute E for W (wind load).

The ultimate concrete strength f_c' in USD is reduced for workmanship and other uncertainties by use of ϕ factors as shown in Table (5.1).

Table (5.1): Reduction Factors for Ultimate Concrete Strength (f_c')

Design consideration	$\boldsymbol{\phi}$
Moment (tension-controlled)	0.90
Shear	0.75
Compression members, spiral	0.75
Compression members, tied	0.65
Unreinforced footings	0.60
Bearing on concrete	0.65

5.2 Design of R.C. Spread Footings

Steps in design of square or rectangular footings with a concentric load and no moments are as follows:

1. Compute the footing plan dimensions using the allowable soil pressure (q_a):

   Working load; $P_w = DL + LL$

Area of footing; $A = \dfrac{P_w}{q_a}$

For square footing; $B = \sqrt{A}$

For rectangular footing; $B \cdot L = A$

A rectangular footing may have a number of solutions unless either (B or L) is fixed.

2. Convert the working load to an ultimate value (P_u) and find the ultimate design pressure (q_u) as;

$$q_u = \frac{P_u}{A}$$

3. Compute the effective footing depth (d) from diagonal tension shear (punching shear or two-way action shear) or for rectangular footing from wide beam shear (one-way action shear).

   a. Punching shear [see Fig. (5.1)]:

   - For rectangular column section ($b \times c$):

     $P_u = b_o \cdot d \cdot (v_c)_p$

     where b_o = critical perimeter given by:

     $b_o = 2(b+d) + 2(c+d)$ for central column

     $b_o = 2\left(b + \frac{d}{2}\right) + (c+d)$ for edge column

     $b_o = \left(b + \frac{d}{2}\right) + (c + \frac{d}{2})$ for corner column

   - For round column (diameter = a):

     $P_u = b_o \cdot d \cdot (v_c)_p$

     where b_o for central column is given by:

     $b_o = \pi(a+d)$

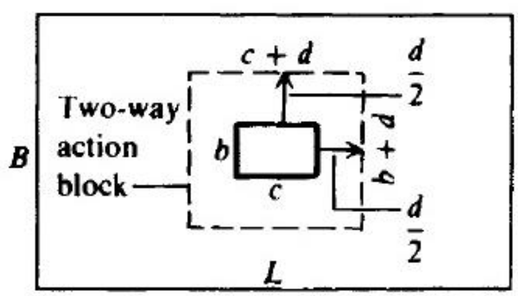

Fig. 5.1 Critical section for two-way action (punching) shear

b. Wide beam shear [see Fig. (5.2)]:

$$L' = \frac{L - c - 2d}{2}$$

$$L' \times 1 \times q_u = d \times 1 \times (v_c)_w$$

$$\left(\frac{L - c - 2d}{2}\right) q_u = d \cdot (v_c)_w$$

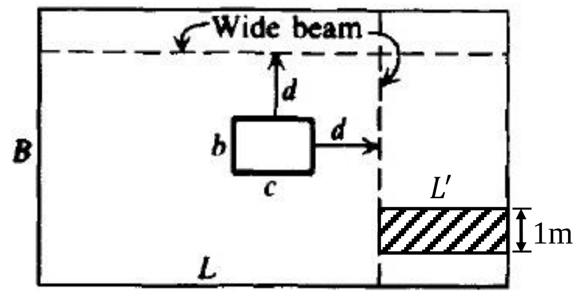

Fig. 5.2 Critical section for wide beam shear

Allowable stresses (ACI: 318-14; Art. 22.6.5.2 and Table 22.5.5.1)

- Allowable stress for punching shear $(v_c)_p$ should be the least of (a), (b) and (c);

$$(a)\ (v_c)_p = 0.33\phi\sqrt{f_c'} \qquad for\ \beta \le 2 \qquad (MPa)$$

$$(b)\ (v_c)_p = 0.17\left(1 + \frac{2}{\beta}\right)\phi\sqrt{f_c'} \qquad for\ \beta > 2 \qquad (MPa)$$

$$(c)\ (v_c)_p = 0.083\left(2 + \frac{\alpha_s d}{b_o}\right)\phi\sqrt{f_c'} \qquad (MPa)$$

where

$$\phi = 0.75$$

$$\beta = \frac{Column\ section\ length}{Column\ section\ width}$$

$$\alpha_s = \begin{cases} 40 & \text{for columns in the center of the footing} \\ 30 & \text{for columns at an edge of a footing} \\ 20 & \text{for columns at a corner of the footing} \end{cases}$$

b_o = the critical perimeter as defined above.

- Allowable stress for one-way shear:

$$(v_c)_w = 0.17\phi\sqrt{f_c'} \qquad (MPa)$$

Note: (ACI: 318-19; Art. 13.3.1.2)

Minimum depth: $d_{min} = 150\ mm$

$$h = d + \frac{\phi}{2} + 75\ mm$$

4. Compute the required steel for bending. The bending moment is computed at the critical section shown in Fig. (5.3). For the length (l) shown, the bending moment per unit width is;

$$M_u = \frac{q_u \cdot l^2}{2}$$

$$M_u = \phi\, b\, d^2 \rho\, f_y \left(1 - 0.59 \frac{\rho\, f_y}{f_c'}\right)$$

- Check $\varepsilon_t \geq 0.005$ (for tension controlled sections) (ACI: 318-19; Table 21.2.2)

  where

$$\varepsilon_t = \frac{(d_t - c)}{c} \times 0.003$$

$$c = \frac{a}{\beta_1} \quad , \quad a = \frac{A_s \cdot f_y}{0.85 f_c' \cdot b}$$

$$\beta_1 = 0.85 - \frac{(f_c' - 28)}{7} \cdot 0.05 \quad , \quad 0.65 \leq \beta_1 \leq 0.85$$ (ACI: 318-19; Table 22.2.2.4.3)

d_t = distance from extreme-compression fiber to extreme-layer of tension steel.

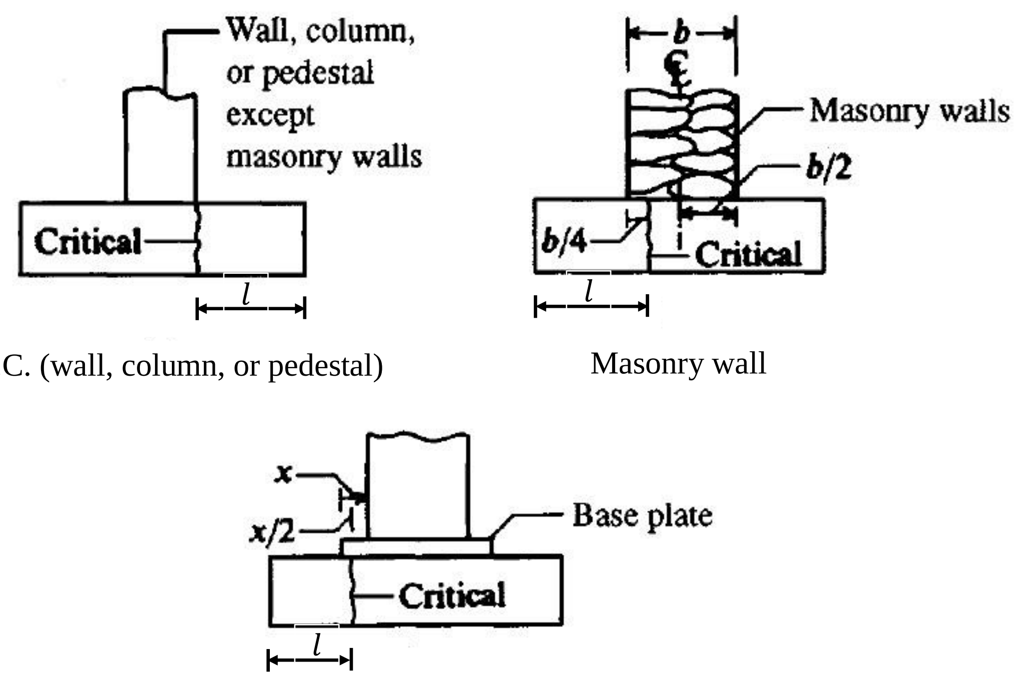

R.C. (wall, column, or pedestal)

Masonry wall

Steel column

Fig. 5.3 Critical sections for computing bending moment

- Check $A_s \geq A_{s,min}$

  $A_{s,min} = 0.0018\ A_g$ (ACI: 318-19; Art. 8.6.1.1)

- Check spacing $S \leq S_{max}$

  $$S_{max} = smaller\ of \begin{cases} 2h \\ 450\ mm \end{cases}$$ (ACI: 318-19; Art. 8.7.2.2)

5. Check the column bearing and use dowels if allowable bearing stress is exceeded. If not, use minimum dowel area.

$$(A_s)_b = (f_b - (f_c)_b) \cdot \frac{A_{col}}{f_y}$$

$$(A_s)_{b,min} = \begin{cases} 0.005\ A_{col} \\ 4\ bars\ at\ least\ (with\ diameter\ not\ less\ than \\ \quad 4\ mm\ of\ the\ column\ bar\ diameter) \end{cases}$$ (ACI: 318-19; Art. 16.3.4.1)

where;

f_b: actual bearing stress, $f_b = \dfrac{P_u}{A_{col}}$

$(f_c)_b$: allowable bearing stress

$(f_c)_b = 0.85\phi\ f_c' \cdot \psi \leq f_c'$ (ACI: 318-19; Table 22.8.3.2)

$\phi = 0.65$

$$\psi = \sqrt{\frac{A_2}{A_1}} \leq 2$$

$A_1 = A_{col.} = b \cdot c$

[See Fig. (5.4)]

$A_2 = (b + 4d)(c + 4d)$

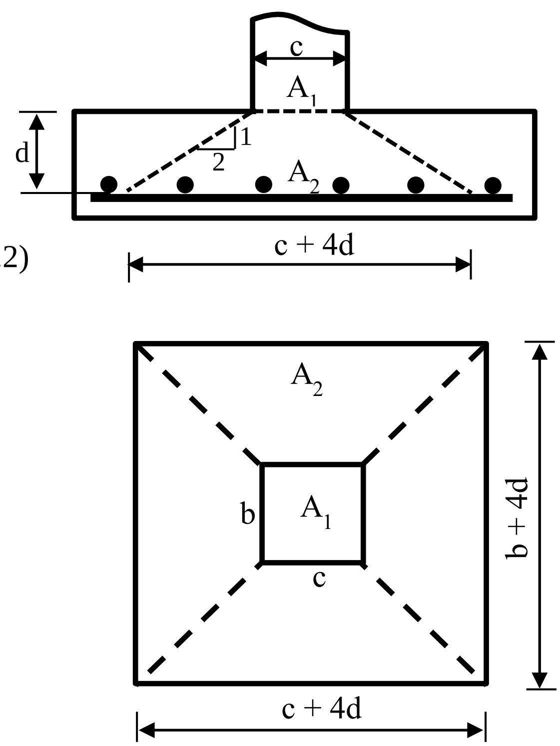

Fig. 5.4 A_1 and A_2 for allowable bearing stress

6. Check development lengths and lap splices [see Fig. (5.5)].

a. Development length for flexure:

$$L_d = 0.019 \frac{A_b \cdot f_y}{\sqrt{f_c'}} \geq 0.058\, d_b \cdot f_y \qquad (for\ d_b \leq 35\ mm)$$

$$L_d = 1.4\, L_d \qquad (for\ top\ bars\ with\ more\ than\ 300\ mm\ of\ concrete\ cast\ below\ the\ bars)$$

b. Development length for compression bars:

$$L_d = 0.24\, f_y \cdot d_b / \sqrt{f_c'}$$

$$= 0.044\, f_y \cdot d_b$$

$$= 200\ mm$$

c. Lap splices for compression bars:

$L_s = 1.7\, L_d$

where

L_d = development length for compression.

7. Make a design sketch.

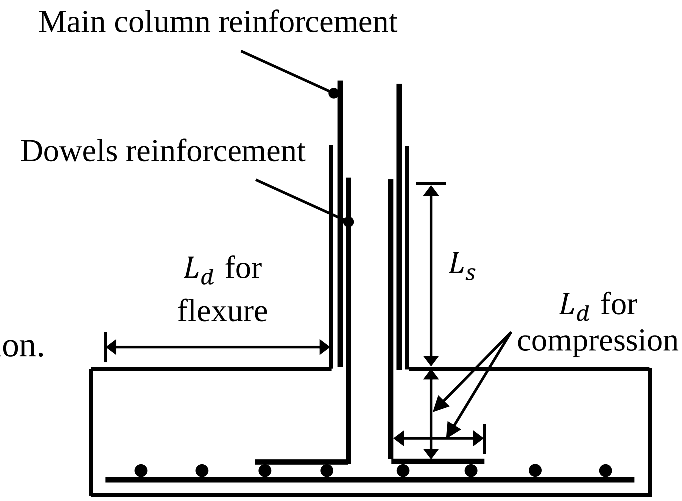

Fig. 5.5 Development lengths and lap splices

5.3 Design of Plain Concrete Spread Footings

For plain concrete footings, the moment requirement is usually the most critical in specifying the footing depth. So, it is required to satisfy the moment requirement and then check for shear.

$$\frac{M_u}{Z} \leq f_t$$

where;

Z: elastic modulus = $\dfrac{d^2}{6}$

f_t: allowable tensile stress:

$f_t = 0.42\phi\sqrt{f_c'}$

where ϕ = 0.6

Note: For plain concrete footing:

$h = d + 50\ mm$ (ACI: 318-19; Art. 14.5.1.7)

$h_{min} = 200\ mm$ (ACI: 318-19; Art. 14.3.2.1)

5.4 Rectangular Footings

Rectangular footings are necessary when;

1. The space in one direction is limited.
2. An overturning moment is present.

Notes:

1. The depth is controlled by wide beam shear (W.B.S.) if $\frac{L}{B} > 1.2$ or when an overturning or eccentric loading is present.
2. Reinforcement in long direction is distributed across the entire width of footing (as in square footing).
3. Reinforcement in short direction is distributed more under column-zone (with width = B) with a percentage (γ) of the total reinforcement where [see Fig. (5.6)]:

$$\gamma = \frac{2}{1+\beta}$$ (ACI: 318-19; Art. 13.3.3.3)

where

$$\beta = \frac{footing\ length}{footing\ width}$$

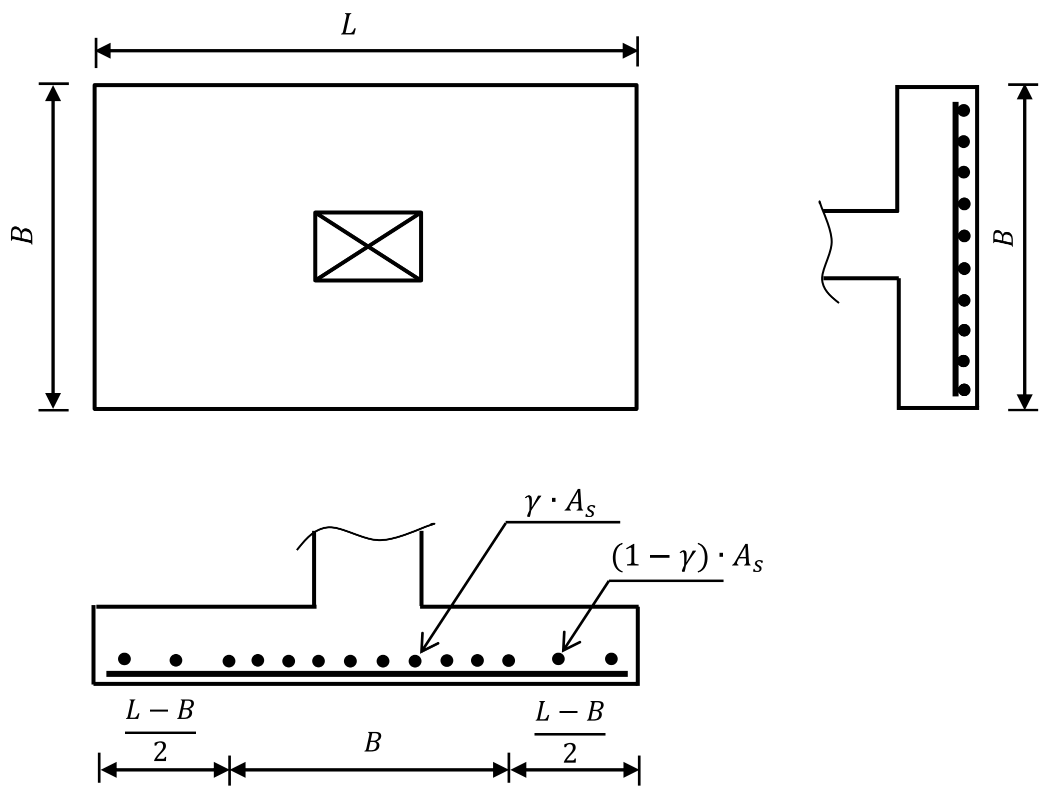

Fig. 5.6

5.5 Eccentrically Loaded Spread Footings

First we will consider the case of eccentrically loaded footing about one axis [see Fig. (5.7)]. Let M be the resultant moment around the centerline of the footing given by:

$$M = m + H \cdot z + V \cdot a$$

Then, from static equilibrium, we get:

$$\sum M_{₵} = 0$$

$$M - V \cdot e = 0$$

or $$e = \frac{M}{V}$$

The soil pressure distribution beneath the footing can be computed from principles of mechanics of materials to get:

$$q = \frac{V}{A} + \frac{M \cdot x}{I_y}$$

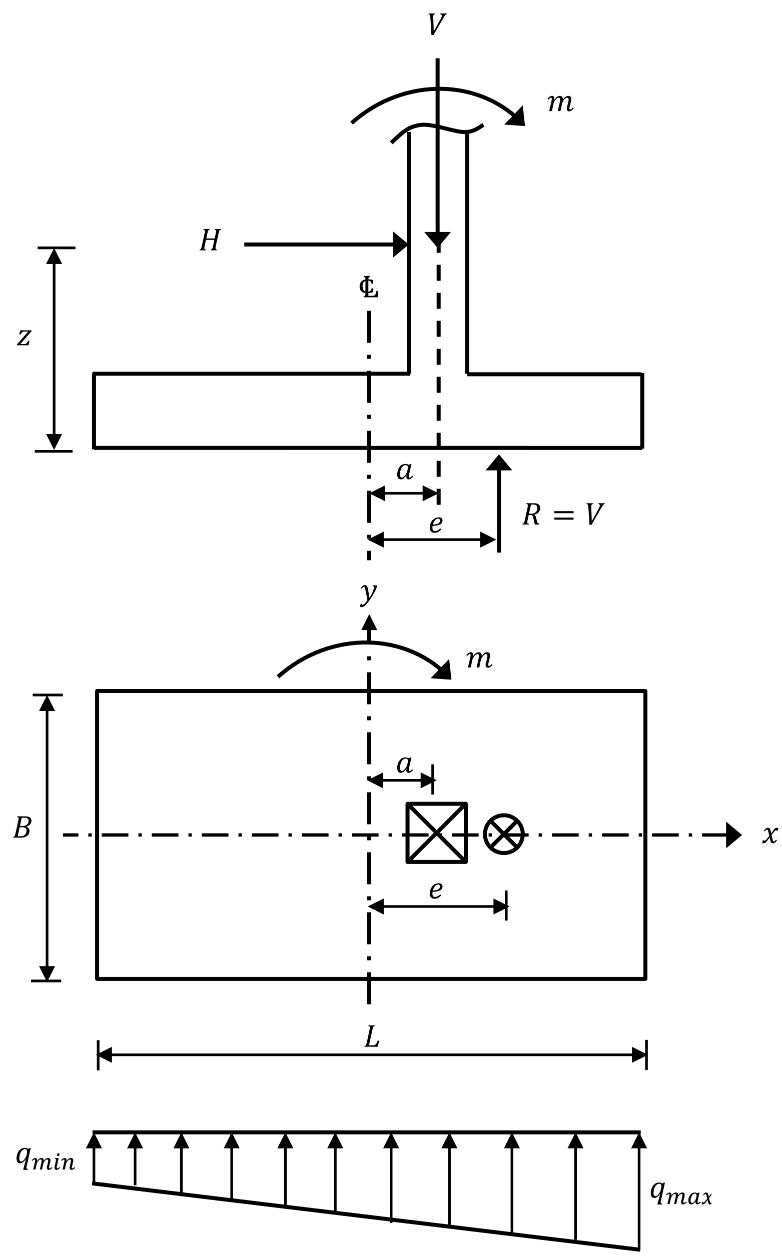

Fig. 5.7

The above formula can be generalized for the case when the eccentricity about both axes which yields [see Fig. (5.8)]:

$$q = \frac{V}{A} + \frac{M_x \cdot y}{I_x} + \frac{M_y \cdot x}{I_y}$$

and $$e_x = \frac{M_y}{V} \quad , \quad e_y = \frac{M_x}{V}$$

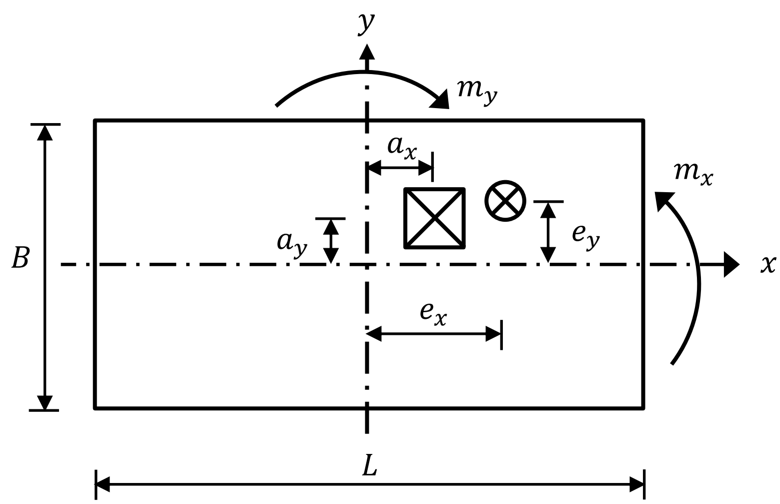

Fig. 5.8

where

$M_x = m_x + H_y \cdot z_y + V \cdot a_y$

$M_y = m_y + H_x \cdot z_x + V \cdot a_x$

V= Vertical load (column load).

a_x, a_y = Coordinates of the vertical load (column).

H_x, H_y = Components of horizontal force in the directions of x and y, respectively (positive components directed in the positive directions of coordinate axes).

z_x, z_y = lever arms of the horizontal components measured to the base of footing.

m_x, m_y = applied moments about x and y axes, respectively. Moments directed toward the first quarter are taken positive as shown in Fig. (5.8).

e_x, e_y = coordinates (eccentricities) of the soil pressure resultant (R).

x, y = coordinates of the point at which the soil pressure is computed.

A = area of footing; $A = B \cdot L$

I_x, I_y = moments of inertia about x and y axes:

$$I_x = \frac{L \cdot B^3}{12} \qquad I_y = \frac{B \cdot L^3}{12}$$

Three general cases can be recognized for the distribution of soil pressure depending on the value of eccentricity:

<u>Case I</u>: Uniform soil pressure ($e = 0$) [see Fig. (5.9)]

If $e = 0$, the soil pressure will be uniform.

$$e = \frac{M}{V} = 0 \;\rightarrow\; M = 0$$

or $$m + H \cdot z + V \cdot a = 0$$

$$Thus, \quad a = -\frac{m + H \cdot z}{V}$$

and the soil pressure is given by:

$$q = \frac{V}{A} \le q_a$$

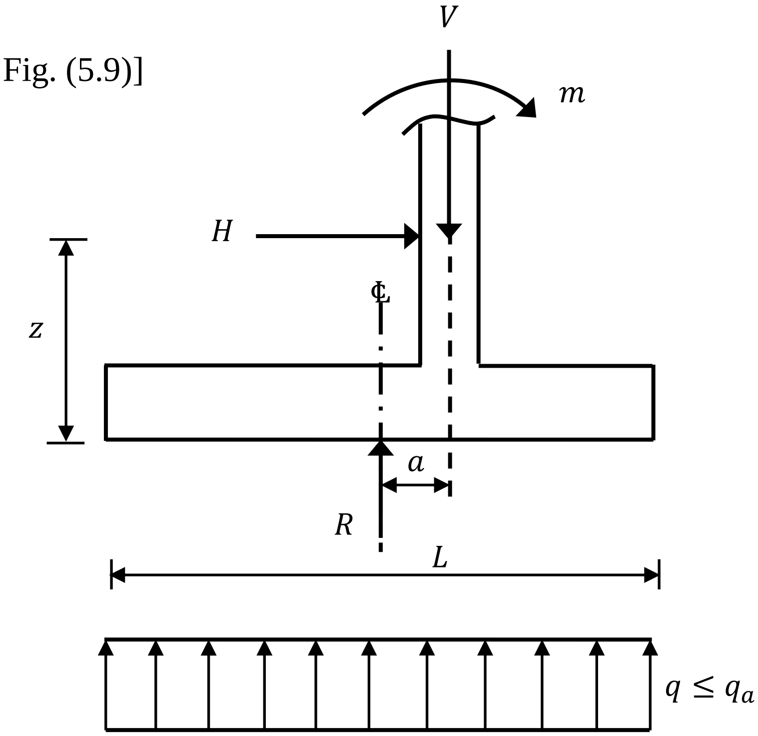

Fig. 5.9

<u>Case II</u>: Eccentricity at middle third $(e \le \frac{L}{6})$[see Fig. (5.10)]

$$q = \frac{V}{A} + \frac{M \cdot x}{I_y} \le q_a$$

For eccentricity about both axes:

$$q = \frac{V}{A} + \frac{M_x \cdot y}{I_x} + \frac{M_y \cdot x}{I_y} \le q_a$$

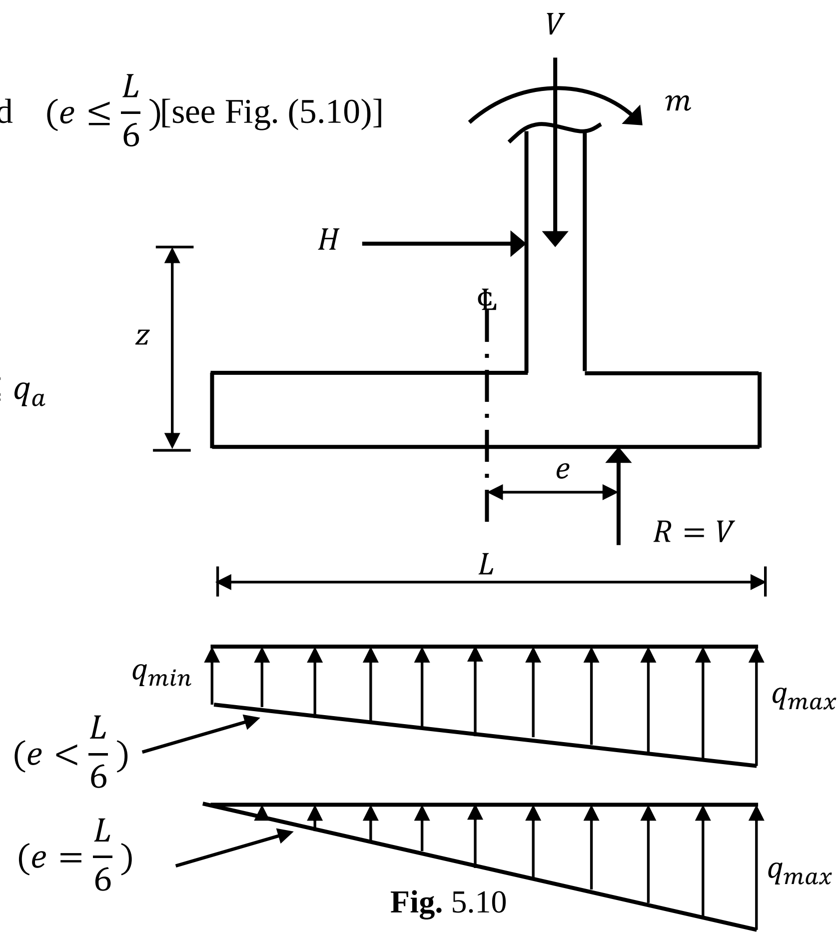

Fig. 5.10

Case III: Eccentricity out of middle third $\left(e > \frac{L}{6}\right)$ [see Fig. (5.11)]

$$\frac{L'}{3} = \frac{L}{2} - e$$

$$L' = 3\left(\frac{L}{2} - e\right)$$

$$V = \frac{1}{2} q_{max} \cdot BL'$$

Put: $q_{max} = q_a$

$$\therefore \ \frac{2V}{3B\left(\frac{L}{2} - e\right)} = q_a$$

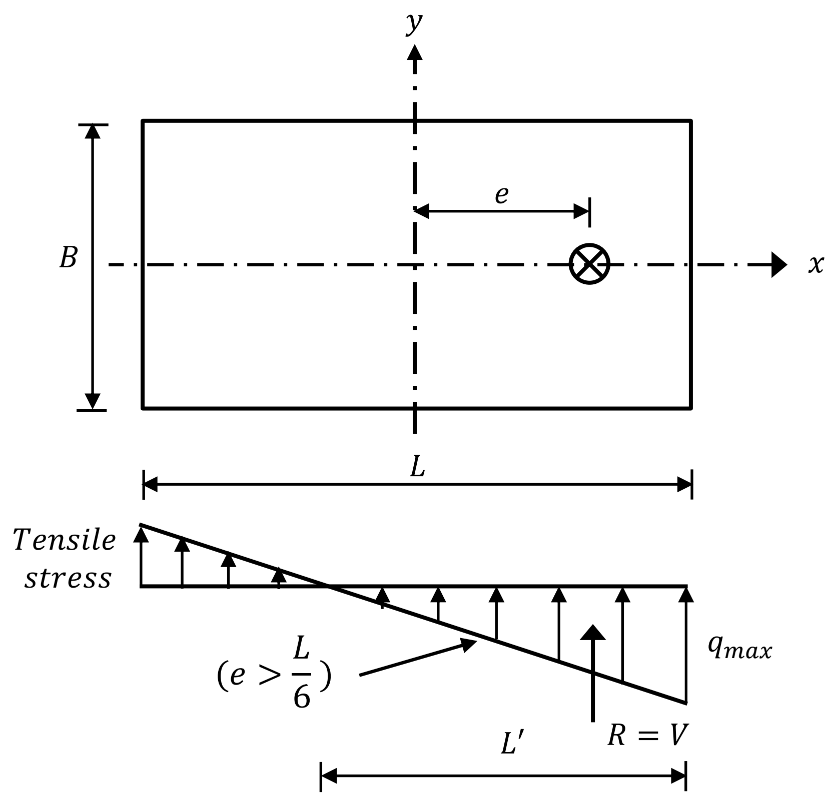

Fig. 5.11

CHAPTER 6

COMBINED FOOTING DESIGN

6.1 Introduction

When a footing supports a line of two or more columns, it is called a *combined footing*. A combined footing may have either rectangular or trapezoidal shape or be a series of pads connected by narrow rigid beams called a *strap footing*.

Combined footings are necessary when:

1. The columns as very close that the area of individual foundation for each column will overlap [Fig. (6.1)].

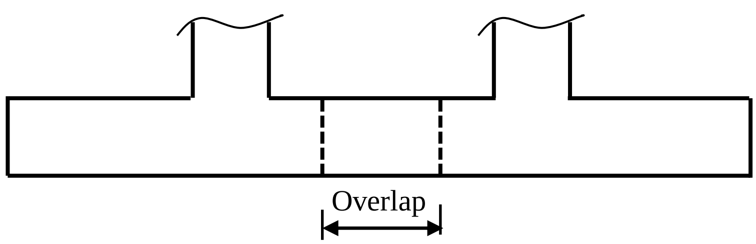

Fig. 6.1

2. There is a space limitation that the column is not possible to place at the center of spread footing. Columns located off center will result in a nonuniform soil pressure. In order to avoid the nonuniform soil pressure, the footing geometry is made such that the column loads in the center of the footing. The three types of combined footing are shown in Fig. (6.2).

6.2 Rectangular Combined Footing

It is used when the load on the exterior column is less than that on the interior column. The footing dimensions are made in such a way to produce a uniform soil pressure. The basic assumption in design is that the footing is rigid so that the soil pressure is linear. The design steps are as follows [see Fig. (6.3)]:

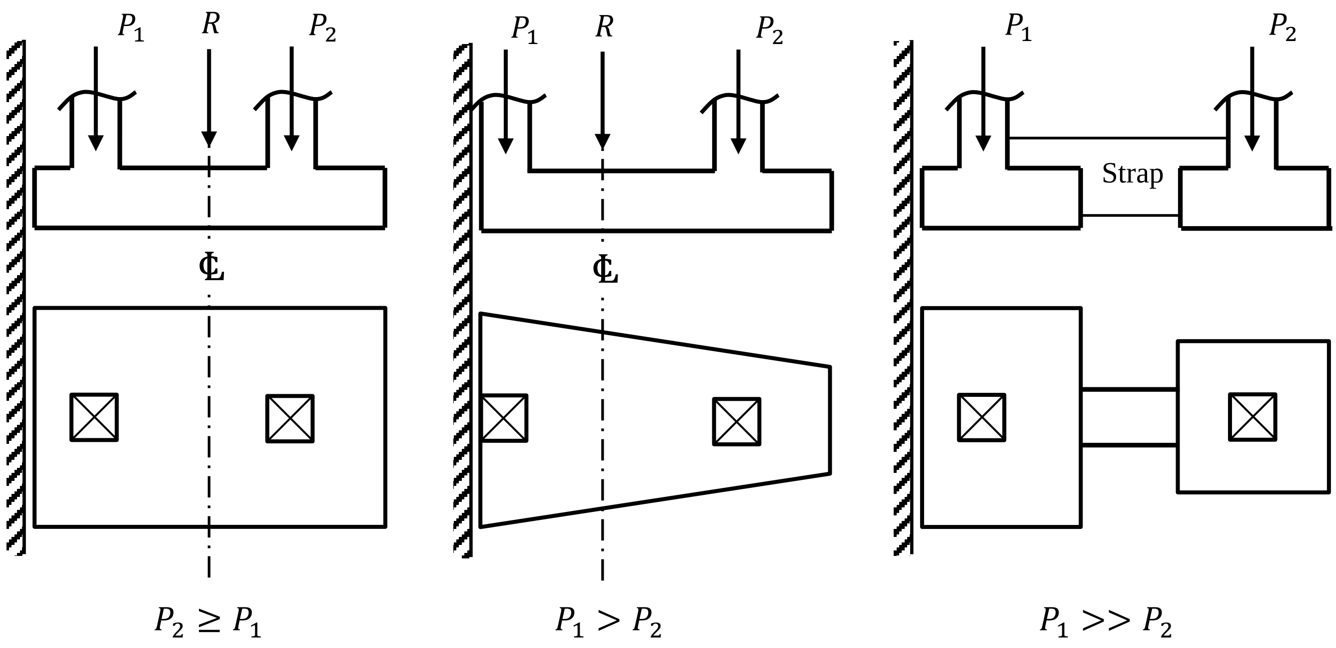

Rectangular Combined footing Trapezoidal Combined footing Strap footing

Fig. 6.2 Possible types of combined footing

1. Find the footing length (L):

$$\bar{x} = \frac{P_{u2} \times S + M_{u1} + M_{u2}}{P_{u1} + P_{u2}}$$

For uniform soil pressure, the resultant of factored loading should act at the centroid of footing, or:

$$L = 2(c + \frac{w_1}{2} + \bar{x})$$

$$L_{min} = S + \frac{w_1 + w_2}{2} + c$$

If $L < L_{min}$, use other shape (trapezoidal or strap).

2. Find the footing width (B) and the ultimate soil pressure (q_u):

$$B = \frac{\sum P_w}{q_a \cdot L}$$

$$A = B \cdot L$$

$$q_u = \frac{\sum P_u}{A}$$

3. Find the depth based on D.T.S. or W.B.S.
4. Find the required flexural steel for the design bending moments at critical sections.
5. Check column bearing on the base.
6. Prepare a final design sketch.

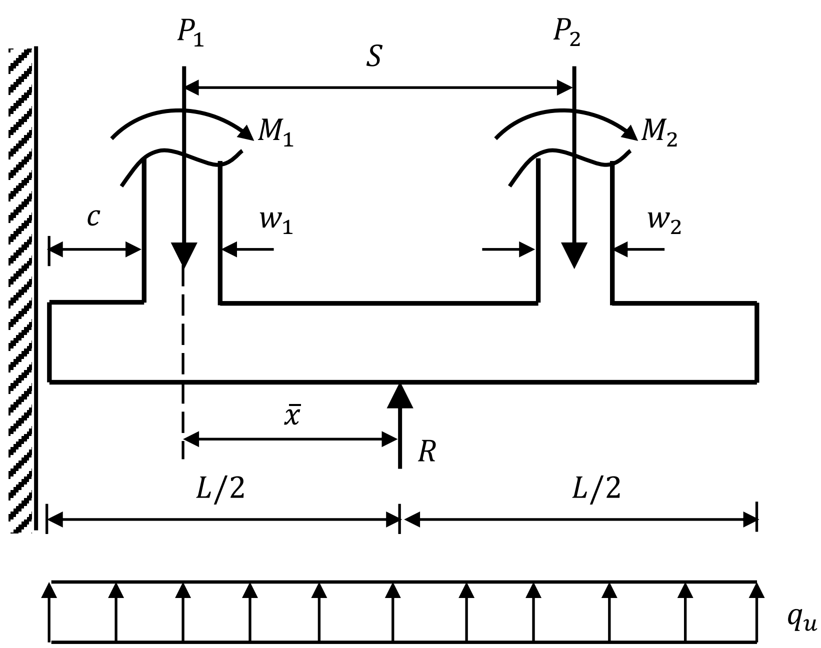

Fig. 6.3 Rectangular combined footing

Notes

1. For the long direction, the minimum area of flexural reinforcement shall be the larger of (a) or (b) [ACI: 318-19; Art. 9.6.1.2]:

$$(a)\ A_{s,min} = \frac{0.25\sqrt{f_c'}}{f_y} b_w \cdot d$$

$$(b)\ A_{s,min} = \frac{1.4}{f_y} b_w \cdot d$$

2. For the bending reinforcement in the short direction [see Fig. (6.4)]:

   - The zones closest to the columns are most effective and should be reinforced for flexure.

   - For the remainder zones, use T & S steel.

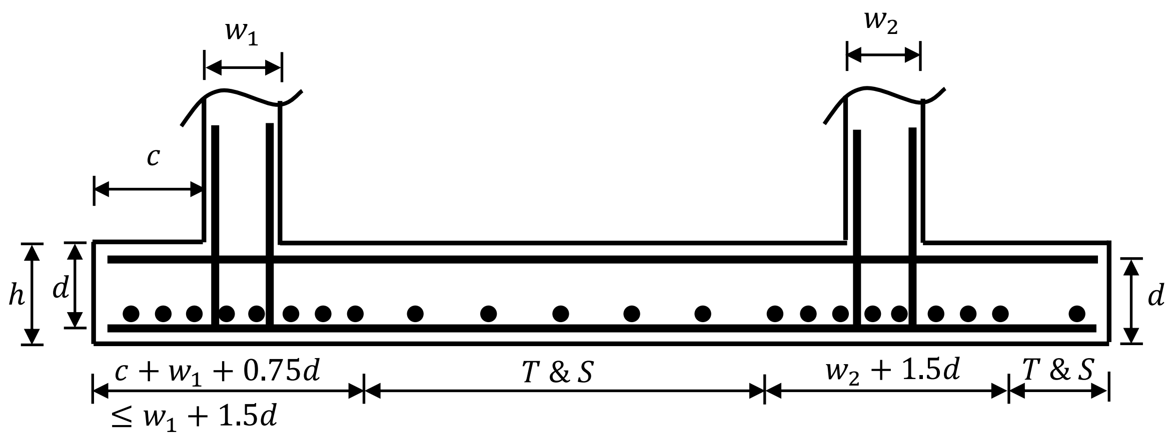

Fig. 6.4 Details of reinforcement in short direction

6.3 Trapezoidal Combined Footing

A combined footing will be trapezoid-shaped if the column which has too limited space for a spread footing carries the larger load. In this case doubling the centroid distance will not provide sufficient length to reach the interior column. The footing geometry necessary for this type is illustrated in Fig. (6.5).

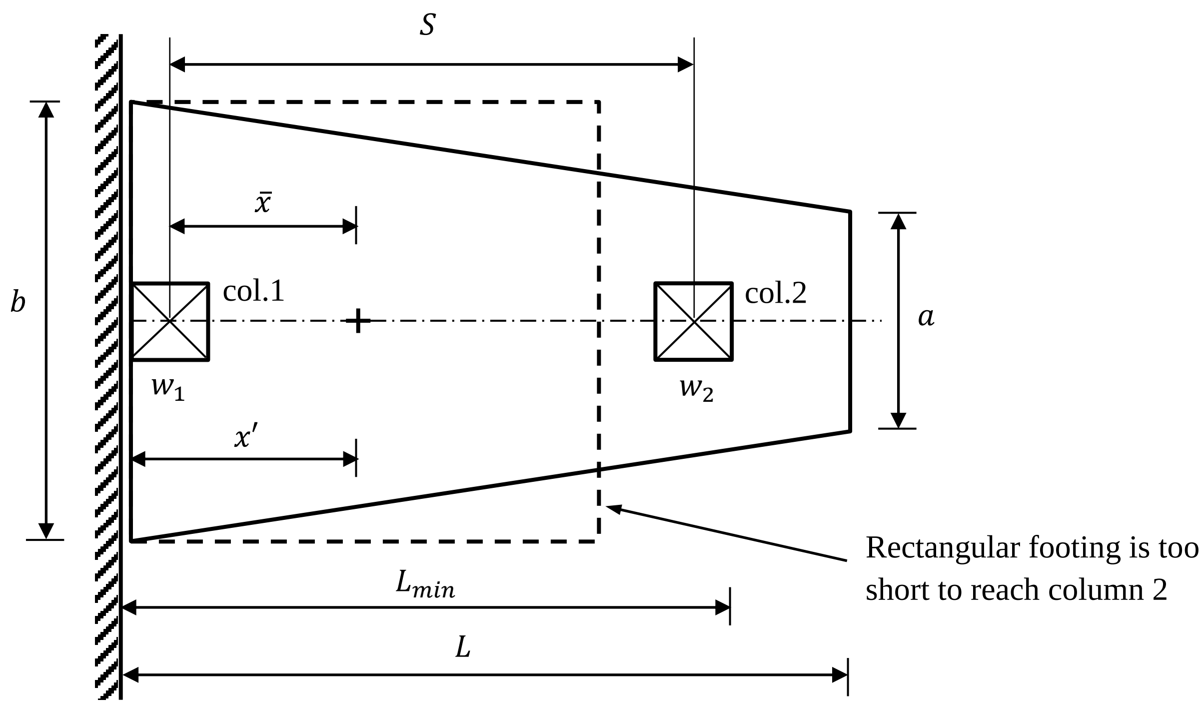

Fig. 6.5 Geometry of trapezoidal combined footing

$$x' = \bar{x} + \frac{w_1}{2}$$

$$L_{min} = S + \frac{w_1 + w_2}{2}$$

- If $x' > \frac{L_{min}}{2}$ → Rectangular C.F.
- If $\frac{L_{min}}{3} < x' < \frac{L_{min}}{2}$ → Trapezoidal C.F.

- If $\frac{L_{min}}{3} > x'$ $\rightarrow$ Strap footing

Dimensions of Combined Footing

- Take $L \geq L_{min}$
- Compute the required area: $A = \frac{\sum P_w}{q_a}$
- Find a and b from the following equations:

$$A = \frac{a+b}{2} \times L \qquad (1)$$

$$x' = \frac{2a+b}{a+b} \times \frac{L}{3} \qquad (2)$$

6.4 Strap (or Cantilever) Footing

A strap footing is used to connect an eccentrically loaded column footing to an interior column as shown in Fig. (6.6). The strap is used to transmit the moment caused from eccentricity to the interior column footing so that a uniform soil pressure is computed beneath both footings.

The strap footing may be used as an alternative to the rectangular or trapezoidal footing if:

1. The exterior column load is very large $\left(x' < \frac{L_{min}}{3}\right)$.
2. The distance between columns is large and/or the allowable soil pressure is relatively large so that the additional footing area is not needed.

6.4.1 Basic Considerations for Strap Footing Design

1. Strap must be rigid ($I_{strap}/I_{footing} > 2$). This rigidity is necessary to control rotation of the exterior footing.
2. Footings should be proportioned for approximately equal soil pressure and avoidance of large difference in B to reduce differential settlement.
3. Strap should be out of contact with soil so that no soil reactions are developed.
4. Design the strap as a beam if the clear span is greater than $4h$, where h is the overall depth. Otherwise, the strap should be designed as a deep beam.

Footings Dimensions

$$q_u = \frac{\sum P_u}{\sum P_w} \cdot q_a$$

$$R_1 = P_{u1} \cdot \frac{S}{S'} \qquad ; \qquad R_2 = \sum P_u - R_1$$

The eccentricity e is to be assumed.

$$L_1 = 2(e + x) \qquad ; \qquad B_1 = \frac{R_1}{q_u \cdot L_1}$$

$$B_2 = \sqrt{\frac{R_2}{q_u}}$$

Check B_1 and B_2 for differential settlement.

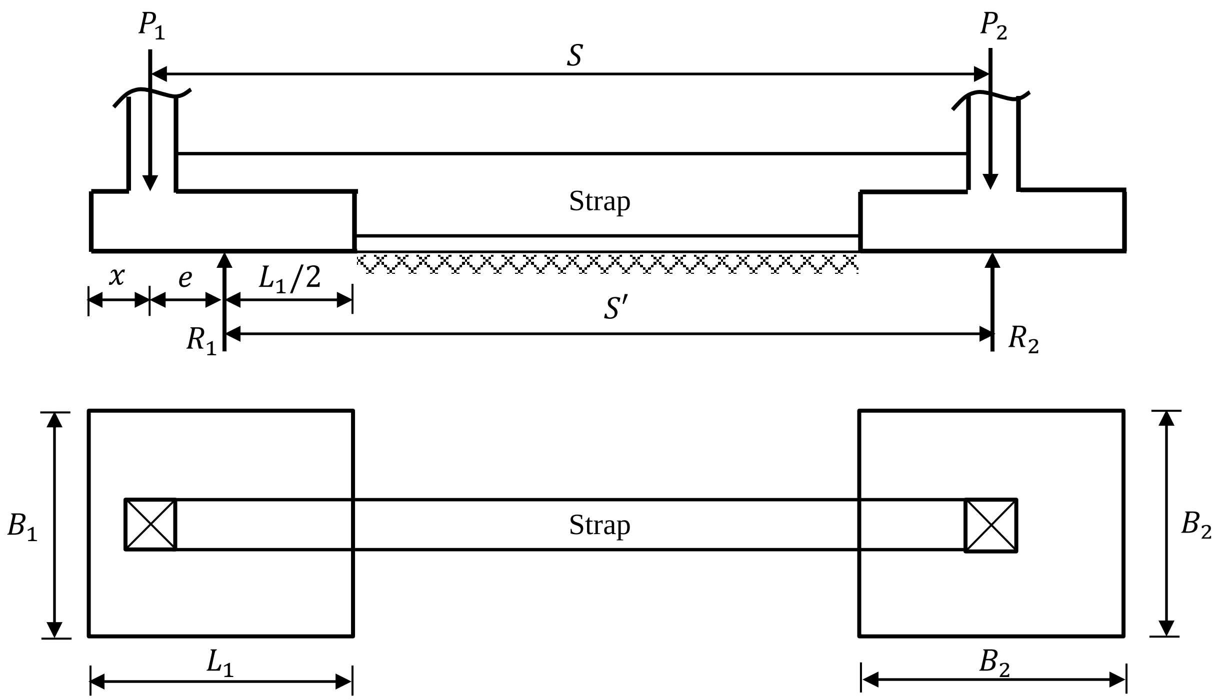

Fig. 6.6 Assumed loading and geometry of strap footing

CHAPTER 7
MAT (RAFT) FOUNDATION DESIGN

7.1 Introduction

A mat foundation is a large concrete slab used to interface one or more columns in several lines with the base soil. Mats are commonly used beneath silo clusters, chimney and various tower structures. Buoyancy rafts and basements (or box foundations) have an important function in that they utilize the principle of buoyancy to reduce the net load on the soil. In this way the total settlement of the foundation is reduced and it follows that the differential settlement will also be reduced.

A mat foundation may be used:

1. Where the soil has a low bearing capacity and/or column loads are so large that more than 50% of the area is covered by conventional spread footings.
2. For deep basements to provide the floor slab for the basement. A particular advantage for basements at or below GWT is to provide a water barrier.
3. If the soil conditions at the site vary so that raft foundation is necessary to reduce the differential settlement.
4. If there are any compressible soil lenses in the subsoil, it is better to design a raft foundation to bridge these compressible lenses.

Mat foundations may be supported by piles in situations such as high groundwater (to control buoyancy) or where the base soil is susceptible to large settlements. We should note that a portion of the mat contact stresses will penetrate the ground to a greater depth or have a greater intensity at a shallower depth, both factors tend to increase settlements unless there is stress compensation from excavated soil so that the “net” increase in pressure is controlled.

7.2 Types of Mat Foundations

Figure (7.1) illustrates several possible mat-foundation configurations. The most common mat design consists of a flat concrete slab with continuous two-way reinforcement top and bottom.

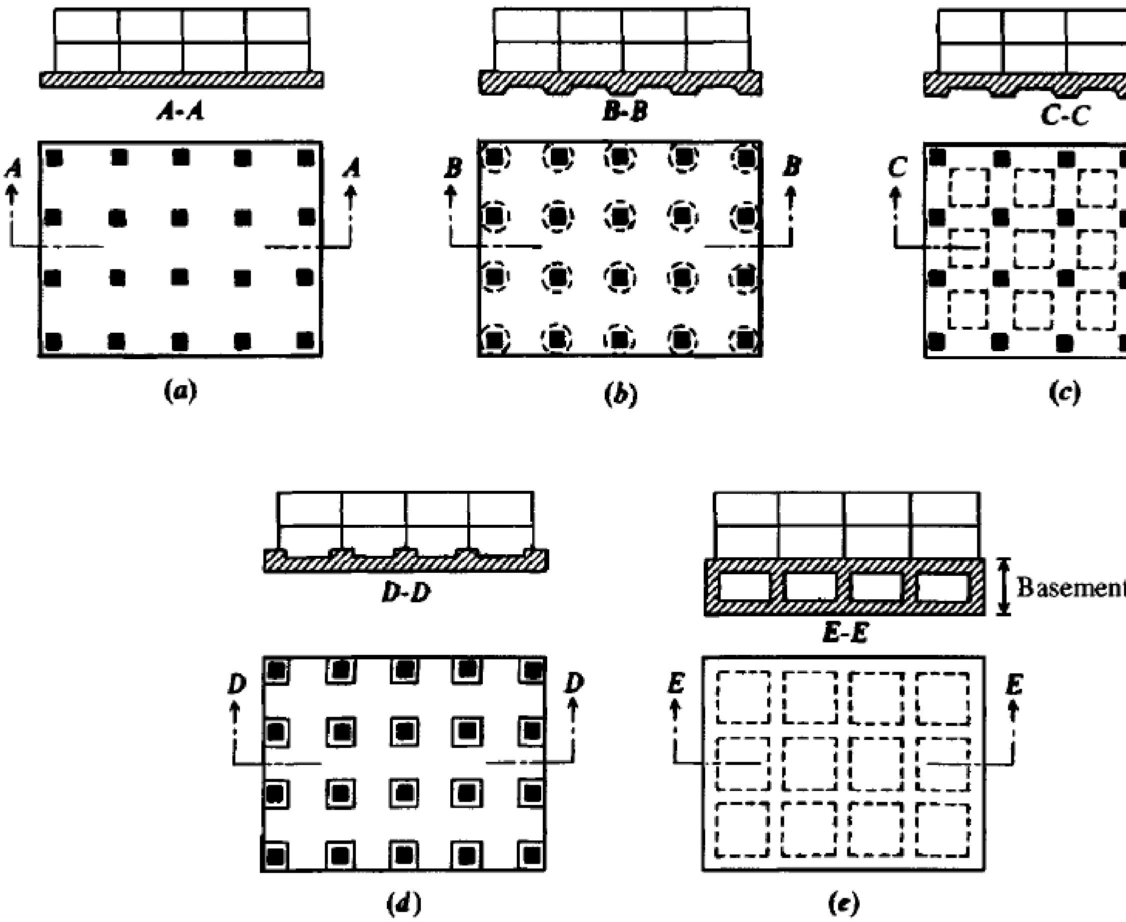

Fig. 7.1 Common types of mat foundations; (a) flat plate; (b) plate thickened under columns; (c) beam-and-slab (waffle slab); (d) plate with pedestals; (e) basement walls as part of mat

7.3 Bearing Capacity of Mat Foundations

A mat must be stable against a deep shear failure which may result in either a rotational failure (G.S.F.) or a vertical (punching) failure. The bearing capacity equations of conventional shallow foundations [Table (3.1)] may be used to compute the soil capacity, e.g.,

$$q_{ult} = c \cdot N_c \cdot s_c \cdot d_c \cdot i_c + \bar{q} \cdot N_q \cdot s_q \cdot d_q \cdot i_q + 0.5\gamma \cdot B \cdot N_\gamma \cdot s_\gamma \cdot d_\gamma \cdot i_\gamma$$

or $$q_{ult} = 5.14 s_u (1 + s_c' + d_c' - i_c') + \bar{q}$$

When the bearing capacity is based on standard penetration test (SPT) in sands and sandy gravel, one may use the Meyerhof formula as follows:

$$q_a = \frac{N}{0.08}\left(\frac{S_a}{25}\right) K_d \qquad kPa$$

where

$$K_d = 1 + 0.33\frac{D_f}{B} \leq 1.33$$

S_a = allowable settlement (mm)

For CPT, the allowable bearing capacity can be estimated as:

$$q_a = \frac{q_c}{20} \qquad kPa$$

where: q_c = cone-point resistance (kPa)

7.4 Mat Settlements

Mat foundations are commonly used where settlements may be problem as where a site contains erratic deposits or lenses of compressible materials, suspended boulders, etc. The settlement to be controlled via:

1. Lower soil contact pressure.
2. Displaced volume of soil (floating effect). Theoretically if the weight of excavation equals the combined weight of the structure and mat, the system "float" in the soil mass and no settlement occurs.
3. Bridging effects due to:
   a. Mat rigidity.
   b. Superstructure-rigidity contribution to the mat.

The floating effect should enable most mat settlements to be limited to 50-80 mm. A problem of more considerable concern is the differential settlement. Again the mat tends to reduce this value. It can be seen that bending moments and shear forces induced in the superstructure depends on relative movement Δ between beam ends [Fig. (7.2)]. Mat continuity results in a somewhat less assumed amount of differential settlement relative to the total expected settlement versus a spread footing as follows:

Foundation type	Expected max settlement (mm)	Expected differential settlement (mm)
Spread	25	20
Mat	50	20

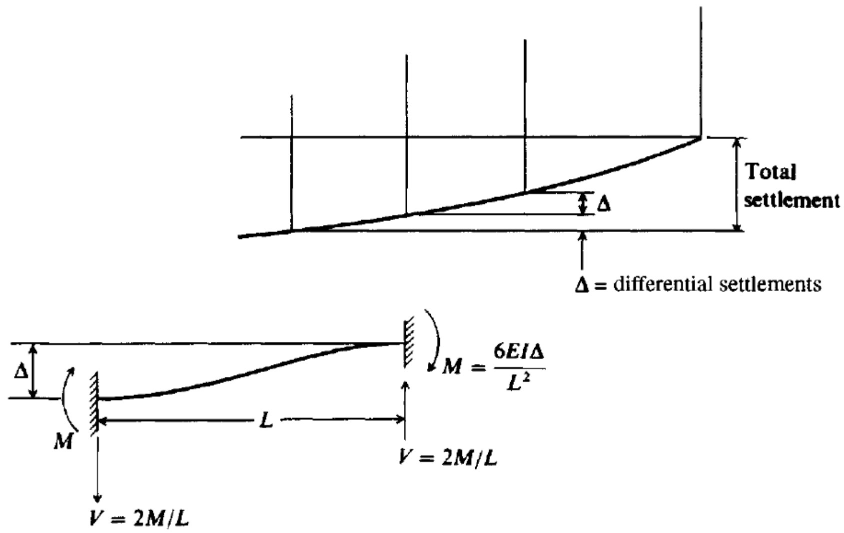

Fig. 7.2 Reduction of bending moments in superstructure by using mat foundation. Bending moment *M* is based on differential settlement between columns and not on total settlement.

7.5 Design of Mat Foundations

There are several methods which can be used to design a mat foundation:

1. Approximate rigid (conventional) method.

   used when:

   - columns are regularly spaced.
   - the distance between adjacent columns or the adjacent column loads do not differ by over about (20%).
   - column spacing < (1.75/λ), where:

$$\lambda = \sqrt[4]{\frac{k_s \cdot B}{4EI}}$$

k_s = modulus of sub-grade reaction.

= the pressure required to produce unit deflection (units; F/L^3).

$\approx 40\ q_{ult}$ kN/m^3

B = width of strip of mat between centers of adjacent bays.

E = modulus of elasticity of concrete.

I = moment of inertia of the strip of width (B).

This method is not recommended at present because of the substantial amount of approximations and the wide availability of computer programs that are relatively easy to use (the finite grid method in particular).

2. Approximate flexible method: This method was suggested by ACI committee 336 (1988).
3. Discrete element methods: In these the mat is divided into elements by gridding. These methods include the following:
   a. Finite-difference method (FDM)
   b. Finite-element method (FEM)
   c. Finite-grid method (FGM)

7.6 Conventional (Rigid) Method of Mat Analysis

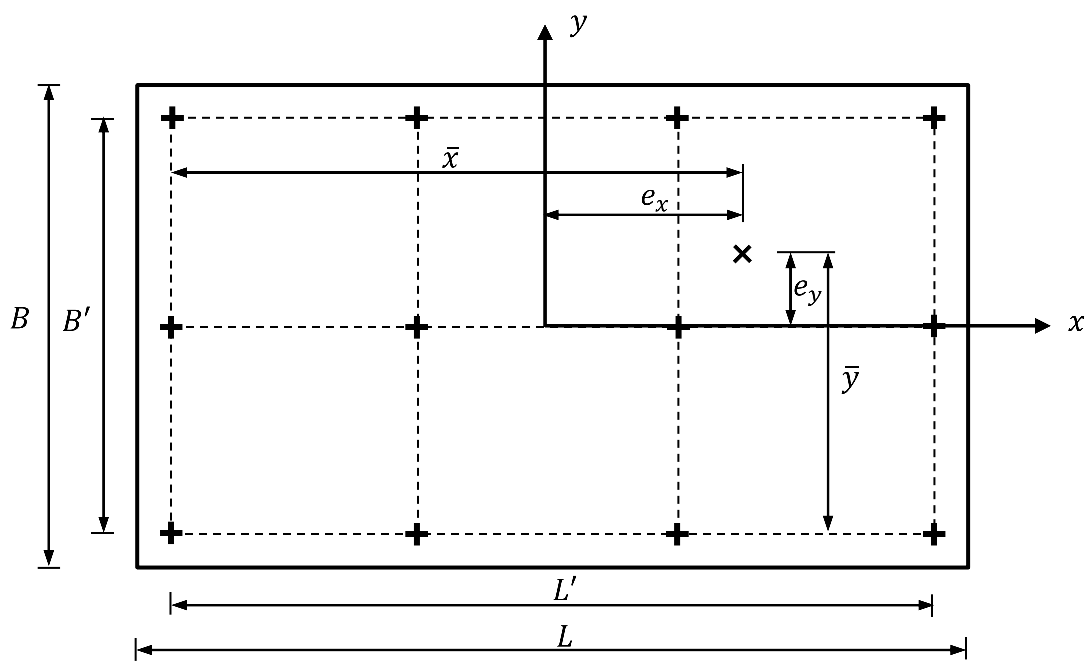

Fig. 7.3 Rigid Mat Design

<u>Design steps</u> [see Fig. (7.3)]:

1. Find the magnitude of resultant of working loads (R_w) and the eccentricity in both directions (e_x and e_y).

$$R_w = \sum (P_w)_i$$

$$\bar{x} = \frac{\sum (P_w)_i \cdot x_i'}{\sum (P_w)_i} \quad , \quad \bar{y} = \frac{\sum (P_w)_i \cdot y_i'}{\sum (P_w)_i}$$

$$e_x = \bar{x} - \frac{L'}{2} \quad , \quad e_y = \bar{y} - \frac{B'}{2}$$

2. Compute the actual soil pressure (based on working loads) at different points beneath the mat:

$$q = R\left(\frac{1}{A} + \frac{e_x \cdot x}{I_y} + \frac{e_y \cdot y}{I_x}\right) \leq q_a$$

where

$$A = B \cdot L$$

$$I_x = \frac{L \cdot B^3}{12} \qquad I_y = \frac{B \cdot L^3}{12}$$

3. Covert the actual soil pressure to ultimate values for USD.
4. Find depth to satisfy shear requirements.
5. Find bending moments in the several mat strips by constructing the bending moment diagram for each strip (noting that each strip must satisfy the condition of vertical equilibrium), [or simply using ($\omega \cdot l^2/10$)].
6. Find the reinforcing steel according to the ACI-Code requirements.

CHAPTER 8

PILE FOUNDATIONS - SINGLE PILE ANALYSIS

8.1 Introduction

Piles are structural members of timber, concrete, and/or steel that are used to transmit surface loads to lower levels in the soil mass. This transfer may be by vertical distribution of the load along the pile shaft or a direct application of load to a lower stratum through the pile point. A vertical distribution of the load is made using a *friction* (or *floating*) pile and a direct load application is made by a point, or *end-bearing*, pile [See Fig. (8.1)].

Piles are commonly used for the following purposes:

1. To carry the superstructure loads into or through a soil stratum. Both vertical and lateral loads may be involved.
2. To resist uplift, or overturning, forces, such as for basement mats below the water table or to support tower legs subjected to overturning from lateral loads such as wind.
3. To compact loose, cohesionless deposits through a combination of pile volume displacement and driving vibrations. These piles may be later pulled.
4. To control settlements when spread footings or a mat is on a marginal soil or is underlain by a highly compressible stratum.
5. In offshore construction to transmit loads above the water surface through the water and into the underlying soil.

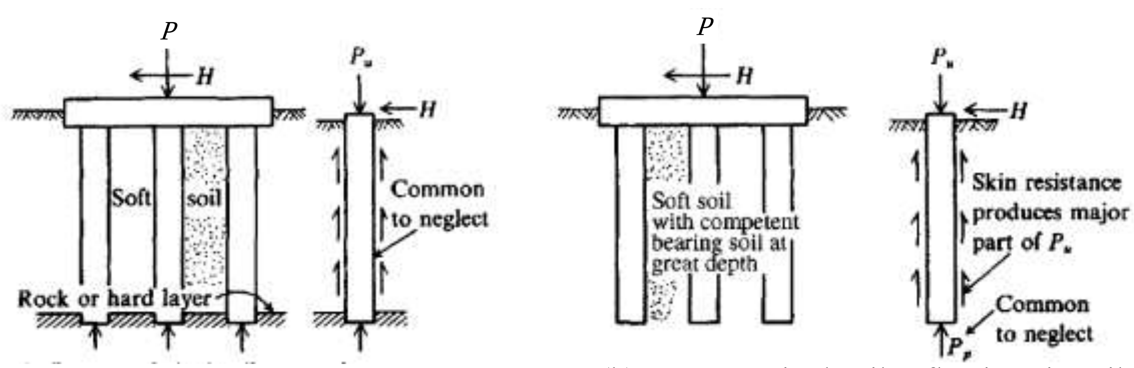

(a) Group and single pile on rock or very firm soil stratum (end bearing pile)

(b) Group or single pile "floating" in soil mass (friction pile)

Fig. 8.1 Types of piles based on their resistance

8.2 Classification of Piles

Piles may be classified in a number of ways [see Table (8.1) and Fig. (8.2)]:

(i) by the material of which they are formed (timber piles, steel piles, concrete piles: precast, prestressed, cast in place).

(ii) by their manner of installation (driven piles, driven and cast-in-place piles, jacked piles, bored and cast-in-place piles, and composite piles).

(iii) by their effect on the soil during installation (displacement piles: driven and jacked piles, and non-displacement piles: bored piles).

(iv) by their action in transferring loads to the soil (end bearing piles and friction piles).

Table 8.1 Typical pile characteristics and uses

Pile type	Timber	Steel	Cast-in-place concrete piles (shells driven without mandrel)	Cast-in-place concrete piles (shells withdrawn)
Maximum length	35 m	Practically unlimited	10–25 m	36 m
Optimum length	9–20 m	12–50 m	9–25 m	8–12 m
Applicable material specifications	ASTM-D25 for piles; P1-54 for quality of creosote; C1-60 for creosote treatment (Standards of American Wood Preservers Assoc.)	ASTM-A36, A252, A283, A572, A588 for structural sections ASTM-A1 for rail sections	ACI	ACI†
Recommended maximum stresses	Measured at midpoint of length: 4–6 MPa for cedar, western hemlock, Norway pine, spruce, and depending on Code. 5–8 MPa for southern pine, Douglas fir, oak, cypress, hickory	$f_s = 0.35\text{–}0.5 f_y$	$0.33 f_c'$; $0.4 f_c'$ if shell gauge ≤ 14; shell stress = $0.35 f_y$ if thickness of shell ≥ 3 mm $f_c' \geq 18$ MPa	$0.25\text{–}0.33 f_c'$
Maximum load for usual conditions	450 kN	Maximum allowable stress × cross section	900 kN	1300 kN
Optimum load range	80–240 kN	350–1050 kN	450–700 kN	350–900 kN
Disadvantages	Difficult to splice Vulnerable to damage in hard driving Vulnerable to decay unless treated Difficult to pull and replace when broken during driving	Vulnerable to corrosion HP section may be damaged or deflected by major obstructions	Hard to splice after concreting Considerable displacement	Concrete should be placed in dry More than average dependence on quality of workmanship

Table 8.1 (continued)

Pile type	Timber	Steel	Cast-in-place concrete piles (shells driven without mandrel)	Cast-in-place concrete piles (shells withdrawn)
Advantages	Comparatively low initial cost Permanently submerged piles are resistant to decay Easy to handle	Easy to splice High capacity Small displacement Able to penetrate through light obstructions	Can be redriven Shell not easily damaged	Initial economy
Remarks	Best suited for friction pile in granular material	Best suited for end bearing on rock Reduce allowable capacity for corrosive locations or provide corrosion protection	Best suited for friction piles of medium length	Allowable load on pedestal pile is controlled by bearing capacity of stratum immediately below pile

Typical illustrations

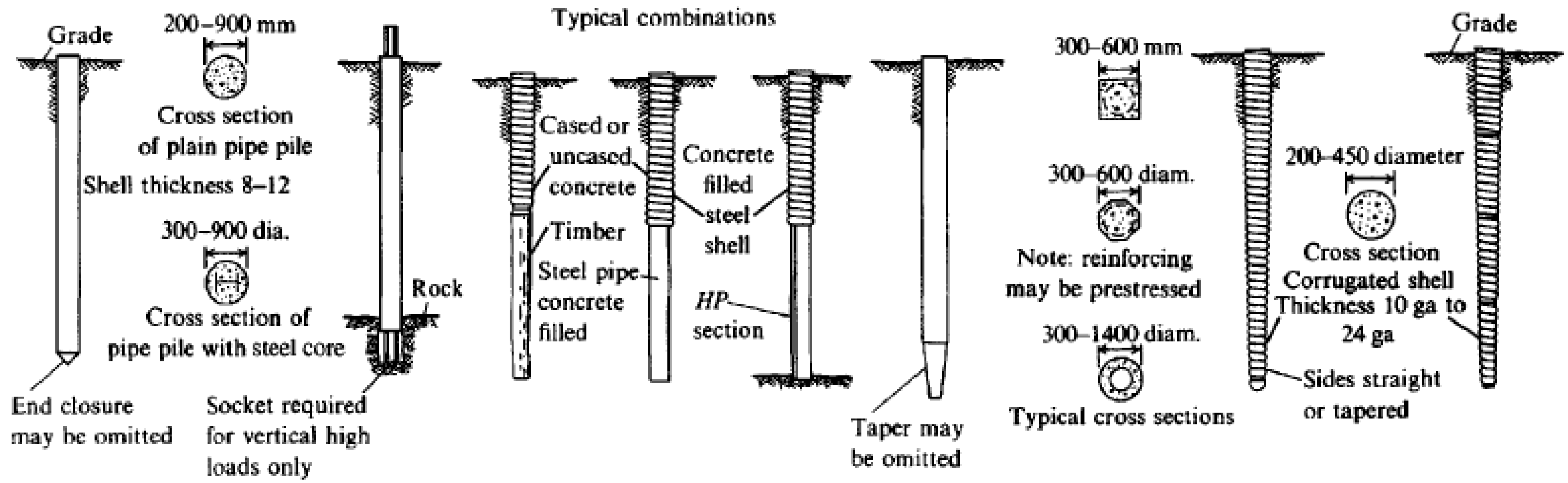

Table 8.1 (continued)

Pile type	Concrete-filled steel pipe piles	Composite piles	Precast concrete (including prestressed)	Cast in place (thin shell driven with mandrel)	Auger-placed pressure-injected concrete (grout) piles
Maximum length	Practically unlimited	55 m	10–15 m for precast 20–30 m for prestressed	6–35 m for straight sections 12 m for tapered sections	5–25 m
Optimum length	12–36 m	18–36 m	10–12 m for precast 18–25 m for prestressed	12–18 m for straight 5–12 m for tapered	10–18 m
Applicable material specifications	ASTM A36 for core ASTM A252, A283 for pipe ACI Code 318 for concrete	ACI Code 318 for concrete ASTM A36 for structural section ASTM A252 for steel pipe ASTM D25 for timber	ASTM A15 reinforcing steel ASTM A82 cold-drawn wire ACI Code 318 for concrete $f'_c \geq 28$ MPa precast $f'_c \geq 35$ MPa prestressed	ACI	See ACI
Recommended maximum stresses	$0.40 f_y$ reinforcement < 205 MPa 0.35–$0.50 f_y$ for shell < 175 MPa $0.33 f'_c$ for concrete	Same as concrete in other piles Same as steel in other piles Same as timber piles for composite	$0.33 f'_c$ unless local building code is less $0.4 f_y$ for reinforced unless prestressed	$0.33 f'_c$; $f_s = 0.4 f_y$ if shell gauge ≤ 14 use $f_y = 0.35 f_y$ if shell thickness ≥ 3 mm	$0.25 f'_c$
Maximum load for usual conditions	1800 kN without cores 18000 kN for large sections with steel cores	1800 kN	8500 kN for prestressed 900 kN for precast	675 kN	700 kN
Optimum load range	700–110 kN without cores 4500–14 000 kN with cores	250–725 kN	350–3500 kN	250–550 kN	350–900 kN
Disadvantages	High initial cost Displacement for closed-end pipe	Difficult to attain good joint between two materials	Difficult to handle unless prestressed High initial cost Considerable displacement Prestressed difficult to splice	Difficult to splice after concreting Redriving not recommended Thin shell vulnerable during driving Considerable displacement	Dependence on workmanship Not suitable in compressible soil

Table 8.1 (continued)

Pile type	Concrete-filled steel pipe piles	Composite piles	Precast concrete (including prestressed)	Cast in place (thin shell driven with mandrel)	Auger-placed pressure-injected concrete (grout) piles
Advantages	Best control during installation No displacement for open-end installation Open-end pipe best against obstruction High load capacities Easy to splice	Considerable length can be provided at comparatively low cost	High load capacities Corrosion resistance can be attained Hard driving possible	Initial economy Tapered sections provide higher bearing resistance in granular stratum	Freedom from noise and vibration Economy High skin friction No splicing
Remarks	Provides high bending resistance where unsupported length is loaded laterally	The weakest of any material used shall govern allowable stresses and capacity	Cylinder piles in particular are suited for bending resistance	Best suited for medium-load friction piles in granular materials	Patented method

Typical illustrations

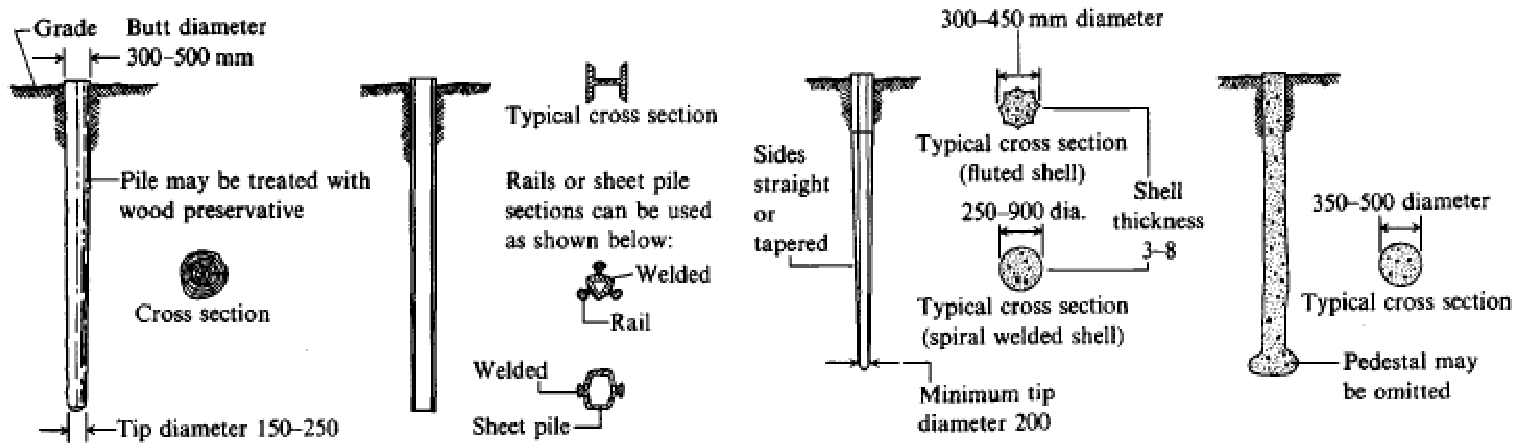

*Additional comments in *Practical Guidelines for the Selection, Design and Installation of Piles* by ASCE Committee on Deep Foundations, ASCE, 1984, 105 pages.

†ACI Committee 543, "Recommendations for Design, Manufacture, and Installation of Concrete Piles," *JACI*, August 1973, October 1974; also in ACI MCP 4 (reaffirmed 1980).

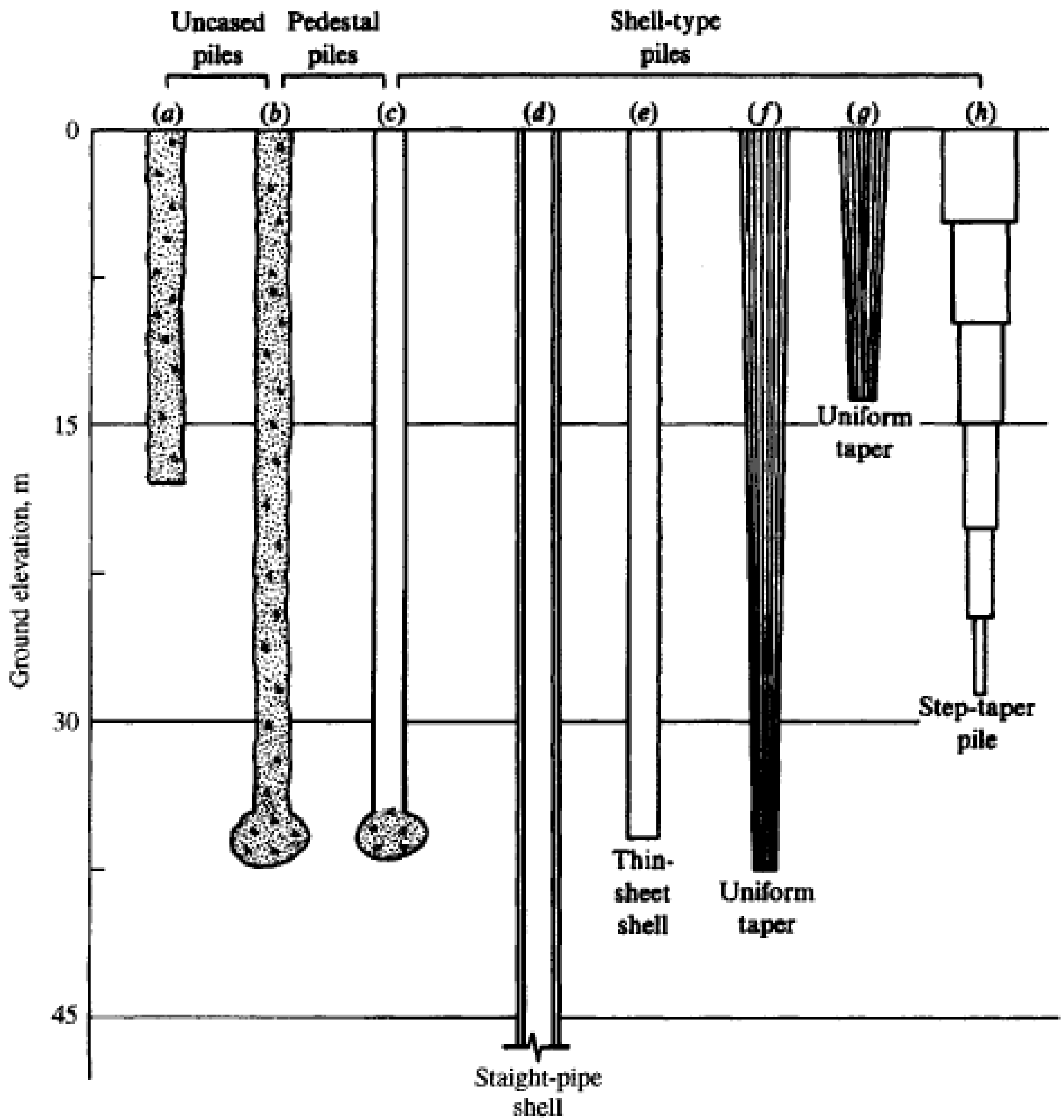

Fig. 8.2 Some common types of cast-in-place (patented) piles: *(a)* Commonly used uncased pile; *(b)* Franki uncased pedestal pile; *(c)* Franki cased pedestal pile; *(d)* welded or seamless pipe; *(e)* Western cased pile; *(f)* Union or Monotube pile; *(g)* Raymond standard; *(h)* Raymond step-taper pile. Depths shown indicate usual ranges for the various piles. Current literature from the various foundation equipment companies should be consulted for design data.

8.3 Static Pile Capacity

The net ultimate load capacity of a single pile is given by [see Fig. (8.3)]

$$Q_u = Q_b + Q_s - W_p \qquad \text{(Compression)}$$

$$T_u = Q_s + W_p \qquad \text{(Tension)}$$

where

Q_u: ultimate pile capacity.

T_u: ultimate pullout (tension) capacity.

Q_b: ultimate point capacity.

Q_s: skin friction resistance.

W_p: weight of pile.

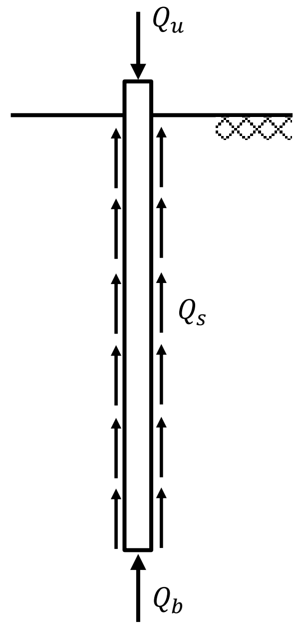

Fig. 8.3 Components of pile carrying capacity

The allowable pile capacity is obtained as:

Driven pile: $$Q_a = \frac{Q_u}{F_s} \quad ; \quad T_a = \frac{T_u}{F_s}$$

Bored pile: $$Q_a = \frac{Q_u}{F} \le \frac{Q_b}{F_1} + \frac{Q_s}{F_2}$$

where

F_s: safety factor ≈ 2.5

F_1: safety factor ≈ 3

F_2: safety factor ≈ 1

F: safety factor ≈ 2

8.4 Point Bearing Capacity

The ultimate point bearing capacity of a pile can be computed using either laboratory or penetration test data. If laboratory data are used, the point capacity can be computed as:

$$Q_b = A_b\left(c \cdot N_c' + \bar{q} \cdot N_q'\right)$$

where

A_b: area of pile point, effective in bearing (generally include any plug).

c: soil cohesion (or undrained shear strength).

N_c': bearing capacity factor for cohesion adjusted for shape and depth.

N_q': bearing capacity factor for overburden effects and includes shape and depth effects.

$\bar{q}$: effective overburden pressure at pile point.

8.4.1 Piles in Clay ($\phi = 0$)

For piles driven into clays and clayey silts, the bearing capacity factors N_c' and N_q' can be taken as follows [Fig. (8.4)].

$N_q' = 1$

$N_c' = 9 \qquad \frac{D}{B} \geq 5$

$c = s_u$

$\therefore Q_b = A_b(9s_u)$

where

s_u = undrained shear strength

Note: if $\frac{D}{B} < 5$, use Skempton's values of N_c instead of N_c' .

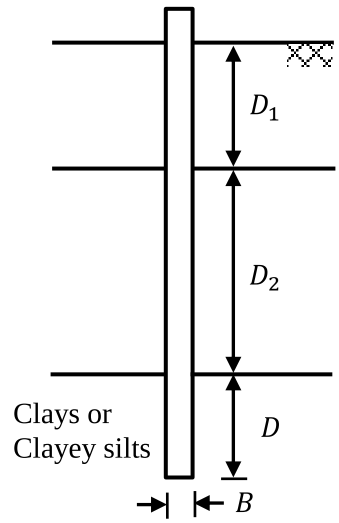

Fig. 8.4

8.4.2 Piles in Sand

A. Berezantsev (1961)

For piles driven into cohesionless soils, the point bearing capacity can be expressed as (N_c' = 0):

$$Q_b = A_b\left(\bar{q} \cdot N_q'\right) \leq A_b(11000) \quad kN$$

where N_q' represents Berezantsev's B.C. factor [Fig. (8.5)].

Berezentsev's values can be used provided that $\frac{D}{B} \geq 5$. For lesser penetrations, values for shallow foundations must be used. If soft clay or silts overlies the bearing stratum of sand or gravel then $\frac{D}{B}$ ratio should be calculated on the penetration into the bearing stratum only [Fig. (8.6)].

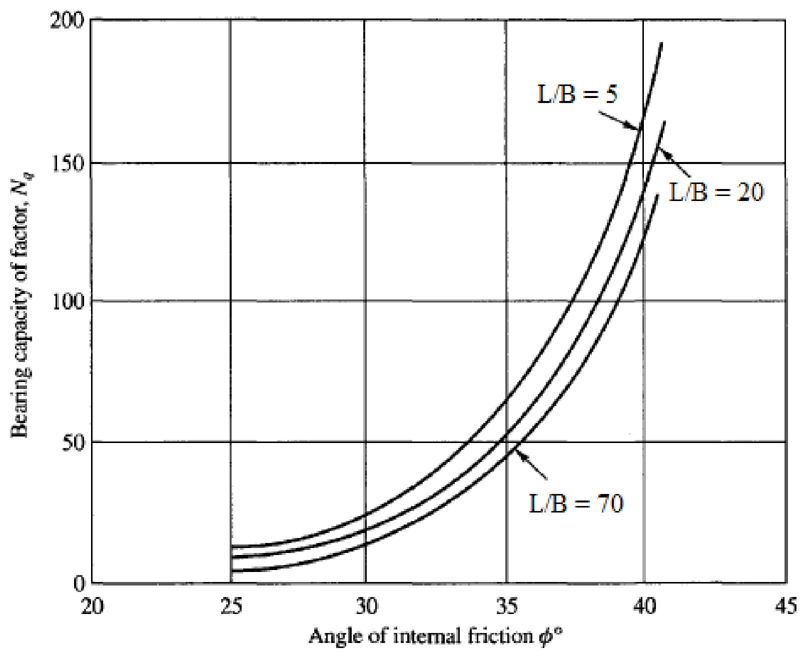

Fig. 8.5 Berezantsev's bearing capacity factor, N_q'

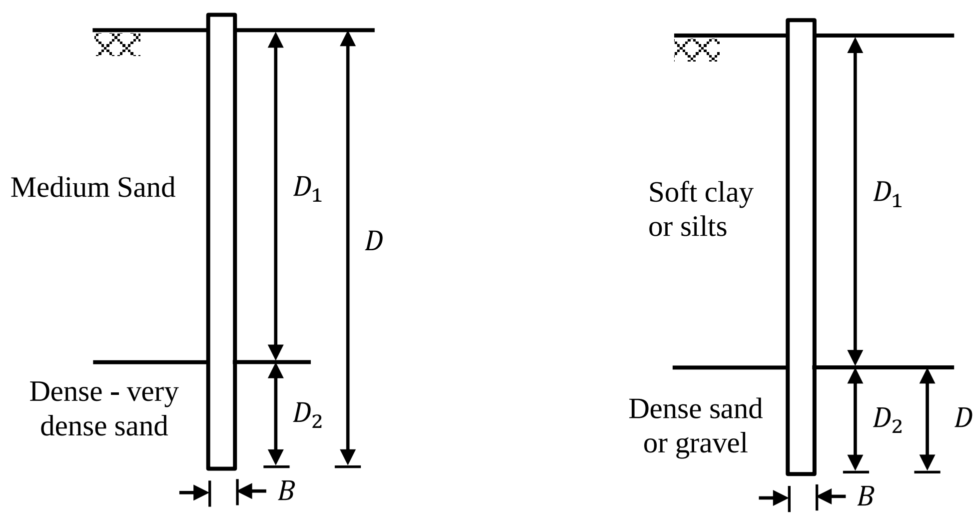

Fig. 8.6

B. <u>Meyerhof (1951, 1976)</u>

For a cohesionless soil and if $\left(\frac{L}{B} \geq \frac{L_c}{B}\right)$ then $\left[Q_b \leq A_b(50\tan\phi)N_q' \quad kN\right]$.

In using Meyerhof's factors;

- Compute ($R_1 = L/B$) and obtain ($R_2 = L_c/B$) from Fig. (8.7) at the given (ϕ) angle.
- Enter the curves with (ϕ):
  i) If ($R_1 > 0.5\ R_2$) and ($\phi < 30^o$), obtain factors from the upper N_i' curves.
  ii) If ($R_1 < 0.5\ R_2$) use a linear ratio between the lower and upper N_i' curves
  for example; $N_c'' = N_c + (N_c' - N_c)\frac{R_1}{0.5\ R_2}$
- If ($\phi > 30^o$), and depending on (L/B), project to the reduced curves shown in the upper right part of Fig. (8.7) and interpolate as necessary.

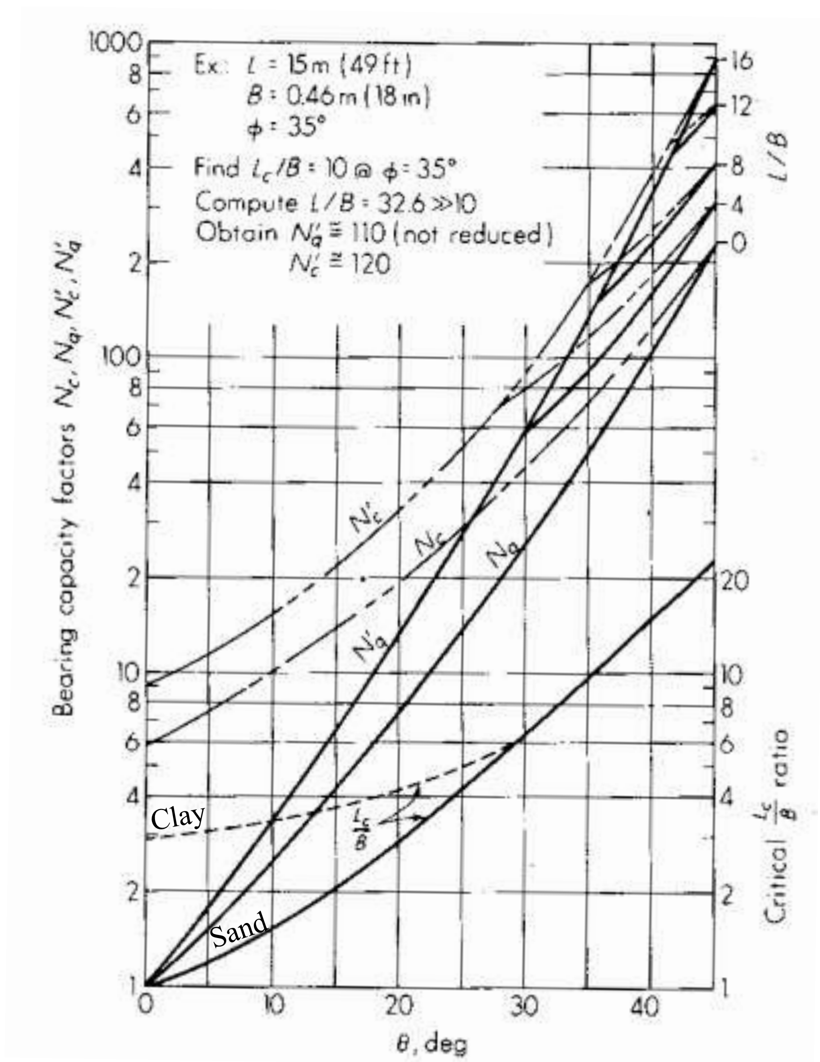

Fig. 8.7 Bearing-capacity factors for deep foundations. [After Meyerhof (1976).]

8.5 Point Bearing from Field Tests

SPT

For standard penetration test (SPT) data, Meyerhof proposed.

$$Q_b = A_b(40\,N)\frac{D}{B} \le A_b(380\,N) \qquad kN$$

where

N = average of the SPT numbers in a zone of about 8B above to 3B below the pile point.

B = width or diameter of pile point.

D = pile penetration depth into bearing stratum.

CPT

For cone penetration data with $\frac{D}{B} \ge 10$:

$$Q_b = A_b \cdot q_c \qquad \text{(units of } q_c\text{)}$$

where

q_c = average of the cone resistance in a zone similar to that for N above.

8.6 Skin Friction Capacity

In general, the skin resistance capacity is computed as [Fig. (8.8)]:

$$Q_s = \sum A_s \cdot f_s$$

where

A_s : effective pile surface area on which (f_s) acts.

= perimeter (p) × embedment increment (ΔL)

f_s: skin resistance per unit area (i.e., shear stress).

$= \alpha \cdot c + k \cdot \bar{\sigma}_v \cdot \tan\delta \le 100\ kPa$

α : adhesion factor.

k : lateral earth pressure coefficient.

$\bar{\sigma}_v$: vertical stress (average).

δ : friction angle between soil and pile material.

L : pile length.

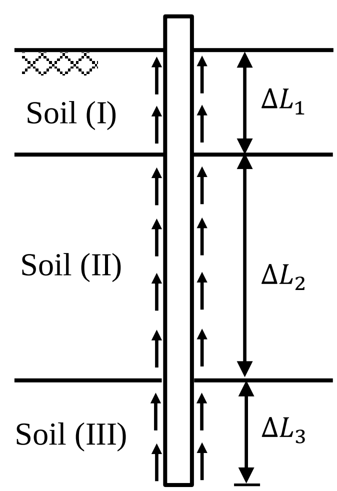

Fig. 8.8

8.6.1 Piles in Clay

α – method (Tomlinson – 1971):

$$f_s = \alpha \cdot c$$

where

α: coefficient from Table (8.2) or from Fig. (8.9).

c: average cohesion (undrained shear strength).

Table 8.2 Values of adhesion factors for piles driven into stiff to very stiff cohesive soils for design

Case	Soil conditions	Penetration ratio‡	Adhesion factor, α
1	Sands or sandy gravels overlying stiff to very stiff cohesive soil	< 20	1.25
		> 20	Fig. 8.9
2	Soft clays or silts overlying stiff to very stiff cohesive soil	$8 < PR \leq 20$	0.40
		> 20	Fig. 8.9
3	Stiff to very stiff cohesive soils without overlying strata	$8 < PR \leq 20$	0.40
		> 20	Fig. 8.9

† After Tomlinson (1971).

‡ Penetration ratio $PR = \dfrac{\text{depth of penetration into cohesive soil}}{\text{diameter of pile}}$

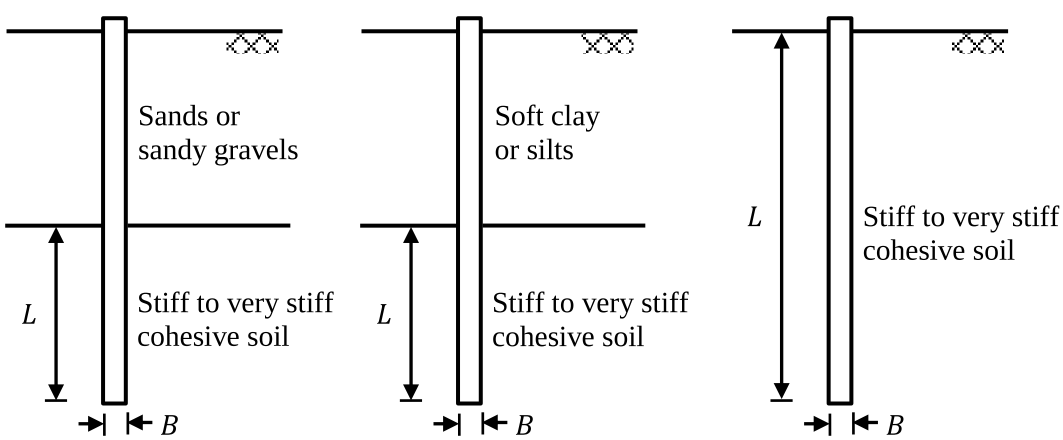

Case (1) Case (2) Case (3)

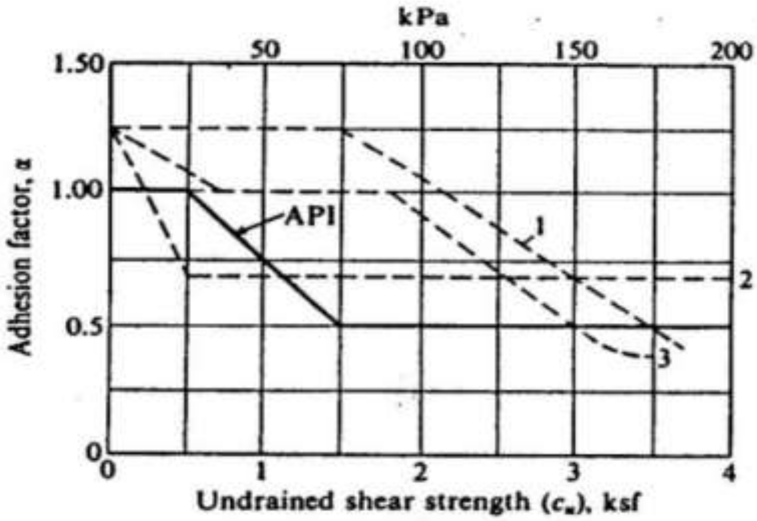

Fig. 8.9 $\alpha - c_u$ relation for different soil conditions

Notes

1. For soft clay, α = 1.0
2. For bored and cast-in-place piles in cohesive soil, Skempton has shown that:

$$f_s = 0.45\ c\ \leq 100\ kN/m^2$$

3. For belled piles, neglect the adhesive over a distance equals twice shaft diameter above the top of bell.

8.6.2 Piles in Sand

The average value of skin friction over the length of pile embedded in sand can be expressed as:

$$f_s = \bar{\sigma}_v \cdot k \cdot \tan\delta$$

Broms (1965) has related the values of k and δ to the effective angle of shearing resistance for various pile materials and relative densities as shown in Table (8.3).

Table 8.3 Values of k and δ

Pile type	δ	k (loose)	k (dense)
Steel	20^{o}	0.5	1.0
Concrete	0.75 ϕ	1.0	2.0
Wood	2/3 ϕ	1.5	4.0

Notes:

1. For short term capacity, use undrained parameters [c_u , ϕ_u , γ and $\bar{q}$, $\bar{\sigma}v$].
2. For long term capacity, use drained parameters [c', ϕ', γ' and $\bar{q}$, $\bar{\sigma}v'$].
3. For normally consolidated clay, the undrained condition is the critical situation.
4. For free draining material, the drained condition is the usual condition for analysis.
5. For fissured clay, use (0.75 c_u) for the prediction of point bearing capacity.
6. In the case of bored piles, the skin friction resistance may be calculated on the assumption that the ϕ value will be representative of loose condition. Similarly, the ϕ value used to obtain the bearing capacity factor N_q' must correspond to loose conditions [see Fig. (8.10)].

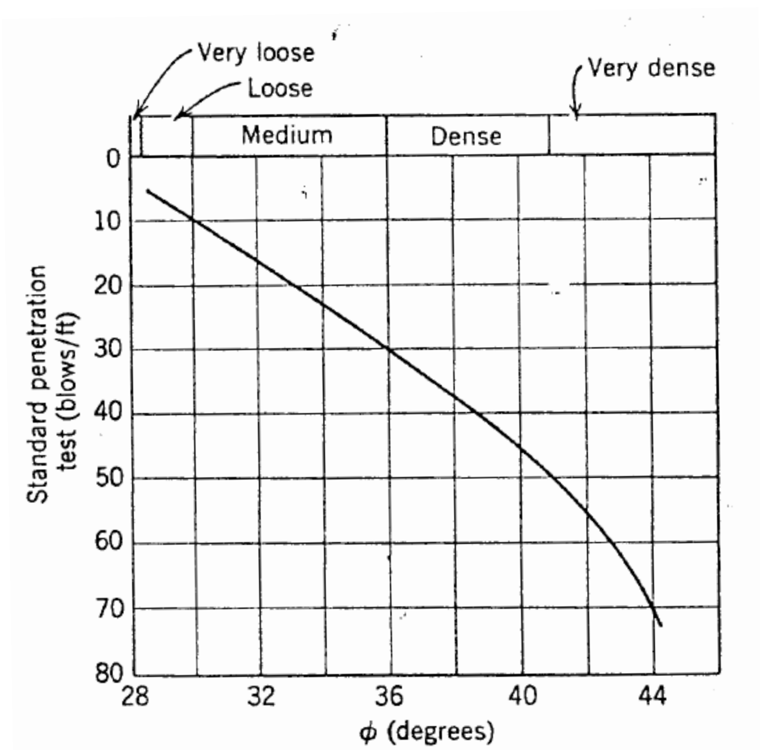

Fig. 8.10 Correlation between friction angle and penetration resistance (From Peck, Hanson, and Thornburn, 1953)

8.7 Pile Loading Test-Axial Compression (ASTM-D1143)

A loading test is made usually for one or other of the following reasons:

1. To determine the load-settlement relationship, particularly in the region of the anticipated working load.
2. To serve as a proof test to ensure that failure does not occur before load is reached which is a selected multiple of the chosen working load. The value of multiple is then treated as a factor of safety.
3. To determine the ultimate carrying capacity as a check on the value calculated from dynamic or static formulae.

8.7.1 Loading Systems

The following methods are used for providing the load or downward force on the pile to be tested:

a) Anchored reaction frame [Fig. (8.11)].
b) Weighted platform [Fig. (8.12)].

8.7.2 Loading Procedures (Standard Loading Procedure)

Unless failure occurs first, load the pile to 200% of the anticipated pile design load. Applying the load in increments of 25% of the design load. Maintain each load increment until the rate of settlement is not greater than 0.01 in. (0.25 mm)/hr but no longer than 2 hrs. Provided that the test pile has not failed, remove the total test load anytime after 12 hrs if the butt settlement over a one-hour period is not greater than 0.01 in. (0.25 mm); otherwise allow the total load to remain on the pile for 24 hrs. After the required holding time, remove the test load in decrements of 25% of the total test load with 1 hr between decrements. If pile failure occurs, continue jacking the pile until the settlement equals 15% of the pile diameter or diagonal dimension.

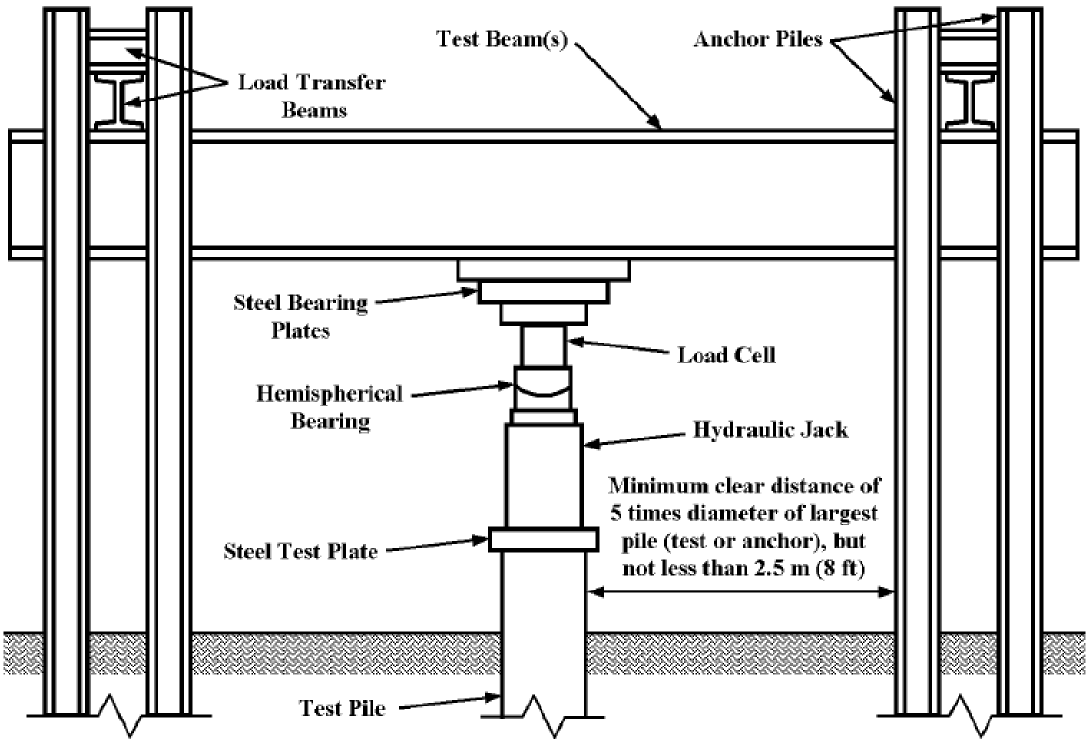

Fig. 8.11 Schematic of hydraulic jack acting against anchored reaction frame

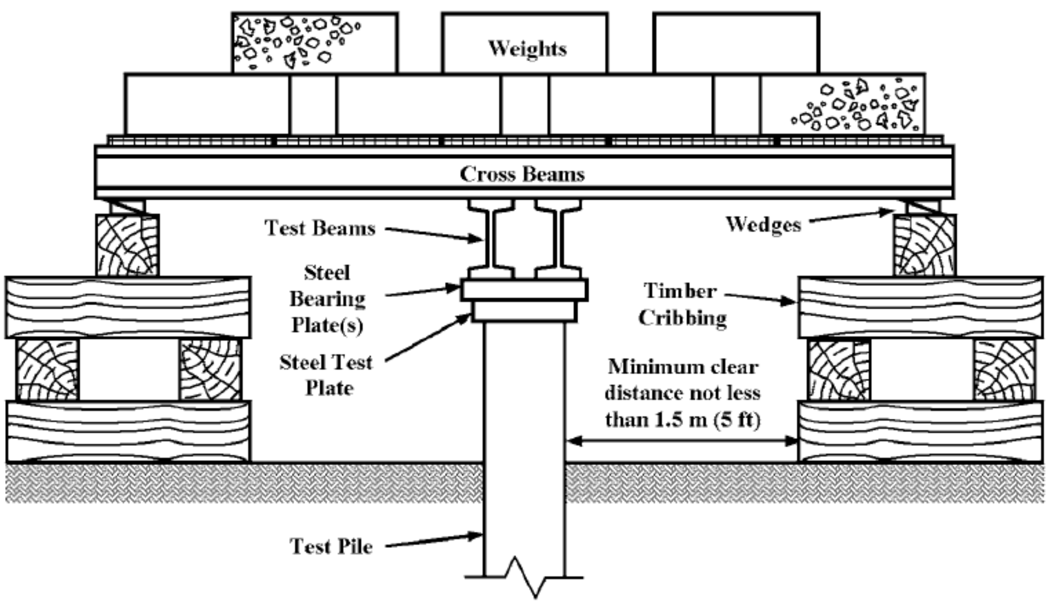

Fig. 8.12 Schematic of direct loading on a single pile using weighted platform

8.7.3 Presenting the Results

The result of a test is plotted as in Fig. (8.13) giving the curves of load and settlement versus time and of load versus the maximum settlement reached at each stage of loading. The unloading of the pile is also plotted to complete the cycle of loading.

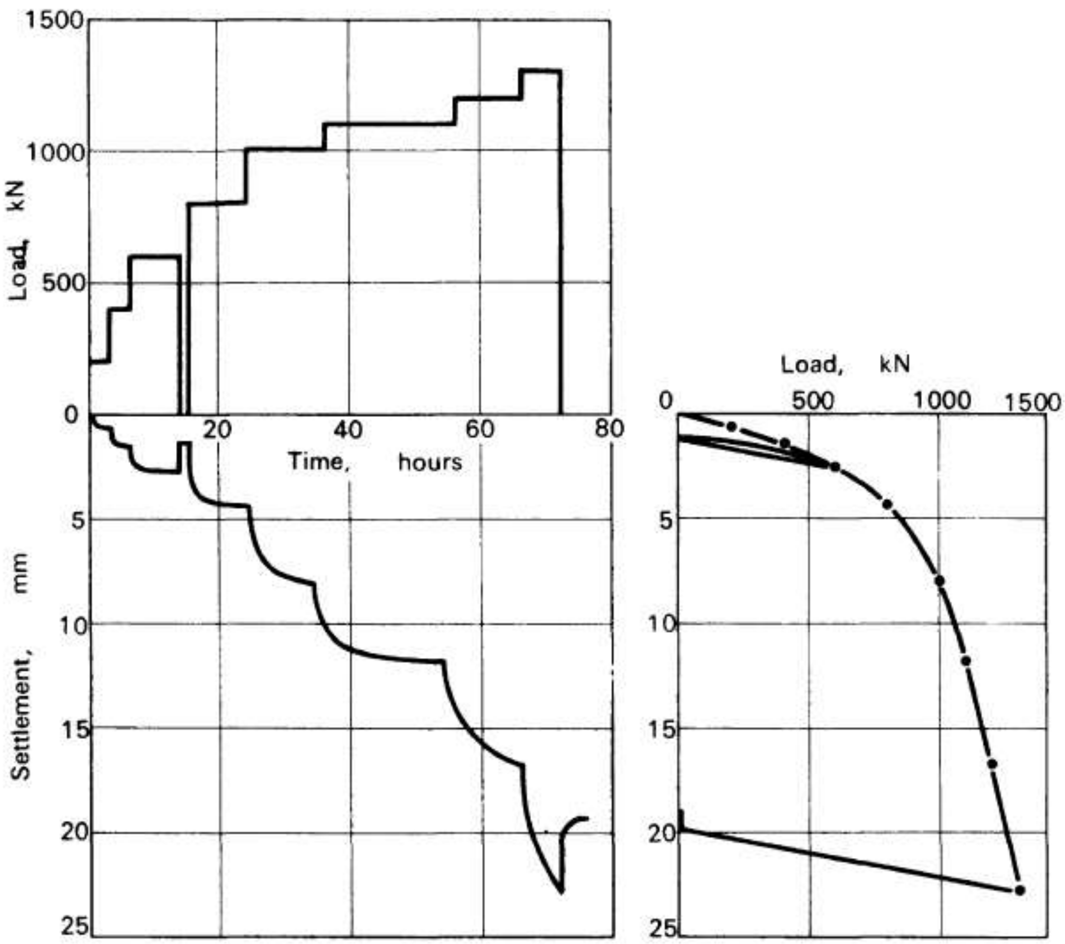

Fig. 8.13 Method of presenting the result of a load test, giving plottings of load and settlement versus time and of load versus the maximum settlement at each stage of loading

8.8 Pile Capacity – Dynamic Analysis

Estimating the ultimate capacity of a pile while it is being driven into the ground at the site has resulted in numerous equations being presented to the engineering profession. Unfortunately, none of the equations is consistently reliable or reliable over an extended range of pile capacity. Because of this, the best means for predicting pile capacity by dynamic means consists in driving a pile, recording the driving history, and load testing the pile. It would be reasonable to assume that other piles with a similar driving history at that site would develop approximately the same load capacity.

8.8.1 Pile Driving

Piles are inserted into the ground using a pile hammer resting or clamped to the top of the pile cap, which is, in turn, connected to the pile. Pile hammers are the devices used to impart sufficient energy to the pile that it penetrates the soil. The common types of pile hammers are [see Fig. (8.14)]:

1. Drop hammers
2. Single-acting hammers
3. Double-acting hammers
4. Diesel hammers
5. Vibratory drivers

8.8.2 The Rational Pile Formula

Nearly all the dynamic pile formulas currently used are based on the rational pile formula by simplifying certain terms. The rational formula depends upon impulse-momentum principle:

Energy = Work + (Impact loss + cap loss + pile loss + soil loss)

For the derivation of the rational pile formulas, refer to Fig. (8.15) and the following list of symbols:

E_h = manufacturer's hammer-energy rating (FL)

h = height of all of ram (L)

P_u = ultimate pile capacity (F)

s = amount of point penetration (mm) per blow for the last 150 mm (s_{min} = 1.25 mm) (L)

W_p = weight of pile including weight of pile cap, all or part of the soil "plug," driving shoe, and capblock (also includes anvil for double-acting steam hammers) (F)

W_r = weight of ram (for double-acting hammers include weight of casing) (F)

$$\left\{\left(\frac{W_p}{W_r}\right)_{min} = 1\right\}.$$

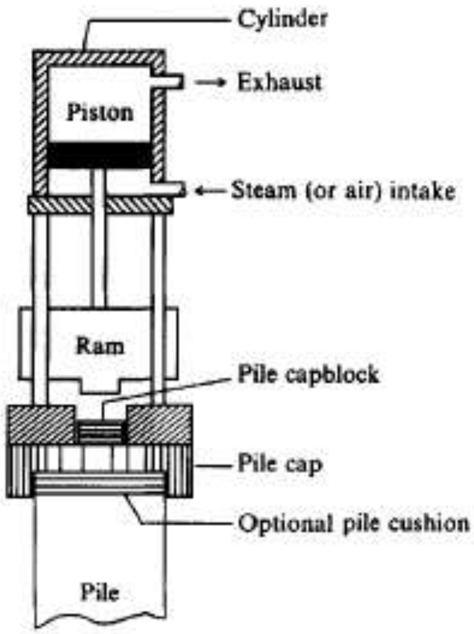

(*a*) Single-acting hammer. At bottom of stroke, intake opens with steam pressure raising ram. At top of lift steam is shut off and intake becomes exhaust, allowing ram to fall.

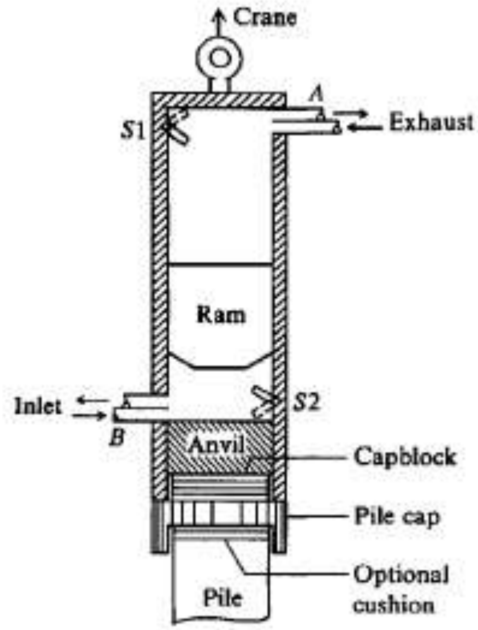

(*b*) Double-acting hammer. Ram in down position trips *S*2, which opens inlet and closes exhaust valves at *B* and shuts inlet and opens exhaust at *A*; hammer then rises from steam pressure at *B*. Ram in up position trips *S*1, which shuts inlet *B* and opens exhaust; valve *A* exhaust closes; steam enters and accelerates ram downward.

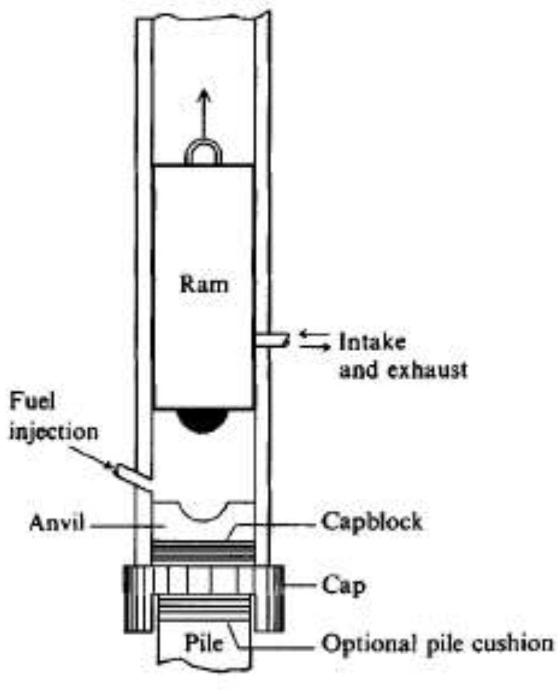

(*c*) Diesel hammer. Crane initially lifts ram. Ram is released and falls; at select point fuel is injected. Ram collides with anvil, igniting fuel. Resulting explosion drives pile and lifts ram for next cycle.

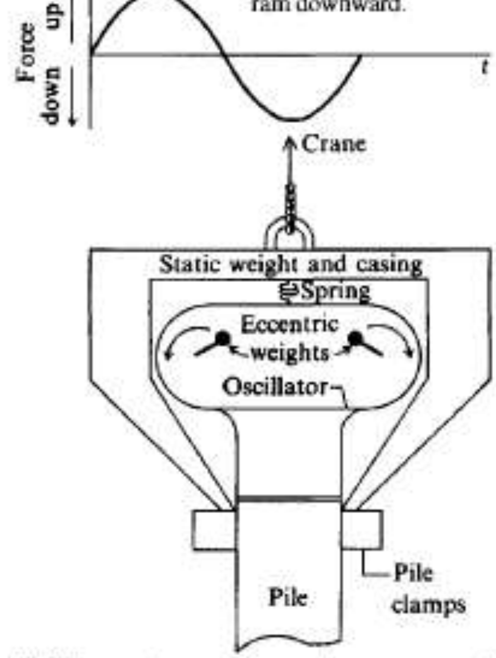

(*d*) Vibratory hammer. External power source (electric motor or electric-driven hydraulic pump) rotates eccentric weights in relative directions shown. Horizontal force components cancel—vertical force components add.

Fig. 8.14 Schematics of several pile hammers.

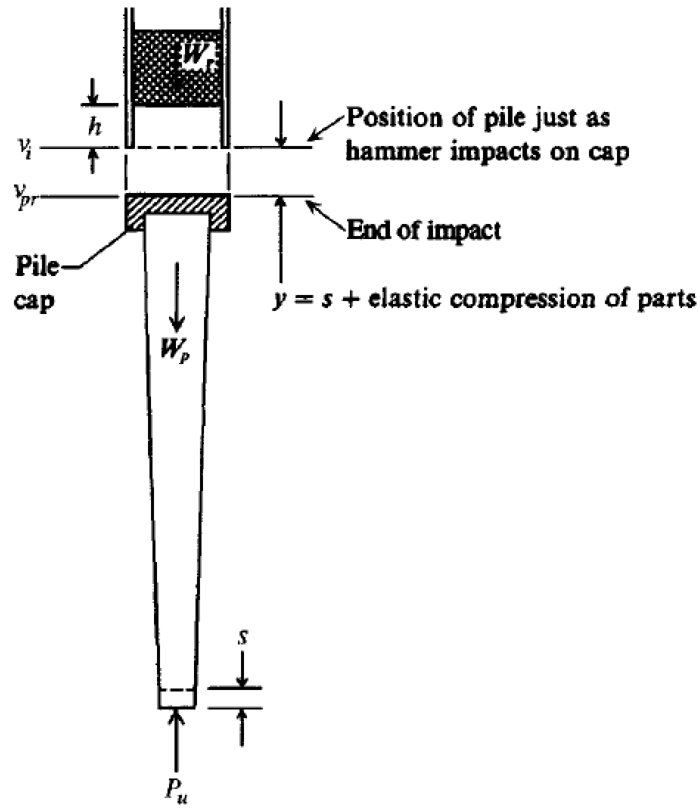

Fig. 8.15 Significance of certain terms used in the dynamic pile-driving equations.

8.8.3 Some of the Dynamic Pile Formulas

1. *The Engineering News Record (ENR) Formula*:

$$P_u = \frac{166.64\ E_h}{s + 2.54}$$

2. *Boston Building Code Formula*:

$$P_u = \frac{141.64\ E_h}{s + 2.54\sqrt{\dfrac{W_r}{W_p}}}$$

CHAPTER 9

PILE FOUNDATIONS - GROUPS

9.1 Introduction

The pile foundations are rarely to consist of a single pile. Generally, there will be a minimum of two or three piles under a foundation element or footing to allow for misalignments and other inadvertent eccentricities. Fig. (9.1) presents some typical pile clusters for illustrative purposes only since the designer must make up the group geometry to satisfy any given problem. When several piles are clustered, it is reasonable to expect that the soil pressure will overlap as shown in Fig. (9.2). With sufficient overlap, either the soil will fail in shear or the pile group will settle excessively. To avoid the overlap, the spacing of the piles could be increased, but large spacing is impractical since a pile cap is usually cast over a group of piles. Therefore, large spacings will require massive and heavy pile caps.

The code of practice (CP 2004) requires a minimum spacing for:

- End bearing piles; S_{min} = 2 × least width of the pile.
- Friction piles ; S_{min} = 3 × least width of the pile.

The National Building Code states that the minimum distance between centers of piles;

- For piles not driven to rock; $S_{min} = 2d \geq 760\ mm$
- For piles driven to rock ; $S_{min} = d + 300\ mm$

where d = pile diameter or the diagonal dimension of square or H piles (mm).

9.2 The Carrying Capacity of Pile Groups

In general, the ultimate load which can be supported by a group of N-piles may not be equal to n times the ultimate load of a single isolated pile. Both theory and experience have shown that pile groups may fail as units before the load per pile becomes equal to the safe design load. Terzaghi and Peck (1967) proposed that the group capacity will be the lesser of;

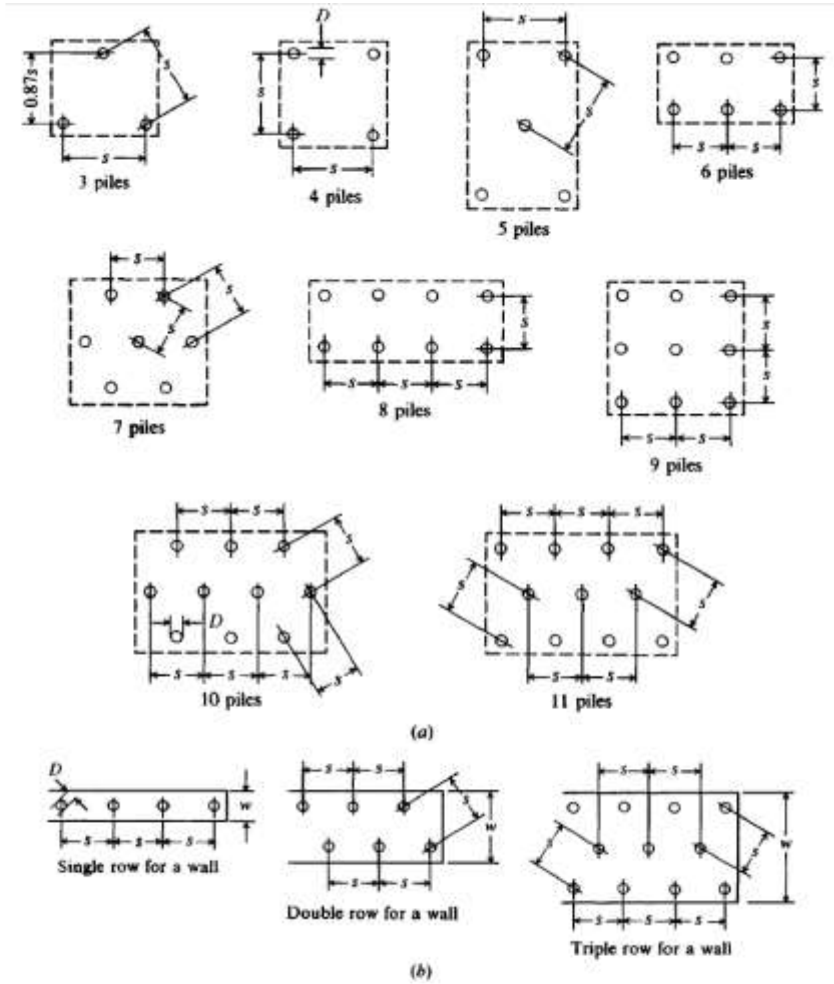

Fig. 9.1 Typical pile-group patterns: (*a*) for isolated pile caps; (*b*) for foundation walls.

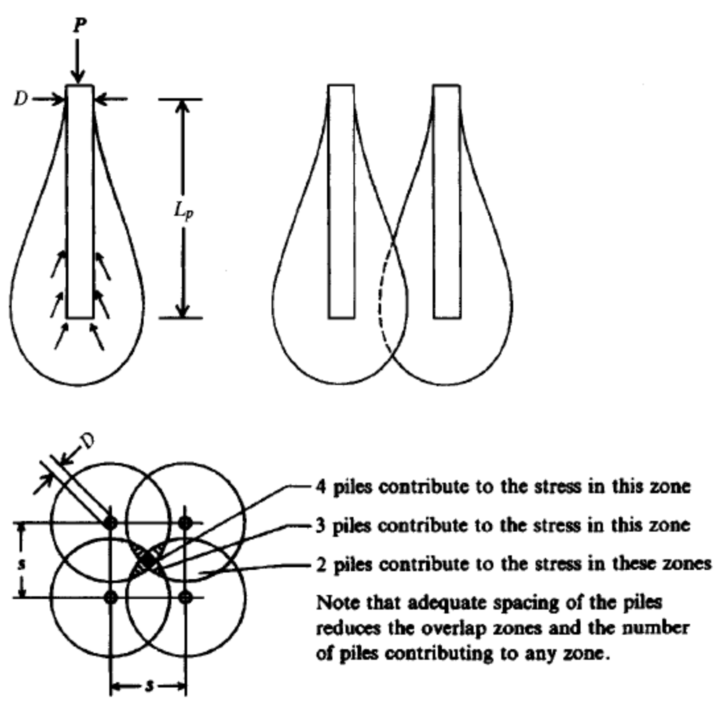

Fig. 9.2 Stresses surrounding a friction pile and the summing effects of a pile group.

(i) Sum of the capacity of the individual piles:

$$G_u = N \cdot Q_u$$

(ii) Block capacity (or block action) [see Fig. (9.3)]:

$$G_u = G_b + G_s$$

where:

Q_u = ultimate carrying capacity of a single pile

N = number of piles in a group

G_u = ultimate pile group capacity

G_s = skin resistance pile group capacity

G_b = point bearing pile group capacity

The allowable pile group capacity is given by:

$$G_a = \frac{G_u}{F_s}$$

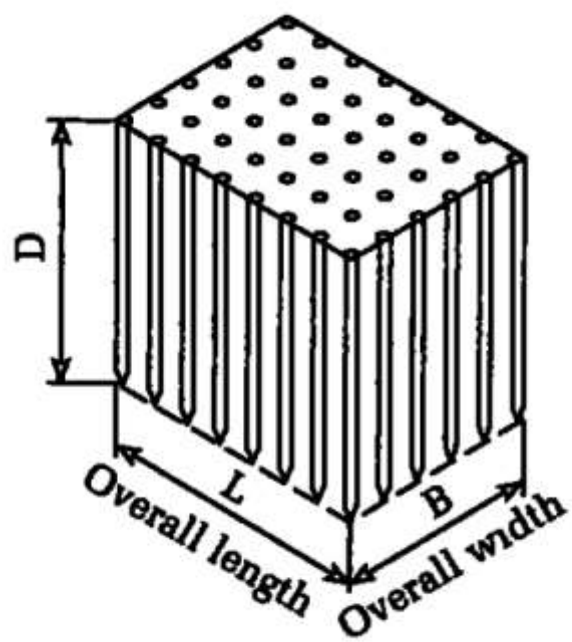

Fig. 9.3 Pile group acting as a block foundation.

9.3 Efficiency of Pile Groups

The efficiency of a pile group is the ratio of the actual group capacity to the sum of the individual pile capacities:

$$E_g = \frac{G_u}{\sum Q_u}$$

where

E_g = group efficiency

There are several equations for calculating the pile group efficiency. Some of these are given below:

i) Converse-Labarre (for floating piles of rectangular configurations)

$$E_g = 1 - \left(\frac{\theta}{90}\right) \cdot \left[\frac{(n-1)m + (m-1)n}{m \cdot n}\right]$$

where

n = no. of piles in the row.

m = no. of rows.

$\theta = \tan^{-1}\frac{d}{s}$ (θ is in degrees)

d = pile diameter.

s = pile spacing (c/c).

ii) Poulos and Davis (for pile groups in clay)

$$\frac{1}{E_g} = 1 + \frac{N^2 \cdot (Q_u)^2}{(G_u)^2}$$

where

N = no. of piles in the group.

iii) Take E_g = 1 for bearing piles in sand.

9.4 Settlement of Pile Groups

The soil stresses on underlying strata under group are greater than those of a single pile under the same load. To estimate stresses under the group it is assumed that the group area acts as a buried raft foundation. It is common practice to simplify the stresses computations as follows:

a. Friction Piles [Fig. (9.4a)]

$$h = \frac{L_p - h_o}{3}$$

b. Point Bearing Piles [Fig. (9.4b)]

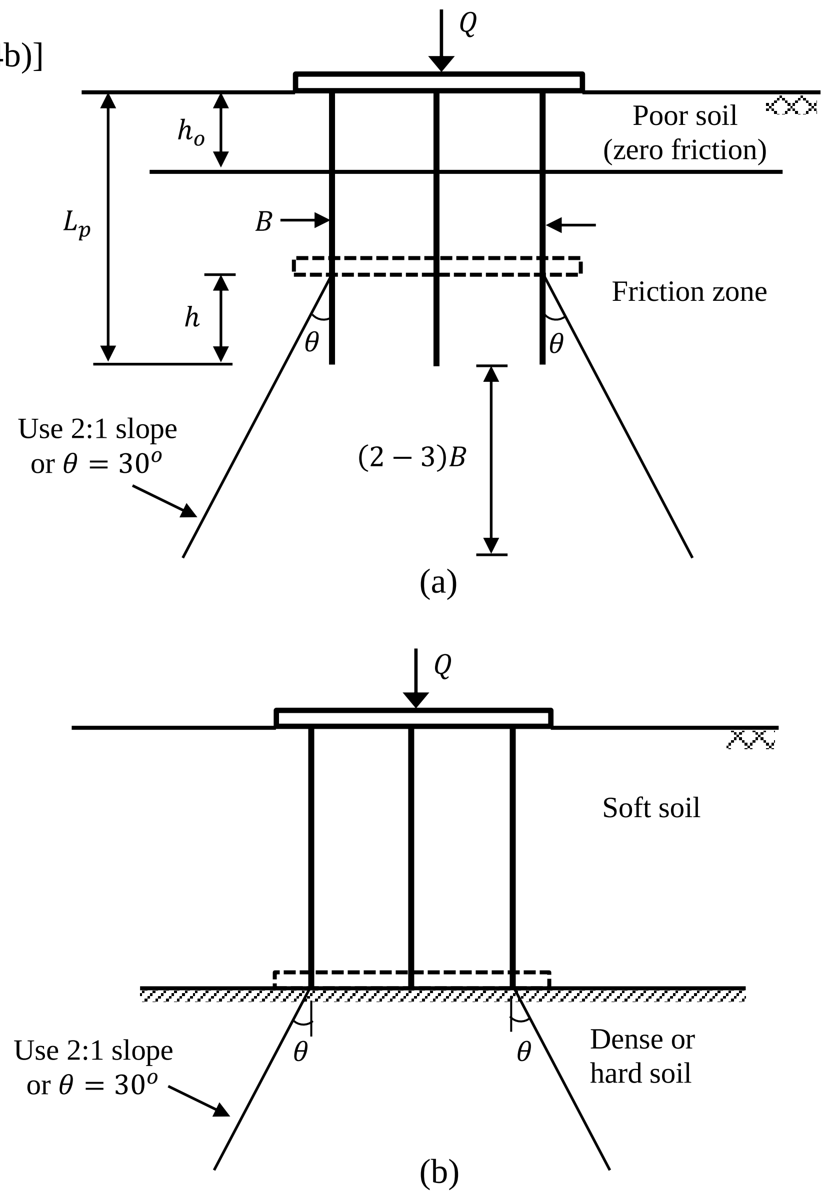

Fig. 9.4 Simplified computation of soil stresses beneath a pile group; (a) friction piles, (b) point-bearing piles

9.5 Pile Caps

Unless a single pile is used, a cap is necessary to spread the vertical and horizontal loads and any overturning moments to all the piles in the group. The cap is usually of reinforced concrete poured directly on the ground. Caps for offshore structures are often fabricated from steel shapes.

Under an eccentric loading or a concentric loading plus moment, the load on each pile can be calculated as follows [see Fig. (9.5)]:

$$M_y = m_y + V \cdot e_x$$

$$M_x = m_x + V \cdot e_y$$

$$P_v = \frac{V}{N} + \frac{M_y \cdot x}{\sum x^2} + \frac{M_x \cdot y}{\sum y^2}$$

$$P_h = \frac{H}{N}$$

where

N = total number of piles

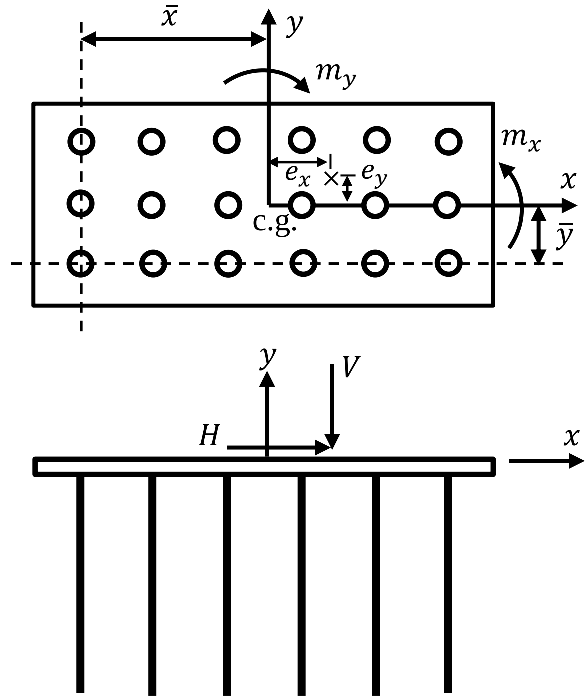

Fig. 9.5 An eccentric loading on group of vertical piles

Notes:

1. The origin of the coordinate axes is taken at the c.g. of the piles.
2. The center of gravity of piles group is calculated as follows:

$$\bar{x} = \frac{\sum N_i \cdot x_i}{\sum N_i} \quad , \quad \bar{y} = \frac{\sum N_i \cdot y_i}{\sum N_i}$$

The structural design of pile caps of reinforced concrete requires consideration of the following [see Fig. (9.6)]:

1. Bending moment is taken at the same sections as for a reinforced concrete spread footing.

2. Pile caps must be reinforced for both +ve and –ve B.M.
3. Pile-cap shear is computed at critical sections (W.B.S. & D.T.S.).
4. Pile caps should end at least 150 mm beyond the outside face of exterior piles.
5. Piles should be embedded at least 150 mm into the cap. If the embedment < 150 mm, the pile should be assumed hinged to the cap.
6. Pile-cap reinforcing bars are placed 75 mm above the top of the pile.
7. The minimum thickness of pile cap above the top of the bottom reinforcing bars is 300 mm.
8. Tension connectors should be attached to the pile to ensure that the pile and cap retain continuity if any of the piles are subjected to tension forces.
9. For fixed-head pile connections, additional reinforcing should be placed around the pile to ensure that the pile does not pull out from or crack pile cap.

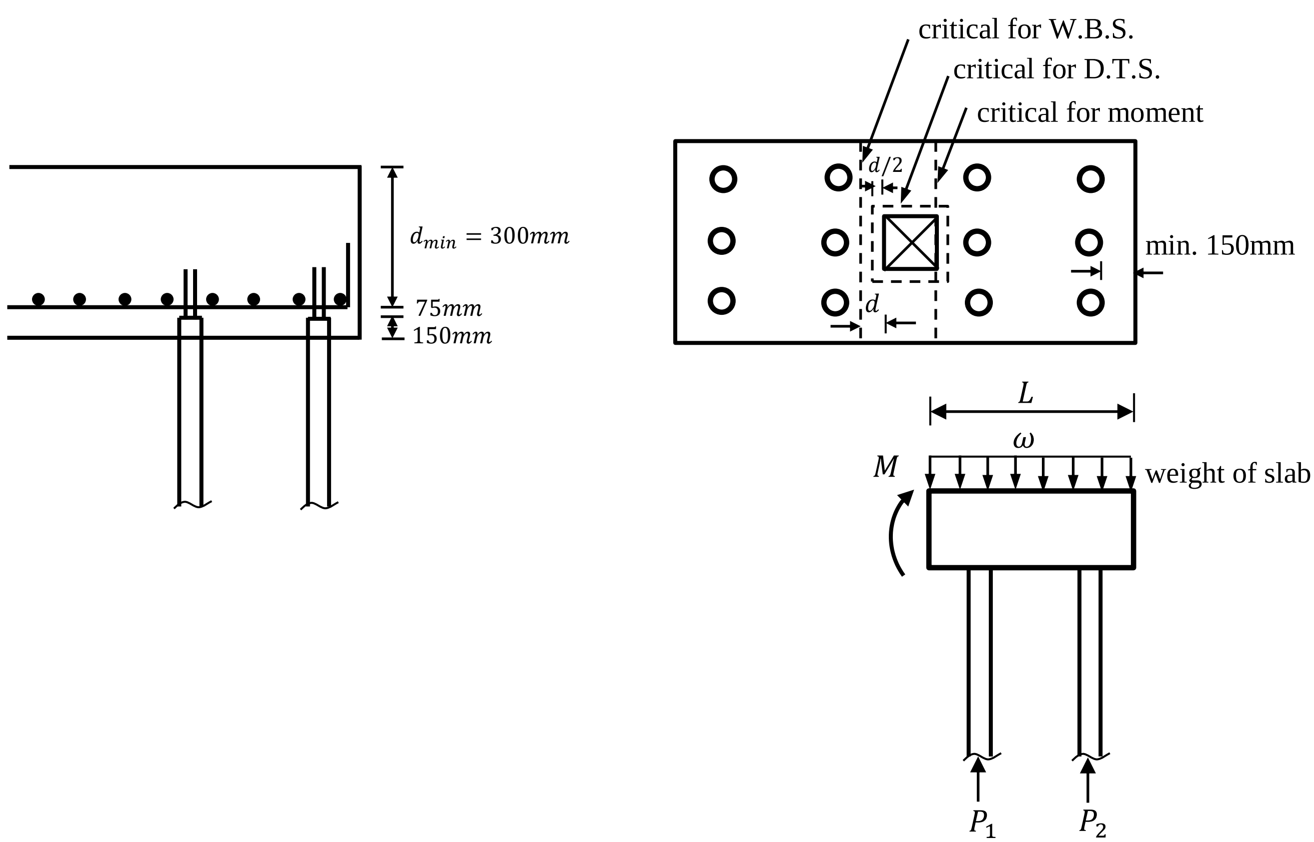

Fig. 9.6 Critical pile cap locations for shear, moment, and bond according to ACI-318.

9.6 Negative Skin Friction

Where piles are driven through strata of soft clay into firmer materials, they will be subjected to loads caused by negative skin friction in addition to the structural loads if the ground settles relative to the piles. Such settlement may be due to the weight of superimposed fill, or ground water lowering, or a result of disturbance of clay caused by pile driving, [particularly large displacement piles in sensitive clays leading to reconsolidation of the disturbed clay under its own weight {see Fig. (9.7)}].

The load transferred to the pile depends on:

- pile material.
- type of soil.
- amount and rate of relative movement between the soil and the pile.
- elastic compression of pile under the working load.

9.6.1 Evaluation of Negative Skin Friction

For a single pile; $Q_{ns} = \sum A_s \cdot f_s = \sum (p_1 \cdot l) \cdot f_s$

For a pile in a group; $Q_{ns} = \frac{1}{N}(W + \sum A_s \cdot f_s) = \frac{1}{N}[W + \sum (p_2 \cdot l) \cdot f_s]$

$$Q_a = \frac{Q_u}{F_s} - Q_{ns}$$

where

f_s = shear stress along pile shaft.

= $c'_a + k_s \cdot \bar{\sigma}_v{}' \cdot \tan \delta'_a$ [see Table (9.1)].

c'_a = adhesion between soil and pile in drained conditions.

≈ 0 for normally consolidated clay.

δ'_a = angle of friction between soil and pile in drained conditions.

p_1 = perimeter of pile.

p_2 = perimeter of group.

N = number of piles in the group.

l = length of zone of negative skin friction.

W = weight of soil block (fill) held in between the piles.

Q_{ns} = ultimate negative skin friction load.

Table 9.1 Bjerrum suggested values for negative skin friction

Soil	δ_a'	k_s	f_s
Silt	30^o	0.45	$0.25\ \bar{\sigma}_v{}'$
Clay (low plasticity)	20^o	0.50	$0.20\ \bar{\sigma}_v{}'$
Clay (plastic)	15^o	0.55	$0.15\ \bar{\sigma}_v{}'$
Clay (high plasticity)	10^o	0.60	$0.10\ \bar{\sigma}_v{}'$

9.6.2 Reducing Negative Skin Friction

Several methods have been developed to reduce the expected negative skin friction on deep foundations. These include:

- using piles with shafts of small cross-sectional area compared with the points.
- driving piles inside a casing with the space between pile and casing filled with a viscous material and the casing withdrawn.
- coating the piles with bitumen.

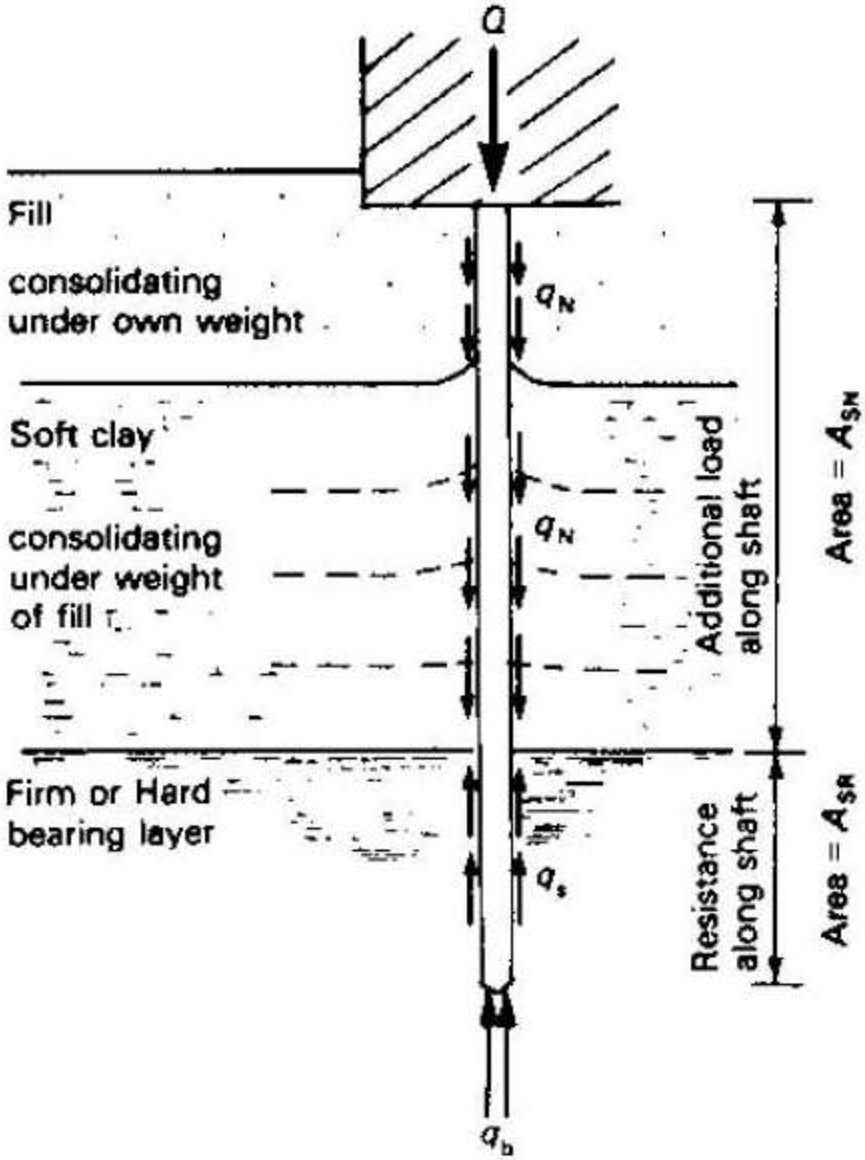

Fig. 9.7 Negative skin friction

CHAPTER 10

LATERAL EARTH PRESSURE

10.1 Introduction

The design of many structures such as retaining walls and sheet-pile walls, excavations, buried pipes, thrust blocks and others, requires the determination of lateral earth pressures. Lateral pressures can be grouped into three states

1- Active state: A state of active stress occurs when the soil deposit yields in such a manner that the deposit tends to stretch horizontally-for example, a retaining wall moving away from its backfill.
2- At-rest state: The at-rest lateral pressure is the lateral pressure that exists in soil deposits that have not been subject to lateral yielding.
3- Passive state: A state of passive stress occurs when the movement is such that the soil tends to compress-for example, when a thrust block moves against the soil.

Fig. (10.1) illustrates the lateral pressures with usual range of values for cohesionless and cohesive soils.

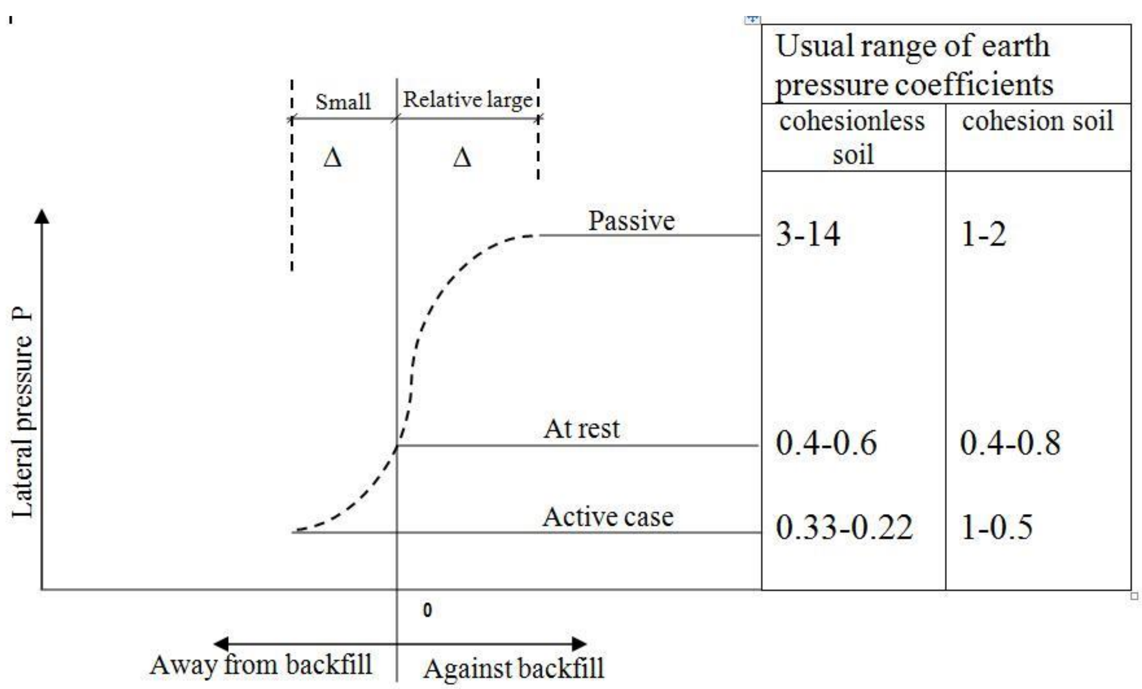

Fig. 10.1 Illustration of active and passive pressures with usual range of values for cohesionless and cohesive soils

The lateral pressure at any level can be determined as:

$$p_a = \sigma_v \cdot K_a - 2c\sqrt{K_a}$$
$$p_p = \sigma_v \cdot K_p + 2c\sqrt{K_p}$$

where

c: soil cohesion

p_a: active lateral earth pressure

p_p: passive lateral earth pressure

K_a: coefficient of active earth pressure

K_p: coefficient of passive earth pressure

σ_v: vertical stress at the required level.

10.2 Coulomb Earth Pressure Theory

Assumptions:

1- The soil is isotropic and homogeneous and possesses both internal friction and cohesion.

2- The rupture surface is a plane surface. The backfill surface is planar.

3- The friction forces are distributed uniformly along the plane of rupture surface and, $f = tan\ \phi$, (f = friction coefficient).

4- The failure wedge is a rigid body.

5- There is wall friction.

6- Failure is a plane-strain problem, consider a unit length of an infinitely long body.

Consider the equilibrium of the assumed failure condition [Fig. (10.2)], the max. value of active wall force (P_a) is found to be:

$$P_a = \frac{1}{2}\gamma H^2 K_a \qquad \text{(cohesionless soil)}$$

$$K_a = \frac{\sin^2(\alpha + \phi)}{\sin^2\alpha \sin(\alpha - \delta)\left[1 + \sqrt{\dfrac{\sin(\phi + \delta)\sin(\phi - \beta)}{\sin(\alpha - \delta)\sin(\alpha + \beta)}}\right]^2}$$

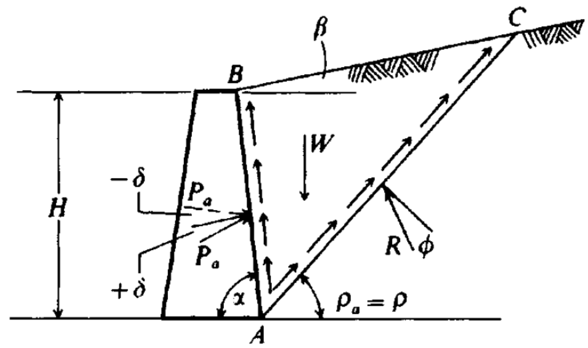

Fig. 10.2 Coulomb active pressure wedge

and the min. value of passive resistance force (P_p) is found to be [Fig. (10.3)]:

$$P_p = \frac{1}{2}\gamma H^2 K_p \qquad \text{(cohesionless soil)}$$

$$K_p = \frac{\sin^2(\alpha-\phi)}{\sin^2\alpha\,\sin(\alpha+\delta)\left[1-\sqrt{\dfrac{\sin(\phi+\delta)\sin(\phi+\beta)}{\sin(\alpha+\delta)\sin(\alpha+\beta)}}\right]^2}$$

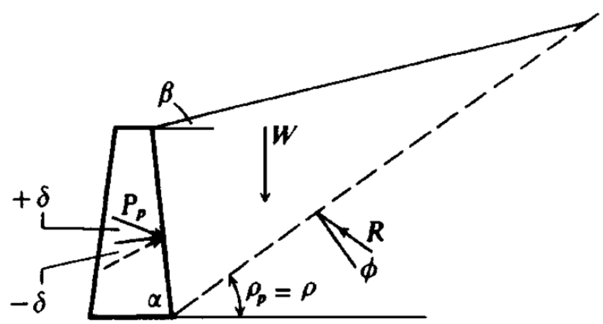

Fig. 10.3 Coulomb passive pressure wedge

For a smooth vertical wall with horizontal backfill:

$$K_a = \frac{1-\sin\phi}{1+\sin\phi} \qquad , \qquad K_p = \frac{1+\sin\phi}{1-\sin\phi}$$

See Tables (10.1) and (10.2) for (K_a and K_p)-values and Table (10.5) for (δ)-values.

Table 10.1 Active-earth-pressure coefficients K_a based on the Coulomb equation

ALPHA = 90 BETA = −10

δ	φ = 26	28	30	32	34	36	38	40	42
0	0.354	0.328	0.304	0.281	0.259	0.239	0.220	0.201	0.184
16	0.311	0.290	0.270	0.252	0.234	0.216	0.200	0.184	0.170
17	0.309	0.289	0.269	0.251	0.233	0.216	0.200	0.184	0.169
20	0.306	0.286	0.267	0.249	0.231	0.214	0.198	0.183	0.169
22	0.304	0.285	0.266	0.248	0.230	0.214	0.198	0.183	0.168

ALPHA = 90 BETA = −5

δ	φ = 26	28	30	32	34	36	38	40	42
0	0.371	0.343	0.318	0.293	0.270	0.249	0.228	0.209	0.191
16	0.328	0.306	0.284	0.264	0.245	0.226	0.209	0.192	0.176
17	0.327	0.305	0.283	0.263	0.244	0.226	0.208	0.192	0.176
20	0.324	0.302	0.281	0.261	0.242	0.224	0.207	0.191	0.175
22	0.322	0.301	0.280	0.260	0.242	0.224	0.207	0.191	0.175

ALPHA = 90 BETA = 0

δ	φ = 26	28	30	32	34	36	38	40	42
0	0.390	0.361	0.333	0.307	0.283	0.260	0.238	0.217	0.198
16	0.349	0.324	0.300	0.278	0.257	0.237	0.218	0.201	0.184
17	0.348	0.323	0.299	0.277	0.256	0.237	0.218	0.200	0.183
20	0.345	0.320	0.297	0.276	0.255	0.235	0.217	0.199	0.183
22	0.343	0.319	0.296	0.275	0.254	0.235	0.217	0.199	0.183

ALPHA = 90 BETA = 5

δ	φ = 26	28	30	32	34	36	38	40	42
0	0.414	0.382	0.352	0.323	0.297	0.272	0.249	0.227	0.206
16	0.373	0.345	0.319	0.295	0.272	0.250	0.229	0.210	0.192
17	0.372	0.344	0.318	0.294	0.271	0.249	0.229	0.210	0.192
20	0.370	0.342	0.316	0.292	0.270	0.248	0.228	0.209	0.191
22	0.369	0.341	0.316	0.292	0.269	0.248	0.228	0.209	0.191

ALPHA = 90 BETA = 10

δ	φ = 26	28	30	32	34	36	38	40	42
0	0.443	0.407	0.374	0.343	0.314	0.286	0.261	0.238	0.216
16	0.404	0.372	0.342	0.315	0.289	0.265	0.242	0.221	0.201
17	0.404	0.371	0.342	0.314	0.288	0.264	0.242	0.221	0.201
20	0.402	0.370	0.340	0.313	0.287	0.263	0.241	0.220	0.201
22	0.401	0.369	0.340	0.312	0.287	0.263	0.241	0.220	0.201

ALPHA = 90 BETA = 15

δ	φ = 26	28	30	32	34	36	38	40	42
0	0.482	0.440	0.402	0.367	0.334	0.304	0.276	0.251	0.227
16	0.447	0.408	0.372	0.340	0.310	0.283	0.258	0.234	0.213
17	0.447	0.407	0.372	0.339	0.310	0.282	0.257	0.234	0.212
20	0.446	0.406	0.371	0.338	0.309	0.282	0.257	0.234	0.212
22	0.446	0.406	0.371	0.338	0.309	0.282	0.257	0.234	0.212

Table 10.2 Passive-earth-pressure coefficients K_p based on the Coulomb equation

ALPHA = 90 BETA = −10

δ	φ = 26	28	30	32	34	36	38	40	42
0	1.914	2.053	2.204	2.369	2.547	2.743	2.957	3.193	3.452
16	2.693	2.956	3.247	3.571	3.934	4.344	4.807	5.335	5.940
17	2.760	3.034	3.339	3.679	4.062	4.493	4.983	5.543	6.187
20	2.980	3.294	3.645	4.041	4.488	4.997	5.581	6.255	7.039
22	3.145	3.490	3.878	4.317	4.816	5.389	6.050	6.819	7.720

ALPHA = 90 BETA = −5

δ	φ = 26	28	30	32	34	36	38	40	42
0	2.223	2.392	2.577	2.781	3.004	3.250	3.523	3.826	4.163
16	3.367	3.709	4.094	4.529	5.024	5.591	6.243	7.000	7.883
17	3.469	3.828	4.234	4.694	5.218	5.820	6.516	7.326	8.277
20	3.806	4.226	4.704	5.250	5.879	6.609	7.462	8.468	9.665
22	4.064	4.532	5.067	5.684	6.399	7.236	8.222	9.397	10.809

ALPHA = 90 BETA = 0

δ	φ = 26	28	30	32	34	36	38	40	42
0	2.561	2.770	3.000	3.255	3.537	3.852	4.204	4.599	5.045
16	4.195	4.652	5.174	5.775	6.469	7.279	8.229	9.356	10.704
17	4.346	4.830	5.385	6.025	6.767	7.636	8.661	9.882	11.351
20	4.857	5.436	6.105	6.886	7.804	8.892	10.194	11.771	13.705
22	5.253	5.910	6.675	7.574	8.641	9.919	11.466	13.364	15.726

ALPHA = 90 BETA = 5

δ	φ = 26	28	30	32	34	36	38	40	42
0	2.943	3.203	3.492	3.815	4.177	4.585	5.046	5.572	6.173
16	5.250	5.878	6.609	7.464	8.474	9.678	11.128	12.894	15.076
17	5.475	6.146	6.929	7.850	8.942	10.251	11.836	13.781	16.201
20	6.249	7.074	8.049	9.212	10.613	12.321	14.433	17.083	20.468
22	6.864	7.820	8.960	10.334	12.011	14.083	16.685	20.011	24.352

ALPHA = 90 BETA = 10

δ	φ = 26	28	30	32	34	36	38	40	42
0	3.385	3.712	4.080	4.496	4.968	5.507	6.125	6.840	7.673
16	6.652	7.545	8.605	9.876	11.417	13.309	15.665	18.647	22.497
17	6.992	7.956	9.105	10.492	12.183	14.274	16.899	20.254	24.633
20	8.186	9.414	10.903	12.733	15.014	17.903	21.636	26.569	33.270
22	9.164	10.625	12.421	14.659	17.497	21.164	26.012	32.601	41.863

ALPHA = 90 BETA = 15

δ	φ = 26	28	30	32	34	36	38	40	42
0	3.913	4.331	4.807	5.352	5.980	6.710	7.563	8.570	9.768
16	8.611	9.936	11.555	13.557	16.073	19.291	23.494	29.123	36.894
17	9.139	10.590	12.373	14.595	17.413	21.054	25.867	32.409	41.603
20	11.049	12.986	15.422	18.541	22.617	28.080	35.629	46.458	62.759
22	12.676	15.067	18.130	22.136	27.506	34.930	45.584	61.626	87.354

10.3 Rankine Earth Pressures

Rankine used essentially the same assumptions as Coulomb, except that he assumed no wall adhesion or friction.

$$P_a = \frac{1}{2}\gamma H^2 K_a \qquad \text{(cohesionless soil)}$$

$$K_a = \cos\beta \frac{\cos\beta - \sqrt{\cos^2\beta - \cos^2\phi}}{\cos\beta + \sqrt{\cos^2\beta - \cos^2\phi}}$$

$$P_p = \frac{1}{2}\gamma H^2 K_p \qquad \text{(cohesionless soil)}$$

$$K_p = \cos\beta \frac{\cos\beta + \sqrt{\cos^2\beta - \cos^2\phi}}{\cos\beta - \sqrt{\cos^2\beta - \cos^2\phi}}$$

See Tables (10.3) and (10.4) for (K_a) and (K_p) values.

For ($c - \phi$) soils:

$$P_a = \frac{1}{2}\gamma (H - z)^2 K_a$$

$$z = \frac{2c}{\gamma\sqrt{K_a}}$$

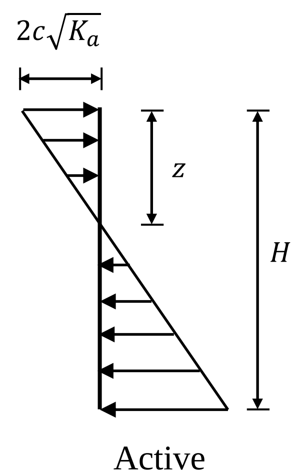

Fig. 10.4 Active lateral earth pressure distribution for a ($c - \phi$) soil

$$P_p = \frac{1}{2}\gamma H^2 K_p + 2c\sqrt{K_p}H$$

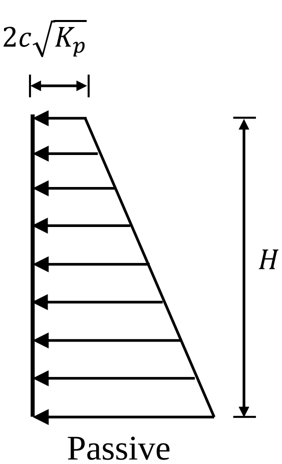

Fig. 10.5 Passive lateral earth pressure distribution for a ($c - \phi$) soil

Table 10.3 Rankine active earth pressure coefficients K_a, values not given for $\beta > \phi$

β	$\phi = 26$	28	30	32	34	36	38	40	42
0	0.3905	0.3610	0.3333	0.3073	0.2827	0.2596	0.2379	0.2174	0.1982
5	0.3959	0.3656	0.3372	0.3105	0.2855	0.2620	0.2399	0.2192	0.1997
10	0.4134	0.3802	0.3495	0.3210	0.2944	0.2696	0.2464	0.2247	0.2044
15	0.4480	0.4086	0.3729	0.3405	0.3108	0.2834	0.2581	0.2346	0.2129
20	0.5152	0.4605	0.4142	0.3739	0.3381	0.3060	0.2769	0.2504	0.2262
25	0.6999	0.5727	0.4936	0.4336	0.3847	0.3431	0.3070	0.2750	0.2465
30	—	—	0.8660	0.5741	0.4776	0.4105	0.3582	0.3151	0.2784
35	—	—	—	—	—	0.5971	0.4677	0.3906	0.3340
40	—	—	—	—	—	—	—	0.7660	0.4668

Table 10.4 Rankine passive earth pressure coefficients K_p

β	$\phi = 26$	28	30	32	34	36	38	40	42
0	2.5611	2.7698	3.0000	3.2546	3.5371	3.8518	4.2037	4.5989	5.0447
5	2.5070	2.7145	2.9431	3.1957	3.4757	3.7875	4.1360	4.5272	4.9684
10	2.3463	2.5507	2.7748	3.0216	3.2946	3.5980	3.9365	4.3161	4.7437
15	2.0826	2.2836	2.5017	2.7401	3.0024	3.2926	3.6154	3.9766	4.3827
20	1.7141	1.9176	2.1318	2.3618	2.6116	2.8857	3.1888	3.5262	3.9044
25	1.1736	1.4343	1.6641	1.8942	2.1352	2.3938	2.6758	2.9867	3.3328
30	—	—	0.8660	1.3064	1.5705	1.8269	2.0937	2.3802	2.6940
35	—	—	—	—	—	1.1239	1.4347	1.7177	2.0088
40	—	—	—	—	—	—	—	0.7660	1.2570

Table 10.5 Friction angles δ between various foundation materials and soil or rock*

Interface materials	Friction angle, δ, degrees†
Mass concrete or masonry on the following:	
Clean sound rock	35°
Clean gravel, gravel-sand mixtures, coarse sand	ϕ
Clean fine to medium sand, silty medium to coarse sand, silty or clayey gravel	ϕ
Clean fine sand, silty or clayey fine to medium sand	ϕ
Fine sandy silt, nonplastic silt	ϕ
Very stiff and hard residual or preconsolidated clay	ϕ
Medium stiff and stiff clay and silty clay	ϕ
Steel sheet piles against the following:	
Clean gravel, gravel-sand mixture, well-graded rock fill with spalls	22°
Clean sand, silty sand-gravel mixture, single-size hard rock fill	17
Silty sand, gravel, or sand mixed with silt or clay	14
Fine sandy silt, nonplastic silt	11
Formed concrete or concrete sheetpiling against the following:	
Clean gravel, gravel-sand mixtures, well-graded rock fill with spalls	22–26
Clean sand, silty sand-gravel mixture, single-size hard rock fill	17–22
Silty sand, gravel, or sand mixed with silt or clay	17
Fine sandy silt, nonplastic silt	14
Various structural materials	
Masonry on masonry, igneous and metamorphic rocks:	
Dressed soft rock on dressed soft rock	35°
Dressed hard rock on dressed soft rock	33
Dressed hard rock on dressed hard rock	29
Masonry on wood (cross grain)	26
Steel on steel at sheet-pile interlocks	17
Wood on soil	14–16‡

*May be stress-dependent (see text) for sand.

†Single values $\pm 2°$. Alternate for concrete poured on soil is $\delta = \phi$.

‡May be higher in dense sand or if sand penetrates wood.

CHAPTER 11

RETAINING WALLS

11.1 <u>Introduction</u>

Retaining walls (R.W.) are structures used to provide stability for earth or other material where conditions disallow the mass to assume its natural slope. Retaining walls are classified into six principal types [Fig. (11.1)]:

a. Gravity wall: which depends upon its weight for stability.

b. Cantilever wall: is a R.C. wall that utilizes cantilever action to retain the mass behind the wall. Stability of this wall is partially achieved from the weight of the soil on the heel portion of the base slab.

c. Counterfort wall: is similar to a cantilever R.W. except that it is used where the cantilever is long or for very high pressure behind the wall and has counterforts, which tie the wall and base together, built at intervals along the wall to reduce the B.M. and S.F. The counterfort is behind the wall and subjected to tensile forces. A “Buttressed” retaining wall is similar to counterfort wall, except that the bracing is in front of the wall and is in compression instead of tension.

d. Crib wall: which are built-up members of pieces of precast concrete, metal, or timber and are supported by anchor pieces embedded in the soil for stability.

e. Semigravity wall: which are walls intermediate between a true gravity and a cantilever wall.

f. Bridge abutments: are often retaining walls with wing wall extension to retain the approach fill and provide protection against erosion.

Terms used in retaining-wall design are shown in Fig. (11.2).

Retaining walls must be of adequate proportions to resist overturning and sliding as well as being structurally adequate. Fig. (11.3) shows the general proportions of some retaining-wall components that can be used in the preliminary design.

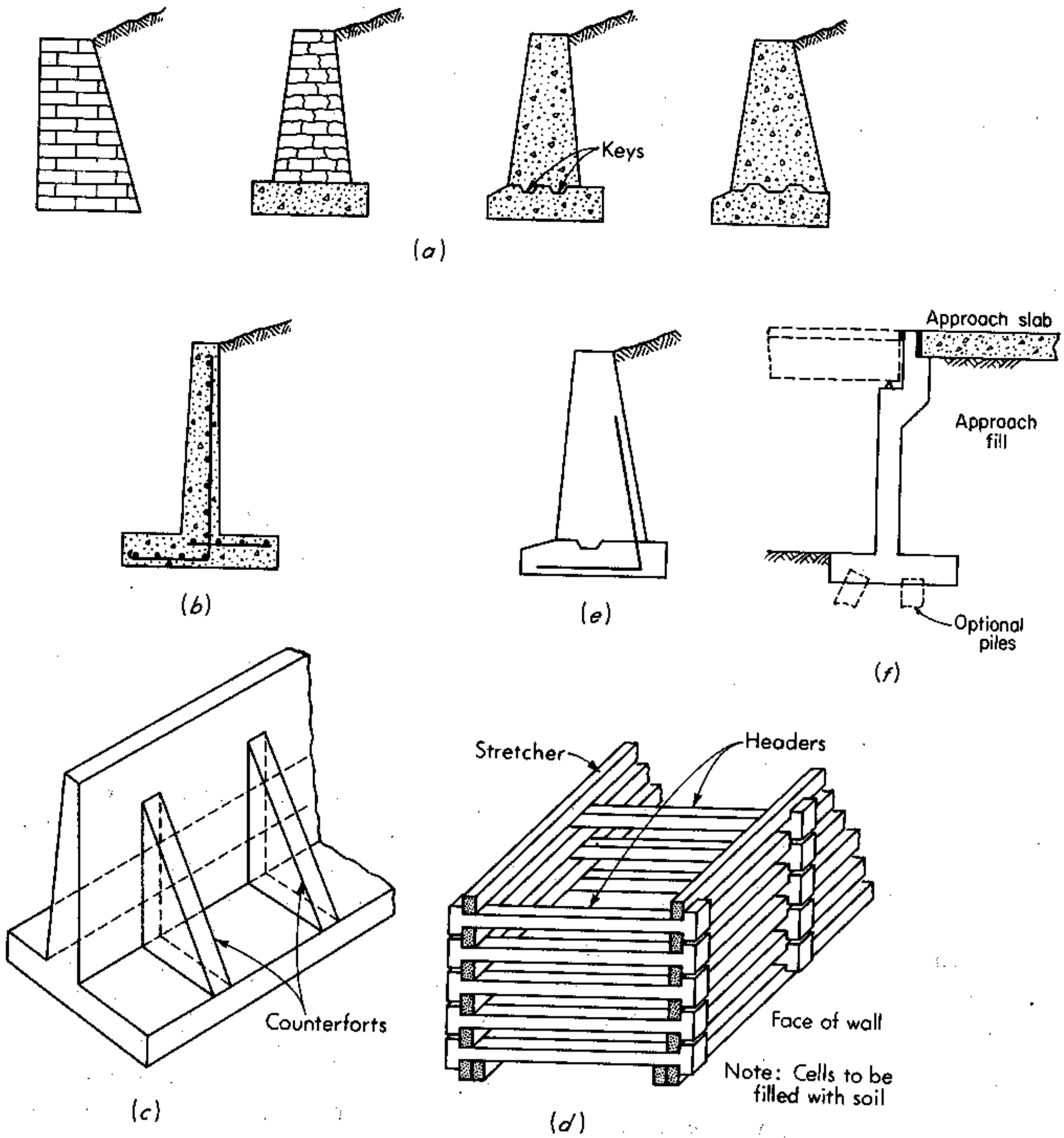

Fig. 11.1 Types of retaining walls. (*a*) Gravity walls of stone masonry, brick, or plain concrete. Weight provides overturning and sliding stability; (*b*) cantilever wall; (*c*) counterfort, or buttressed wall. If backfill covers counterforts, the wall is termed a counterfort; (*d*) crib wall; (*e*) semigravity wall (small amount of steel reinforcement is used); (*f*) bridge abutment.

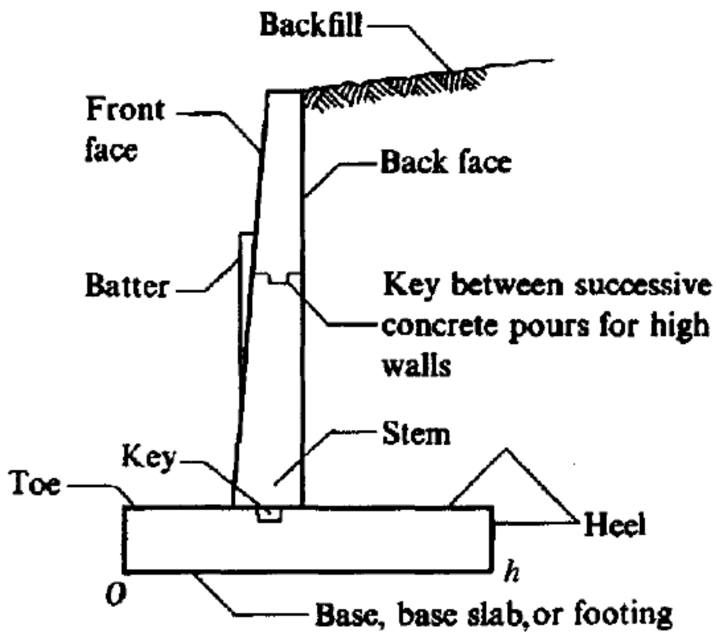

Fig. 11.2 Principal terms used with retaining walls.

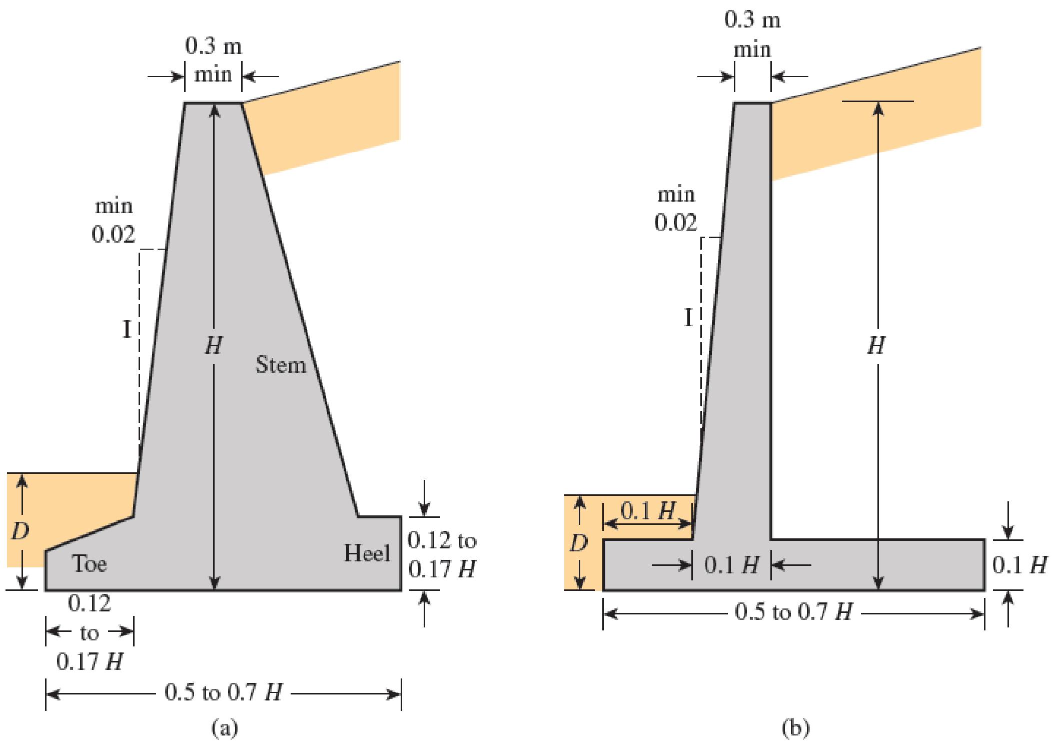

Fig. 11.3 Approximate dimensions for various components of retaining walls for initial stability checks: (*a*) gravity wall; (*b*) cantilever wall

The base-slab dimensions should be such that the resultant of the vertical loads within the middle third. If the resultant falls outside the middle-third, the toe pressure will be excessively larger, only a part of the footing will be effective.

11.2 Stability of Retaining Walls

A retaining wall may fail in any of the following ways:

- It may *overturn* about its toe. [See Fig. (11.4a)]
- It may *slide* along its base. [See Fig. (11.4b)]
- It may fail due to the loss of *bearing capacity* of the soil supporting the base. [See Fig. (11.4c)]
- It may undergo deep-seated shear failure. [See Fig. (11.4d)]
- It may go through excessive settlement.

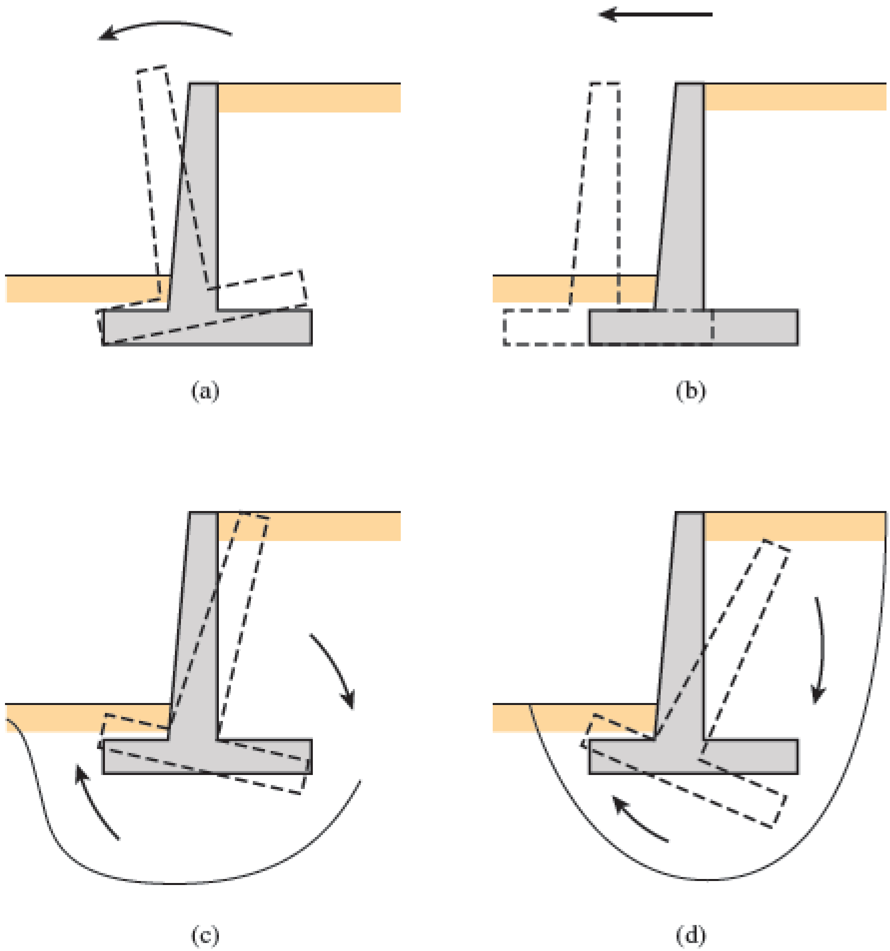

Fig. 11.4 Failure of retaining wall: (a) by overturning; (b) by sliding; (c) by bearing capacity failure; (d) by deep-seated shear failure

The checks for stability against sliding, overturning, and bearing capacity failure will be described below. The Rankine theory will be used in estimating the lateral earth pressure acting on the wall.

Referring to Fig. 11.5:

1. Sliding

$$F_s = \frac{P_{resisting}}{P_{driving}} = \frac{F_r + P_p}{P_{ah}}$$

F_s = 1.25 – 2.0

2. Overturning

$$F_o = \frac{resisting\ moment}{overturning\ moment} = \frac{M_r + P_p \bar{y}_p}{M_o}$$

$$M_o = P_{ah}\ \bar{y}_a$$

$$M_r = \sum W_i \cdot x_i + P_{av} \cdot x_{av} = W_c \cdot x_c + W_s \cdot x_s + P_{av} \cdot x_{av}$$

F_o = 1.5 – 2.0

3. Stability against B.C. failure

$$q = \frac{R}{B} \mp \left(\frac{6R \cdot e}{B^2}\right) \leq q_a$$

$$R = W_c + W_s + P_{av}$$

$$e = \frac{B}{2} - \bar{x}$$

$$\bar{x} = \frac{M_r + P_p \cdot \bar{y}_p - M_o}{R}$$

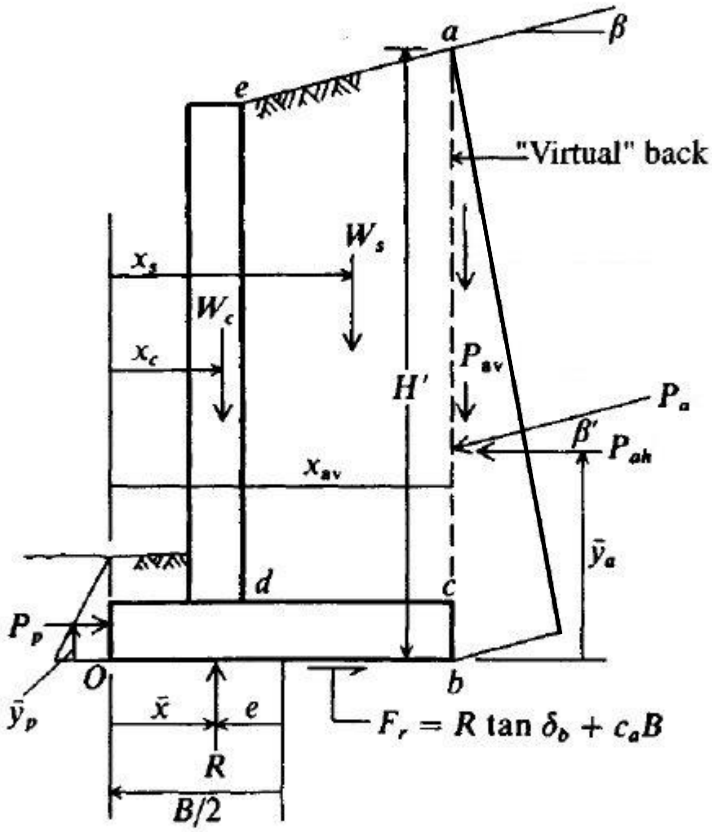

Fig. 11.5 Wall pressure for overall stability against overturning and sliding. W_c = weight of all concrete (stem and base); W_s = weight of soil in zone *acde*. Find moment arms x_i any way practical – usually using parts of known geometry. Use this lateral pressure for base design and bearing capacity.

11.3 <u>Base Key</u>

Where sufficient sliding stability is not possible (usually for walls with large H) a base key has been used [Fig. (11.6)]. It was common practice to put the key beneath the stem. This was convenient from the view of simply extending the stem reinforcement through the base and into the key.

Considering the labor involved with a key, for the low cantilever wall in current practice a key should not be required since it would be more economical to simply increase the base dimension *B* until the sliding stability is adequate.

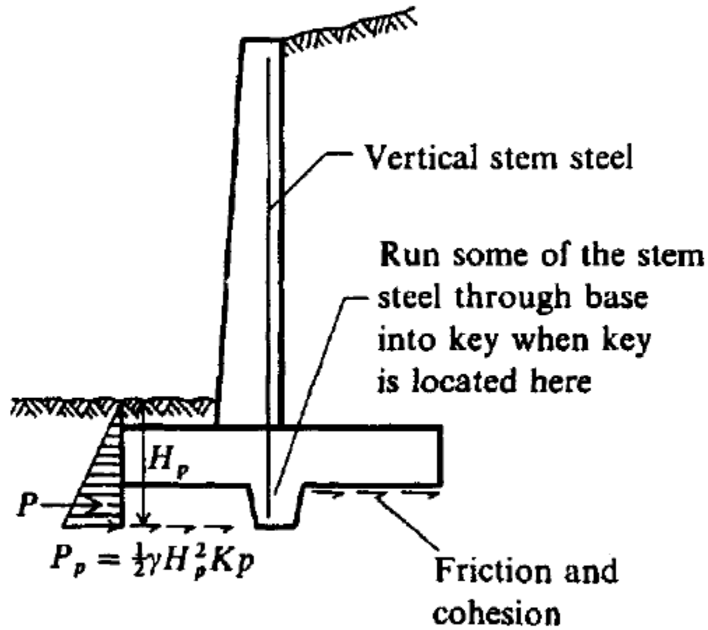

Fig. 11.6 Stability against sliding by using a base key

CHAPTER 12

SHEET-PILE WALLS

12.1 Introduction

Sheet-pile walls are widely used for both large and small water front structures. Piers jutting into the harbor consisting of two rows of sheet-piling are widely used. Sheet piling is also used for slope stability and erosion protection. There are four types of sheet-pile walls as shown in Fig. (12.1).

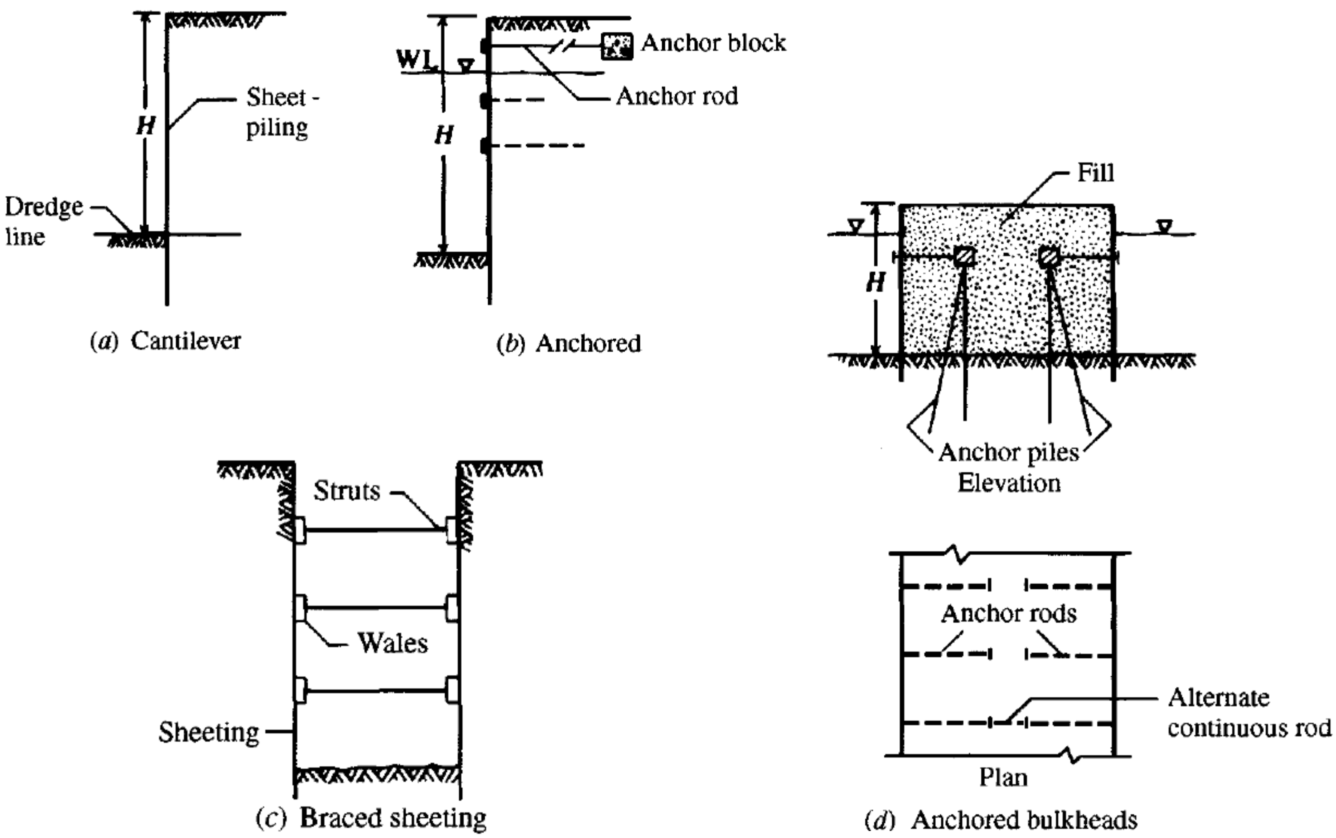

Fig. 12.1 Sheet-pile structures

12.2 Types of Sheetpiling

Sheet piling materials may be of timber, reinforced concrete, or steel. Steel sheetpiling is the most common type used because of several advantages over other materials. Principal advantages are as follows:

Table 12.1 (a) Steel sheetpiling sections produced in the United States*

	Section index	Depth d, in. / mm	Driving distance, in. / mm	Weight lb/ft / kg/m	Weight lb/ft² / kg/m²	Section modulus* per pile, in.³ / m³ × 10⁻³	Moment of inertia per pile, in.⁴ / m⁴ × 10⁻⁶
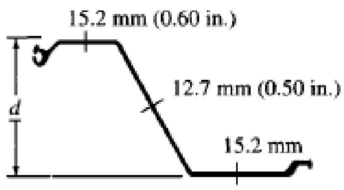	PZ40	16.1	19.69	65.6	40.0	99.6	805.4
		410	**500**	**97.6**	**195.3**	**1.632**	**335.23**
	PZ35	14.9	22.64	66.0	35.0	91.4	681.5
		380	**575**	**98.2**	**170.9**	**1.498**	**283.7**
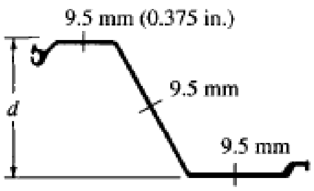	PZ27	12	18	40.5	27.0	45.3	276.3
		305	**460**	**60.3**	**131.8**	**0.742**	**115.0**
	PZ22	9	22	40.3	22.0	33.1	154.7
		230	**560**	**60.0**	**107.4**	**0.542**	**64.39**
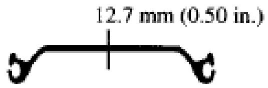	PS31	—	19.69	50.9	31.0	3.3	5.3
			500	**75.7**	**151.4**	**0.054**	**2.206**
	PS27.5	—	19.69	45.1	27.5	3.3	5.3
			500	**67.1**	**134.3**	**0.054**	**2.206**
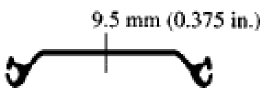	PSA23	—	16.00	30.7	23.0	3.2	5.5
			405	**45.7**	**112.3**	**0.052**	**2.290**
	Box pile	31.0	45.28	261.2	—	480.7	7618
		787	**1150**	**388.7**	**—**	**7.877**	**3170.9**

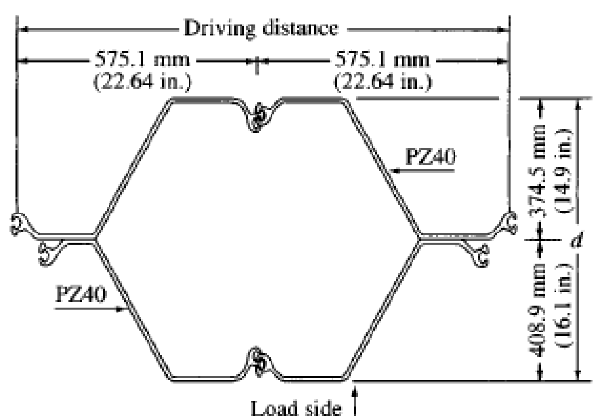

*These sections are now available only from Bethlehem Steel Corporation.

Steel grades: A328 with F_y = 270 MPa (39 ksi)
A572 with F_y = 345 and 415 MPa (50 and 60 ksi)
A690 with F_y = 345 MPa (50 ksi) for marine environments

Table 12.1 (b) Steel sheetpiling sections produced in Europe

	Section index	Depth d, mm	Driving distance, mm	Weight kg/m	Weight kg/m²	Section modulus per pile, $m^3 \times 10^{-3}$	Moment of inertia per pile, $m^4 \times 10^{-6}$
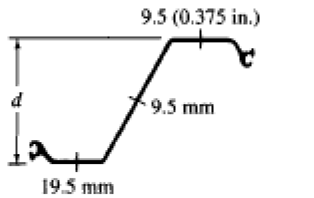	AZ 13	303	670	72.0	107	0.870	132.0
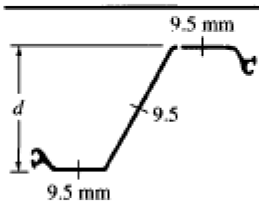	AZ 18	380	630	74.4	118	1.135	215.40
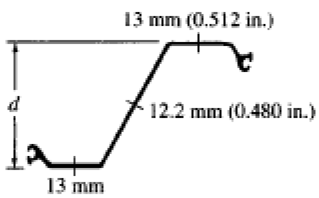	AZ 26	427	630	97.8	155	1.640	349.70
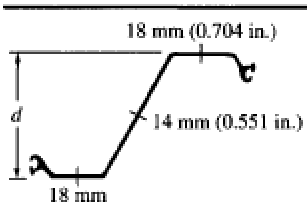	AZ 36	460	630	122.2	194	2.270	521.60
	AS500-12.0	—	500	72.3	145	0.047	1.80
							
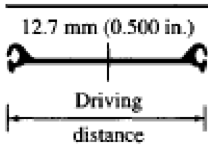	AS500-12.7	—	500	75.2	150	0.047	1.80
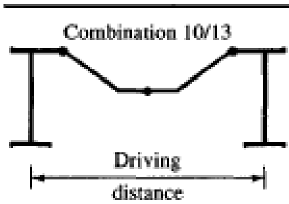	HZ775A / ZH9.5	775	1585	184	222	4.80	1859.9

1. It is resistant to high driving stresses as developed in hard or rocky materials.
2. It may be reused several times.
3. It is of relatively light weight.
4. It has a long service life either above or below water with modest protection.
5. It is easy to increase the pile length by either welding or bolting.
6. Joints are less apt to deform when wedged full with soil and stones during driving.

Steel sheetpiling is available in several shapes and joints [see Table (12.1)].

12.3 Safety Factors

The conventional methods use:

F = 1.2 to 1.5 (with respect to embedment depth)

F = 1.5 to 2.0 (with respect to passive resistance)

12.4 Cantilever Sheetpiling

The solution of this problem is to assume that the pile is subjected, on the backfill side, to active pressure to the dredge line. Under the influence of the active pressure the wall tends to rotate, developing passive pressure in front of the wall and active pressure behind the wall. At the pivot point O the soil behind the wall goes from active to passive pressure, with active pressure in front of the wall for the remainder of the distance to the bottom of the pile [Fig. (12.2)]. In the classical design of cantilever sheetpiling, simplifying assumption as indicated in Fig. (12.2c) is made.

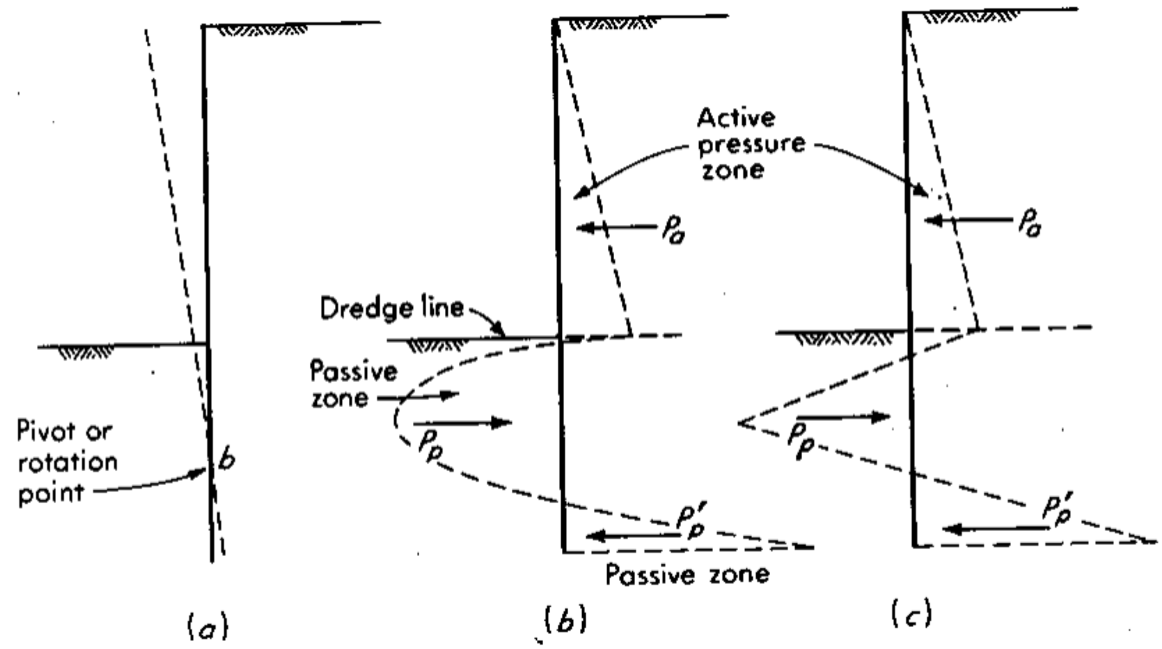

Fig. 12.2 (a) Assumed elastic line of the sheetpiling; (b) probable and as obtained in finite-element solution qualitative soil-pressure distribution; (c) simplified pressure diagram for computational purposes (granular soil and no water as shown).

12.4.1 <u>Cantilever Sheetpiling in Granular Soil</u>

Steps in the solution of a cantilever wall in a granular soil are as follows:

1. Sketch the given conditions [as in Fig. (12.3)].
2. Evaluate the active and passive earth pressure coefficients.
3. Compute the pressures, $\bar{p}_a$, the distance a, $\bar{p}_p'$ and the resultant pressure R_a and its location $\bar{y}$.
4. Insert values from step (3) into the following equation and evaluate (Y) using trial and error, starting with (Y= 0.75H).

$$Y^4 + Y^3\frac{\bar{p}_p'}{C} - Y^2\frac{8R_a}{C} - Y\left[\frac{6R_a}{C^2}\left(2\bar{y}C + \bar{p}_p'\right)\right] - \frac{6R_a\,\bar{y}\,\bar{p}_p' + 4R_a^2}{C^2} = 0$$

5. Total required length of the pile:

   L = H + D

   D = Y + a

6. Compute the max. B.M which occurs at the point of zero shear find the required section modulus and select a suitable section.
7. Add (20-50)% to the computed embedment depth or reduce passive resistance from step (3).

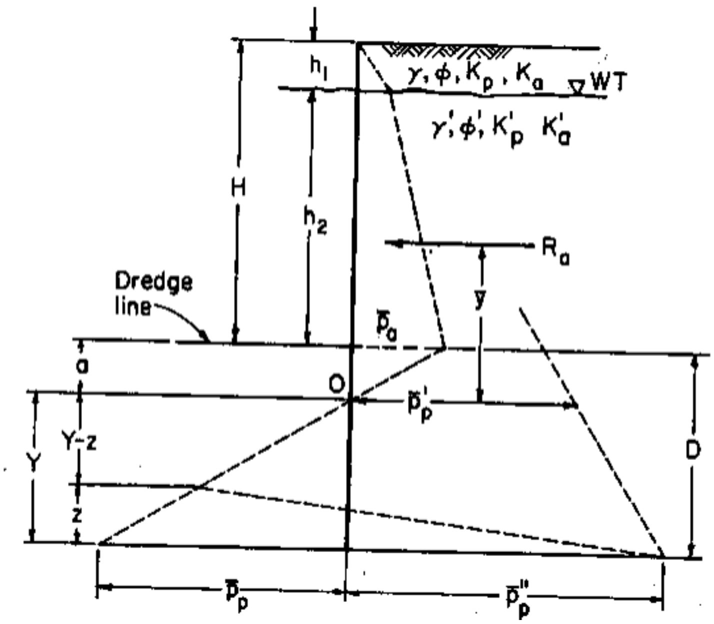

If ϕ below the water table is same as above, then $K'_p = K_p$ and $K'_a = K_a$

$$a = \frac{\bar{p}_a}{\gamma'(K'_p - K'_a)} = \frac{\bar{p}_a}{C}$$

$$\bar{p}_p = CY$$

$$\bar{p}'_p = \gamma h_1 K'_p + (h_2 + a)\gamma' K'_p - \gamma' a K'_a$$

$$\bar{p}''_p = \bar{p}'_p + CY$$

$$z = \frac{\bar{p}_p \cdot Y - 2R_a}{\bar{p}_p + \bar{p}''_p}$$

Fig. 12.3 Cantilever sheetpiling pressure diagram for a granular soil. The diagram illustrates the possibility of different soil properties below the water table. If other stratification exists, the pressure diagram should be appropriately modified.

12.4.2 <u>Cantilever Sheet Pile in Cohesive Soils (ϕ = 0)</u>

Design steps:

1. Sketch the given conditions [as in Fig. (12.4)].
2. Evaluate the active and passive pressure coefficients.
3. Calculate weigh of overburden and surcharge load at the dredge level.
4. Compute the resultant pressure (R_a) and its location $\bar{y}$.
5. Insert values from step (3 & 4) into the following equation and evaluate (D).

$$D^2(4c - \bar{q}) - 2DR_a - \frac{R_a(12c\bar{y} + R_a)}{2c + \bar{q}} = 0$$

6. Compute the max. bending moment which occurs at the point of zero shear, find the

required section modulus and select a suitable section.

7. Add (20-50)% to the computed depth or reduce passive resistance and/or cohesion from step (5).

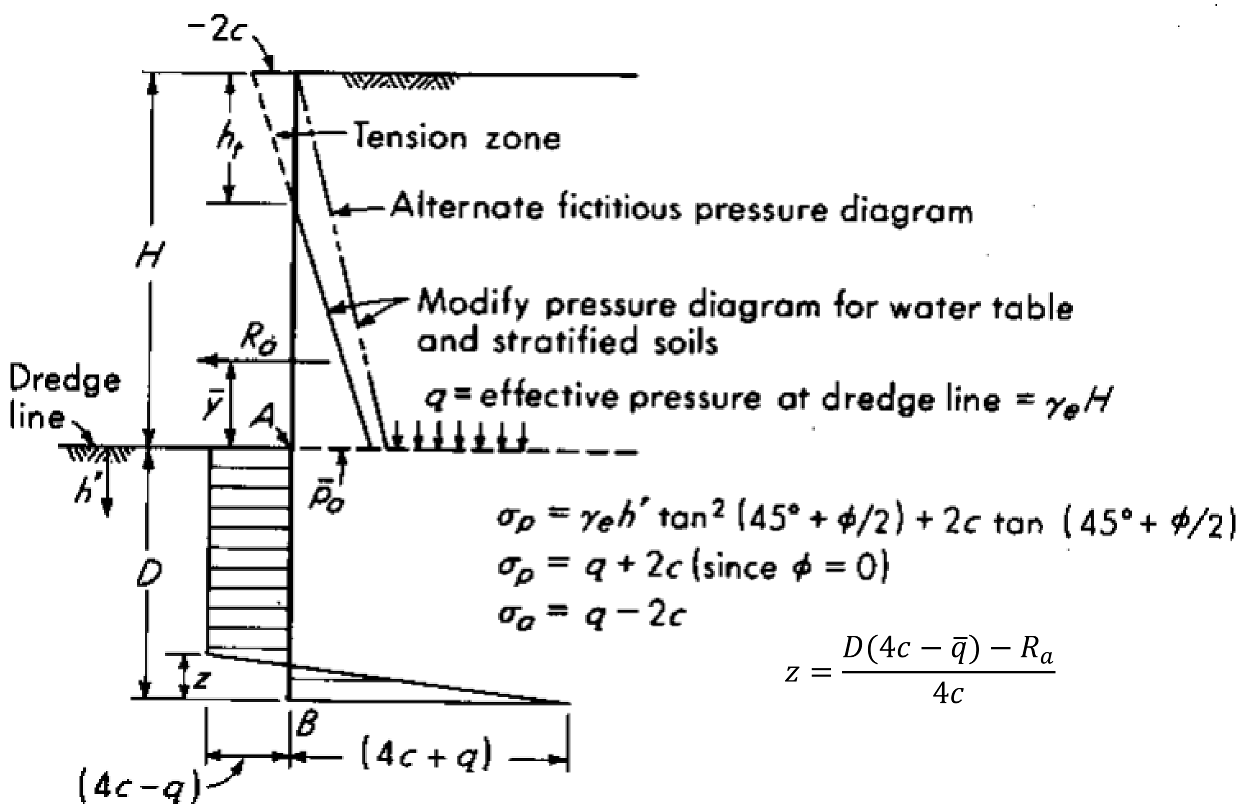

Fig. 12.4 Sheetpiling in cohesive soil. The undrained shear strength (ϕ = 0) case shown is conservative.

12.5 <u>Anchored Sheetpiling; Free-Earth Support</u>

The use of an anchor member tends to reduce the lateral deflection, the bending moment, and the depth of penetration of the pile.

The free-earth support method assumes that the piling is rigid and may rotate at the anchor-rod level, with failure occurring by a rotation about the anchor rod as shown in Fig. (12.5).

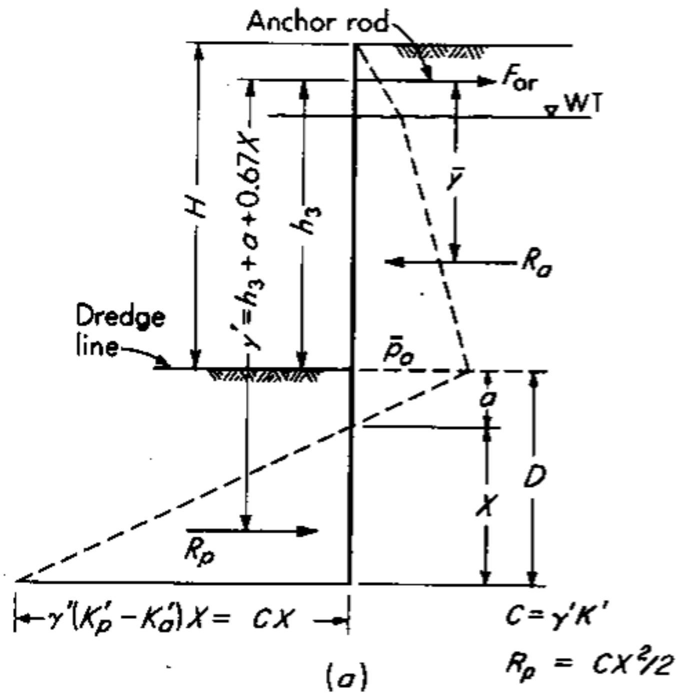

Fig. 12.5 Anchored sheetpiling, free-earth method. (a) All granular soil; (b) cohesive soil below dredge line with granular-soil backfill

Design steps:

1. Select appropriate value for active and passive earth pressure coefficients.
2. a- calculate a, R_a, $\bar{y}$.

   b- calculate $\bar{q}$, R_a, $\bar{y}$.
3. Take moment about tie rod level.

   a- $a = \dfrac{\bar{p}_a}{C}$

   $$2X^3 + 3X^2(h_3 + a) - \frac{6R_a\bar{y}}{C} = 0$$

   Solve for (X).

   b- $$R_a\bar{y} - D(4c - \bar{q})\left(h_3 + \frac{D}{2}\right) = 0$$

   Solve for (D).
4. Compute tie rod tension $F_{ar} = R_a - R_p$

a- $R_p = \frac{CX^2}{2}$

b- $R_p = D(4c - \bar{q})$

5. Determine max. B.M at point of zero shear.
6. Select pile section for the max. moment.
7. Add (20 -50)% to penetration depth or divide (K_p) and/or (c) by (1.5-2.0) in steps (3 & 4).
8. Design deadman and wales.

12.5.1 Capacity of Deadman

If the anchor is a deadman, its capacity will depend on its length (L) and the ratio ($\frac{d_2}{H}$). Three cases will be considered [Fig. (12.6)].

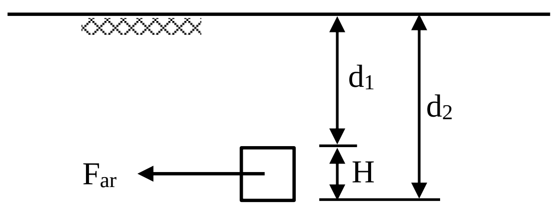

Fig. 12.6

a- $L > 1.5H$

$\frac{d_1}{H} \leq (0.5 - 0.7)H$

$F_{ar} = \frac{P_p - P_a}{F}$

P_p, P_a : Rankine active and passive earth pressure forces per unit of anchor width.

F: safety factor (1.2-1.5).

b- $L \leq 1.5H$

$F_{ar} = \frac{0.65\, \gamma\, d_2^2 L\, K_p}{F}$ $(Granular\ soil)$

K_p: Rankine value

$F_{ar} = \frac{McHL}{F}$ $[cohesive\ (\phi = 0)\ soil]$

$M = 9$ $(for\ \frac{d_2}{H} \geq 3)$

$$= \frac{9d_2}{H} \qquad \left(for \quad 0 \le \frac{d_2}{H} < 3\right)$$

$$F_{ar} = \frac{P_p L}{F} \qquad (c - \phi\ soil)$$

c- $\dfrac{d_2}{H} > 6.5$

$$F_{ar} = \frac{0.65\, \gamma\, d_2^2 L\, K_p}{F} \qquad (for\ all\ values\ of\ L)$$

12.5.2 Location of Deadman

In order to develop the full capacity, the deadman should be located so that the passive zone is outside the active wedge [the shaded area of Fig. (12.7)].

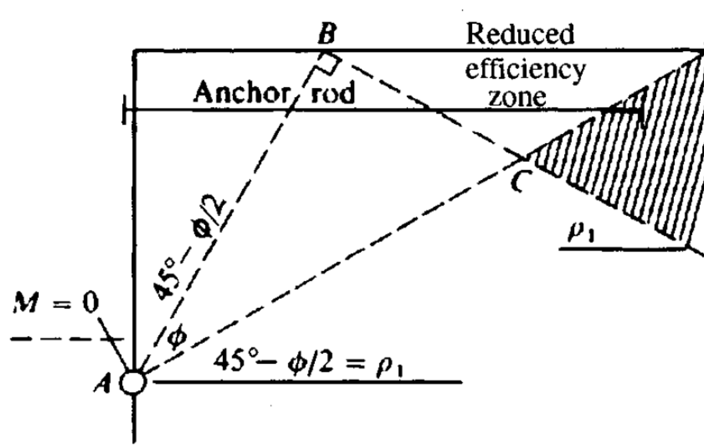

Fig. 12.7 Locating anchor so active and passive zones do not intersect gives maximum efficiency.

12.6 Braced Cuts-General

Sometimes construction works requires ground excavations with vertical or near-vertical faces- for example, basements of buildings in developed areas or underground transportation facilities at shallow depths below the ground surface. The vertical faces of the cuts need to be protected by temporary bracing systems to avoid failure that may be accompanied by considerable settlement or by bearing capacity failure of nearby foundations.

Fig. (12.8) shows two types of braced cuts commonly used in construction work. One type uses the soldier beam, [Fig. (12.8a)] which is driven into the ground before excavation and is a vertical steel or timber beam. Laggings, which are horizontal timber planks, are placed between soldier beams as the excavation proceeds. When the excavation reaches the desired depth, wales (horizontal steel beams) and struts are installed. The struts are horizontal compression members. Fig. (12.8b) shows another type of braced excavation. In this case, interlocking sheet piles are driven into the soil before excavation. Wales and struts are inserted immediately after excavation reaches the appropriate depth.

12.6.1 Pressure Envelope for Braced-Cut Design

To design braced excavations (that is, to select wales, struts, sheet piles, and soldier beams), an engineer must estimate the lateral earth pressure to which the braced cuts will be subjected. The analysis based on the lateral earth pressure theories does not provide the relationships for estimation of variation of lateral pressure with depth, which is a function of several factors such as the type of soil, experience of the construction crew, equipment used, and so forth. For that reason, empirical pressure envelopes were developed for braced cuts. Fig. (12.9) shows the pressure envelopes suggested by Peck (1969), to which the following guidelines apply.

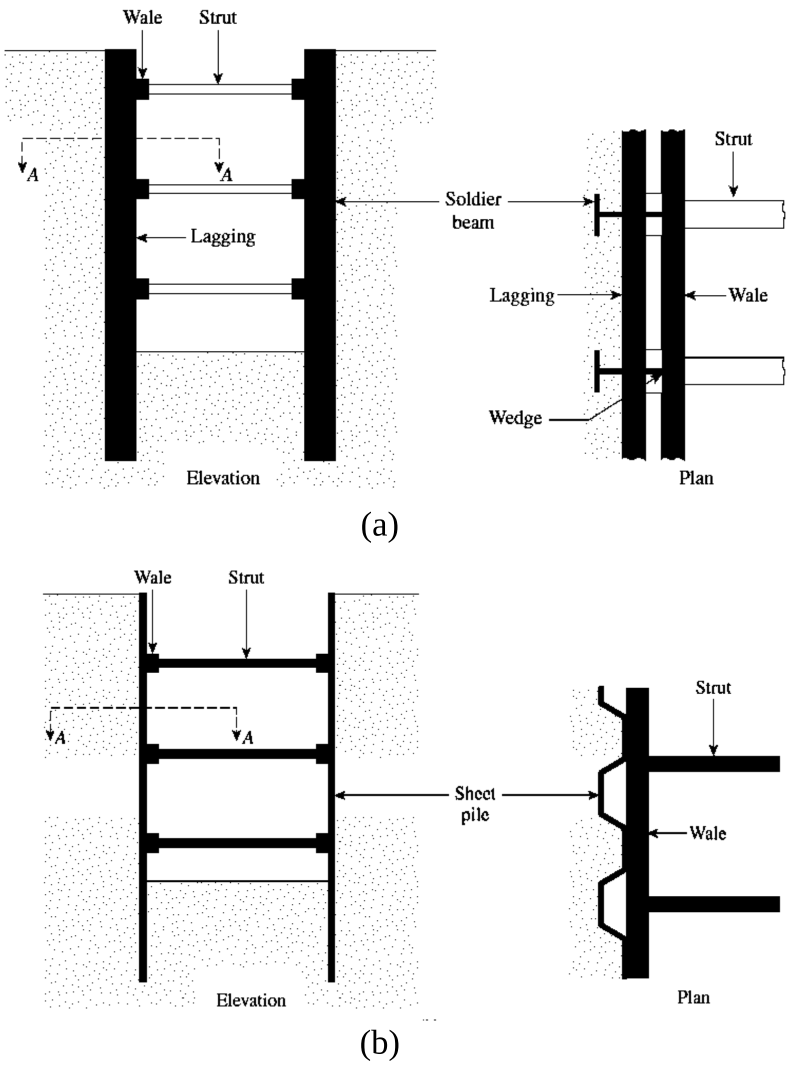

Fig. 12.8 Types of braced cut: (a) use of soldier beams; (b) use of sheet piles

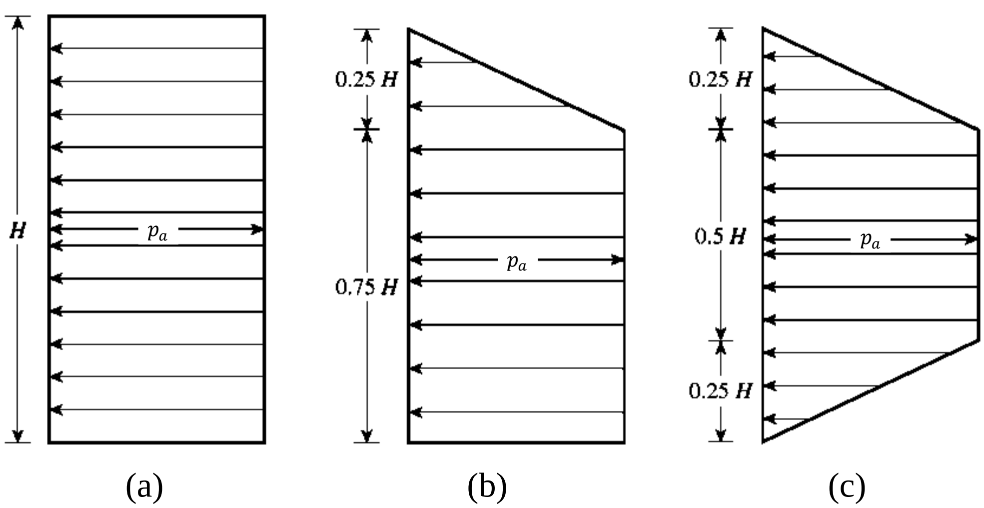

Fig. 12.9 Apparent-pressure envelope for (a) cuts in sand, (b) cuts in soft to medium stiff clay, and (c) cuts in stiff clay

Cuts in sand [Fig. (12.9a)]

$$p_a = 0.65\gamma H K_a$$

where,

γ = unit weight of soil

H = height of the cut

K_a = Rankine active pressure coefficient

Cuts in soft to medium stiff clay [Fig. (12.9b)]

This pressure envelope is applicable for the condition; $\gamma H/c > 4$

where, c is the undrained cohesion (ϕ = 0)

It is the larger of

$$p_a = \gamma H\left[1 - \frac{4c}{\gamma H}\right] \qquad or \qquad p_a = 0.3\gamma H$$

Cuts in stiff clay [Fig. (12.9c)]

It is applicable to the condition; $\gamma H/c \leq 4$

$p_a = 0.2\gamma H$ to $0.4\gamma H$

$(p_a)_{av.} = 0.3\gamma H$

12.6.2 Design of Various Components of a Braced Cut

a. Struts

They are actually horizontal columns subject to bending. The load carrying capacity of columns depends on the slenderness ratio. For braced cuts in clayey soils, the depth of the first strut below the ground surface should be less than the depth of tensile crack ($z_c = 2c/\gamma$).

The following is a step-by-step outline of the procedure used to design the struts:

1. Draw the pressure envelope for the braced cut. Also show the proposed strut levels, [A, B, C and D in the Fig. (12.10a)]. The sheet piles or soldier beams are assumed to be hinged

at the strut levels, except for the top and bottom ones.

2. Determine the reactions for the two simple overhang beams (top and bottom) and all the simple beams in between. These reactions are (A, B1, B2, C1, C2 and D) in Fig. (12.10b).
3. The strut load in the figure may be calculated as follows:

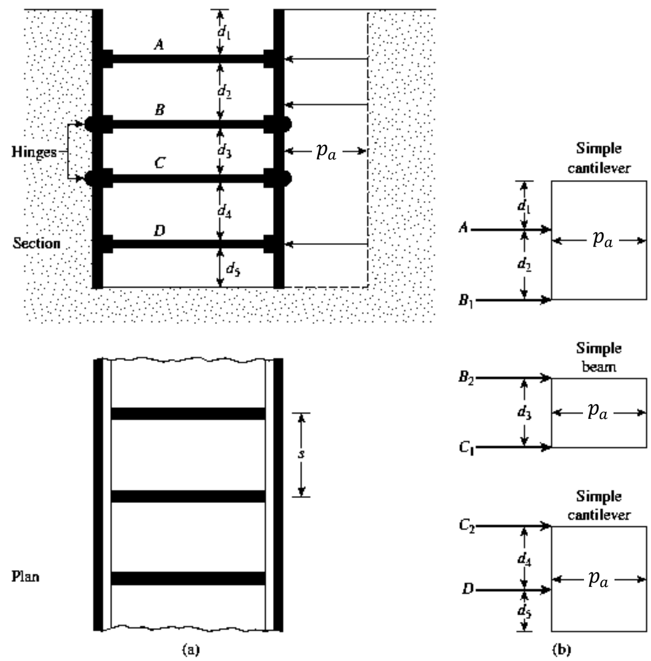

Fig. 12.10 Determination of strut loads: (a) section and plan of the cut; (b) method for determining strut loads

$P_A = (A).(S)$

$P_B = (B_1+B_2).S$

$P_C = (C_1+C_2).S$

$P_D = (D).(S)$

where:

P_A, P_B, P_C and P_D = loads to be taken by the individual struts at levels A, B, C, and D, respectively.

A, B_1, B_2, C_1, C_2 and D = reactions calculated in step (2) (unit: force per unit length of the braced cut)

S = horizontal spacing of the struts.

4. Knowing the strut loads at each level and the intermediate bracing conditions allows selection of the proper sections from the steel construction manual.

b. Sheet piles

1. For each of the sections shown in Fig. (12.10b), determine the maximum bending moment.
2. Determine the value of maximum bending moments (M_{max}) obtained in step (1). Note that the unit of this moment will be (F.L/L), for example (kN.m/m) length of the wall.
3. Obtain the required section modulus of the sheet piles.
4. Choose a sheet pile having a section modulus greater than or equal to the required section modulus.

c. Wales

Wales may be treated as continuous horizontal members if they are spliced properly. Conservatively, they may also be treated as though they are pinned at the struts. For the section shown in Fig. (12.10a), the maximum moment for the wales (assuming that they are pinned at the struts) is:

At level A, $M_{max} = A(S)^2/8$

At level B, $M_{max} = (B_1+B_2)(S)^2/8$

At level C, $M_{max} = (C_1+C_2)(S)^2/8$

At level D, $M_{max} = D(S)^2/8$

Determine the section modulus of the wales.

12.6.3 Bottom Heaving of a Cut in Clay

Braced cuts in clay may become unstable as a result of heaving of the bottom of the excavation. The failure surface for such a case is shown in Fig. (12.11). Bjerrum and Eide (1956) proposed the following equation for the factor of safety;

$$F.S = \frac{cN_c}{\gamma H + q}$$

where;

N_c = The bearing capacity factor, [Fig. (12.12)]

$$(N_c)_{rectangular} = (N_c)_{squre}\left(0.84 + \frac{0.16B}{L}\right)$$

A factor of safety of about (1.5) is generally recommended.

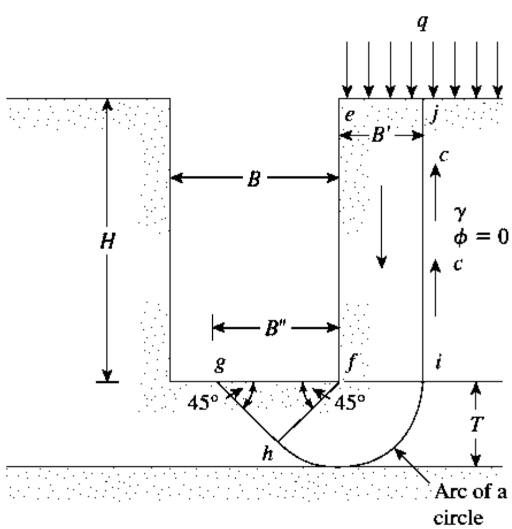

Fig. 12.11 Heaving in braced cuts in clay

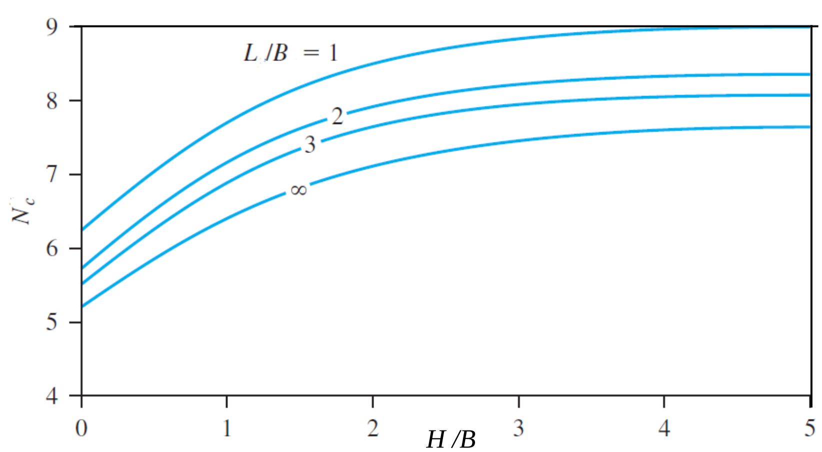

Fig. 12.12 Variations of N_c with L/B and H/B